PROCEEDINGS of the I·R·E AND WAVES and ELECTRONS

The Institute of Radio Engineers

INCORPORATED

RCA Victor

THREADLESS SEWING MACHINE
ONIC TECHNIQUE ENABLES THE PRODUCTION OF SEAMLESS FABRIC JOINTS

MARCH, 1946

Volume 34 Number 3

Published in Two Sections

Section I—Proceedings of the I.R.E. Section

Reflex-Klystron Oscillators
Transmission of F-M Wave
R-C Parallel-T Network Analysis
Modulation-Frequency Feedback
Low-Pass Filter
Matrix Algebra

Section II—Waves and Electrons Section

Induction Heating in Tube Manufacture
Fine Wires in Tube Industry
Three-Beam Microoscillograph
Television Synchronizing Generators
Negative Voltage Feedback
Fractional-Mu Oscillator

REPORTS of the Theory, Practice, and Applications of Electronics and Electrical Communication

Radio Communication • Sound Broadcasting • Television • Marine and Aerial Guidance • Tubes • Radio-Frequency Measurements • Engineering Education • Electron Optics • Sound and Picture Electrical Recording and Reproduction • Power and Manufacturing Applications of Radio-and-Electronic Technique •

YOUR TUBE PROBLEMS

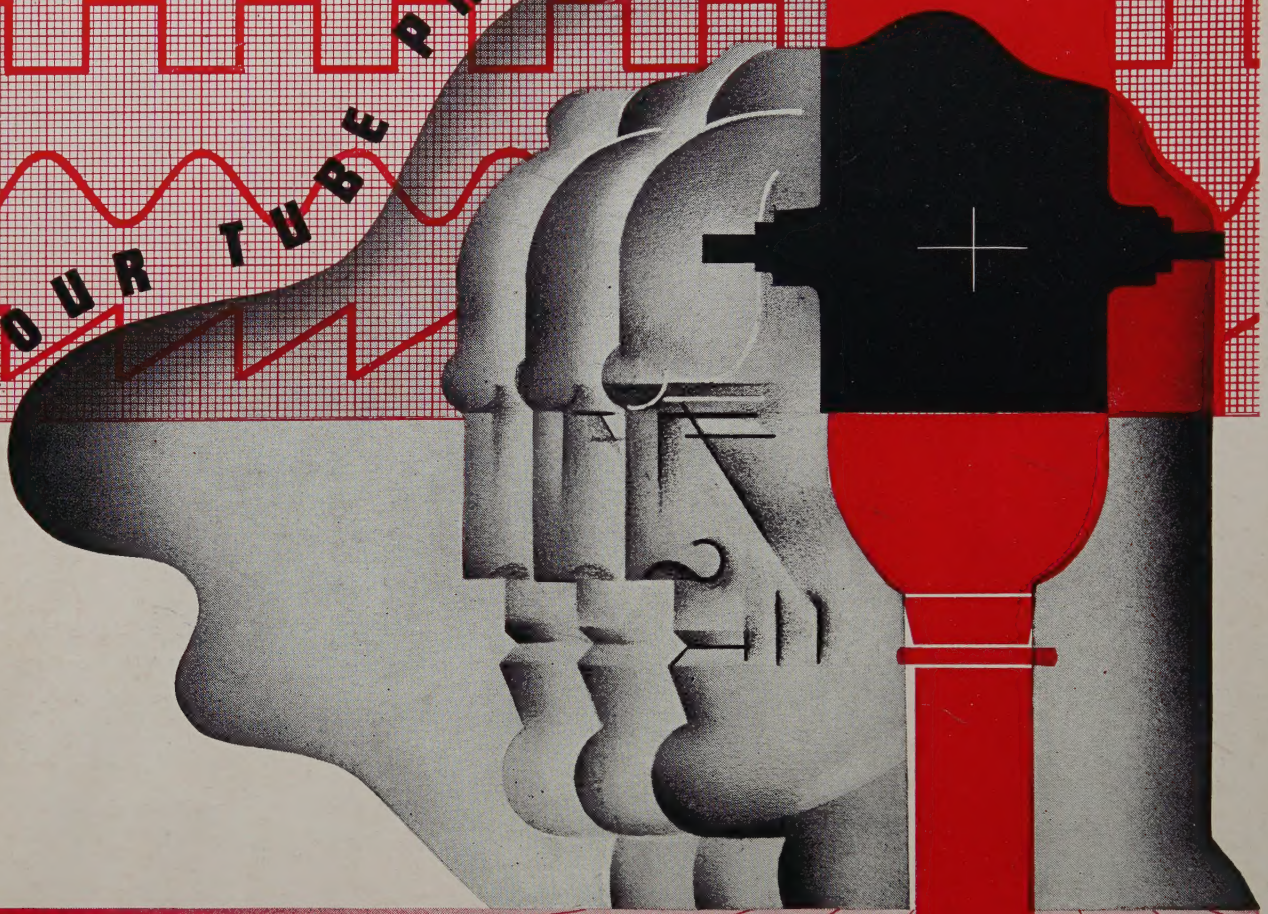

FOR DECADES AMPEREX RESEARCH PROGRAMS, CREATIVE ENGINEERING AND PRECISION MANUFACTURE HAVE BEEN SUCCESSFUL IN TRANSLATING THE TUBE HOPES AND NEEDS OF EQUIPMENT DESIGNERS INTO ACTUAL TUBES FOR PROJECTED SOCKETS.

Perhaps it is getting more power into smaller space for induction or dielectric heating • or higher power at higher frequencies for communications • or unusual ruggedness for operation under unusual conditions • or a marriage of seemingly antagonistic characteristics • or any one of a host of other "bugs".

ASK AMPEREX TO BRING ITS LONG EXPERIENCE TO BEAR ON YOUR TUBE QUESTIONS . . . YOUR ONLY OBLIGATION IS A STATEMENT OF YOUR PROBLEM.

AMPEREX

POWER TUBE SPECIALISTS SINCE 1925

COMMUNICATION
RECTIFICATION
INDUSTRIAL
ELECTRO-MEDICAL
SPECIAL PURPOSE

AMPEREX
ELECTRONIC CORPORATION

25 WASHINGTON STREET, BROOKLYN 1, N. Y., CABLES: "ARLAB"

In Canada and Newfoundland: ROGERS MAJESTIC LIMITED, 622 Fleet Street West, Toronto 2B, Canada

BOARD OF DIRECTORS, 1946

Frederick B. Llewellyn
President

Edmond M. Deloraine
Vice-President

William C. White
Treasurer

Haraden Pratt
Secretary

Alfred N. Goldsmith
Editor

Hubert M. Turner
Senior Past President

William L. Everitt
Junior Past President

1944–1946
Raymond F. Guy
Lawrence C. F. Horle

1945–1947
Stuart L. Bailey
Keith Henney
Benjamin E. Shackelford

1946–1948
Walter R. G. Baker
Virgil M. Graham
Donald B. Sinclair

1946
Ralph A. Hackbusch
Frederick R. Lack
George T. Royden
William O. Swinyard
Wilbur L. Webb
Edward M. Webster

●

Harold R. Zeamans
General Counsel

George W. Bailey
Executive Secretary

William H. Crew
Assistant Secretary

●

BOARD OF EDITORS
Alfred N. Goldsmith
Chairman

●

PAPERS COMMITTEE
Frederick B. Llewellyn
Chairman

●

PAPERS PROCUREMENT COMMITTEE
Dorman D. Israel
General Chairman

Edward T. Dickey
Vice General Chairman

●

PROCEEDINGS OF THE I.R.E. AND WAVES AND ELECTRONS

Published Monthly in two sections by

The Institute of Radio Engineers, Inc.

VOLUME 34 — *March, 1946* — NUMBER 3

SECTION I—PROCEEDINGS OF THE I.R.E. SECTION

Continuing Service ..... F. H. R. Pounsett 96 P

Reflex-Klystron Oscillators ... Edward Leonard Ginzton and Arthur E. Harrison 97 P

The Transmission of a Frequency-Modulated Wave Through a Network ..... Walter J. Frantz 114 P

Analysis of a Resistance-Capacitance Parallel-T Network and Applications ..... A. E. Hastings 126 P

The Application of Modulation-Frequency Feedback to Signal Detectors ..... Geoffrey Builder 130 P

The Ideal Low-Pass Filter in the form of a Dispersionless Lag Line ..... Marcel J. E. Golay 138 P

Applications of Matrix Algebra to Filter Theory ..... Paul I. Richards 145 P

Discussion on "Electron Transit Time in Time-Varying Fields," by Arthur B. Bronwell ..... L. A. Ware, H. B. Phillips, and Arthur B. Bronwell 151 P

Contributors to the PROCEEDINGS OF THE I.R.E. SECTION ..... 152 P

Advertising Index ..... 86 A

SECTION II—WAVES AND ELECTRONS SECTION FOLLOWS AFTER PAGE 152 P.

EDITORIAL DEPARTMENT

Alfred N. Goldsmith
Editor

Helen M. Stote
Publications Manager

Ray D. Rettenmeyer
Technical Editor

Winifred Carrière
Assistant Editor

William C. Copp
Advertising Manager

Lillian Petranek
Assistant Advertising Manager

Responsibility for the contents of papers published in the PROCEEDINGS OF THE I.R.E. and WAVES AND ELECTRONS rests upon the authors.

Statements made in papers are not binding on the Institute or its members.

MEMBER AUDIT BUREAU OF CIRCULATIONS

Changes of address (with advance notice of fifteen days) and communications regarding subscriptions and payments should be mailed to the Secretary of the Institute, at 450 Ahnaip St., Menasha, Wisconsin or 330 West 42nd Street, New York 18, N. Y. All rights of republication, including translation into foreign languages, are reserved by the Institute. Abstracts of papers, with mention of their source, may be printed. Requests for republication privileges should be addressed to The Institute of Radio Engineers.

Copyright, 1946, by The Institute of Radio Engineers, Inc.

The Chairmen of the Sections of the Institute have been invited to express to the membership, in such editorial form as they may desire, views which they believe will be contributory to the future of the engineering profession. Thoughtful analyses and forward-looking discussions of this nature have been received. There follows, accordingly, a statement from the Chairman of the Toronto Section of the Institute.

The Editor

Continuing Service

F. H. R. Pounsett

Due credit has been reflected on our membership for its technical effort during the war. However, we must avoid becoming too embroiled in the present confusion of reconversion of facilities, men, and minds, and missing opportunities for further service: a service which, if properly performed, will be of lasting benefit to our industry, our Institute, and incidentally ourselves.

It is well, at a turning point like this, to look back at the fundamental concepts of our charter. What are the objects of our Institute? As stated in the Constitution; "Its aims shall include the advancement of the theory and practice of radio, and allied branches of engineering and of the related arts and sciences, their application to human needs, and the maintenance of a high professional standing among its members."

Headquarters, backed by the splendid response to the Building-Fund Campaign, and the recently acquired executive assistance, is taking care of the general realigning of our affairs to cope with present conditions of expansion and broadening of interest. The Sections must, in turn, organize to serve their particular areas as required by local conditions and plan to make The Institute of Radio Engineers of maximum benefit to the membership and the community. The avenues along which the Toronto Section has been extending its activities during the past eighteen months are briefly outlined here in the hope that they may be of interest or possibly of benefit to members elsewhere.

Education

Meetings are arranged to acquaint members and guests not only with the interesting war developments but also with the industrially useful phases of wartime developments with which many have lost touch during the past six years because of the pressure of their particular jobs.

Many members can exert considerable influence towards adjusting the curricula of engineering schools and rehabilitation schools in line with the present requirements of industry. Surplus test equipment and prototypes from war plants can be well directed to the laboratories of these schools.

Rehabilitation

Returned Service technical personnel, not necessarily members, are invited to Section meetings. Group contact, as well as personal counseling can be helpful to these men, especially those who were not in technical work before the war but, because of their war experience, are now seriously considering continuing it as a vocation. Many members are serving on advisory councils of rehabilitation schools which offer electronic courses.

Canadian Radio Technical Planning Board

This needs no elucidation. Several members have taken an active part on the various panels and committees as representatives of the I.R.E., particularly recommended by the Section.

Regional Organization

Our Section executive has played an active part in organizing the Canadian Council of the I.R.E. The Regional Scheme, recently proposed at Headquarters will offer all Sections a similar opportunity to co-operate with others in their territories to their mutual advantage.

The Profession

Members have been encouraged to upgrade their membership wherever possible. They have also been encouraged to join the Provincial Association of Professional Engineers (the registering body).

By intermembership in the Provincial Association and the active participation of the Section with the Canadian Council of the I.R.E. in the formation of the Canadian Council of Professional Engineers and Scientists (CCPES), the relationship of the employee engineer to his employer and to organized labor with regard to collective bargaining has been beneficially clarified on a Dominion-wide basis.

Reflex-Klystron Oscillators*

EDWARD LEONARD GINZTON†, ASSOCIATE, I.R.E., AND
ARTHUR E. HARRISON†, SENIOR MEMBER, I.R.E.

Summary—**A comprehensive analysis of reflex klystrons is developed by considering the electrons as particles acted upon by forces which modify their motion. The analysis is similar to earlier explanations of electron bunching in a field-free drift space and predicts a similar current distribution when bunching takes place in a reflecting field. The effect of the bunched electron beam is treated qualitatively by considering the effect of the beam admittance upon a simple equivalent circuit. A quantitative mathematical analysis based upon oscillator theory is also derived and the results are presented in a series of universal curves which are used to explain the operating characteristics of these tubes. Power output, efficiency, starting current, electronic tuning, and modulation properties are discussed. Some general remarks on reflex-oscillator design considerations are also included.**

Introduction

REFLEX-klystron oscillators are an important member of an extensive family of velocity-modulation tubes invented independently by R. H. Varian and W. W. Hansen at Stanford University, W. C. Hahn and G. F. Metcalf at Schenectady, and O. Heil in Germany. Velocity-modulation tubes are now quite generally known as klystrons, and perform the same functions at frequencies in the microwave region that triodes and pentodes do at lower frequencies. The mechanism of energy conversion is different, but analogies between klystrons and the electrical circuits used with conventional tubes are often useful. Klystrons with one or more resonators are used as oscillators, and multiresonator klystrons often replace conventional vacuum tubes for other applications.

A reflex klystron utilizes a single resonator, and obtains feedback by reflecting the electron beam so that it passes through the resonator a second time. This type of oscillator was described briefly by Hahn and Metcalf,[1] and has been discussed in greater detail in other papers.[2–4] The operation of these tubes can be explained by a ballistic or kinematic analysis; i.e., the electrons may be considered as particles which follow Newton's laws of motion. An understanding of the application of such a kinematic analysis to the principles of operation of the ordinary two-resonator klystron will be assumed. These principles have been presented in papers by Varian[5] and Webster,[6,7] and a similar analysis will be developed for the reflex-klystron oscillator.

The analysis has been subdivided into two parts. The first section derives the transit-time relationships for the reflex type of klystron from the laws of motion. Then these relations are expanded to explain electron bunching, and the similarity between reflection-field bunching and bunching in a field-free drift space is shown. A second section applies these relationships to a derivation of the efficiency, power output, and electronic tuning of a reflex-klystron oscillator. The dependence of these characteristics on the beam current, beam voltage, reflector voltage, load, and other klystron design factors will be shown.

Operating Principles of a Reflex Klystron

A simplified drawing of a reflex klystron is shown in Fig. 1. The tube is a figure of revolution about the axis AA. The cathode surface K provides a source of electrons when it is indirectly heated by F. The electrons are accelerated by the voltage E_0, which is known as the beam voltage, or as the acceleration voltage because it determines the velocity which the electrons have acquired when they reach the anode plane. The emission current is controlled by the voltage E_g which is applied to the grid G. The cylindrical portion of the control-grid structure acts as a focusing element and gives a collimated beam which continues along the axis of the tube past the anode plane. In many klystron designs, the grid is not used and this electrode is only a focusing

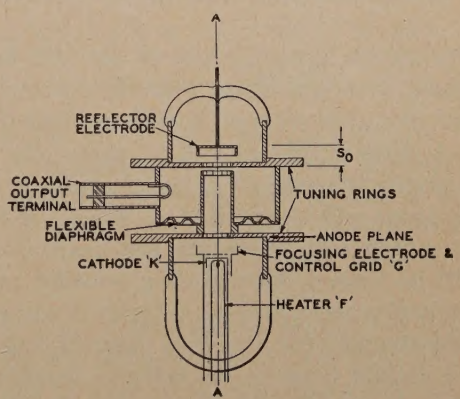

Fig. 1—Cross-section view of a reflex klystron.

* Decimal classification: R355.9. Original manuscript received by the Institute, August 3, 1945.

† Sperry Gyroscope Company, Inc., Garden City, Long Island, N. Y.

[1] W. C. Hahn and G. F. Metcalf, "Velocity-modulated tubes," PROC. I.R.E., vol. 27, pp. 106–117; February, 1939.

[2] A. E. Harrison, "Klystron Technical Manual," Sperry Gyroscope Company, Inc., Great Neck, Long Island, New York, 1944.

[3] A. E. Harrison, "Kinematics of reflection oscillators," *Jour. Appl. Phys.*, vol. 15, pp. 709–711; October, 1944.

[4] J. R. Pierce, "Reflex oscillators," PROC. I.R.E., vol. 33, pp. 112–118; February, 1945.

[5] R. H. Varian and S. F. Varian, "A high-frequency oscillator and amplifier," *Jour. Appl. Phys.*, vol. 10, pp. 321–327; May, 1939.

[6] D. L. Webster, "Cathode-ray bunching," *Jour. Appl. Phys.*, vol. 10, pp. 501–508; July, 1939.

[7] D. L. Webster, "The theory of klystron oscillations," *Jour. Appl. Phys.*, vol. 10, pp. 864–872; December, 1939.

element. Fig. 2 shows the reflex klystron connected to the proper power supplies. The standard diagram for velocity-modulation tubes has been used, and the operating voltages have been labeled with the designations which will be used throughout this discussion.

This electron-gun structure is quite similar to a triode tube; it has a cathode, a control grid, and an anode. In a klystron, however, the electron gun is merely the source of an electron beam and the radio-frequency portion of the klystron is independent of the electron source.

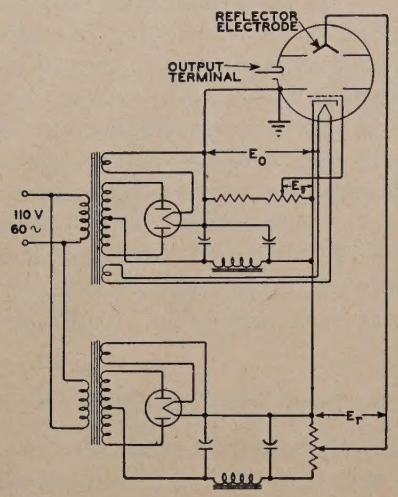

Fig. 2—Circuit diagram for a reflex oscillator and power supply.

The beam travels along the axis of the tube beyond the anode plane with a uniform velocity corresponding to E_0, the acceleration voltage, until it reaches the resonator gap. A radio-frequency voltage across the resonator gap will modify the velocity of the electrons in the beam. Some electrons will be speeded up when the field has a direction which will accelerate the beam. Other electrons will be slowed down during another part of the radio-frequency cycle, and the velocity of some electrons will not be changed because they pass the gap when the resonator voltage is zero. The velocity variation will be assumed to be small, and the average velocity of the electrons in the beam will be identical to the velocity corresponding to the acceleration voltage, since an equal number of electrons will be slowed down and speeded up during one radio-frequency cycle.

Beyond the resonator gap, the electrons encounter a retarding electric field produced by the potential between the reflector and the anode (E_0+E_r). This reflecting field brings the electrons to rest and returns them to the cavity resonator. The shape of the reflector electrode is designed to preserve the focus of the beam. The beam current is constant when the beam leaves the resonator gap, but electron bunching takes place while the electrons are in the reflection space, and the beam is density modulated when it returns to the cavity resonator.

If space-charge effects and the focusing action of the reflector shape are neglected, the bunching action is analogous to the motion of objects in a gravitational field.[3] An Applegate diagram, in Fig. 3, is a convenient method of illustrating the bunching action. This diagram represents the resonator-gap voltage as a function of time, and plots the position in the reflection space of a number of electrons which pass the resonator gap at selected intervals during a complete cycle. The opposite action of the radio-frequency field on the electrons leaving the resonator and those returning to the resonator after bunching has been shown on the diagram.

An electron which has been speeded up by the action of the radio-frequency field will travel farther into the reflecting field and will take longer than the average

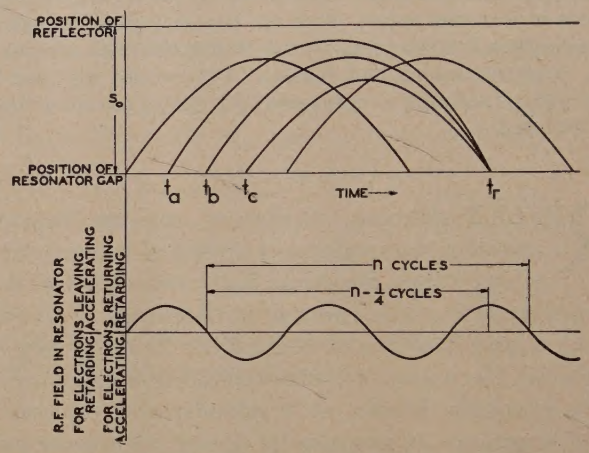

Fig. 3—Applegate diagram for a reflex-klystron oscillator.

time to return to the resonator. This behavior is similar to throwing a ball into the air; the harder the ball is thrown, the longer it takes to return to the ground. Reference to Fig. 3 will show that an electron which passes the resonator gap early in the cycle at time t_a is accelerated and requires a longer time to return than an electron leaving at time t_b when the radio-frequency field is zero. The electrons which leave at time t_c later in the cycle require less than the average transit time and all of these electrons return to the resonator in a bunch at time t_r. Bunching of the electron beam is the result, and the uniform flow of beam current is converted into an equivalent direct current with a superimposed alternating component.

The arrival time t_r of a group of electrons returning to the resonator depends upon the physical dimensions of the klystron, and also depends upon the acceleration voltage and the reflector voltage. In general, the transit time for the electron with average velocity, leaving at time t_b, may correspond to any number of cycles of the radio-frequency field, and this number need not be an integer. But in order to sustain oscillations, the electron bunch must arrive during the time when the radio frequency is retarding the returning electrons, so

that the electron velocity is reduced and some of the kinetic energy of the electrons is transferred into electromagnetic energy in the cavity-resonator field.

The electron which is to become the center of the bunch leaves at the time t_b when the radio-frequency voltage is zero and changing from acceleration to deceleration. At an integral number of cycles later, the radio-frequency voltage will again be zero, but for the returning electron, the field will be changing from deceleration to acceleration. This time is indicated by n cycles in Fig. 3. Since a maximum retarding field is required for maximum energy transfer from the bunched electron beam, the transit time for an electron which enters the reflecting field with average velocity must correspond to one-quarter cycle less than an integral number of cycles. This transit-time requirement may be verified by inspection of Fig. 3.

Most of the electrons are collected by the metal walls of the tube after they have given up energy to the resonator field. Other electrons may have been lost by interception by the grid structures. A few electrons may survive these chances of getting collected and will be decelerated near the cathode surface, then reaccelerated with the newly emitted electrons. Upon re-entering the reflection space, these electrons will behave differently from the electrons which are going through the round-trip cycle for the first time. These electrons which make multiple transits may produce undesirable effects, but in most cases the effect of these electrons may be neglected. More important factors, such as space-charge debunching forces, will be neglected in order to simplify the analysis. *This theory is not intended for designing klystrons, but to help in understanding many of the phenomena which occur.*

Transit-Time Relationships in the Reflection Space

It was mentioned previously that the electrons which pass the resonator gap when the radio-frequency voltage is zero enter the reflecting field without any change in velocity, and are defined as electrons with average velocity. Electrons which pass the resonator gap at a time t_b (see Fig. 3) when the radio-frequency field is changing from accleration to deceleration, become the center of the bunch. The electrons in the bunch have different velocities, and these velocities are continually changing during the time the electrons are in the reflection space; however, it is convenient to consider that the bunch moves as a unit along a path determined by the electron which is to become the center of the bunch. Note that the lines in Fig. 3 representing electrons leaving at times t_a, t_b, and t_c appear to converge about the center of the bunch.

A brief review of electron ballistics will derive the equations which are useful in determining the relationships between the transit time and the tube-design parameters. The calculation of the transit time from the tube voltages and the reflector-electrode spacing will not be accurate because the effect of the nonuniform field and the effect of space charge have been neglected. Although the effects of space charge are quite important, the assumption simplifies the analysis considerably, and the result is quite useful.

In the derivations which follow, the terminology will be defined as it is introduced. In addition, a glossary of symbols is included in an appendix. The average electron velocity v_0 is determined by the acceleration voltage E_0, and the relation may be obtained from the fact that the kinetic energy gained by an electron of mass m and charge e is equal to the potential energy which accelerates the electron. This relation may be stated

$$1/2(mv_0^2) = E_0 e. \tag{1}$$

Equation (1) is then rewritten in the form

$$v_0 = \sqrt{\frac{2e}{m}E_0}. \tag{2}$$

Other laws of motion of particles may be used to determine the transit time. If the deceleration is denoted by a, then the position of a particle as a function of time is given by

$$s = v_0 t - 1/2(at^2). \tag{3}$$

When t is equal to the average transit time T_0 the electron has returned to the resonator, the electron velocity is again v_0, but in the opposite direction, and s is equal to zero; i.e.,

$$0 = v_0 T_0 - 1/2(aT_0^2). \tag{4}$$

There are two solutions to (4). T_0 equal to zero corresponds to an electron which has not traversed the reflection space, and is disregarded. The other solution is

$$T_0 = \frac{2v_0}{a}. \tag{5}$$

The deceleration a may be evaluated from the familiar equation for the force acting on a particle. This force is given by the product of the charge on the electron and the gradient of the potential between the anode and the reflector electrode. If the reflector field is assumed to be uniform, the gradient is simply the sum of the voltages on the reflector electrode divided by s_0, the reflector spacing. Therefore,

$$F = ma - e\frac{E_0 + E_r}{s_0}. \tag{6}$$

Substitution of (6) and (2) in (5) gives

$$T_0 = \frac{2v_0}{\frac{e}{m}\frac{E_0 + E_r}{s_0}} = 4s_0\frac{\sqrt{\frac{m}{2e}E_0}}{E_0 + E_r} \tag{7}$$

for the average transit time.

It is usually more convenient to express the transit time in terms of a number of oscillation cycles rather than as a time interval. This equivalent number of cycles will be designated N, and is defined by

$$N = fT_0 \tag{8}$$

where f is the frequency of oscillation. Equation (7) may therefore be written

$$N = 4fs_0 \frac{\sqrt{\frac{m}{2e}E_0}}{E_0 + E_r}. \tag{9}$$

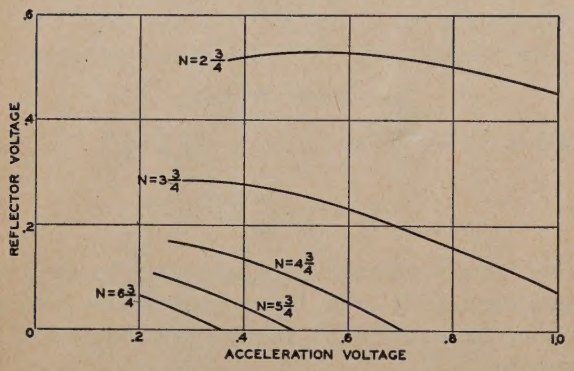

Fig. 4—Family of curves showing voltage modes in a reflex oscillator.

If oscillation is to be at maximum strength, the number of cycles during the transit time in the reflection space must satisfy the relation mentioned in the discussion of Fig. 3; i.e.,

$$N = n - 1/4 \tag{10}$$

where n is any integer greater than zero. Oscillation at the same frequency will occur for a number of values of N, and each value of N may be provided by the proper choice of the acceleration voltage and the reflector voltage. A series of curves showing the reflector voltage required to give constant frequency for any value of acceleration voltage is shown in Fig. 4. Each curve represents a different value of N. The value of N may be estimated from the frequency, reflector spacing, and voltages involved. These transit times are an important factor in the behavior of reflex klystrons, and the importance of transit time will be discussed in greater detail in the sections which follow. In practice, transit time corresponding to values of N between $1\frac{3}{4}$ and $10\frac{3}{4}$ cycles are typical.

Electron-Bunching Relationships

It is obvious that electron bunching must occur in a reflex klystron because the velocity variation introduced by the resonator voltage produces a variation of the transit times of electrons which pass the resonator gap at different times during a cycle. This variation of transit time may be expected from (5), which may be rewritten in terms of a varying velocity instead of the average velocity, and becomes

$$T = \frac{2v}{a} \tag{11}$$

when T and v are varying quantities. The current distribution in the bunched beam is similar to the bunching in a two-resonator klystron, but the manner in which the electrons become grouped is different and there is a phase difference of 180 degrees between the two types of bunching.

These differences between reflection-field bunching and field-free bunching are introduced because the transit time is proportional to the electron velocity in a reflex klystron; while the transit time in the field-free drift space between the resonators in a two-resonator klystron is inversely proportional to the velocity. As a result, the electron bunch in a reflex klystron is formed around the electron which passed the resonator gap when the radio-frequency voltage was changing from acceleration to decleration. In contrast, the bunch in a two-resonator klystron forms around the electron which passed the input resonator gap when the radio-frequency field was changing from deceleration to acceleration.[3]

The existence of a field-free bunching space in addition to the reflection space requires a modification of this analysis. A discussion of this effect is given in a number of references[1–3] and will not be repeated here.

An analysis of the bunching process in a reflex klystron may be made, following the method used by Webster[6] for the two-resonator type of klystron. Negligible transit time across the resonator gap will be assumed in the preliminary analysis, and the factors which must be modified when this assumption is invalid will be discussed in a later section.

The electrons approach the resonator gap with average velocity v_0, which is determined by the acceleration voltage E_0 as shown in (2). The velocity of the electrons will be modified by the radio-frequency voltage at the resonator gap, and after passing the gap the velocity will be

$$v = \sqrt{\frac{2e}{m}}\sqrt{E_0 + E_1 \sin \omega t_1} \tag{12}$$

where E_1 is the peak value of the radio-frequency voltage at the resonator gap, ω is the angular frequency and equal to $2\pi f$, and t_1 is the time required for an electron to pass the resonator gap. The transit time of an electron will be given by (11), and may be rewritten in a form similar to (7).

$$T = 4s_0 \frac{\sqrt{\frac{m}{2e}E_0}}{E_0 + E_r}\sqrt{1 + \frac{E_1}{E_0}\sin \omega t_1}. \tag{13}$$

Equation (7) may be substituted in (13) to give

$$T = T_0 \sqrt{1 + \frac{E_1}{E_0} \sin \omega t_1}. \tag{13a}$$

When the ratio of E_1/E_0 is small, an approximate form of (13a) may be used

$$T = T_0 \left(1 + \frac{E_1}{2E_0} \sin \omega t_1\right). \tag{14}$$

Returning electrons will arrive at the resonator gap at a time t_2, which will be the sum of the transit time (T) and the departure time (t_1).

$$t_2 = t_1 + T_0 \left(1 + \frac{E_1}{2E_0} \sin \omega t_1\right). \tag{15}$$

The number of electrons which return to the resonator during a time interval dt_2 will be equal to the product of the instantaneous beam current in the reverse direction

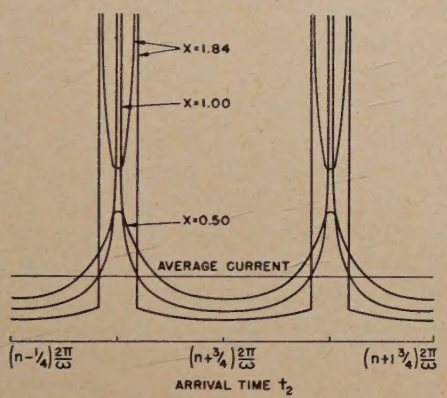

Fig. 5—Instantaneous beam current. Two complete cycles are shown and three values of the bunching parameter are represented.

I_2 and the time interval dt_2. This same number of electrons originally passed the resonator gap during an interval dt_1, when the beam current in the forward direction was equal to I_0, the direct beam current. If these expressions for the number of electrons are equated,

$$I_2 dt_2 = I_0 dt_1 \tag{16}$$

and the instantaneous bunched current is given by

$$I_2 = I_0 dt_1/dt_2. \tag{17}$$

Differentiating both sides of (15) gives

$$dt_2 = dt_1 \left(1 + \omega T_0 \frac{E_1}{2E_0} \cos \omega t_1\right) \tag{18}$$

or

$$dt_2 = dt_1 \left(1 + \pi f T_0 \frac{E_1}{E_0} \cos \omega t_1\right). \tag{18a}$$

Substituting (8) in (18a) gives

$$dt_2 = dt_1 \left(1 + \pi N \frac{E_1}{E_0} \cos \omega t_1\right) \tag{18b}$$

which may be rewritten

$$dt_2 = dt_1(1 + x \cos \omega t_1). \tag{18c}$$

The quantity x is known as the bunching parameter, and is defined by

$$x = \pi N \frac{E_1}{E_0}. \tag{19}$$

Other expressions for the bunching parameter may be obtained by substitution in (19), but these expressions will not be similar to the other equations for the bunching parameter when bunching occurs in a field-free drift space.

Substituting (18c) in (17) gives

$$I_2 = \frac{I_0}{1 + x \cos \omega t_1}. \tag{20}$$

Equation (20) is identical in form to the expression for the bunched current in a double-resonator klystron.[6]

The equations for the instantaneous current express this current as a function of t_1, the departure time of the electrons when they enter the reflecting field. It is more desirable to know the relation between the instantaneous current and t_2, the arrival time of the returning electrons. This relationship is easily obtained if a curve of t_1 versus t_2 is available, and a family of such curves is illustrated in Fig. 5 for several different values of the bunching parameter x. This graphical representation of the relationship is necessary because (15) cannot be solved explicitly for t_1. Rewriting (15) in terms of the bunching parameter x gives a form which is convenient for computation of the curves in Fig. 5. Equation (15) then becomes

$$t_2 = t_1 + T_0 + \frac{x}{\omega} \sin \omega t_1. \tag{21}$$

Note that the slope of the curves in Fig. 5 may become negative when the bunching parameter is greater than unity. This negative slope corresponds to a negative value of I_2 indicated by (20) when x is greater than unity. The beam current never becomes negative; this sign merely means that electrons departing at a later time return before electrons which left earlier but traveled farther into the reflecting field. Since electrons leaving at three different times may arrive simultaneously, the beam current is the sum of the absolute magnitudes of the values obtained from (20) for the three values of t_1. Additional discussion of this point, based on an analysis of bunching in a field-free drift space, has been published.[8]

Curves of instantaneous current, corresponding to the

[8] D. L. Webster, "Velocity modulation currents," *Jour. Appl. Phys.*, vol. 13, pp. 786–787; December, 1942.

t_1 versus t_2 curves in Fig. 5, are shown in Fig. 6. The current peaks when the bunching parameter is unity, or greater, are quite large, but are not infinite if the transit time in the resonator gap is finite.[9,10] However, it is

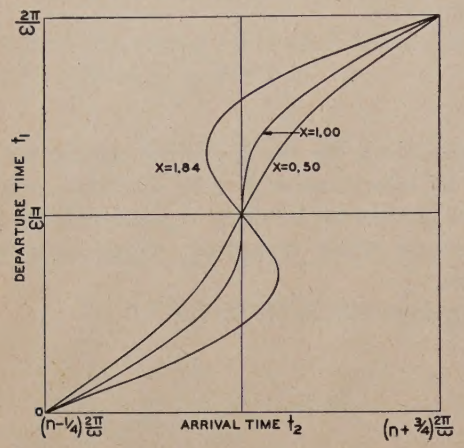

Fig. 6—Electron-arrival-time curves for three values of the bunching parameter.

convenient to treat the gap length as infinitesimal, and correction factors which can be applied when the transit time through the gap is appreciable will be given in the next section.

Since the instantaneous beam current is identical to that given by Webster[6] for the field-free case, the current may be expressed by a Fourier series with coefficients which are Bessel functions of the first kind.

$$I_2 = I_0[1 + 2J_1(x)\sin(\omega t_2 - 2\pi N) + 2J_2(2x)\sin 2(\omega t_2 - 2\pi N) + \cdots + 2J_n(nx)\sin n(\omega t_2 - 2\pi N)]. \quad (22)$$

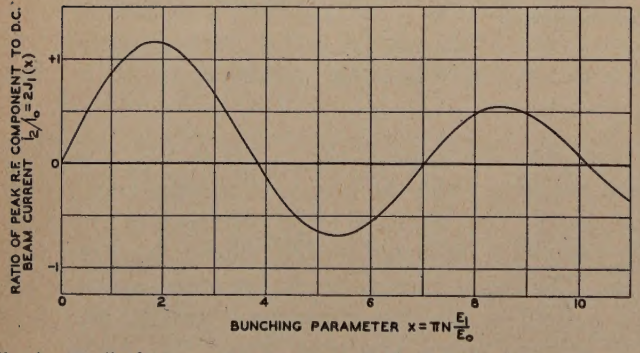

Fig. 7—Radio-frequency component of the bunched beam current.

Only the second term is of particular interest in an oscillator, and the fundamental component of the radio-frequency current in the beam, which will be designated i_2, is given by

$$i_2 = 2I_0J_1(x)\sin(\omega t_2 - 2\pi N). \quad (23)$$

[9] L. J. Black and P. L. Morton, "Current and power in velocity-modulation tubes," PROC. I.R.E., vol. 32, pp. 477–482; August, 1944.

[10] A. E. Harrison, "Graphical methods for analysis of velocity-modulation bunching," PROC. I.R.E., vol. 33, pp. 20–33; January, 1945.

The higher harmonics are unimportant because reflex klystrons are designed to operate with a high effective Q.

Fig. 7 shows the peak value of the radio-frequency component of the bunched beam current as a function of the bunching parameter. The peak value has been divided by I_0 so that the ordinates of the curve are equal to $2J_1(x)$. This Bessel function output curve is characteristic of klystron tubes, and may be considered analogous to the plate-current versus grid-voltage charteristic of conventional tubes.

Transit-Time Effects in the Resonant Cavity

The previous discussion has ignored the effect of the transit time of the electrons in the resonator gap. If the electron crosses the gap in a small fraction of an oscillation cycle, then the change in kinetic energy will be determined by the potential difference across the gap at that instant. However, if an electron requires a full cycle to traverse the resonator gap, the electron will be accelerated during half of the cycle and decelerated during the remainder of the cycle. As a result, the net change in kinetic energy will be zero if the gap voltage is very small compared to the beam voltage.

This effect may be expressed in terms of a "beam coupling coefficient" of the gap. The expression for the bunching parameter in (19) must be modified by this beam coupling coefficient β when the transit time across the resonator gap is an appreciable fraction of a cycle, and

$$x = \beta\pi N \frac{E_1}{E_0} \quad (24)$$

gives the correct value for the bunching parameter. Equations (24) and (19) become identical when β has a value of unity.

It is necessary to know the transit time across the gap in order to evaluate β. If the distance is d, and the electron velocity has the average value v_0, then the transit time is d/v_0. The transit angle δ is given by

$$\delta = 2\pi f d/v_0. \quad (25)$$

If the averaging process mentioned in the previous paragraph is performed, the value β may be shown to be

$$\beta = \frac{\sin \delta/2}{\delta/2}. \quad (26)$$

In practice, β is always less than unity, but in many cases it is convenient to assume it is equal to unity. Since this coefficient appears in most of the equations which describe the behavior of reflex-klystron oscillators, it will be referred to frequently in the next section on oscillator theory, which will utilize the fundamental principles derived here to explain the electrical characteristics of these tubes.

General Theory of Oscillators

The basic principles of electron bunching discussed in the preceding sections can be used to derive the typical electrical characteristics of reflex-klystron oscillators. The analysis is quite similar to the analysis of oscillators in the more familiar radio-frequency region. Certain outstanding differences will be apparent; the most important is the dependence of the frequency of oscillation on the input voltages. These differences are the result of the dependence of the bunching action on transit time, and emphasize the fact that analogies to conventional vacuum tubes cannot always be used to describe the behavior of klystrons, although some of the concepts and terminology are equally useful in discussion of velocity-modulation tubes.

There are several methods which might be used to analyze the operation of a reflex-klystron oscillator. All of these methods are essentially the same and merely represent differing viewpoints in approaching the problem. Pierce[4] has described a method which equates the admittance of the resonator of a reflex oscillator and the transadmittance of the bunched electron beam. A variation of this method, using impedances instead of admittances, was used in an analysis of double-resonator klystron oscillators.[11] This variation of the analysis is desirable for a double-resonator klystron oscillator because the relation between the output current and input voltage in tightly coupled tuned circuits is usually given in the form of a transfer impedance. A reflex-klystron oscillator is much simpler to analyze because a single resonator is used.

The effect of the reflected beam in a reflex-klystron oscillator can be explained quite easily by assuming that the radio-frequency component of the bunched beam introduces an admittance Y_2 in parallel with the resonant circuit. This method reduces the analysis to a simple circuit problem in which a change in the value of Y_2 may change the resonant frequency or losses in the circuit. The results are correct; in fact, it can be shown that the various methods of analysis are mathematically identical. The advantage of the method to be used here is primarily convenient in visualizing the problem, since the effect of varying components in a circuit is often more easily understood than the effect of varying parameters in an equation.

The Equivalent Circuit of a Reflex-Klystron Oscillator

An equivalent circuit for a reflex-klystron oscillator based on the method outlined above, is shown in Fig. 8. The cavity resonator and its coupled load are represented by the parallel resistance-inductance-capacitance circuit. The copper losses and other resonator losses such as loading caused by the beam itself or secondary electrons, are represented by an equivalent shunt resistance R_S, and the coupled load or output circuit considered as another parallel resistance R_L. Then the effective resistance R_{SL} would be given by the expression for two resistances in parallel

$$R_{SL} = \frac{R_S R_L}{R_S + R_L}. \tag{27}$$

The equivalent capacitance C represents the capacitance of the resonator gap. The value of this capacitance can be estimated to a satisfactory approximation from the formula for a parallel-plate capacitor, using the area and spacing of the resonator grids forming the gap. The value of the equivalent inductance L is chosen to make the resonant frequency of the equivalent circuit equal to the resonant frequency of the cavity.

If the reflex klystron is oscillating, or if energy is coupled into the cavity resonator from an external source, then a voltage will exist across the resonator gap. This voltage is represented by the voltage E across the capacitance C in the equivalent diagram in Fig. 8, and the value of E is given by

$$E = E_1 \sin \omega t \tag{28}$$

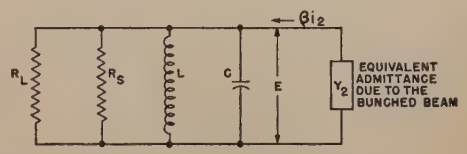

Fig. 8—Equivalent circuit for a reflex-klystron oscillator.

where E_1 is the peak value of the voltage across the resonator gap, and ω and t represent the angular frequency of oscillation and time.

The bunching action produces a radio-frequency current i_2 which depends upon the beam current I_0 and the bunching parameter x, as shown in (23).

$$i_2 = 2I_0 J_1(x) \sin (\omega t - 2\pi N). \tag{23}$$

N represents the number of oscillation cycles during the time an electron is in the reflection space. A current βi_2 is shown flowing out of the "fictitious" admittance Y_2, which represents the effect of the bunched beam current in the equivalent diagram. This direction for the current is chosen because Y_2 represents the source of power. The beam coupling coefficient β is introduced in order to include the effect of the decreased energy transfer from the beam to the resonator when the gap transit time is large. This factor must be included in each step of the derivation in which it should appear; but a value of unity, corresponding to negligible-gap transit time, will be assumed in most cases in order to simplify the discussion of this analysis.

[11] A. E. Harrison, "Klystron oscillators," *Electronics*, vol. 17, pp. 100–107; November, 1944.

Admittances are used in this discussion because admittances can be added when considering parallel circuits. Equation (27), expressed in the form of the sum of two conductances (the real part of an admittance), would be written

$$\frac{1}{R_{SL}} = \frac{1}{R_S} + \frac{1}{R_L}. \tag{29}$$

The total admittance of the resonator Y_S would include the susceptance terms for the inductance and capacitance as well as the conductance terms in (29).

$$Y_S = \frac{1}{R_S} + \frac{1}{R_L} - \frac{j}{\omega L} + j\omega C. \tag{30}$$

This form will be quite convenient in the analysis of a reflex oscillator because real and imaginary terms may be considered separately.

An evaluation of the admittance Y_2 which is added to the resonator admittance may be obtained from the fact that a voltage E must cause a current βi_2 to flow. The magnitude of Y_2 will be determined by the ratio of the peak value of βi_2 and the peak voltage E_1.

$$Y_2 = \frac{2\beta I_0 J_1(x)}{E_1}. \tag{31}$$

The phase of Y_2 is determined by the transit time in the reflection field. If the transit time corresponds to $(n-\frac{1}{4})$ cycles, where n is an integer, then the electrons in the bunch will be retarded, and the beam will transfer energy to the radio-frequency field in the resonator. This relation was explained in the discussion of Fig. 3. Under these conditions Y_2 will be a pure negative conductance. A transit time of $(n+\frac{1}{4})$ cycles corresponds to a transfer of energy from the radio-frequency field to the electron beam, and in this case Y_2 is a positive conductance; i.e., the beam represents an additional loss in the circuit.

Other values of transit time cause Y_2 to be complex since the radio-frequency component of the bunched beam current will not be in phase with the resonator voltage. The phase angle of i_2 will be represented by ϕ, and ϕ will be considered zero when the transit time in the reflection field corresponds to $(n-\frac{1}{4})$ cycles. The expression for i_2 in (23) may be rewritten

$$i_2 = 2I_0 J_1(x) \sin [\omega t - 2\pi(n - 1/4) - \phi]. \tag{32}$$

Comparison of (23) and (32) shows that the phase angle ϕ is defined by

$$\phi = 2\pi N - 2\pi(n - 1/4). \tag{33}$$

N may have any value and is determined by the transit time in the reflection space, but n is always an integer. If the transit time is correct for maximum output, then the phase angle ϕ is zero, and N is given by (10).

$$N = n - 1/4. \tag{10}$$

Decreasing either the acceleration voltage or the reflector voltage increases the transit time in the reflection space and increases the angle ϕ.

It will be convenient to express i_2 in the vector form instead of the sinusoidal form in (32).

$$i_2 = 2I_0 J_1(x)[\cos \phi - j \sin \phi]. \tag{34}$$

Since Y_2 is a negative admittance when ϕ is equal to zero, as defined in the discussion following (31), the complex admittance is

$$Y_2 = \frac{-\beta i_2}{E_1} = \frac{2\beta I_0 J_1(x)}{E_1}[-\cos \phi + j \sin \phi]. \tag{35}$$

Both components of the admittance are plotted in Fig. 9. The conductance, which is the real term in (35), is shown as a solid line, and the susceptance is a dash line. The vertical scale in Fig. 9 is purely arbitrary, since I_0, $J_1(x)$ and E_1 are unspecified.

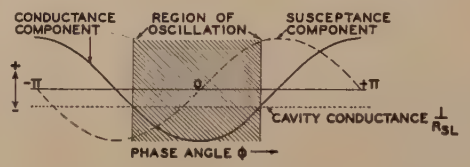

Fig. 9—Conductance and susceptance components of the beam admittance.

A qualitative analysis of a reflex oscillator may be obtained from inspection of Fig. 9. As the phase angle is increased from a negative value toward zero, the conductance changes from a positive value, indicating a loss, to a negative value representing a source of power. Oscillation will occur when the negative conductance is equal in magnitude to the conductance of the cavity; i.e., when the source of power is just sufficient to supply the losses in the resonator and the load. The magnitude of the circuit conductance is indicated by the horizontal dotted line in Fig. 9. The shaded portion shows the region in which oscillation will occur.

When ϕ is equal to zero, corresponding to the transit time for maximum output, the beam susceptance is zero and the tube will oscillate at the natural frequency of the cavity resonator. Note that the equivalent capacitance of the resonator corresponds to a positive susceptance in (30). Increasing the phase angle until ϕ is positive introduces an additional positive susceptance in parallel with C, and the frequency of oscillation becomes less than the natural frequency of the resonator. A negative susceptance might be considered a negative capacitance which decreases the effect of C, or it might be viewed as an inductance in parallel with L. Either viewpoint indicates that the resonant frequency of the system will be increased when ϕ is negative.

The value of this analysis can be demonstrated by experimental verification of the theory. If the beam current is kept quite small so that oscillation does not

occur, the magnitude of the beam conductance and susceptance components will be sinusoidal, as shown by Fig. 9, and the effective Q and resonant frequency of the cavity will vary as the phase of the feedback is changed by varying the reflector voltage. These changes were measured; the results of the experiment are shown in Fig. 10 and agree quite closely with the theoretical prediction.

A casual inspection of Figs. 9 and 10 might suggest that the tuning effect becomes small for large values of the phase angle ϕ near the points where oscillation fails to occur, because the sine function is not changing

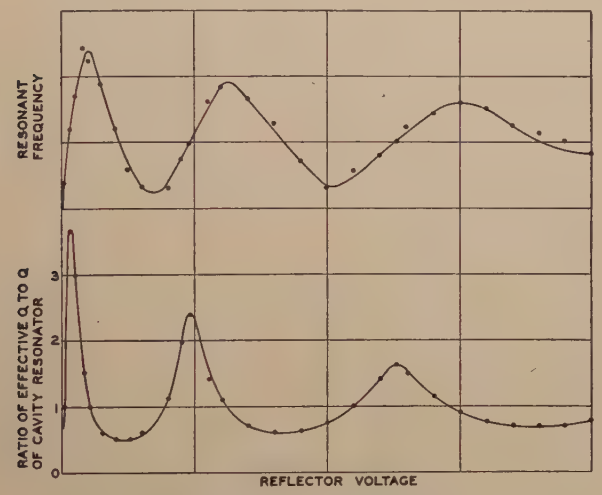

Fig. 10—Experimental curves showing the effect of the beam admittance.

rapidly. This behavior is correct for the conditions represented by Fig. 10, but when the beam current is large enough to maintain oscillation; i.e., when the beam current is much greater than the starting current, the sinusoidal variation of frequency does not occur. Actually, the scale in Fig. 9 depends upon the ratio $J_1(x)/E_1$, and this ratio decreases as the strength of oscillation increases. As a result, the tuning effect decreases rapidly as the transit time in the reflection space approaches the value required to make the phase angle ϕ equal to zero, and the frequency deviation is actually proportional to the tangent of the phase angle rather than the sine. This effect will be apparent from the quantitative analysis which follows.

Analysis of Reflex-Oscillator Characteristics

If the shunt resistance of a resonator is independent of frequency, the analysis is simplified because the power output and efficiency relations are obtained by considering only the conductance component of the beam admittance. After the strength of oscillation has been determined, the frequency of oscillation can be obtained from the magnitude of the beam susceptance. If the beam conductance is greater than the value required to supply the losses in the resonator and its load, the strength of oscillation will increase until the value of the negative beam conductance is reduced to the conductance of the resonator and its load. This means that the conductance of the system is zero when the klystron is oscillating. The sum of the susceptances must also be zero, and this relation determines the frequency of oscillation.

The starting current is one of the important characteristics of an oscillator, and will be used to illustrate this method of analysis. The starting current is the lowest value of beam current I_0 which will allow oscillation to exist. The sum of the cavity conductance and the beam conductance from (35) must be zero for oscillation to occur.

$$\frac{1}{R_{SL}} - \frac{2\beta I_0 J_1(x)}{E_1}\cos\phi = 0. \tag{36}$$

The peak resonator voltage E_1 and x are related, and the analysis is simplified if x is used as the variable. E_1 may be expressed in terms of x by rewriting (24).

$$x = \beta\pi N\frac{E_1}{E_0} \tag{24}$$

$$E_1 = \frac{E_0 x}{\beta\pi N}. \tag{37}$$

Substituting (37) in (36) and rearranging terms gives

$$\frac{x}{2J_1(x)} = \frac{\beta^2\pi N I_0 R_{SL}}{E_0}\cos\phi \tag{38}$$

$$\frac{x}{2J_1(x)} = \frac{\beta^2\pi N I_0 R_S R_L}{E_0(R_S + R_L)}\cos\phi. \tag{38a}$$

Weak oscillation corresponds to extremely small resonator voltage, and the bunching parameter x is almost zero under these conditions. The $J_1(x)$ Bessel function is equal to $x/2$ for small values of x, therefore the left side of the equation will be unity when I_0 is equal to the starting current. The current will be a minimum for the starting conditions only if the phase is correct; i.e., $\cos\phi$ must be a maximum and ϕ is equal to zero, the phase for maximum output. When these conditions are imposed on (38), we obtain an expression for the starting current.

$$I_{\text{Start}} = \frac{E_0}{\beta^2\pi N R_{SL}}. \tag{39}$$

Reasonable values which might be substituted into (39) in order to give some idea of the current required for oscillation follow:

$$\beta^2 = 1.0$$

$$E_0 = 300 \text{ volts}$$

$$N = 4\tfrac{3}{4} \text{ cycles}$$

$$R_{SL} = 20{,}000 \text{ ohms}.$$

Representative values have been chosen, and indicate that a beam current of one milliampere will maintain oscillation.

The term $x/2J_1(x)$ in (38) and (38a) is one form of a very important parameter in the analysis of any oscillator. It was used and explained in an article[11] on double-resonator klystron oscillators and will appear as a co-ordinate in many of the illustrations which follow. The basic parameter, which applies to conventional vacuum tubes as well as velocity-modulation types, may be defined as the magnitude of the ratio of the small-signal transadmittance of a tube to the large-signal transadmittance. This ratio is a measure of the saturation effect at high input levels and the term "transreduction factor" has been proposed for this ratio. The term is not limited to analysis of oscillators but is equally useful in amplifiers and other vacuum-tube circuits. When used in an analysis of klystron operation based on small variations of velocity, the value of the parameter has the convenient mathematical equivalent $x/2J_1(x)$, which has been mentioned.

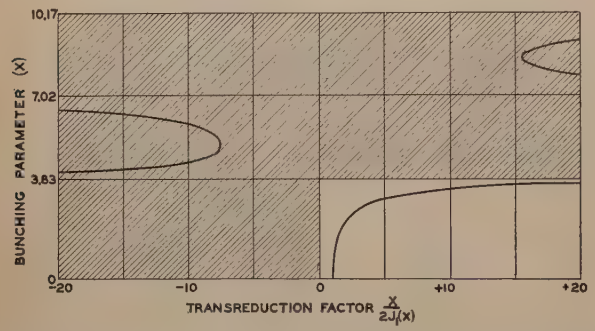

Fig. 11—Bunching parameter x as a function of beam current and other variables. The unshaded portion is the normal operating region for a reflex oscillator.

Increasing the beam current above the starting current value will greatly increase the output. This can be shown by deriving the expression for the power delivered to the resonator and load. This power will be designated P_2, and is the power delivered by the bunched beam to the shunt resistance R_{SL}. The value of P_2 is given by one half of the product of E_1, the peak resonator voltage, and the peak value of the in-phase component of i_2. This product must be reduced by the beam coupling coefficient β, in order to include the effect of finite transit time across the resonator gap.

$$P_2 = 1/2(E_1\beta i_2 \cos\phi) = \beta E_1 I_0 J_1(x) \cos\phi. \qquad (40)$$

Substituting the expression for E_1 in (37) into (40)

$$P_2 = \frac{E_0 I_0 \cos\phi}{\pi N} x J_1(x). \qquad (41)$$

In order to compute P_2, it is necessary to know the dependence of E_1 or x upon the beam current, I_0. Equations (24) or (37) do not furnish this information, but the relation can be obtained indirectly from (38). Values may be substituted in (38) or (38a) to obtain the value of the transreduction factor $x/2J_1(x)$ corresponding to the assumed value of the beam current I_0. The relation between the bunching parameter x and $x/2J_1(x)$ can be obtained from a table of Bessel functions, or from Fig. 7, which is a curve of $2J_1(x)$ as a function of x. This relation between x and $x/2J_1(x)$ is

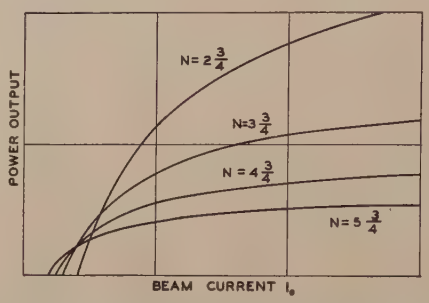

Fig. 12—Power output as a function of beam current. Several modes corresponding to different transit times are shown.

given in Fig. 11 for all values of x between zero and 10.17, corresponding to the third zero of the Bessel function, but only the unshaded region is of importance in the normal operation of a reflex-klystron oscillator. The value of $x/2J_1(x)$ computed from (38) or (38a) is used with Fig. 11 to obtain values for x and $J_1(x)$ corresponding to the assumed value of the beam current I_0, and the power can then be computed from (41).

Curves of power delivered by the bunched beam as a function of beam current I_0, computed in the manner described above, are shown in Fig. 12 for various values of N. Those curves not only show the increase of power as the current is increased above the starting value, but also indicate that the maximum power from a reflex oscillator and the starting current are inversely proportional to N, the number of cycles during transit in the reflection field. In other words, increasing the number of cycles required for bunching, either by reducing the reflector voltage or actually changing the tube design by increasing the reflector spacing, will decrease the output which can be obtained but will permit the tube to be operated with a smaller beam current.

It would be interesting to investigate the region in Fig. 11 where $x/2J_1(x)$ has a negative value. The negative sign has the same significance as the negative portion of the Bessel-function curve; i.e., when the bunching parameter x is greater than 3.83, the Bessel function becomes negative and the phase of the bunched beam is shifted 180 degrees.[10] Reference to (35) will illustrate the effect of this phase shift. Oscillation can occur only when the equivalent beam conductance is negative. Normally, this condition is met when the phase angle ϕ is zero and the Bessel function has a positive value. However, if the phase angle is 180 degrees, corresponding to the usual region of nonoscillation, but the resonator

voltage is made large enough to give a negative value of $J_1(x)$, then the beam conductance defined by (35) is also negative. Oscillation would not be self-starting, but *might* be maintained if the beam current was sufficiently high and the correct value of resonator voltage was obtained by overdriving the resonator.

If any of the variables other than current are changed,

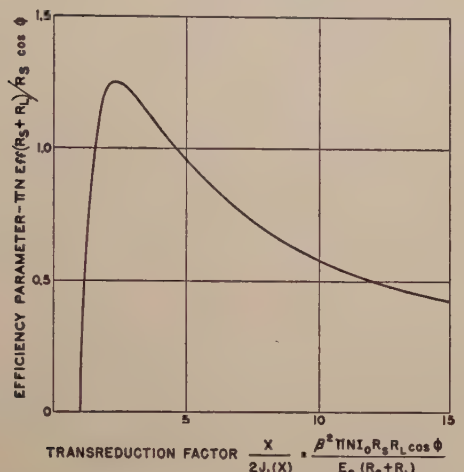

Fig. 13—Universal curve for the efficiency of a reflex-klystron oscillator.

such as the load resistance or the phase angle ϕ, the use of curves to show the effect of each variable becomes quite complicated. Fortunately, all of the variables can be combined into dimensionless parameters and the characteristics can be presented in a universal curve as illustrated by Fig. 13. The transreduction factor $x/2J_1(x)$ in (38) is one example of a useful dimensionless parameter and the efficiency parameter to be derived below is another example.

The power delivered by the bunched beam, defined by (41), is not all useful power since some is absorbed by the resonator losses. We are more interested in the power delivered to the load, which will be designated P_L. Then

$$P_L = \frac{R_S}{R_L + R_S} P_2 = \frac{R_S E_0 I_0 \cos \phi}{\pi N (R_L + R_S)} x J_1(x). \quad (42)$$

If we divide the power output by the beam power input we obtain the efficiency of the klystron oscillator. Equation (42) can be rearranged so that the efficiency (abbreviated "Eff.") and the other factors involved are related to a dimensionless efficiency parameter $xJ_1(x)$.

$$x J_1(x) = \frac{\pi N}{\cos \phi} \frac{R_L + R_S}{R_S} \text{Eff.} \quad (43)$$

Fig. 13 combines these two dimensionless parameters in a single curve which relates the output characteristics of a reflex-klystron oscillator to the design factors which may be varied. The vertical co-ordinate is $xJ_1(x)$ and $x/2J_1(x)$ is the horizontal co-ordinate.

Effect of Voltage, Current, and Load on Klystron Output

Most of the output characteristics which are typical of reflex-klystron oscillators can be predicted by inspection of Fig. 13. Consider the case when the load, beam current, and acceleration voltage remain fixed, but the reflector voltage is varied. Assume that the phase angle ϕ is $\pi/2$ for zero reflector voltage; i.e., when the reflector electrode is at cathode potential. Cos ϕ will be zero, corresponding to an operating point at the origin in Fig. 13. Increasing the negative reflector voltage will decrease ϕ and cos ϕ will vary from zero to a maximum of unity and then decrease again. The value of N will also vary, but if N is large this variation is not important in a qualitative analysis, and N will be assumed a constant for the range of each voltage mode.

When cos ϕ is zero, the transreduction factor $x/2J_1(x)$ is also zero, since the value of $x/2J_1(x)$ is determined by (38) or (38a).

$$\frac{x}{2J_1(x)} = \frac{\beta^2 \pi N I_0 R_{SL}}{E_0} \cos \phi. \quad (38)$$

Oscillation will not occur until cos ϕ has increased until the value of $x/2J_1(x)$ is unity. As cos ϕ increases beyond this point, the output will increase as shown by Fig. 13. When cos ϕ is unity, $x/2J_1(x)$ will have its maximum value and the output will also be maximum. This is true for the region where the efficiency curve is decreasing because the cos ϕ term increases faster than the efficiency parameter in Fig. 13 decreases. As the reflector voltage is increased beyond the value giving maximum output, the phase angle becomes negative, and cos ϕ decreases until the output is again zero.

As the reflector voltage is increased further, the sign of cos ϕ will become negative and the beam-conductance term in (35) has a positive value. This positive beam conductance represents an additional loss, therefore

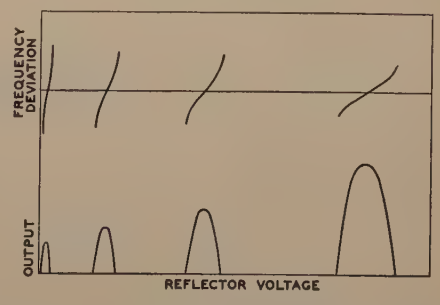

Fig. 14—Power-output and frequency characteristics when the reflector voltage of a reflex klystron is varied.

oscillation does not occur. When the transit time has changed by an amount equivalent to one complete cycle, the phase is again correct for oscillation and another output mode will occur. Normally, there are several of these voltage modes, and oscillation does not occur in

the region between modes where the phase angle is incorrect. This behavior is illustrated by Fig. 14.

The higher reflector-voltage modes correspond to smaller values of N and the output is greater for two reasons: first, the ordinate $xJ_1(x)$ in Fig. 13 becomes greater as N is decreased, since decreasing N corresponds to moving from right to left on the curve in Fig. 13; second, the efficiency for a particular value on the curve is inversely proportional to N. Eventually it is no longer possible to observe modes with higher reflector voltage because N has become so low that the starting current is greater than the beam current. The last mode observed may have the highest output of the series, or it may have less output than the previous mode. The latter case corresponds to a point in Fig. 13 to the left of the maximum of the curve.

The maximum theoretical efficiency of a reflex-klystron oscillator is less than the value for a double-resonator oscillator, and is inversely proportional to N. The efficiency for any value of N can be calculated from Fig. 13. If most of the power is transferred to the load and the phase angle is adjusted for maximum output, then (43) may be rewritten

$$\text{maximum efficiency} = \frac{xJ_1(x)}{\pi N} = \frac{1.25}{\pi N}. \qquad (44)$$

The assumptions used in this derivation are not valid for small values of N, and theoretical efficiencies between 20 and 30 per cent are indicated when better approximations are made in the computation of efficiency for values of N less than two.

It is interesting to note that the efficiency obtainable for any mode is independent of the beam coupling coefficient. If the transit time across the resonator gap is large, making the value of β less than unity, then it is theoretically possible to overcome this disadvantage by increasing the beam current. The power output will be greater because the same maximum efficiency requires more power input. If sufficient beam current is available so that the load resistance R_L is small in comparison with the shunt resistance of the resonator R_S, the effect of a small value of β may be counteracted by decreasing the load; i.e., increasing the value of R_L.

If the output load impedance is varied (by varying the length of the output line or some other method of impedance transformation), the output will increase to a maximum, then decrease suddenly and the klystron may refuse to oscillate for certain load impedances. This effect occurs first for the higher reflector-voltage modes because the starting current is higher for these modes. When the beam current is constant the load required for maximum output is different for each mode. Heavier loading is required for maximum output from the modes corresponding to the larger values of N.

This effect can be demonstrated conveniently with a dynamic method of observing the output. An alternating voltage can be superimposed upon the reflector voltage, causing the output to be swept through several modes periodically. The output voltage is applied to a cathode-ray oscilloscope with the sweep synchronized with the reflector-voltage modulation. A pattern similar to Fig. 14 will be observed. If the klystron is lightly loaded, all of the modes will be small, but the higher reflector-voltage modes will increase until the mode with the smallest value of N corresponds to the point of maximum efficiency on Fig. 13. Increasing the load further will decrease the output from the highest voltage mode until it disappears when the transreduction factor becomes less than unity. The other modes with larger values of N will continue to increase in output, with the modes disappearing successively until the load is so great that the klystron cannot oscillate at any reflector voltage.

Analysis of Electronic Tuning

The qualitative analysis based on Fig. 9 predicted that the frequency of oscillation would change as the phase of the bunched beam was varied by changing the acceleration voltage or the reflector voltage. This effect is known as electronic tuning. The power output and efficiency relationships were obtained by considering only the conductance components of the beam and cavity admittances. Similarly, the electronic-tuning analysis requires the sum of the susceptances to be zero. The magnitude of the beam susceptance depends upon the strength of oscillation, however. As a result, the imaginary component of the beam admittance depends upon the magnitude of the real component.

Equation (36) may be rewritten

$$\frac{2\beta I_0 J_1(x)}{E_1} = \frac{1}{R_{SL}\cos\phi}. \qquad (45)$$

Then (45) may be substituted in the imaginary term of (35) to obtain the value of the beam susceptance in terms of the phase angle ϕ.

$$\frac{2\beta I_0 J_1(x)}{E_1}\sin\phi = \frac{\sin\phi}{R_{SL}\cos\phi} = \frac{\tan\phi}{R_{SL}}. \qquad (46)$$

Equating all susceptance terms in the resonator and beam admittances to zero gives an expression which may be used to determine the frequency of oscillation. If ω is the angular frequency of oscillation for any phase angle, and ω_0 is the angular frequency corresponding to zero phase; i.e., the resonant frequency of the cavity, then

$$-\frac{1}{\omega L} + \omega C + \frac{\tan\phi}{R_{SL}} = 0. \qquad (47)$$

Rearranging terms gives

$$\frac{R_{SL}}{\omega_0 L}\left(\frac{\omega_0}{\omega} - \omega\omega_0 LC\right) = \tan\phi. \qquad (47a)$$

But $R_{SL}/\omega_0 L$ is equal to the loaded Q of the resonator, Q_L and LC is equal to $1/\omega_0^2$, therefore

$$Q_L\left(\frac{\omega_0}{\omega}-\frac{\omega}{\omega_0}\right)=\tan\phi. \tag{47b}$$

When ω and ω_0 do not differ by more than a few per cent $((\omega_0/\omega)-(\omega/\omega_0))$, may be rewritten

$$\frac{\omega_0}{\omega}-\frac{\omega}{\omega_0}=2\frac{\omega_0-\omega}{\omega}=2\frac{\Delta f}{f} \tag{48}$$

and (47b) becomes the familiar expression for the phase of a parallel-resonant circuit.

$$2Q_L\frac{\Delta f}{f}=\tan\phi. \tag{49}$$

The term $2\,Q_L\Delta f/f$ is a convenient frequency-deviation parameter which is often used in universal curves for resonant circuits. It relates the actual frequency deviation to the loaded Q of the circuit.

Equation (42) and Fig. 13 allow the power output to be calculated as a function of the phase angle ϕ, and the frequency deviation from the resonant frequency of the cavity can be obtained from (49). However, it is more useful to know these characteristics as a function of voltage instead of phase. Equation (9), repeated below,

$$N=4fs_0\frac{\sqrt{\frac{m}{2e}E_0}}{E_0+E_r} \tag{9}$$

may be substituted into (33) to obtain a value of ϕ, and this value of ϕ may then be substituted into (42) and (49), giving the output power and frequency characteristics as a function of reflector voltage. Fig. 14 was obtained in this manner.

Fig. 15 repeats the characteristics shown in Fig. 14 for a single mode and a number of different values of loaded Q. The curves for heavy loading correspond to a load which is almost great enough to prevent oscillation. Curves are also shown for the loading which gives maximum output, and very light loading when most of the power is absorbed by the resonator losses.

A number of interesting conclusions are illustrated by Fig. 15. The slope of the linear portion of the frequency characteristic is inversely proportional to the loaded Q of the resonator. This fact is apparent from (49), but only the trend is indicated by Fig. 15, since actual values of Q_L are not given. Increasing the Q by decreasing the load does not decrease the electronic-tuning bandwidth as might be expected, since this change will increase the bunching and the phase angle may be varied over a larger range before the output decreases appreciably. The bandwidth between zero-output points actually increases as the loading is decreased, and the bandwidth between half-power points is decreased only slightly. Decreased loading causes the amplitude characteristic to become more uniform over a large range of voltage, but the frequency-deviation curve becomes quite nonlinear.

These qualitative conclusions are interesting, but a method of calculating the bandwidths is more valuable. The desired equations may be obtained by evaluating

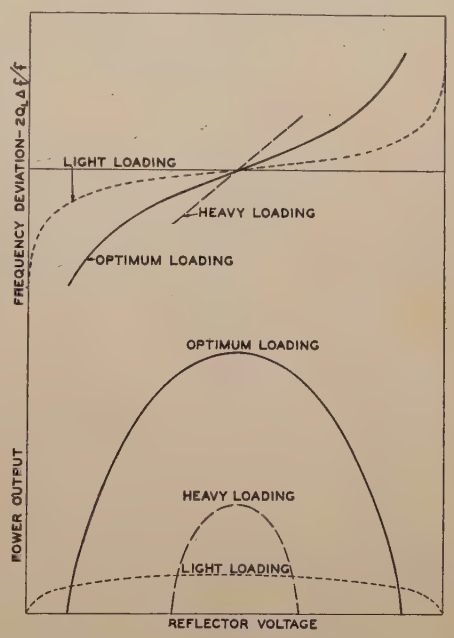

Fig. 15—Power-output and frequency characteristics for different loads.

the phase angle ϕ for the output being considered, and substituting this value of ϕ in (49). This process will be carried out for the zero-power point and also the half-power point. Equation (38a) may be rewritten

$$\cos\phi=\frac{E_0(R_S+R_L)}{\beta^2\pi N I_0 R_S R_L}\cdot\frac{x}{2J_1(x)}. \tag{50}$$

For zero output, the value of $x/2J_1(x)$ is unity; therefore

$$\cos\phi_0=\frac{E_0(R_S+R_L)}{\beta^2\pi N I_0 R_S R_L}, \tag{51}$$

and

$$\tan\phi_0=\sqrt{\frac{1}{\cos^2\phi_0}-1}. \tag{52}$$

Note that $\cos\phi_0$; i.e., the cosine of the phase angle when the output is zero, has a value equal to the reciprocal of the transreduction factor $x/2J_1(x)$ for the operating conditions when the phase angle is zero, corresponding to maximum output. Therefore, (52) may be rewritten

$$\tan \phi_0 = \sqrt{\left(\frac{x}{2J_1(x)}\right)^2 - 1}. \qquad (52a)$$

The bandwidth between zero-output points is obtained by substituting (52) in (49). However, the frequency deviation $\Delta f/f$ is measured from the point of maximum output; therefore, the bandwidth between zero-output points will be twice the value indicated by (49). The term $(2\Delta f/f)_0$ will be introduced to avoid confusion between the bandwidth between the two zero-output points and the frequency deviation from the frequency corresponding to maximum output. Then

$$2Q_L\left(\frac{2\Delta f}{f_0}\right) = 2 \tan \phi_0 = 2\sqrt{\frac{1}{\cos^2 \phi_0} - 1}. \qquad (53)$$

Evaluation of the bandwidth between half-power points is somewhat more complicated, and requires the determination of the bunching-parameter value which corresponds to one half of the maximum output. The power output for any operating condition is the square of the peak voltage E_1 divided by twice the load resistance R_L.

$$P_L = \frac{E_1^2}{2R_L} = \frac{E_0^2 x^2}{2\beta^2\pi^2 N^2 R_L}. \qquad (54)$$

Equation (37) has been substituted for E_1 in (54). The value of the bunching parameter x for maximum output can be obtained from Fig. 11 with cos ϕ equal to unity. This maximum output does not necessarily correspond to the point of optimum efficiency in Fig. 13, but is the maximum output for the given conditions of load and input when the phase angle is zero. These conditions determine the value of $x/2J_1(x)$ and x is then determined from Fig. 11. This value of x divided by $\sqrt{2}$ is the value of the bunching parameter which corresponds to the half-power points. Substituting this value of the bunching parameter in (50) gives

$$\cos \phi_{1/2} = \frac{E_0(R_S + R_L)}{\beta^2\pi N I_0 R_S R_L} \cdot \frac{x/\sqrt{2}}{2J_1(x/\sqrt{2})}. \qquad (55)$$

Equation (55) may also be written

$$\cos \phi_{1/2} = \frac{2J_1(x)}{x} \cdot \frac{x/\sqrt{2}}{2J_1(x/\sqrt{2})}. \qquad (55a)$$

A definition for the bandwidth between half-power points, similar to the definition for zero-output conditions, gives

$$2Q_L\left(\frac{2\Delta f}{f}\right)_{1/2} = 2 \tan \phi_{1/2} = 2\sqrt{\frac{1}{\cos^2 \phi_{1/2}} - 1}. \qquad (56)$$

These expressions may appear complicated, but the evaluation of cos $\phi_{1/2}$ from Fig. 11 is quite simple. The method can be illustrated by a sample calculation. Assume that $x/2J_1(x)$ equal to 2.30 corresponds to the operating conditions when the phase angle is zero. This corresponds to maximum output from the tube. The bunching parameter x for this value of $x/2J_1(x)$ is 2.40, as indicated by the curve in Fig. 11. The value of x for the half-power point would be $2.40/\sqrt{2}$ or 1.70, and corresponds to $x/2J_1(x)$ equal to 1.47. Cos $\phi_{1/2}$ is then 1.47/2.30, or 0.64. Substitution of this value of cos $\phi_{1/2}$ in (56) gives a value of 2.40 for $2Q_L(2\Delta f/f)_{1/2}$.

The calculations for bandwidths between zero-output and half-power points have been made and the results are plotted in Fig. 16 as a function of $x/2J_1(x)$, the transreduction factor. A dotted line has been drawn

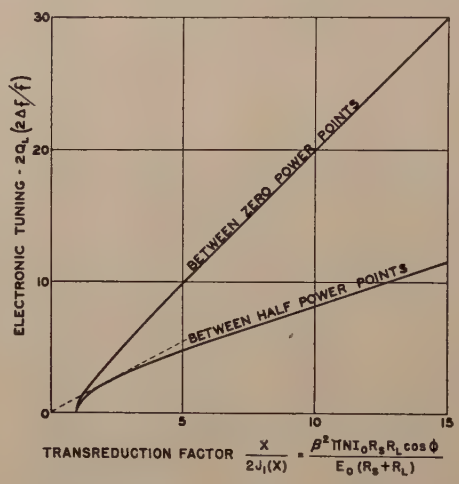

Fig. 16—Universal curves for the electronic tuning of a reflex oscillator.

through the origin and tangent to the curve for the bandwidth between half-power points. Since Q_L is proportional to $R_S R_L/(R_S+R_L)$, this dotted line is proportional to Q_L and $(2\Delta f/f)_{1/2}$ will be a maximum at the point of tangency. In other words, the maximum bandwidth between half-power points occurs when the conductance parameter has a value of approximately 2.30, the same as the value required for optimum output from the tube.

It is interesting to note that the bandwith between half-power points for a single resonant circuit is 2.00 when using these co-ordinates for the frequency deviation. The value for a reflex-klystron oscillator with the load adjusted for maximum bandwidth is 2.40, or 20 per cent greater than the bandwidth associated with the loaded Q of the resonator. Increasing the bunching by increasing the beam current, decreasing the loading, or in any other manner which increases the value of the transreduction factor, will increase the value of $2Q_L(2\Delta f/f)_{1/2}$. However, it is not correct to state that the electronic tuning of a reflex klystron is independent of the loaded Q of the resonator. The frequency deviation in the linear region is inversely proportional to Q_L, but increasing Q_L by reducing the load causes

overbunching and the tube can oscillate over a wider range of voltage variation. As a result, the half-power point is extended into the nonlinear region of the frequency-deviation characteristic and the actual frequency bandwidth $(2\Delta f/f)_{1/2}$ decreases only slightly from the maximum bandwidth when the oscillator is loaded to give maximum output.

Effect of Load Variations

Some of the effects of varying the load have been mentioned in the discussion of Figs. 13 and 15. The previous discussion assumed that the load can be represented by an equivalent shunt resistance R_L. This equivalent resistance has a magnitude similar to the shunt resistance of the cavity resonator; i.e., R_L is

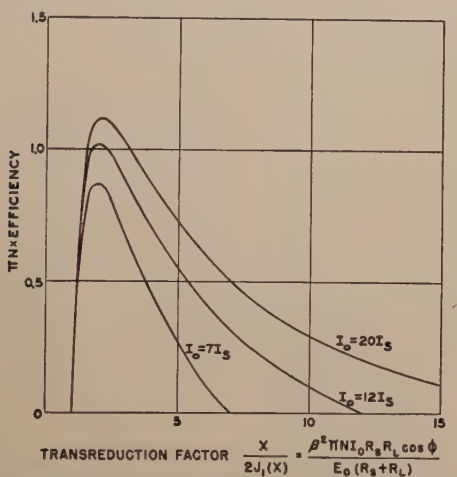

Fig. 17—Efficiency of a reflex oscillator as a function of load. Curves for three values of beam current are shown.

usually several thousand ohms. The characteristic impedance of the coaxial output line is very much smaller, usually in the order of magnitude of 100 ohms for convenient physical dimensions, and the coupling loop must be designed to transform an impedance of perhaps 100 ohms to the required value of several thousand ohms. Some tubes are manufactured with coupling loops which are fixed in size and position; in this case, the equivalent load resistance can be changed only by changing the load itself or by using some type of impedance transformer between the load and the coaxial output terminal. Other tube types may also permit variation of the size or position of the coupling loop as a means of adjusting the load.

If a variable length of line is used as an impedance transformer, the resistive component of the load can be varied, if there are standing waves in the line, but a reactive component may also be introduced. This reactive component will affect the frequency of oscillation. The analysis of this effect will not be considered in detail in this paper. However, the effect is quite important and should not be overlooked when using these tubes.

Frequency changes may also be caused by changing only the resistive component of the load if the phase angle ϕ is not zero. Consider a case illustrated by Fig. 15 when the reflector voltage does not correspond to the adjustment for maximum output and the frequency deviation is not zero. Decreasing the load will decrease the frequency deviation. This effect is also indicated by the magnitude of the beam susceptance in (47). Decreasing the load corresponds to increasing the load resistance R_L, and this change also increases the effective shunt resistance R_{SL}; therefore, decreasing the load will decrease the effective beam susceptance and the frequency deviation will be less. This effect becomes greater when the reflector voltage deviates from the value required for maximum output.

If most of the power is not transferred to the load, then the derivation of the maximum efficiency in (44) does not apply, and the efficiency is dependent upon the load resistance. Actually, R_L must be small compared to R_S if most of the power is to be transferred to the load, and this condition can be obtained only if the beam current available is very much larger than the starting current. The maximum efficiency is less than the theoretical value for practical values of beam current. If the beam current is seven times greater than the starting current, the maximum value of the $x/2J_1(x)$ co-ordinate in Fig. 13 will be 7.0 when R_L is infinite, corresponding to no load. The output will be zero under these conditions and the efficiency will also be zero, since, $(R_L+R_S)/R_S$ becomes infinite. As R_L is decreased corresponding to increasing the load, the output will increase.

A family of curves similar to Fig. 13 can be plotted to show the effect of power division between the resonator losses and the load. The factor $(R_L+R_S)/R_S$ in the ordinate of Fig. 13 is computed for each value of R_L considered, and the ordinates for the revised efficiency curves in Fig. 17 are directly proportional to the output efficiency. Each curve corresponds to some chosen value of beam current I_0 and πN times the efficiency is plotted as a function of R_L. The other variables in the transreduction factor are held constant. The phase angle ϕ has been assumed to be zero in this illustration, corresponding to the voltage adjustment for maximum output, therefore cos ϕ is unity and has not been included in the efficiency co-ordinate.

If the beam current I_0 were equal to the starting current I_S, the transreduction factor $x/2J_1(x)$ would have a value of unity. The load would be zero, corresponding to an infinite value of R_L. When I_0 is seven times greater than I_S, the value of $x/2J_1(x)$ would be 7.0 if the load resistance R_L was infinite. The output would be zero, of course. Decreasing R_L would increase the load, and the efficiency would increase until a maximum was reached. Eventually the load would become too great and the tube would fail to oscillate when R_L was

reduced until $x/2J_1(x)$ had a value of unity. Similar curves are shown for values of I_0 twelve and twenty times greater than the starting current. Note that the actual efficiency is only 90 per cent of the theoretical efficiency when the beam current is twenty times greater than the starting current.

Fig. 17 may also be used to compare the efficiencies for different values of N when the beam current remains constant. These conditions can be met by changing the reflector voltage. Consider that the curve in Fig. 17 for seven times the starting current corresponds to a value of N equal to $2\frac{3}{4}$ cycles, and the curve for 12 times the starting current corresponds to the same beam current but a value of $4\frac{3}{4}$ cycles for N. Then the actual efficiency for optimum loading would be $0.87/2.75\pi$ or 10.1 per cent for N equal to $2\frac{3}{4}$ cycles, and $1.01/4.75\pi$ or 6.8 per cent for N equal to $4\frac{3}{4}$ cycles. Although the loading required for maximum output is less for the mode with the shorter transit time, and therefore a larger proportion of the total power is dissipated in the resonator losses, the improved conversion efficiency for the shorter transit time allows the output efficiency to be greater.

Reflex-Klystron Design Considerations

Most of the previous discussion has been used to predict or explain the electrical characteristics of reflex-klystron oscillators when operating voltages, current, and loading were the only variables. It is interesting to consider the effect of varying the design of the tube itself, although it is necessary to remember that the relation between the lumped constants used in the equivalent circuit and the physical dimensions of the cavity resonator is not clearly defined. However, considering the effect of changing these constants can be quite useful in a qualitative analysis of the factors which are important in the design of klystrons.

Reference to the equivalent circuit in Fig. 8 will indicate that increasing the ratio of the small-signal beam admittance to the circuit capacitance will increase the amount of electronic tuning. This ratio may be increased by increasing the beam current I_0, increasing the transit time in the reflection space (increasing the value of N), or by decreasing the circuit capacitance. Decreasing the capacitance by increasing the resonator-gap spacing may not be satisfactory because the transit time across the gap may become excessive. This change would reduce the beam coupling coefficient, which has the same effect as reducing the beam current. Therefore we will only consider reducing the capacitance by decreasing the area of the resonator gap.

Either increasing the beam current without changing the capacitance, or reducing the area of the gap without changing the current, corresponds to increasing the current density. Therefore the problem of increasing the electronic tuning in a klystron design becomes a problem of increasing the current density. This conclusion assumes that N is already large and that additional transit time in the reflection space will not increase N appreciably.

It is equally interesting to analyze the factors affecting electronic tuning from the viewpoint that increased electron bunching permits heavier loading of the oscillator, and therefore increases the electronic tuning because the loaded Q has been reduced. Reference to Figs. 11 and 13 will emphasize the fact that the bunching parameter x has a value of 2.40 when the oscillator is adjusted for maximum output. If the beam current is increased, with no design change in the resonator, the resonator voltage E_1 will be increased and the value of the bunching parameter will increase. The magnitude of E_1 is determined by the radio-frequency current i_2 and the loaded shunt resistance R_{SL}.

$$E_1 = 2I_0R_{SL}J_1(x). \tag{57}$$

Since E_1 must be constant if x remains constant, an increase in I_0 must be accompanied by a decrease in the loaded shunt resistance R_{SL}. Therefore the increased beam current permits the oscillator to be operated with a greater load, and reducing the Q of the loaded circuit increases the electronic tuning.

The effect of decreasing the capacitance may also be related to the loaded Q of the resonator. One of the relations giving the Q of a circuit is

$$Q_L = \omega CR_{SL} = \omega C\frac{R_SR_L}{R_S + R_L}. \tag{58}$$

The unloaded Q of the circuit will be

$$Q = \omega CR_S, \tag{59}$$

therefore (58) may be rewritten

$$Q_L = Q\frac{R_L}{R_S + R_L}. \tag{60}$$

Decreasing the circuit capacitance by reducing the resonator-gap area without changing the gap spacing does not change the unloaded Q appreciably, but does increase the shunt resistance R_S. This change will not affect the loaded shunt resistance R_{SL}, since R_L is usually much smaller than R_S; therefore, the oscillator will operate with the same degree of bunching if the beam current and the load resistance R_L are unchanged However, (60) indicates that the loaded Q will decrease when the shunt resistance is increased, and the electronic tuning will be increased.

Note that the changes discussed in all of the preceding paragraphs correspond to increasing the curent density in the electron beam. The various explanations of the electronic tuning are merely different ways of looking at the problem.

The design of an efficient, high-power reflex-klystron oscillator would require a different approach. The important design factor would be the transit time in the reflection space, therefore N must be small. As pointed out in the discussion of (44), the analysis is not valid for small values of N, but the trend is indicated correctly. Decreasing N increases the starting current, and if the beam current is already as large as permitted by a practical design, then the load required for optimum output cannot be very great and the electronic tuning will be small. It is also apparent that the theoretical efficiency will not be attained if a large part of the total power goes into the resonator losses. In spite of this factor, however, the efficiency will be greater than that of a reflex klystron designed for a larger value of N. If it were possible to increase the beam current sufficiently so that most of the power could be transferred to the load, then the klystron would have as much electronic tuning as a design with a larger value of N and smaller beam current.

Acknowledgment

The presentation of reflex-oscillator characteristics with universal curves, and the form of these curves, were suggested in an unpublished report by D. R. Hamilton. Credit is also due G. E. Hackley for some of the experimental work which verified the theory.

Appendix I

Glossary of Symbols

E_0 = beam voltage or acceleration voltage.
E_r = reflector voltage (voltage between cathode and reflector electrode).
E_g = control-grid voltage.
E = instantaneous value of radio-frequency voltage across resonator gap.
E_1 = peak value of radio-frequency voltage across resonator gap.
I_0 = average beam current (value of direct current).
I_{start} = minimum value of beam current required to maintain oscillation
I_2 = instantaneous value of bunched beam current.
i_2 = fundamental component of radio-frequency current in the bunched beam.
ϕ = phase angle of bunched beam current.
v = velocity of an electron.
v_0 = average velocity of an electron (corresponds to E_0).
s = distance measured from resonator gap.
s_0 = spacing between resonator gap and reflector electrode.
F = retarding force due to reflecting field.
a = deceleration caused by retarding force F.
e = charge of an electron.
m = mass of an electron.
t = time.
t_1 = departure time when an electron leaves the resonator gap.
t_2 = arrival time when an electron returns to the resonator.
T = transit time in the reflection field.
T_0 = transit time in the reflection field of an electron with average velocity v_0.
N = number of oscillation cycles during transit of the reflection space.
f = frequency of oscillation.
ω = $2\pi f$.
ω_0 = 2π times the resonant frequency of the cavity.
x = bunching parameter equal to $\beta\pi N\frac{E_1}{E_0}$.
J_n = Bessel function of first kind and nth order.
J_1 = Bessel function of first kind and first order.
d = spacing of resonator gap.
δ = transit angle across the resonator gap.
β = moudlation coefficient equal to $\frac{\sin \delta/2}{\delta/2}$.
R_S = shunt resistance of the cavity resonator.
R_L = equivalent load resistance.
R_{SL} = loaded shunt resistance of the cavity resonator.
L = equivalent inductance of the cavity resonator.
C = equivalent capacitance of resonator gap.
Q = unloaded Q of the cavity resonator.
Q_L = loaded Q of the cavity resonator.
Y_s = total admittance of the cavity resonator.
Y_2 = equivalent admittance due to the bunched beam.
P_2 = power delivered to the resonator and load.
P_L = power delivered to the load.
Eff. = efficiency (ratio of radio-frequency output power to beam-power input).
$x/2J_1(x)$ = transreduction factor (magnitude of the ratio of small-signal transadmittance to large-signal transadmittance).
$xJ_1(x)$ = universal efficiency parameter for reflex klystrons.
$2Q_L\Delta f/f$ = frequency deviation from resonant frequency of the cavity.
$2Q_L(2\Delta f/f)_0$ = bandwidth between zero-power-output points.
$2Q_L(2\Delta f/f)_{1/2}$ = bandwidth between half-power points (frequently called electronic-tuning bandwidth).

The Transmission of a Frequency-Modulated Wave Through a Network*

WALTER J. FRANTZ†, ASSOCIATE, I.R.E.

Summary—**A practical method for calculating the effect of a four-terminal network upon a frequency-modulated wave being transmitted through it is developed and demonstrated. The form of the solution is simple enough to be applied by anyone familiar with electric circuits. No knowledge of calculus or higher mathematics is required; nor is the solution restricted in any way, being equally accurate and practical for large and small values of modulation index, and for any physical network.**

In order to determine whether or not a particular network problem involving a frequency-modulated input wave may be analyzed from the "instantaneous frequency" viewpoint, a test, or validity condition, has been developed. This test quickly classifies the problem either as one for which only a complete, straightforward analysis determines the response, or as one for which a quasi-steady state exists. The quasi-steady state is a condition under which the amplitude—instantaneous-input-frequency envelope and the phase-shift—instantaneous-input-frequency envelope of the output wave approach closely enough to the steady-state-amplification—frequency and phase-shift—frequency characteristics of the network.

Introduction

WITH THE increasing use of a frequency-modulated wave for circuit alignment and test, spectrum analysis, altitude or time-delay measurement, and the transmission of intelligence, there arises the need for a practical and dependable method of calculating the response of a network to a frequency-modulated input wave.

Suppose that it is desired to picture accurately the steady-state amplification—frequency characteristic of a tuned one-megacycle amplifier with an effective Q of 100. The layout of Fig. 1 is often used for visual circuit test and alignment in the communications industry.

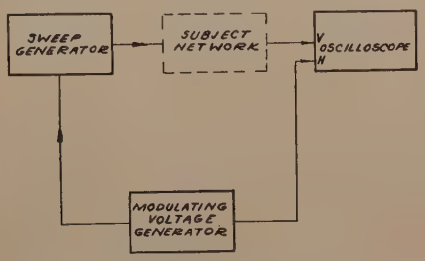

Fig. 1—Block layout of a visual network test and alignment position.

Since the modulating voltage is applied also to the horizontal plates of the oscilloscope, the horizontal axis is linear in instantaneous frequency of the input frequency-modulated wave. In Fig. 2, (a) is the oscillogram obtained when the frequency-modulated signal generator is operating at a center frequency of one megacycle, a total sweep width of 50 kilocycles, and a modulating frequency of 100 cycles per second; the amplification—frequency characteristic of the amplifier has been fairly well pictured. If the modulating frequency is increased to 1000 cycles per second, the pattern (b) departs considerably from the steady-state amplification—frequency characteristic of the network. The two traces are the frequency upsweep and the downsweep. The upsweep trace leans to the right and the downsweep trace leans to the left. In Fig. 2, (c) is the oscillogram obtained for a total sweep width of 150 kilocycles and a modulating frequency of 333 cycles per second, while (d) is the oscillogram obtained for a total sweep width of 150 kilocycles and a modulating frequency of 1000 cycles per second.

These oscillograms will be referred to quantitatively later in the article. They are presented here only to persuade those unfamiliar with the problem that it is real, important, and frequently encountered. The problem is probably given the most attention by the designers of high-quality frequency-modulated transmitters and receivers.

It is the purpose of this paper to devise a simple test by which one may determine whether or not the effects of a network upon a frequency-modulated wave being transmitted through it differ appreciably from the steady-state amplification—frequency and phase-shift—frequency characteristics of the network, and, if so, to offer a general and practical method of calculating these effects as a function of either time or instantaneous input frequency.

The Response-Envelope Equation

The following procedure is a rigorous and general method of obtaining the output-voltage envelope for a network driven by a frequency-modulated wave:

1. Measure or calculate the steady-state amplification—frequency and phase-shift—frequency characteristics of the network in question.
2. Express the frequency-modulated input wave in terms of its steady-state spectrum of sinusoidal side frequencies.
3. Pass the individual side frequencies through the network, altering the amplitude and phase of each according to the steady-state amplification and phase characteristics of the network at the particular frequency of the side frequency.
4. Plot the sum of the altered side frequencies point by point to obtain the output wave as a function of time.
5. Draw a smooth curve through the carrier-voltage peaks to obtain the response envelope of the output voltage.

* Decimal classification: R414×R140. Original manuscript received by the Institute, May 28, 1945; revised manuscript received, October 23, 1945.

† RCA Laboratories, Princeton, N. J.

Such a procedure, however, is not a solution to the frequency-modulated transmission problem. The method is rigorous and general, but not practical. Calculating the response pattern of (a) in Fig. 2 by the method just outlined, for example, would require the labor of a staff of clerks for several years, because it would be necessary to calculate about 100,000 points for a smooth curve of the radio-frequency voltage oscillations during one modulation cycle, each point being the sum of the instantaneous values of more than 500 side-frequency voltages.

It is fortunate that the operations outlined by steps 2, 3, 4, and 5 can be done analytically, initiating a practical equation for the output or response-voltage envelope in terms of the network parameters and the frequency-modulated input-wave parameters. This equation will be derived with time as the independent variable and transformed to a function of instantaneous input frequency to correspond with the abscissae of Fig. 2. The method used in this report for bridging steps 2, 3, 4, and 5 is very similar to the pattern followed by Cherry and Rivlin.[1] The problem has also been

(a)

Modulating frequency $=100$ $(v=2\pi=100)$
Total frequency excursion $=50,000$ $(K=2\pi\times25,000)$

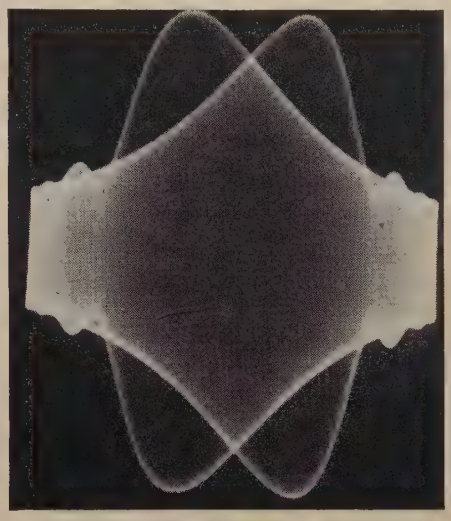

(b)

Modulating frequency $=1000$ $(v=2\pi\times1000)$
Total frequency excursion $=50,000$ $(K=2\pi\times25,000)$

(c)

Modulating frequency $=333$ $(v=2\pi\times333)$
Total frequency excursion $=150,000$ $(K=2\pi\times75,000)$

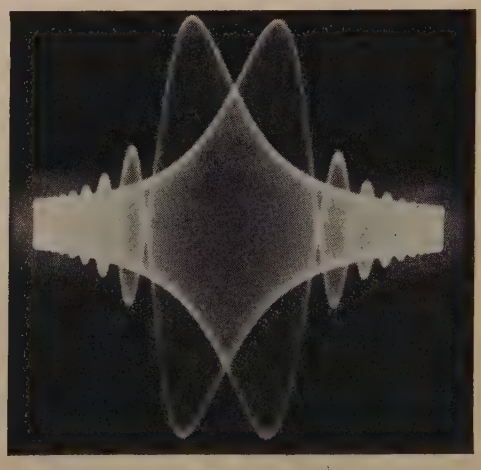

(d)

Modulating frequency $=1000$ $(v=2\pi\times1000)$
Total frequency excursion $=150,000$ $(K=2\pi\times75,000)$

Fig. 2—Experimental amplitude—instantaneous-input-frequency and phase-shift—instantaneous-input-frequency response of a tuned amplifier to a frequency-modulated wave.
Effective Q of amplifier $=100$ $(p=0.01)$
Center frequency $=10^6$ $(\omega_0=2\pi\times10^6)$

[1] E. C. Cherry and R. S. Rivlin, "Nonlinear distortion, with particular reference to the theory of frequency-modulated waves," Part II, *Phil. Mag.*, vol. 33, pp. 272–293; April, 1942.

considered by Kulp, who developed a solution which is practical when the modulation index of the frequency-modulated input wave is small.[2]

First a unit frequency-modulated wave is defined. The equations derived in this paper are based upon unit magnitude of the input signal.

$$\omega_0 = 2\pi \times \text{the center frequency} \tag{1}$$

$$K = 2\pi \times \text{the frequency deviation} \tag{2}$$

$$v = 2\pi \times \text{the modulating frequency} \tag{3}$$

$$m_f = \frac{K}{v} = \text{the modulation index} \tag{4}$$

$$\hat{\omega} = \omega_0 + K \cos vt = 2\pi \times \text{the instantaneous input frequency.} \tag{5}$$

It has been shown that[3]

$$\begin{aligned} e_{in} &= \sin(\omega_0 t + m_f \sin vt) \\ &= J_0(m_f) \sin \omega_0 t \\ &\quad + \sum_{n=1}^{\infty} (J_{2n-1}(m_f)\{\sin[\omega_0 + (2n-1)v]t \\ &\quad - \sin[\omega_0 - (2n-1)v]t\} \\ &\quad + J_{2n}(m_f)\{\sin[\omega_0 + 2nv]t + \sin[\omega_0 - 2nv]t\}). \end{aligned} \tag{6}$$

The series (6) is absolutely convergent, allowing the convenience of a partial summation with any desired accuracy.

$$\begin{aligned} e_{in} &\approx J_0(m_f) \sin \omega_0 t \\ &\quad + \sum_{n=1}^{N} (J_{2n-1}(m_f)\{\sin[\omega_0 + (2n-1)v]t \\ &\quad - \sin[\omega_0 - (2n-1)v]t\} \\ &\quad + J_{2n}(m_f)\{\sin[\omega_0 + 2nv]t + \sin[\omega_0 - 2nv]t\}). \end{aligned} \tag{7}$$

The choice of N depends upon m_f and the accuracy required of the analysis. The choice of N is not ordinarily difficult, because the Bessel coefficients of the series become negligible rather abruptly for a given argument as the order is increased beyond a certain value. For example, J_n (10,000)'s are relatively important up to $n=10{,}000$ and slightly above, but are insignificant beyond $n=10{,}050$.

For pure sinusoidal input of angular velocity ω to a linear network, the output wave can differ from the input wave only in amplitude and phase. By the rules of algebraic steady-state circuit analysis E_{out} can be expressed in general as the product of E_{in} and a complex function of ω. (See Appendix.)

$$E_{out}\{=\}E_{in}f(\omega) \tag{8}$$

where

$$|f(\omega)| = \frac{\text{amplitude of } E_{out}}{\text{amplitude of } E_{in}} \tag{9}$$

and where

$$\text{arc tangent}\frac{\text{imaginary }[f(\omega)]}{\text{real }[f(\omega)]} = \text{angular phase }[E_{out}] - \text{angular phase }[E_{in}]. \tag{10}$$

The $f(\omega)$ is a dimensionless transfer-voltage ratio. If I_{out} were used instead of E_{out}, $f(\omega)$ would be the transfer admittance.

The next step is to approximate $f(\omega)$ by a finite Fourier series about ω_0 in a period Ω equal to or greater than the interval containing the side-frequency voltage of (7). From (7) it is obvious that this interval extends from (ω_0-2Nv) to (ω_0+2Nv), a total width of $4Nv$.

$$f(\omega) \approx \sum_{m=0}^{M}\left(A_m \cos\left[\frac{2\pi m}{\Omega}(\omega-\omega_0\right] + B_m \sin\left[\frac{2\pi m}{\Omega}(\omega-\omega_0)\right]\right). \tag{11}$$

The notation $\approx$ used in (11) means "approximately equals only in the interval $(\omega_0-2Nv) \leqq \omega \leqq (\omega_0+2Nv)$." It is sufficient that the partial sum represent the function only in the interval $(\omega_0-2Nv) \leqq \omega \leqq (\omega_0+2Nv)$ since N has previously been chosen large enough that only relatively insignificant side frequencies of the frequency-modulated input voltage lie outside that interval. The choice of M depends upon the accuracy with which it is desired to approximate $f(\omega)$ and the nature of $f(\omega)$.

The reason for expressing $f(\omega)$ as a series approximation is to make the method general. If an analytical solution to steps 2, 3, 4, and 5 can be obtained for the terms of the series approximation, the problem is then solved for any $f(\omega)$, since any physical network characteristic can be approximated by such a finite series as (11). The Fourier series was chosen in preference to other series approximations because the analytical solution to steps 2, 3, 4, and 5 is not difficult for sinusoidal network terms, because engineering personnel are most familiar with the use of the Fourier series, and because the Fourier series, being periodic, is well behaved and known everywhere outside the interval of approximation. The power and real exponential series were avoided because such series increase without bound outside the chosen interval as the argument becomes large. Although N has been chosen large enough so that the side frequencies outside the interval $(\omega_0-2Nv) \leqq \omega \leqq (\omega_0+2Nv)$ are small enough to be neglected in comparison with the amplitude of the side frequencies within the interval, the products of the side frequencies and the value of the

[2] M. Kulp, "Spektra und Klirrfaktoren frequenz- und amplitudenmodulierter Schwingungen," Part II, *Elek. Nach. Tech.*, vol. 19, pp. 96–109; June, 1942.

[3] John R. Carson, "Notes on the theory of modulation," Proc. I.R.E., vol. 10, pp. 57–64; February, 1922

series outside the interval of approximation might not be negligible in comparison with the products of the side frequencies and the series approximation within the interval.

The A_m's and B_m's of (11) are the complex Fourier coefficients defined by the following integrals.

$$A_0 = \frac{1}{\Omega}\int_{\omega_0-\Omega/2}^{\omega_0+\Omega/2} f(\omega)d\omega \tag{12}$$

$$A_{m>0} = \frac{2}{\Omega}\int_{\omega_0-\Omega/2}^{\omega_0+\Omega/2} f(\omega)\cos\left[\frac{2\pi m}{\Omega}(\omega-\omega_0)\right]d\omega \tag{13}$$

$$B_m = \frac{2}{\Omega}\int_{\omega_0-\Omega/2}^{\omega_0+\Omega/2} f(\omega)\sin\left[\frac{2\pi m}{\Omega}(\omega-\omega_0)\right]d\omega. \tag{14}$$

These integrals can seldom be evaluated analytically, because either the $f(\omega)$ is known only numerically, or, if known analytically, the integrals are too difficult to handle. Numerical methods of obtaining the values of the integrals are nearly always preferable. These methods have been organized well enough so that, for example, a 24-point numerical analysis of a function takes only a few hours.[4,5]

Bridging steps 3, 4, and 5 analytically yields the following general equation for the output frequency-modulated voltage envelope. (See Appendix.)

$$E_{\text{out}}\{=\}\sum_{m=0}^{M} D_m(A_m\cos\psi_m + B_m\sin\psi_m) \tag{15}$$

where D_m and ψ_m are calculated as functions of either time t or instantaneous angular input velocity $\hat{\omega}$ as follows (see Appendix):

$$D_m(t)=\cos\left[\frac{K}{v}\sin vt\left(1-\cos\frac{2\pi mv}{\Omega}\right)\right] - j\sin\left[\frac{K}{v}\sin vt\left(1-\cos\frac{2\pi mv}{\Omega}\right)\right] \tag{16}$$

$$\psi_m(t)=\left[\frac{K}{v}\cos vt\sin\frac{2\pi mv}{\Omega}\right] \tag{17}$$

$$D_m(\hat{\omega})=\cos\left[\frac{\sqrt{K^2-(\hat{\omega}-\omega_0)^2}}{v}\left(1-\cos\frac{2\pi mv}{\Omega}\right)\right] \pm j\sin\left[\frac{\sqrt{K^2-(\hat{\omega}-\omega_0)^2}}{v}\left(1-\cos\frac{2\pi mv}{\Omega}\right)\right] \tag{18}$$

$$\psi_m(\hat{\omega})=\frac{\hat{\omega}-\omega_0}{v}\sin\frac{2\pi mv}{\Omega}. \tag{19}$$

[4] J. B. Scarborough, "Numerical Mathematical Analysis," Johns Hopkins University Press, Baltimore, Md., 1930, chap. 17, pp. 388–404.

[5] R. P. G. Denman, "Thirty-six and seventy-two ordinate schedules for general harmonic analysis," *Electronics*, vol. 15, pp. 44–47; September, 1942. Corrections by F. W. Grover, *Electronics*, vol. 16, pp. 214–215; April, 1943.

The amplitude and phase shift of E_{out} can be plotted as a function of time by calculating the magnitude and phase of (15) for several equally spaced values of t between $vt=0$ and $vt=2\pi$. As a function of instantaneous input frequency the amplitude and phase shift of E_{out} can be determined by calculating the magnitude and phase of (15) for several equally spaced values of $\hat{\omega}$ between $(\hat{\omega}-\omega_0)=-K$ and $(\hat{\omega}-\omega_0)=K$. As a function of instantaneous input frequency E_{out} has two values, one corresponding to the frequency downsweep and one corresponding to the frequency upsweep. The sign of the imaginary part of $D_m(\hat{\omega})$ is negative for the downsweep of frequency and positive for the upsweep. (See Appendix.)

It should be noted that E_{out} (15) is unusual in that it describes the amplitude and phase of a frequency-modulated oscillation. The arc tangent of the quotient of the imaginary and real parts of E_{out} is equal to the deviation between the instantaneous angular phase of the output wave and the instantaneous angular phase of the frequency-modulated input wave. When using (15) to compute points for a response envelope it must be remembered that D_m, A_m, and B_m are complex quantities, and that the summation is a complex summation. The magnitude of E_{out} is the absolute value of the complex summation rather than the sum of the absolute values of $D_m(A_m\cos\psi_m+B_m\sin\psi_m)$.

The Validity Condition Upon the "Instantaneous-Frequency" Method of Analysis

It is not surprising that the response of the networks of a final working frequency-modulation design can usually be justified from the "instantaneous-frequency" premise. A quasi-steady state usually results from careful design for a practical application; the quasi-steady state is often necessary. When the "instantaneous-frequency" method of analyzing the effect of a network upon a frequency-modulated wave is valid (that is, when a quasi-steady state exists) the response envelope approaches the steady-state amplification—frequency and phase-shift—frequency characteristics of the network. At any instant of time the frequency-modulated output wave deviates from the frequency-modulated input wave in amplitude and phase in a manner no different from that of a steady-state output wave whose constant frequency is equal to the instantaneous frequency of the frequency-modulated wave. Letting the quasi-steady-state response envelope $E^1_{\text{out}}(\hat{\omega})$ approach $f(\omega)$, equation (11),

$$E_{\text{out}}{}^1(\hat{\omega}) \rightarrow f(\omega) \approx \sum_{m=0}^{M}(A_m\cos\psi_m{}^1 + B_m\sin\psi_m{}^1) \tag{20}$$

where

$$\psi_m{}^1(\hat{\omega}) = \frac{2\pi m}{\Omega}(\hat{\omega}-\omega_0). \tag{21}$$

Equation (20) is equivalent to (15) if $D_m \rightarrow 1$ and

$\psi_m \rightarrow \psi_m{}^1$. The discrepancy between the angles ψ_m and $\psi_m{}^1$ is given by

$$\psi_m{}^1 - \psi_m = \frac{2\pi m}{\Omega}(\hat{\omega} - \omega_0) - \frac{\hat{\omega} - \omega_0}{v} \sin \frac{2\pi m v}{\Omega}. \quad (22)$$

For small discrepancies this becomes

$$\psi_m{}^1 - \psi_m \approx \frac{\hat{\omega} - \omega_0}{6v}\left(\frac{2\pi m v}{\Omega}\right)^3. \quad (23)$$

The maximum discrepancy between $\psi_m{}^1$ and ψ_m occurs at the ends of the sweep where $\hat{\omega} - \omega_0 = K$, the maximum frequency deviation.

$$\psi^1 - \psi_m \approx \frac{K}{6v}\left(\frac{2\pi m v}{\Omega}\right)^3 \text{maximum}. \quad (24)$$

The discrepancy between D_m and 1 is given by

$$D_m - 1 = \cos\left[\frac{\sqrt{K^2 - (\hat{\omega} - \omega_0)^2}}{v}\left(1 - \cos\frac{2\pi m v}{\Omega}\right)\right] \pm j \sin\left[\frac{\sqrt{K^2 - (\hat{\omega} - \omega_0)^2}}{v}\left(1 - \cos\frac{2\pi m v}{\Omega}\right)\right] - 1. \quad (25)$$

For small discrepancies this becomes

$$D_m - 1 \approx \pm \frac{j}{2} \frac{\sqrt{K^2 - (\hat{\omega} - \omega_0)^2}}{v}\left(\frac{2\pi m v}{\Omega}\right)^2. \quad (26)$$

This discrepancy is maximum at the center of the frequency sweep $\hat{\omega} - \omega_0 = 0$, where the time rate of change of frequency is maximum. Neglecting the factor $\pm j$, this maximum discrepancy becomes

$$\boxed{D_m - 1 \approx \frac{Kv}{2}\left(\frac{2\pi m}{\Omega}\right)^2 \text{maximum}} \quad (27)$$

The discrepancy given by (24) is nearly always negligible if the discrepancy given by (27) is negligible. Therefore, if the discrepancy given by (27) for a particular problem is small enough to be considered negligible, the validity condition upon the "instantaneous-frequency" method of analysis has been fulfilled. One can establish quantitative ideas about how small the value of (27) must be to be considered negligible by studying the examples in the next section. Most engineers have already established their own personal landmarks concerning the allowable distortion of the terms of a Fourier approximation to a nonsinusoidal function. Fortunately, (27) gives the phase discrepancy of the terms of the Fourier approximation as proportional to m^2, so only the shortest period terms ($m = M$) need usually be considered. The terms for m less than M are distorted much less than the Mth.

A practical procedure which has proven quite satisfactory for using (27) follows. First, decide how far the magnitude of the response envelope can differ from the network characteristic in its most hard-to-follow region before a quasi-steady state ceases to exist. This magnitude may vary from one tenth of one per cent of the peak value of the network characteristic to 50 per cent of the peak, depending entirely upon the requirements and specifications of the equipment being designed. M is then determined such that the sum of the absolute values of all the coefficients of the Fourier approximation beyond the Mth terms is equal to or less than the allowable difference decided upon. It should be pointed out that the sum of the absolute values of the coefficients of the Fourier approximation always converges (and always converges quite rapidly beyond a certain coefficient) since there can be no discontinuities in the function or its derivatives for a physical network characteristic. How to avoid creating extrinsic discontinuities at the ends of the period of the approximation will be discussed in the example in the next section.

Thirdly, the phase displacement of this Mth term of the approximation is investigated by (27). A quasi-steady state is assumed to exist if the discrepancy is less than one third radian or about 20 degrees. This sort of procedure is quite similar to common video-frequency-amplifier design practice. Amplifiers for nonsinusoidal waves are commonly designed to be down less than three decibels, that is, to have less than 45 degrees phase shift, at the frequency of the last significant harmonic of the signal to be amplified. That design criterion is somewhat less conservative than the allowable 20 degrees phase shift assumed here for the last significant harmonic of the network characteristic.

The procedure outlined above is, of course, not foolproof. It is certainly feasible to imagine a Fourier approximation of functions for which the above procedure would not insure the desired fidelity of the output envelope. Such functions, however, are seldom, if ever, encountered in physical networks.

Step-by-Step Procedure for Testing the Validity of the "Instantaneous-Frequency" Method of Analysis

The steps necessary for determining whether or not a quasi-steady state exists are organized and demonstrated in this section. The test is applied to the problems which, when tried experimentally, yielded (a) and (b) in Fig. 2.

A. Investigate the spectrum of the frequency-modulated wave applied to the network, deciding how wide a frequency band need be considered in order to include all the nonnegligible side frequencies of the wave.

Example: The frequency-modulated wave applied to a tuned amplifier to produce (b) in Fig. 2 experimentally is described by the following parameters, which are repeated here for convenience:

$\omega_0 = 2\pi \times 10^6$ ($2\pi \times$ the center frequency)

$K = 2\pi \times 25{,}000$ ($2\pi \times$ the frequency deviation)

$v = 2\pi \times 1000$ ($2\pi \times$ the modulating frequency)

$$m_f = \frac{K}{v} = 25 \quad \text{(the modulation index).}$$

The steady-state spectrum of the frequency-modulated wave is given by (6). The Bessel amplitude coefficients $J_n(m_f)$ of the side frequencies are as follows:[6]

$J_0(25) = 0.0963$	$J_{11}(25) = -0.1682$	$J_{22}(25) = 0.2246$	$J_{33}(25) = 0.001267$
$J_1(25) = -0.1254$	$J_{12}(25) = -0.0729$	$J_{23}(25) = 0.2306$	$J_{34}(25) = 0.000550$
$J_2(25) = -0.1063$	$J_{13}(25) = 0.0983$	$J_{24}(25) = 0.1998$	$J_{35}(25) = 0.000229$
$J_3(25) = 0.1083$	$J_{14}(25) = 0.1751$	$J_{25}(25) = 0.1529$	$J_{36}(25) = 0.000092$
$J_4(25) = 0.1323$	$J_{15}(25) = 0.0978$	$J_{26}(25) = 0.1061$	$J_{37}(25) = 0.000036$
$J_5(25) = -0.0660$	$J_{16}(25) = -0.0577$	$J_{27}(25) = 0.06778$	$J_{38}(25) = 0.000013$
$J_6(25) = -0.1587$	$J_{17}(25) = -0.1717$	$J_{28}(25) = 0.04028$	$J_{39}(25) = 0.000005$
$J_7(25) = -0.0102$	$J_{18}(25) = -0.1758$	$J_{29}(25) = 0.02245$	$J_{40}(25) = 0.000002$
$J_8(25) = 0.1530$	$J_{19}(25) = -0.0814$	$J_{30}(25) = 0.01181$	$J_{41}(25) = 0.000001$
$J_9(25) = 0.1081$	$J_{20}(25) = 0.0520$	$J_{31}(25) = 0.005889$	
$J_{10}(25) = -0.0752$	$J_{21}(25) = 0.1646$	$J_{32}(25) = 0.002795$	

The amplitudes of the side frequencies are certainly negligible beyond the 35th side frequency for any practical application. Therefore, the interval $2\pi \times 0.965 \times 10^6 \leqq \omega \leqq 2\pi \times 1.035 \times 10^6$ contains all the nonnegligible side frequencies.

B. Measure or calculate the steady-state complex-network characteristic $f(\omega)$.

Example: The amplification—frequency and phase-shift—frequency characteristics of a network can be measured. The real part of $f(\omega)$ is then obtained by multiplying the amplification by the cosine of the phase-shift angle. The imaginary part of $f(\omega)$ is obtained by multiplying the amplification by the sine of the phase-shift angle.

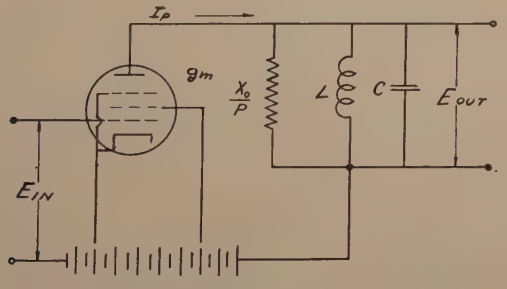

Fig. 3—Simplified schematic of a tuned amplifier.

For several networks, however, it is practical to calculate the network characteristic from its circuit. Fig. 3 is the simplified schematic of a tuned amplifier, for which

$$X_L = -X_C = jX_0 \quad \text{at} \quad \omega_0 \tag{28}$$

[6] Eugen Jahnke and Fritz Emde, "Table of Functions with Formulae and Curves," Dover Publications, New York, N. Y., 1943, p. 179.

$$p = \frac{1}{Q_L} + \frac{X_0}{R_p} = \text{power factor of plate circuit} \tag{29}$$

$$g_m = \frac{-I_p}{E_{in}} \tag{30}$$

$$Z = \frac{1}{\dfrac{p}{X_0} + \dfrac{1}{j\dfrac{\omega}{\omega_0}X_0} - \dfrac{1}{j\dfrac{\omega_0}{\omega}X_0}}$$

$$= X_0 \left[\frac{p}{p^2 + \left(\dfrac{\omega^2 - \omega_0^2}{\omega\omega_0}\right)^2} - j \frac{\dfrac{\omega^2 - \omega_0^2}{\omega\omega_0}}{p^2 + \left(\dfrac{\omega^2 - \omega_0^2}{\omega\omega_0}\right)^2} \right] \tag{31}$$

$$E_{out} = E_{in} g_m Z = E_{in} f(\omega) \tag{32}$$

$$\frac{f(\omega)}{g_m X_0} = \frac{p}{p^2 + \left(\dfrac{\omega^2 - \omega_0^2}{\omega\omega_0}\right)^2} - j \frac{\dfrac{\omega^2 - \omega_0^2}{\omega\omega_0}}{p^2 + \left(\dfrac{\omega^2 - \omega_0^2}{\omega\omega_0}\right)^2}. \tag{33}$$

In Fig. 4, (a) is a plot of the real part of $f(\omega)/g_m X_0$ and (b) is the imaginary part. The square root of the sum of the squares of the real and imaginary parts is the amplification—frequency characteristic (c). The arc tangent of the quotient of the imaginary and real parts of $f(\omega)/g_m X_0$ is the phase-shift—frequency characteristic (d).

C. Approximate the network characteristic by a finite Fourier series over an interval equal to or greater than the essential interval determined in step A.

Example: Unless the network-characteristic function and its derivatives at one end point of the essential interval chosen in step A happen to be equal to the function and its derivatives, respectively, at the opposite end point of the interval, it is necessary to take the following steps to avoid extrinsic discontinuities which would needlessly burden and reduce the accuracy of the Fourier approximation. First, the period for the Fourier approximation should be chosen slightly larger than the interval over which the approximation must accurately

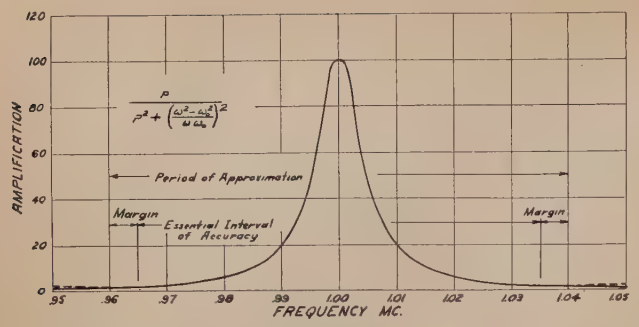

(a)

(a)—Real part of $\frac{f(\omega)}{g_m X_0}$

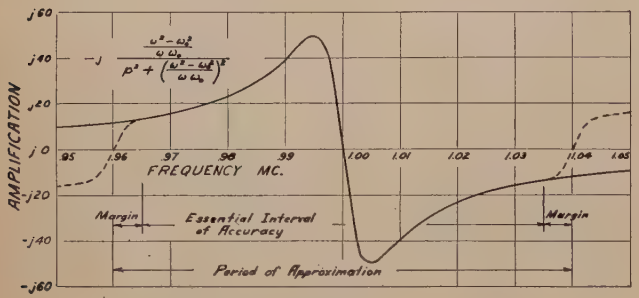

(b)

(b)—Imaginary part of $\frac{f(\omega)}{g_m X_0}$

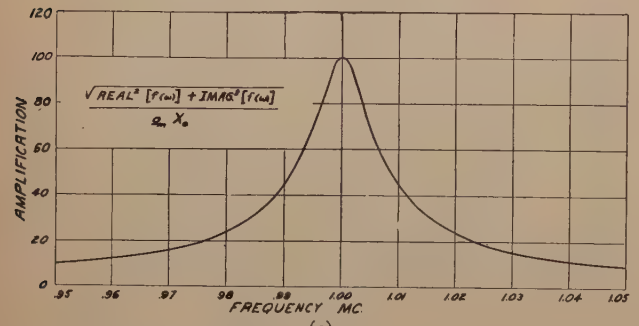

(c)

(c)—Magnitude of $\frac{f(\omega)}{g_m X_0}$

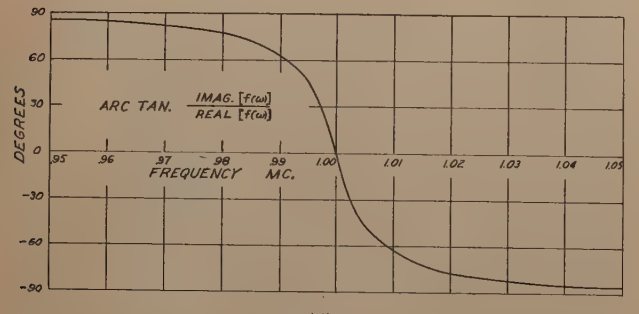

(d)

(d)—Phase of $f(\omega)$.

Fig. 4—Complex-network characteristic of a tuned amplifier.

$$\frac{f(\omega)}{g_m X_0} = \frac{p}{p^2 + \left(\frac{\omega^2 - \omega_0^2}{\omega\omega_0}\right)^2} - j\frac{\frac{\omega^2 - \omega_0^2}{\omega\omega_0}}{p^2 + \left(\frac{\omega^2 - \omega_0^2}{\omega\omega_0}\right)^2}$$

represent the network characteristic. Second, the function should be altered in the two margins where the chosen period overlaps the essential interval of approximation in such a way that the new function has no discontinuities either within the chosen period or at its end points. The artificial function constructed within the margins should be as smooth as possible to avoid its contributing to the higher-order terms of the Fourier approximation.

Recall that the essential interval of approximation was $2\pi\times0.965\times10^6 \leqq \omega \leqq 2\pi\times1.035\times10^6$; let Ω, the period of approximation, be slightly greater, say, $2\pi\times0.960\times10^6 \leqq \omega \leqq 2\pi\times1.040\times10^6$. Then construct an artificial function in the margins of overlap of the intervals ($2\pi\times0.960\times10^6 \leqq \omega \leqq 2\pi\times0.965\times10^6$ and $2\pi\times1.035\times10^6 \leqq \omega \leqq 2\pi\times1.040\times10^6$) that smoothly joins the ends of the period. This artificial function has been dotted into (b) of Fig. 4. In Fig. 4, (a) is so nearly continuous at the end points that no alteration is necessary. The essential interval of approximation and the period of approximation are also indicated.

A 24-point numerical analysis[4] of this improved function in the indicated period yields its Fourier coefficients. When using numerical methods to obtain these coefficients, one must be careful that the signs of the coefficients are correct to place the approximation about ω_0 as required by (11).

$A_0 = 17.9 + j0$	
$A_1 = 26.8 + j0$	$B_1 = 0 - j33.1$
$A_2 = 17.8 + j0$	$B_2 = 0 - j14.3$
$A_3 = 12.2 + j0$	$B_3 = 0 - j14.5$
$A_4 = 8.2 + j0$	$B_4 = 0 - j6.4$
$A_5 = 5.6 + j0$	$B_5 = 0 - j6.6$
$A_6 = 3.8 + j0$	$B_6 = 0 - j2.6$
$A_7 = 2.6 + j0$	$B_7 = 0 - j3.1$
$A_8 = 1.8 + j0$	$B_8 = 0 - j1.0$
$A_9 = 1.3 + j0$	$B_9 = 0 - j1.5$
$A_{10} = 0.9 + j0$	$B_{10} = 0 - j0.3$
$A_{11} = 0.8 + j0$	$B_{11} = 0 - j0.4$
$A_{12} = 0.4 + j0$	

Because the real part of this network characteristic is nearly symmetrical in the period chosen, the B_m's have a negligible real part. Likewise, the imaginary part of this network characteristic is very nearly skew symmetrical in the period chosen; therefore, the A_m's have a negligible imaginary part.

D. Find the maximum phase shift of the Mth component of the network-characteristic approximation by (27). If the maximum phase shift of the Mth component is less than 20 degrees, a quasi-steady state exists.

Example: Suppose that, for this particular problem, the requirements of a quasi-steady state shall be that the response envelope shall nowhere deviate from the network characteristic more than fifteen per cent of its peak value. Following the suggested procedure, it will be found that the sum of the absolute values of the coefficients of the A_m's and B_m's beyond the sixth is

about 14 per cent of the peak magnitude of the function. Therefore, the terms corresponding to $m=M=6$ are the last significant terms of the series.

The problem solved experimentally in (b) of Fig. 2 will now be tested analytically for a quasi-steady state. The parameters K and v have been given, Ω was chosen in step C, and the largest significant value of $m(M=6)$ has been chosen in the preceding paragraph.

$$D_m-1\approx\frac{Kv}{2}\left(\frac{2\pi m}{\Omega}\right)^2$$

$$\approx\frac{2\pi\times25{,}000\times2\pi\times1000}{2}\left(\frac{2\pi\times6}{2\pi\times80{,}000}\right)^2 \quad (27)$$

$\approx$2.8 radians or 160 degrees.

This large phase discrepancy for $m=6$ indicates that a quasi-steady state does not exist, and that the distortion is quite large. This conclusion is confirmed by (b) in Fig. 2.

The series obtained in step C is also adequate for the problem solved experimentally in (a) of Fig. 2, because the spectrum is even more closely confined. Substituting the parameters for (a) of Fig. 2 into (27),

$$D_m-1\approx\frac{2\pi\times25{,}000\times2\pi\times100}{2}\left(\frac{2\pi\times6}{2\pi\times80{,}000}\right)^2$$

$\approx$0.28 radian or 16 degrees.

Since the phase discrepancy for this Mth term is less than 20 degrees, a quasi-steady state (such as postulated) may be assumed to exist. In Fig. 2, (a) bears out this conclusion nicely; the discrepancy between (a) and the static-network response characteristic is obviously everywhere less than 15 per cent of the peak.

Step-by-Step Procedure for Calculating the Response of a Network to a Frequency-Modulated Wave

The necessary steps for evaluating (15) as a function of either t or $\hat{\omega}$ are organized and demonstrated in this section. The amplitude—instantaneous-input-frequency response and phase-shift—instantaneous-input-frequency response of a tuned amplifier will be calculated using the same parameters that were used experimentally to obtain (b) of Fig. 2.

I. Perform steps A, B, and C of the validity-test procedure.

II ($\hat{\omega}$). Prepare work sheets similar to Table I for several equally spaced values of $(\hat{\omega}-\omega_0)$ between zero and K.

Example: There should be work sheets for enough points to determine smooth curves of the amplitude—instantaneous-input-frequency and phase-shift—instantaneous-input-frequency response. Work sheets for $(\hat{\omega}-\omega_0)=2\pi\times2000,\ 2\pi\times4000,\ 2\pi\times6000,\cdots,\ 2\pi\times24{,}000$ were prepared for the example; Table I is the work sheet for $(\hat{\omega}-\omega_0)=2\pi\times6000$.

Table I

Sample Work Sheet for Calculating E_{out}

III	IV	V	VI	VII	VIII	IX	X	XI	XII	XIII
m	Phase of D_m (degrees)	ψ_m (degrees)	A_m	$A_m\cos\psi$ (V)	(VII) cos (IV)	j(VII) sin (IV)	B_m	$B_m\sin\psi$ (V)	(XI) cos (IV)	j(XI) sin (IV)
0	0	0	17.9+j0	17.9+j0	17.9+j0					
1	4.3	27.0	26.8+j0	23.9+j0	23.9+j0	0+j1.8	0−j33.1	0−j14.9	0−j14.9	1.1+j0
2	17.1	53.8	17.8+j0	10.5+j0	10.0+j0	0+j3.1	0−j14.3	0−j11.5	0−j11.1	3.4+j0
3	38.4	80.3	12.2+j0	2.1+j0	1.6+j0	0+j1.3	0−j14.5	0−j14.3	0−j11.2	8.9+j0
4	68	106	8.2+j0	−2.3+j0	−0.9+j0	0−j2.1	0− j6.4	0− j6.1	0− j2.3	5.7+j0
5	106	132	5.6+j0	−3.7+j0	1.0+j0	0−j3.6	0− j6.6	0− j4.9	0+ j1.3	4.7+j0
6	152	156	3.8+j0	−3.5+j0	3.1+j0	0−j1.6	0− j2.6	0− j1.1	0+ j1.0	0.5+j0
7	205	180	2.6+j0	−2.6+j0	2.4+j0	0+j1.1	0− j3.1	0+ j0	0+ j0	0 +j0
8	266	202	1.8+j0	−1.7+j0	0.1+j0	0+j1.7	0− j1.0	0+ j0.4	0+ j0	0.4+j0
9	333	223	1.3+j0	−1.0+j0	−0.9+j0	0+j0.5	0− j1.5	0+ j1.0	0+ j0.9	0.5+j0
10	407	243	0.9+j0	−0.4+j0	−0.3+j0	0−j0.3	0− j0.3	0+ j0.3	0+ j0.2	−0.2+j0
11	487	262	0.8+j0	−0.1+j0	0.1+j0	0−j0.1	0− j0.4	0+ j0.4	0− j0.3	−0.3+j0
12	572	278	0.4+j0	0.1+j0	−0.1+j0	0−j0.1				
$\hat{\omega}-\omega_0=2\pi\times6000$ or $vt=$ _____				TOTALS	57.9+j0	0+j1.7			0−j36.4	24.7+j0

$Q=(57.9+j0)+(0+j1.7)+(0-j36.4)+(24.7+j0)=82.6-j34.7=89.5/-22.8$ degrees

$R=(57.9+j0)-(0+j1.7)+(0-j36.4)-(24.7+j0)=33.2-j38.1=50.5/-48.9$ degrees

$S=(57.9+j0)+(0+j1.7)-(0-j36.4)-(24.7+j0)=33.2+j38.1=50.5/\ 48.9$ degrees

$T=(57.9+j0)-(0+j1.7)-(0-j36.4)+(24.7+j0)=82.6+j34.7=89.5/\ 22.8$ degrees

II (t). Prepare work sheets similar to Table I for several equally spaced values of vt between zero and $\pi/2$ (90 degrees).

III. Into column III enter the orders of the Fourier coefficients obtained in step C.

This column is the same for all the work sheets.

IV ($\hat{\omega}$). Into column IV enter the value of

$$\frac{\sqrt{K^2-(\hat{\omega}-\omega_0)^2}}{v}\left(1-\cos\frac{2\pi mv}{\Omega}\right)\times 57.3 \text{ degrees.}$$

Example: The parameters K and v are given. The period Ω was chosen in step *C*. A value of $(\hat{\omega}-\omega_0)$ is assigned to each calculation sheet; the value assigned to Table I is $(\hat{\omega}-\omega_0)=2\pi\times 6000$. Thus, for $m=2$,

$$\text{IV} = \frac{\sqrt{(2\pi\times 25{,}000)^2-(2\pi\times 6000)^2}}{2\pi\times 1000}\cdot\left(1-\cos\frac{2\pi\times 2\times 2\pi\times 1000}{2\pi\times 80{,}000}\right)\times 57.3$$

$$=17.1 \text{ degrees}$$

IV (t). Into column IV enter the value of

$$57.3\times\frac{K}{v}\sin vt\left(1-\cos\frac{2\pi mv}{\Omega}\right)\text{ degrees.}$$

V ($\hat{\omega}$). Into column V enter the value of

$$57.3\times\frac{\hat{\omega}-\omega_0}{v}\sin\frac{2\pi mv}{\Omega}\text{ degrees.}$$

Example: For $m=2$ on the work sheet for $(\hat{\omega}-\omega_0)=2\pi\times 6000$,

$$V = 57.3\times\frac{2\pi\times 6000}{2\pi\times 1000}\sin\frac{2\pi\times 2\times 2\pi\times 1000}{2\pi\times 80{,}000}$$

$$= 53.8 \text{ degrees.}$$

V (t). Into column V enter the value of

$$57.3\times\frac{K}{v}\cos vt\sin\frac{2\pi mv}{\Omega}\text{ degrees.}$$

VI. Enter the A_m's obtained in step C into column VI.

Example: From step C, $A_2=17.8+j0$. This column is the same for all the work sheets.

VII. Multiply the A_m's, column VI, by the cosine of the angle in column V and enter the result into column VII.

Example: For $m=2$,

$$(17.8+j0)\cos 53.8 \text{ degrees} = 10.5+j0.$$

VIII. Multiply column VII by the cosine of the angle in column IV and enter the result into column VIII.

Example: For $m=2$,

$$(10.5+j0)\cos 17.1 \text{ degrees} = 10.0+j0.$$

IX. Multiply column VII by j sine of the angle in column IV and enter the result into column IX.

Example: For $m=2$,

$$j(10.5+j0)\sin 17.1 \text{ degrees} = 0+j3.1.$$

X. Enter the B_m's obtained in step C into column X.

Example: From step C, $B_2=0-j14.3$. This column is the same for all the work sheets.

XI. Multiply the B_m's, column X, by the sine of the angle in column V and enter the result into column XI.

Example: For $m=2$,

$$(0-j14.3)\sin 53.8 \text{ degrees} = 0-j11.5.$$

XII. Multiply column XI by the cosine of the angle in column IV and enter the result into column XII.

Example: For $m=2$,

$$(0-j11.5)\cos 17.1 \text{ degrees} = 0-j11.1.$$

XIII. Multiply column XI by j sine of the angle in column IV and enter the result into column XIII.

Example: For $m=2$,

$$j(0-j11.5)\sin 17.1 \text{ degrees} = 3.4+j0.$$

XIV. Total columns VIII, IX, XII, and XIII on each work sheet. (See Table I.)

XV. Calculate the following quantities for each work sheet and express the result in polar form.

$$Q = \text{VIII} + \text{IX} + \text{XII} + \text{XIII}$$
$$R = \text{VIII} - \text{IX} + \text{XII} - \text{XIII}$$
$$S = \text{VIII} + \text{IX} - \text{XII} - \text{XIII}$$
$$T = \text{VIII} - \text{IX} - \text{XII} + \text{XIII}$$

where VIII, IX, XII, and XIII are the totals obtained in step XIV. (See Table I.)

XVI ($\hat{\omega}$). For each of the work sheets prepared for different assigned values of $(\hat{\omega}-\omega_0)$, plot on the response graphs,

Q = the upsweep response at $\omega_0+(\hat{\omega}-\omega_0)$
R = the downsweep response at $\omega_0+(\hat{\omega}-\omega_0)$
S = the upsweep response at $\omega_0-(\hat{\omega}-\omega_0)$
T = the downsweep response at $\omega_0-(\hat{\omega}-\omega_0)$.

The magnitudes of Q, R, S, and T for each work sheet give four points on the desired amplitude—instantaneous-input-frequency response curve. The phases of Q, R, S, and T give four points on the desired phase-shift—instantaneous-input-frequency response curve.

Example: For Table I,

$Q=89.5\,/\underline{-22.8 \text{ degrees}}$ = the upsweep response at $\hat{\omega}=2\pi\times 1.006\times 10^6$

$R=50.5\,/\underline{-48.9 \text{ degrees}}$ = the downsweep response at $\hat{\omega}=2\pi\times 1.006\times 10^6$

$S=50.5\,/\underline{48.9 \text{ degrees}}$ = the upsweep response at $\hat{\omega}=2\pi\times 0.994\times 10^6$

$T=89.5\,/\underline{22.8 \text{ degrees}}$ = the downsweep response at $\hat{\omega}=2\pi\times 0.994\times 10^6$

Plotting the points obtained on work sheets for $(\hat{\omega}-\omega_0)=2\pi\times 2000, 2\pi\times 4000, 2\pi\times 6000, \cdots, 2\pi\times 24{,}000$ determines curves (a) and (b) of Fig. 5. In this particular problem the upsweep response is symmetrical with the downsweep response because the steady-state network characteristic is symmetrical about ω_0. Note that

curve (a) of Fig. 5, the calculated amplitude—instantaneous-input-frequency response, agrees very closely with (b) of Fig. 2, the experimental amplitude—instantaneous-input-frequency response. The reader may be interested in comparing the results of the calculation with the results obtained by Roder on a very similar problem, which he solved by the aid of a differential analyzer. His response curve was plotted as a function of time.[7]

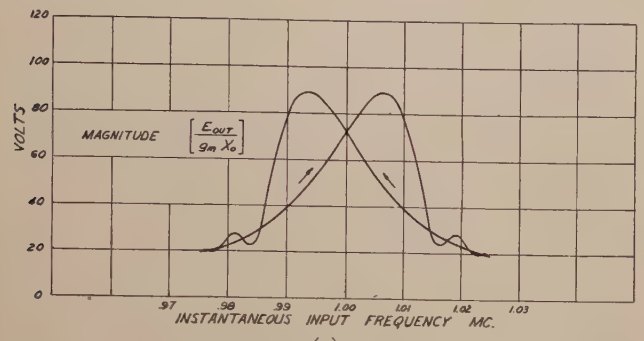

(a)

(a)—Amplitude of $\frac{E_{out}}{g_m X_0}$

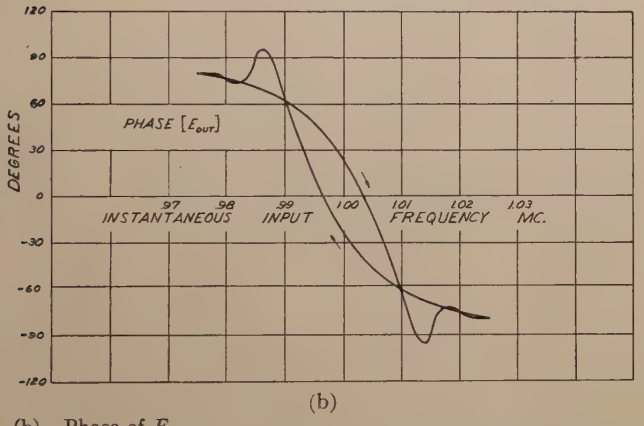

(b)

(b)—Phase of E_{out}.

Fig. 5—Calculated amplitude—instantaneous-input-frequency and phase-shift—instantaneous-input-frequency response of a tuned amplifier to a frequency-modulated wave.

Effective Q of amplifier	$=100$	$(p=0.01)$
Center frequency	$=10^6$	$(\omega_0=2\pi\times10^6)$
Modulating frequency	$=1000$	$(v=2\pi\times1000)$
Total frequency excursion	$=50{,}000$	$(K=2\pi\times25{,}000)$

XVI (t). For each of the work sheets prepared for different assigned values of vt, plot on the response graphs.

Q = the response at $2\pi - vt$
R = the response at vt
S = the response at $\pi + vt$
T = the response at $\pi - vt$.

The magnitudes of Q, R, S, and T for each work sheet give four points on the desired amplitude—time response curve. The phases of Q, R, S, and T give four points on the desired phase-shift—time-response curve.

[7] Hans Roder, "Effects of tuned circuits upon a frequency-modulated signal," PROC. I.R.E., vol. 25, pp. 1617–1648; December, 1937.

APPENDIX

If a steady-state driving voltage $\epsilon^{j\omega t}$ is applied to the input terminals of a linear network, it can be shown that the steady-state solution for the voltage at the output terminals[8] is of the form $R(\omega)\epsilon^{j[\omega t+\theta(\omega)]}$. $R(\omega)$ is the ratio of the peak amplitudes of the output and input voltages, and $\theta(\omega)$ is the phase difference. Abbreviating $\epsilon^{j\omega t}$ as E_{in}^{+} and $R(\omega)\epsilon^{j[\omega t+\theta(\omega)]}$ as E_{out}^{+}, it follows that

$$E_{out}^{+} = E_{in}^{+}R(\omega)\epsilon^{j\theta(\omega)}. \tag{34}$$

Furthermore, if a steady-state driving voltage $\epsilon^{-j\omega t}$ is applied to the input terminals of the same linear network, it can be shown that the voltage at the output terminals is of the form $R(\omega)\epsilon^{-j[\omega t+\theta(\omega)]}$, where R and θ are equal to R and θ of (34). Setting $\epsilon^{-j\omega t}$ as E_{in}^{-} and $R(\omega)\epsilon^{-j[\omega t+\theta(\omega)]}$ as E_{out}^{-} it follows that

$$E_{out}^{-} = E_{in}^{-}R(\omega)\epsilon^{-j\theta(\omega)}. \tag{35}$$

Therefore, if a steady-state driving voltage sin ωt is applied to the input terminals of the network, the output voltage can be determined as follows:

$$E_{in} = \sin \omega t = \frac{\epsilon^{j\omega t} - \epsilon^{-j\omega t}}{2j}. \tag{36}$$

By (34) and (35),

$$E_{out} = \frac{R(\omega)\epsilon^{j[\omega t+\theta(\omega)]} - R(\omega)\epsilon^{-j[\omega t+\theta(\omega)]}}{2j}$$

$$= R(\omega)\sin[\omega t + \theta(\omega)]. \tag{37}$$

$R(\omega)\epsilon^{j\theta(\omega)}$ is now defined as the complex network characteristic, $f(\omega)$. It can be seen from (36) and (37) that

$$E_{out}\{=\}E_{in}f(\omega) \tag{8}$$

where

$$|f(\omega)| = \frac{\text{amplitude of } E_{out}}{\text{amplitude of } E_{in}} \tag{9}$$

and where

$$\arctan\frac{\text{imaginary }[f(\omega)]}{\text{real }[f(\omega)]} = \text{angular phase }[E_{out}] - \text{angular phase }[E_{in}]. \tag{10}$$

The notation $\{=\}$ in (8) means "equals by convention," because the right- and left-hand members of the equation are not mathematically equivalent except when $\theta(\omega)=n\pi$.

Note also from (34) and (35) that

$$E_{out}^{+} = E_{in}^{+}f(\omega) \tag{38}$$

and

$$E_{out}^{-} = E_{in}^{-}f^{*}(\omega) \tag{39}$$

[8] H. Pender and S. Warren, "Electric Circuits and Fields," McGraw-Hill Book Company, New York, N. Y., 1943, pp. 161–163.

where $f^*(\omega)$ = the complex conjugate of $f(\omega)$. (40)

The = signs of (38) and (39) indicate exact mathematical equivalence. Only the $\{=\}$ sign of (8) is restricted.

Equation (7), which expresses the input frequency-modulation voltage as a spectrum of steady-state side frequencies, is repeated here for convenience.

$$\begin{aligned} e_{in} &= J_0(m_f)\sin\omega_0 t \\ &+ \sum_{n=1}^{N}\Big(J_{2n-1}(m_f)\{\sin[\omega_0+(2n-1)v]t \\ &- \sin[\omega_0-(2n-1)v]t\} \\ &+ J_{2n}(m_f)\{\sin[\omega_0+2nv]t+\sin[\omega_0-2nv]t\}\Big). \quad (7) \end{aligned}$$

Since $J_n(z)=(-1)^nJ_{-n}(z)$, equation (7) can be compressed as follows:

$$e_{in} = \sum_{\eta=-2N}^{2N} J_\eta(m_f)\sin(\omega_0+\eta v)t. \quad (41)$$

Changing $\sin(\omega_0+\eta v)t$ to exponential form,

$$2je_{in} = \sum_{\eta=-2N}^{2N} J_\eta(m_f)\left[\epsilon^{j(\omega_0+\eta v)t} - \epsilon^{-j(\omega_0+\eta v)t}\right]. \quad (42)$$

The steady-state output oscillation corresponding to each steady-state oscillation of the frequency-modulated input spectrum is given by (38) and (39).

$$E_{out}^{+}[\text{for } E_{in}^{+} = \epsilon^{j(\omega_0+\eta v)t}] = \epsilon^{j(\omega_0+\eta v)t}f(\omega_0+\eta v) \quad (43)$$

and

$$E_{out}^{-}[\text{for } E_{in}^{-} = \epsilon^{-j(\omega_0+\eta v)}] = \epsilon^{-j(\omega_0+\eta v)t}\,f^*(\omega_0+\eta v) \quad (44)$$

Equation (11) gives the values of $f(\omega_0+\eta v)$ and $f^*(\omega_0+\eta v)$.

$$f(\omega_0+\eta v) \approx \sum_{m=0}^{M}(A_m\cos km\eta v + B_m\sin km\eta v) \quad (45)$$

and

$$f^*(\omega_0+\eta v) \approx \sum_{m=0}^{M}(A_m^*\cos km\eta v + B_m^*\sin km\eta v) \quad (46)$$

where

$$k = \frac{2\pi}{\Omega}. \quad (47)$$

The output-voltage equation can now be written from (42), (43), and (44).

$$\begin{aligned} 2je_{out} = \sum_{m=0}^{M}\sum_{\eta=-2N}^{2N} J_\eta(m_f)\big[&\epsilon^{j(\omega_0+\eta v)t}(A_m\cos km\eta v + B_m\sin km\eta v) \\ &-\epsilon^{-j(\omega_0+\eta v)t}(A_m^*\cos km\eta v + B_m^*\sin km\eta v)\big]. \quad (48) \end{aligned}$$

Changing $\cos km\eta v$ and $\sin km\eta v$ to exponential form,

$$\begin{aligned} 2je_{out} = \sum_{m=0}^{M}\sum_{\eta=-2N}^{2N} J_\eta(m_f)\Big[&\frac{A_m}{2}\left(\epsilon^{j[(\omega_0+\eta v)t+km\eta v]} + \epsilon^{j[(\omega_0+\eta v)t-km\eta v]}\right) \\ &+ \frac{B_m}{2j}\left(\epsilon^{j[(\omega_0+\eta v)t+km\eta v]} - \epsilon^{j[(\omega_0+\eta v)t-km\eta v]}\right) \\ &- \frac{A_m^*}{2}\left(\epsilon^{j[-(\omega_0+\eta v)t+km\eta v]} + \epsilon^{j[-(\omega_0+\eta v)t-km\eta v]}\right) \\ &- \frac{B_m^*}{2j}\left(\epsilon^{j-[(\omega_0+\eta v)t+km\eta v]} - \epsilon^{j-[(\omega_0+\eta v)t-km\eta v]}\right)\Big]. \quad (49) \end{aligned}$$

The Bessel coefficients are combined with the exponentials by the use of the relation,

$$\sum_{\eta=-2N}^{2N} J_\eta(m_f)\epsilon^{j\eta\theta} \approx \epsilon^{jm_f\sin\theta},$$

which is accurate because the $J_\eta(m_f)$'s below $\eta=-2N$ and above $\eta=2N$ are negligible by the definition of N.

$$\begin{aligned} 2je_{out} = \sum_{m=0}^{M}\Big[&\frac{A_m}{2}\left(\epsilon^{j[\omega_0 t+m_f\sin(vt+kmv)]}\right. \\ &\left.+\epsilon^{j[\omega_0 t+m_f\sin(vt-kmv)]}\right) \\ &+\frac{B_m}{2j}\left(\epsilon^{j[\omega_0 t+m_f\sin(vt+kmv)]}\right. \\ &\left.-\epsilon^{j[\omega_0 t+m_f\sin(vt-kmv)]}\right) \\ &-\frac{A_m^*}{2}\left(\epsilon^{j[-\omega_0 t+m_f\sin(-vt+kmv)]}\right. \\ &\left.+\epsilon^{j[-\omega_0 t+m_f\sin(-vt-kmv)]}\right) \\ &-\frac{B_m^*}{2j}\left(\epsilon^{j[-\omega_0 t+m_f\sin(-vt+kmv)]}\right. \\ &\left.-\epsilon^{j[-\omega_0 t+m_f\sin(-vt-kmv)]}\right)\Big]. \quad (50) \end{aligned}$$

Expanding $\sin(vt\pm kmv)$ and factoring the exponentials,

$$\begin{aligned} 2je_{out} = \sum_{m=0}^{M}\Big[&\frac{A_m}{2}\left(\epsilon^{j(\omega_0 t+m_f\sin vt\cos kmv)}\right)\left(\epsilon^{jm_f\cos vt\sin kmv}\right. \\ &\left.+\epsilon^{-jm_f\cos vt\sin kmv}\right) \\ &+\frac{B_m}{2j}\left(\epsilon^{j(\omega_0 t+m_f\sin vt\cos kmv)}\right)\left(\epsilon^{jm_f\cos vt\sin kmv}\right. \\ &\left.-\epsilon^{-jm_f\cos vt\sin kmv}\right) \\ &-\frac{A_m^*}{2}\left(\epsilon^{-j(\omega_0 t+m_f\sin vt\cos kmv)}\right)\left(\epsilon^{jm_f\cos vt\sin kmv}\right. \\ &\left.+\epsilon^{-jm_f\cos vt\sin kmv}\right) \\ &-\frac{B_m^*}{2j}\left(\epsilon^{-j(\omega_0 t+m_f\sin vt\cos kmv)}\right)\left(\epsilon^{jm_f\cos vt\sin kmv}\right. \\ &\left.-\epsilon^{-jm_f\cos vt\sin kmv}\right)\Big]. \quad (51) \end{aligned}$$

Factoring $\epsilon^{\pm j(\omega_0 t + m_f \sin vt \cos kmv)}$ and changing the other exponentials to trigonometric form,

$$2je_{out} = \sum_{m=0}^{M} [A_m \cos (m_f \cos vt \sin kmv)\epsilon^{jm_f \sin vt(\cos kmv-1)}\epsilon^{j(\omega_0 t+m_f \sin vt)}$$
$$+ B_m \sin (m_f \cos vt \sin kmv)\epsilon^{jm_f \sin vt(\cos kmv-1)}\epsilon^{j(\omega_0 t+m_f \sin vt)}$$
$$- A_m^* \cos (m_f \cos vt \sin kmv)\epsilon^{-jm_f \sin vt(\cos kmv-1)}\epsilon^{-j(\omega_0 t+m_f \sin vt)}$$
$$- B_m^* \sin (m_f \cos vt \sin kmv)\epsilon^{-jm_f \sin vt(\cos kmv-1)}\epsilon^{-j(\omega_0 t+m_f \sin vt)}]. \quad (52)$$

$$2je_{out} = \epsilon^{j(\omega_0 t+m_f \sin vt)} \sum_{m=0}^{M} D_m[A_m \cos \psi_m + B_m \sin \psi_m] - \epsilon^{-j(\omega_0 t+m_f \sin vt)} \sum_{m=0}^{M} D_m^*[A_m^* \cos \psi_m + B_m^* \sin \psi_m] \quad (53)$$

where

$$D_m(t) = \cos\left[\frac{K}{v} \sin vt\left(1 - \cos\frac{2\pi mv}{\Omega}\right)\right]$$
$$- j \sin\left[\frac{K}{v} \sin vt\left(1 - \cos\frac{2\pi mv}{\Omega}\right)\right] \quad (16)$$

and where $$\psi_m(t) = \frac{K}{v} \cos vt \sin\frac{2\pi mv}{\Omega}. \quad (17)$$

It is easy to derive $D_m(\hat{\omega})$ and $\psi_m(\hat{\omega})$ from (16) and (17) by starting with (5), which relates $\hat{\omega}$ and t.

$$\hat{\omega} = \omega_0 + K \cos vt \quad (5)$$

$$\cos vt = \frac{\hat{\omega} - \omega_0}{K} \quad (54)$$

$$\sin vt = \frac{\pm\sqrt{K^2 - (\hat{\omega} - \omega_0)^2}}{K}. \quad (55)$$

Substituting for $\sin vt$ in (16),

$$D_m(\hat{\omega}) = \cos\left[\frac{\sqrt{K^2-(\hat{\omega}-\omega_0)^2}}{v}\left(1-\cos\frac{2\pi mv}{\Omega}\right)\right]$$
$$\pm j \sin\left[\frac{\sqrt{K^2-(\hat{\omega}-\omega_0)^2}}{v}\left(1-\cos\frac{2\pi mv}{\Omega}\right)\right]. \quad (18)$$

Substituting for $\cos vt$ in (17),

$$\psi_m(\hat{\omega}) = \frac{\hat{\omega} - \omega_0}{v} \sin\frac{2\pi mv}{\Omega}. \quad (19)$$

Equation (53) can be changed from exponential form to sinusoidal form as follows:

Let $$P = \left|\sum_{m=0}^{M} D_m[A_m \cos \psi_m + B_m \sin \psi_m]\right| \quad (56)$$

and

$$\phi = \arctan \frac{\text{imaginary}\left\{\sum_{m=0}^{M} D_m[A_m \cos \psi_m + B_m \sin \psi_m]\right\}}{\text{real}\left\{\sum_{m=0}^{M} D_m[A_m \cos \psi_m + B_m \sin \psi_m]\right\}}. \quad (57)$$

Then

$$2je_{out} = \epsilon^{j(\omega_0 t+m_f \sin vt)}P\epsilon^{j\phi} - \epsilon^{-j(\omega_0 t+m_f \sin vt)}P\epsilon^{-j\phi} \quad (58)$$

$$e_{out} = \frac{P}{2j}\left[\epsilon^{j(\omega_0 t+m_f \sin vt+\phi)} - \epsilon^{-j(\omega_0 t+m_f \sin vt+\phi)}\right] \quad (59)$$

$$e_{out} = P \sin (\omega_0 t + m_f \sin vt + \phi). \quad (60)$$

The output-voltage-envelope equation, therefore, written in conventional form is

$$E_{out}\{=\} \sum_{m=0}^{M} D_m[A_m \cos \psi_m + B_m \sin \psi_m]. \quad (15)$$

The notation $\{=\}$ again means "equals by convention"; the amplitude of the envelope is the absolute value of the complex summation, and the angular phase difference between the output and input frequency-modulated waves is equal to the phase of the complex summation.

Acknowledgment

The author wishes to express his appreciation for the many suggestions and constructive criticisms of this paper in the draft stage offered by members of the Test Engineering Section of RCA Victor, and to the department management, who supplied laboratory and clerical facilities; Mr. L. C. Smith suggested that this material be prepared for publication, and supervised the work. Mr. M. S. Corrington of the Advanced Development Section recommended changes that strengthened the text, suggested identities which greatly simplified the appendix, and cited additional pertinent references.

Analysis of a Resistance-Capacitance Parallel-T Network and Applications*

A. E. HASTINGS†, ASSOCIATE, I.R.E.

Summary—**A resistance-capacitance parallel-T network is analyzed to find the conditions for a null in output and the transfer characteristic. Its use in the return circuit of a feedback amplifier is considered, and the bandwidth of the resulting tuned amplifier is found. The requirements for stability of the amplifier and for its use as an oscillator are discussed.**

Introduction

NETWORKS which have the property of null balance at one frequency are well known. The Wien bridge is such a network of the four-terminal type, using only resistance and capacitance as elements. A three-terminal equivalent has recently come into use.[1,2] This form has the advantage of a common input and output terminal and does not require a special transformer in many applications.

With such a network in the inverse feedback circuit of an amplifier, there results a tuned amplifier with a number of advantages, particularly at audio frequencies. A number of applications of this amplifier to the design of instruments have been made.[3–6] The purpose of this work is to analyze in some detail the null network and its use in a tuned amplifier.

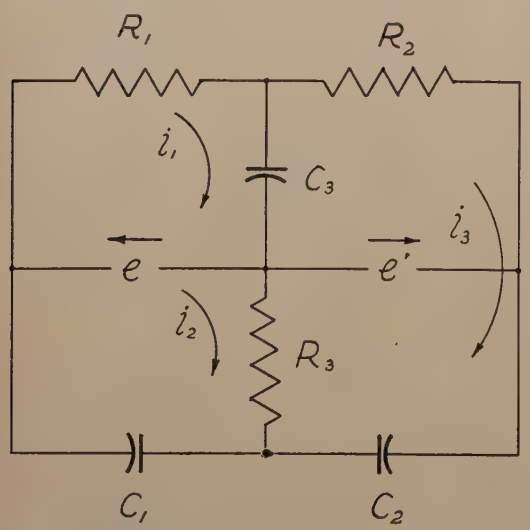

Fig. 1—Parallel-T network with general R's and C's.

Conditions for a Null

A three-terminal parallel-T network which contains only resistive and capacitive elements is shown in Fig. 1. In this illustration, e is the input voltage with angular velocity ω, and it is desired to find the conditions for a null in output voltage e'. The impedance across e' is assumed throughout this analysis to be infinite, a condition which can in most cases be closely approximated. Four independent circuit equations can be written. These are

$$\left.\begin{aligned} e - i_1\left(R_1 - \frac{j}{\omega C_3}\right) + i_3\left(-\frac{j}{\omega C_3}\right) &= 0 \\ e + i_2\left(R_3 - \frac{j}{\omega C_1}\right) - i_3(R_3) &= 0 \\ e' - i_1\left(-\frac{j}{\omega C_3}\right) + i_3\left(R_2 - \frac{j}{\omega C_3}\right) &= 0 \\ e' + i_2(R_3) - i_3\left(R_3 - \frac{j}{\omega C_2}\right) &= 0 \end{aligned}\right\}. \qquad (1)$$

If $e'=0$, for a null, these reduce to a set of four linear homogeneous equations with four variables, e, i_1, i_2, and i_3. The necessary and sufficient condition that the variables shall have values other than zero is that the determinant of the coefficients shall be zero. This gives the conditions on the R's and C's and on ω for a null. Expanding this determinant and equating to zero gives the equation

$$R_1R_2R_3 - \frac{R_3}{\omega_0^2C_2C_3} - \frac{R_3}{\omega_0^2C_1C_3} - j\frac{R_2R_3}{\omega_0C_3} - j\frac{R_1R_3}{\omega_0C_3} + j\frac{1}{\omega_0^3C_1C_2C_3} = 0$$

where ω_0 is the value of ω for a null. Equating both real and imaginary parts of this equation to zero, these conditions are obtained:

$$\omega_0^2 = \frac{C_1+C_2}{R_1R_2C_1C_2C_3} \quad \text{and} \quad (R_1+R_2)(C_1+C_2)R_3 - R_1R_2C_3 = 0.$$

If the T's are made symmetrical, $R_1=R_2=R$ and $C_1=C_2=C$, and the conditions for a null become

$$\omega_0 = \frac{1}{\sqrt{2n}\,RC} \qquad (2)$$

and

* Decimal classification: R140×R363.1. Original manuscript received by the Institute, May 3, 1945; revised manuscript received, August 31, 1945.

† Naval Research Laboratory, Washington, D. C.

[1] W. N. Tuttle, "Bridged-T and parallel-T null circuits for measurements at radio frequencies," PROC. I.R.E., vol. 28, pp. 23–30; January, 1940.

[2] Mathematics Tables Project, "Characteristics of Resistance-Capacitance Electrical Networks," 50 Church St., New York, N. Y., 1942.

[3] H. H. Scott, "A new type of selective circuit and some applications," PROC. I.R.E., vol. 26, pp. 226–236; February, 1938.

[4] L. A. Meacham, "The bridge-stabilized oscillator," PROC. I.R.E., vol. 26, pp. 1278–1295; October, 1938.

[5] H. H. Scott, "An analyzer for sub-audible frequencies," *Jour. Acous. Soc. Amer.*, vol. 13, pp. 360–362; April, 1942.

[6] W. G. Shepherd and R. O. Wise, "Variable-frequency bridge-type frequency-stabilized oscillators," PROC. I.R.E., vol. 31, pp. 256–269; June, 1943.

$$\frac{R_3}{R} = \frac{C_3}{4C} = n \tag{3}$$

where n is a positive number which can be chosen arbitrarily to obtain certain desired characteristics. The network then appears as in Fig. 2.

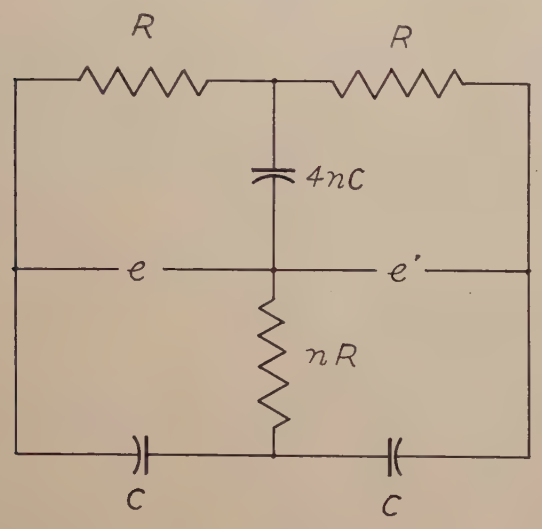

Fig. 2—Network as used in the tuned amplifier.

The null conditions also hold for any impedance across e', since when e' is zero the current distribution is not affected by whatever value of impedance is used in shunt.

Transfer Characteristic

The transfer characteristic β of the network in Fig. 2, with infinite impedance across e', will now be found. This is the ratio of e' to e as a function of frequency. The set of equations (1) represents this circuit if $R_1=R_2=R=R_3/n$ and $C_1=C_2=C=C_3/4n$. Making these substitutions and solving for the voltage ratio, the transfer characteristic is found to be

$$\beta=\frac{e'}{e}=\frac{4n^2\alpha^3-2n\alpha+j(-2n\alpha^2+1)}{4n^2\alpha^3-6n\alpha-2\alpha+j(-8n^2\alpha^2-6n\alpha^2+1)} \tag{4}$$

where $\alpha=\omega RC$. Let the frequency of the applied voltage e be restricted to small variations about the null frequency given by

$$f_0 = \frac{\omega_0}{2\pi} = \frac{1}{2\pi RC\sqrt{2n}}.$$

Then

$$f = f_0\left(1+\frac{\Delta f}{f_0}\right)$$

where $\Delta f/f_0 \ll 1$, and

$$\alpha = 2\pi fRC = 2\pi RCf_0\left(1+\frac{\Delta f}{f_0}\right) = \frac{1}{\sqrt{2n}}\left(1+\frac{\Delta f}{f_0}\right).$$

Substituting this value of α in (4) and making approximations for Δf small,

$$\beta = j\frac{\Delta f\sqrt{2n}}{f_0(2n+1)}. \tag{5}$$

This indicates that, at a frequency near that for a null, the phase of the output voltage e' is shifted 90 degrees from that of the input voltage e, its amplitude is proportional to the frequency deviation from that of the null, and its phase changes discontinuously by 180 degrees as the frequency passes through that of the null. For certain applications it is desired that β change as rapidly as possible with frequency about the null point, or that the slope of the $|\beta|$ versus Δf curve be as great as possible. This slope is

$$s = \frac{d|\beta|}{d(\Delta f)} = \frac{\sqrt{2n}}{(2n+1)f_0}.$$

Now n is still arbitrary, and if the slope is made a maximum by varying n so that $ds/dn=0$, n is found to be $\frac{1}{2}$. For this value, β in (4) becomes

$$\beta = \frac{\alpha^3-\alpha+j(-\alpha^2+1)}{\alpha^3-5\alpha+j(-5\alpha^2+1)}. \tag{6}$$

For Δf small as in (5)

$$\beta = j\frac{\Delta f}{2f_0}.$$

Use in the Feedback Circuit of an Amplifier

The use of a parallel-T network in a vacuum-tube circuit to obtain a tuned amplifier will be discussed. Suppose the output of an amplifier with a flat gain-frequency characteristic is returned to the input in such a way

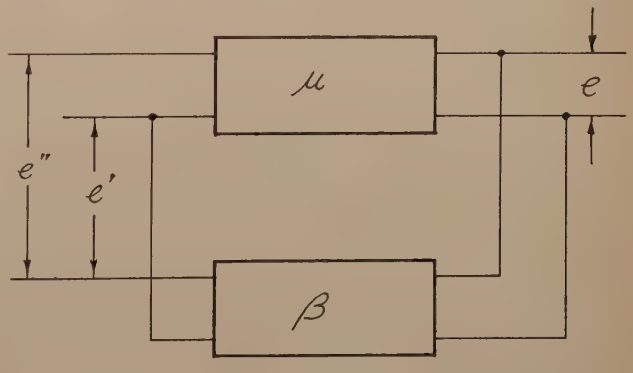

Fig. 3—Arrangement of feedback in the tuned amplifier.

that the amplifier is highly degenerative at any input frequency. A null network inserted in the return circuit will leave the degeneration unchanged at all frequencies except those near the null frequency of the network. At the null frequency the amplifier has no degeneration and operates with maximum gain. Such an arrangement is shown in Fig. 3, where the output of the null network

e' is connected in series with the input e'' in such a way that the resultant input to the amplifier is decreased. The bandwidth of such a tuned amplifier is of interest.

If μ is the normal gain of the amplifier without feedback, A its gain with feedback, and β the transfer characteristic of the feedback network, the well-known relation holds

$$A = \frac{\mu}{1 + \mu\beta}. \tag{7}$$

If β is determined by a parallel-T network, it has the value given in (5), and the gain becomes

$$A = \frac{\mu}{1 + j\dfrac{\mu\Delta f\sqrt{2n}}{f_0(2n+1)}}.$$

If μ is real, the absolute value of the gain is

$$|A| = \frac{\mu}{\sqrt{1 + \dfrac{2n\mu^2(\Delta f)^2}{f_0^2(2n+1)^2}}}.$$

At the null frequency of the network, Δf will be zero, and the gain will be μ. Suppose Δf has a value δ such that the gain is $\sqrt{2}/2$ times that at the null frequency, or

$$\frac{\sqrt{2}}{2}\mu = |A|.$$

Then δ is defined as the half bandwidth, and is given by

$$\delta = \frac{(2n+1)f_0}{\mu\sqrt{2n}}. \tag{8}$$

If n is varied to make the bandwidth smallest for given values of μ and f_0, n is found to be again $\frac{1}{2}$. For this value of n, the half bandwidth becomes

$$\delta = \frac{2f_0}{\mu}. \tag{9}$$

It is seen that the bandwidth increases directly with null frequency and can be made small by increasing the normal gain of the amplifier μ. Since, in a tuned circuit, Q is defined as the ratio of the resonant frequency to the bandwidth,

$$Q = \frac{f_0}{2\delta} = \frac{\mu}{4}.$$

Stability of the Amplifier and Use as an Oscillator

In a practical amplifier of the form here described, it is found that oscillation will occur under certain conditions. This section is concerned with the determination of these conditions. If (6) is rationalized, it becomes

$$\beta = \frac{(\alpha^2 - 1)(\alpha^2 - 1 + j4\alpha)}{\alpha^4 + 14\alpha^2 + 1}.$$

Let this be the value of β in (7),

$$A = \frac{\mu}{1 + \mu\beta}.$$

It is easily proved that if $\mu\beta$ is plotted in the complex plane (Fig. 4) with α as a parameter varying from $-\infty$ to $+\infty$, the result will be a circle of radius $\mu/2$ and center at $(\mu/2, 0)$. For $\alpha=0$ or $\alpha=\infty$, $\beta=1$ and $\mu\beta=\mu$; while for $\alpha=1$, $\beta=0$ and $\mu\beta=0$. It has been shown[7] that

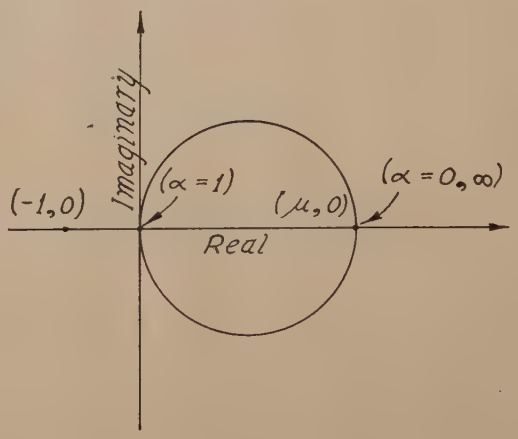

Fig. 4—Plot of $\mu\beta$ in the complex plane (network of Fig. 2).

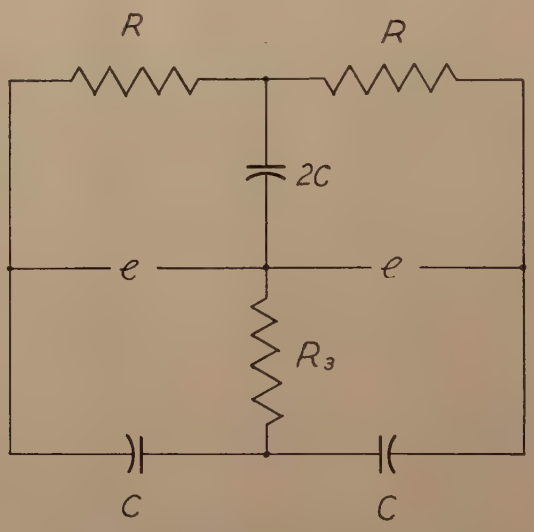

Fig. 5—Network with R_3 arbitrary.

a feedback amplifier becomes unstable if the $\mu\beta$ curve as drawn here encloses the point $(-1, 0)$. If in addition to the selective negative feedback, a positive feedback greater than $1/\mu$ is arranged, the curve of Fig. 4 is

[7] H. Nyquist, "Regeneration theory," *Bell Sys. Tech. Jour.*, vol. 11, pp. 126–147; January, 1932.

shifted to the left to enclose the point $(-1, 0)$, and sustained oscillations with the frequency determined by $\omega = 1/RC$ result. Such an oscillator has been described by Scott.[3]

Even without the addition of a separate positive feedback, a tuned amplifier such as described may be unstable. It is found that the shunt resistance R_3 in Fig. 1 makes a convenient control of feedback. Assume the network shown in Fig. 5. This circuit, if $R_3 = R/2$, is equivalent to that in Fig. 2 with $n = \frac{1}{2}$. As before, it is desired to find the ratio of e' to e for small variations of the frequency about that at the null, and in addition, for small variations of R_3 about $R/2$. Equations (1) again represent this network if $R_1 = R_2 = R$ and $C_1 = C_2 = C = C_3/2$. The solution is

$$\beta = \frac{e'}{e} = \frac{2\alpha^3\left(\frac{R_3}{R}\right) - 2\alpha\left(\frac{R_3}{R}\right) + j\left[-2\alpha^2\left(\frac{R_3}{R}\right) + 1\right]}{2\alpha^3\left(\frac{R_3}{R}\right) - 2\alpha\left(\frac{R_3}{R}\right) - 4\alpha + j\left[-6\alpha^2\left(\frac{R_3}{R}\right) - 2\alpha^2 + 1\right]}. \tag{10}$$

As before, let

$$\alpha = \left(1 + \frac{\Delta f}{f_0}\right)\frac{1}{\sqrt{2n}} = 1 + \frac{\Delta f}{f_0}$$

since $n = \frac{1}{2}$. Also let R_3 be restricted to small variations about $R/2$, or

$$R_3 = \frac{R}{2} + \Delta R = \frac{R}{2}\left(1 + \frac{2\Delta R}{R}\right).$$

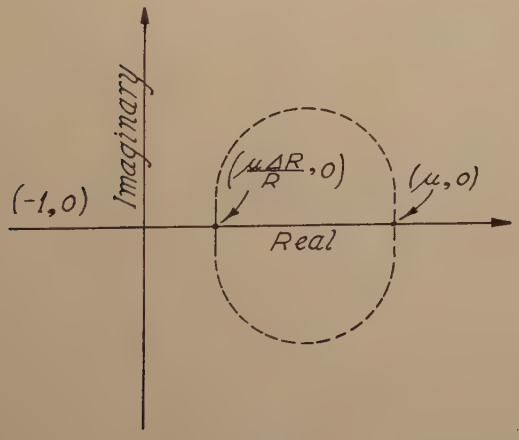

Fig. 6—Plot of $\mu\beta$ in the complex plane (network of Fig. 5).

Substituting these values of α and R_3 in (10) and making approximations,

$$\beta = \frac{\Delta R}{4R} + j\left(\frac{\Delta f}{2f_0} + \frac{\Delta R}{4R}\right). \tag{11}$$

Fig. 6 shows some features of the graph which would be obtained by plotting $\mu\beta$ in the complex plane with α as parameter varying from $-\infty$ to $+\infty$, for a fixed small ΔR. An approximation to that portion of the graph which corresponds to values of α close to 1 is obtained by using β as determined by (11) with Δf as parameter. This approximate graph crosses the axis of reals at the point $(\mu\Delta R/4R, 0)$. The exact graph must then cross in a nearby point $(\mu\Delta R/4R + r, 0)$. When $\Delta R/R$ is small and μ is large, r will be very small an can be neglected. Using $\alpha = 0$ in (10), another point of the exact graph is found as $(\mu, 0)$. It can be proved that these two points are the only points in which the graph meets the real axis and that the graph constitutes a closed curve through the two points as shown in the illustration. If ΔR is such that the curve encloses the point $(-1, 0)$, an amplifier with this network in the feedback circuit will oscillate. The condition for oscillation is then

$$\mu\frac{\Delta R}{4R} < -1$$

or

$$\Delta R < -\frac{4R}{\mu}.$$

Then ΔR may be varied to obtain a stable amplifier of variable selectivity or an oscillator.[6]

Acknowledgment

The writer wishes to acknowledge the valuable assistance of Lieutenant S. C. Kleene, who has reviewed and made contributions to the mathematical part of this work.

The Application of Modulation-Frequency Feedback to Signal Detectors*

GEOFFREY BUILDER†, FELLOW, I.R.E.

Summary—Positive modulation-frequency feedback to the load circuit of a signal detector may be adjusted to make the effective modulation-frequency admittance of the load circuit equal to its direct-current conductance, thus eliminating peak clipping and improving the efficiency of detection. Conversely, negative feedback to the detector tends to increase peak clipping. Incidental effects in the amplifier from which the positive feedback voltage is derived may correspond to positive or negative, voltage or current, feedback depending on the general circuit arrangement. Design formulas and some simple equivalent circuits are given and the major design considerations are outlined. Typical examples include a detector arrangement which provides automatic-volume-control voltages and has a high input impedance and a very low output impedance, as well as Varrell's arrangement which is in agreement with the design procedure outlined in this paper. Attention is also drawn to the great care necessary in the design of detector-amplifier circuits, using multipurpose valves (vacuum tubes), to avoid distortion due to incidental negative modulation-frequency feedback to the detector.

I. Introduction

IT IS well known that the modulation-frequency output of signal detectors may be seriously distorted by "peak clipping" if the detector load-circuit admittance is not uniform; i.e., if its admittance to modulation frequencies differs from its direct-current conductance. It has been stated[1] that quite small amounts of peak clipping may cause objectionable distortion. The cause and nature of peak clipping have been fully discussed and analyzed by Wheeler[2] and are now well known to designers. Although Wheeler deals only with diode detectors, similar effects may occur in other types of detectors, and may also occur in audio-frequency amplifiers.

As a basis for discussion, the simplified equivalent circuit of Fig. 1 will be used to represent a diode detector. The diode is fed from a carrier-frequency source

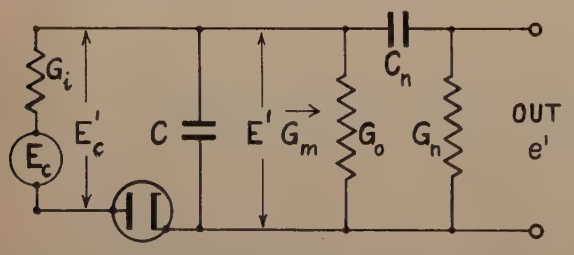

Fig. 1—An equivalent circuit for diode detectors.

of electromotive force E_c and of internal conductance G_i. The detector load circuit comprises a carrier-frequency by-pass capacitor C in parallel with the uniform conductance G_0 of a diode leak resistor and in parallel with a modulation-frequency load of conductance G_n. A capacitor C_n serves to prevent flow of direct current through the modulation-frequency load G_n, and will be assumed throughout to have negligible impedance at modulation frequencies. Neglecting the modulation-frequency admittance of the capacitor C, the total modulation-frequency admittance G_m of the load circuit is given by

$$G_m = G_0 + G_n \tag{1}$$

while its direct-current conductance is G_0.

The effect of nonuniformity in the load circuit can then be summarized, in terms of the equivalent circuit of Fig. 1, as follows:

(a) *Peak Clipping*

Peak clipping occurs when the depth of inward modulation exceeds an amount corresponding to a modulation factor

$$(K_m)_{\max} = G_0(2G_m + G_i)/G_m(2G_0 + G_i). \tag{2}$$

This peak clipping takes the form of clipping of the inward peaks of the detected modulation-frequency wave, and also results in corresponding distortion of the envelope of the modulated carrier-frequency signal E_c' applied to the detector and thus causes distortion in the modulation-frequency output of any other detector or signal rectifier fed from the same carrier-frequency source. An automatic-volume-control voltage derived from the detector output would also be affected by a change in mean direct-current voltage output at high modulation depths, leading to an undesirable variation of the automatic-volume-control voltage with modulation.

(b) *Efficiency*

The addition to the load circuit of the modulation-frequency conductance G_n results in a reduction in the modulation-frequency output voltage, at all depths of modulation, in comparison with the output voltage that would be obtained if the load circuit has a uniform conductance of the value G_0. The carrier-frequency voltage E_c' applied to the diode and the output voltage E' are modulated to a depth K_m' which is less than the depth of modulation K_m of the carrier-frequency signal E_c by an amount given by

$$K_m' = K_m(2G_0 + G_i)/(2G_m + G_i) \tag{3}$$

as compared with

$$K_m' = K_m, \text{ When } G_n = 0. \tag{4}$$

Although the peak-clipping effect is the more important and has received correspondingly greater attention, the reduction in detector efficiency expressed by (3), and corresponding losses incurred in keeping the value of G_0 high to reduce peak clipping, should not be overlooked.

* Decimal classification: R134×R362.2. Original manuscript received by the Institute, August 6, 1945.

† Merino House, 57 York Street, Sydney, Australia.

[1] A. J. Heins van der Venn, "Distortionless detection" (Discussion), *Jour. I.E.E.* (London), Part III, vol. 89, pp. 175–176; September, 1942.

[2] Harold A. Wheeler, "Design formulas for diode detectors," PROC. I.R.E., vol. 26, pp. 745–781; June, 1938.

II. Methods of Eliminating or Reducing the Effects of Nonuniformity of the Load-Circuit Admittance

Many design methods and devices, aimed at reducing or eliminating the effects of nonuniformity in the admittance of the detector load circuit, have been described from time to time, and are briefly summarized in this section.

(*a*) *Equalization of the Direct-Current and Modulation-Frequency Conductances of the Load Circuit*

It is obviously preferable to eliminate the effects of nonuniformity by making the load circuit uniform, or so nearly uniform as to make the effects of nonuniformity negligible for any particular purpose.

Wheeler[2,3] has described the use of modulation-frequency choke coils to reduce the modulation-frequency conductance of the load circuit, but the method does not seem to have been widely used, at least at low modulation frequencies, owing to the practical design and cost factors involved.

Wheeler[2] has also shown that, for many practical purposes, careful design of the load circuit, and particularly the correct selection of the diode leak conductance G_0, can be used to keep the load conductance fairly uniform and thus to reduce peak-clipping effects to an acceptable degree. His methods are widely used, and provide a simple and satisfactory attack on the problem for many purposes.

The simplest device, and one that is very satisfactory in the limited number of cases to which it is applicable, is the direct connection of the detector output to the input control grid of the modulation-frequency signal amplifier. An obvious disadvantage of the device is the application to the control grid of the direct rectified carrier voltage. Although in a limited number of special cases this may be used to provide automatic-volume-control action in the amplifier valve, it is usually a serious limitation. One method of overcoming this difficulty, proposed by Varrell,[4] is to utilize direct-current feedback, without modulation-frequency feedback, in the cathode circuit of the amplifier, to maintain the grid bias substantially constant irrespective of variations in the carrier level applied to the detector.

The success of these methods is limited when an additional modulation-frequency load is applied to the detector for automatic-volume-control or other purposes, or when an automatic-volume-control rectifier is also connected across the same carrier-frequency source from which the signal detector is fed.

(*b*) *Positive Diode Bias*

The application of a positive bias to the diode is well known and has been discussed by Wheeler,[2] Sturley,[5] *The Marconi Review*,[6] Cocking,[7] and others. The optimum value of the bias voltage depends on the carrier-voltage level as well as on the relative values of the load conductances. A wide variety of circuits has therefore been devised to provide a diode bias controlled by the carrier-signal level, and some of the circuit arrangements used are quite complex; but it is not clear to what extent these have been used. An investigation by Williams[8] raises considerable doubt as to the over-all improvement in distortion to be achieved by these methods.

(*c*) *The Reflex Detector*

The reflex or "infinite-impedance" detector ascribed by Weedon[9] to the R.C.A. Licencee Laboratories is mentioned here because it seems likely to have been devised to meet some of the limitations of diode detectors, because it is frequently described as a negative-feedback device, and because it may also be regarded as differing essentially from the diode detector only insofar as a separate electrode, with negative bias, is used for signal injection. It has the advantages of a very high input impedance, independent of its load circuit, and of the existence of a small amount of standing anode current which tends to reduce peak clipping. Disadvantages, which have considerably restricted its use, are that it is not itself suitable as a source of automatic-volume-control voltages, and that the usefulness of its high input impedance is somewhat limited if a normal automatic-volume-control diode rectifier is fed from the same carrier-frequency channel. A further practical difficulty is that the carrier-input level must be fairly closely controlled to prevent the input grid from drawing current, while maintaining a level high enough to ensure effectively linear detection. The detector has been described and discussed in detail by Healy and Ross,[10] Chauvierre,[11] and others.

Reference is often made to the reflex detector as a device utilizing negative feedback. While it is true that its configuration resembles that of an amplifier of the "cathode-follower" type, and while it may perhaps be regarded as a development from an anode-bend detector with the addition of negative current feedback, excessive emphasis on the negative-feedback aspect does not seem wholly desirable in that it tends to hide the essential similarity of the reflex and diode detectors and fails to draw attention to the difference in operating conditions between the reflex detector and the cathode-follower type of amplifier. The matter is of course largely one of definition and perhaps also of personal preference, but there seems no reason why the corresponding aspect of the diode detector itself should not

[3] Harold A. Wheeler, "Peak detector"; United States Patent 1,951,685, March 20, 1934; British Patent 398,882, April 1, 1931.

[4] H. E. Varrell, "Distortionless detection," *Wireless World*, vol. 45, pp. 94–96; August 3, 1939.

[5] K. R. Sturley, "The diode detector with positive bias," *Wireless World*, vol. 44, pp. 220–223; March 9, 1939.

[6] "The reduction of diode-detector distortion by positive bias," *Marconi Rev.*, no. 73, pp. 10–12; April–June, 1939.

[7] W. T. Cocking, "The diode detector," *Wireless World*, vol. 42, pp. 74–76; January 27, 1938; pp. 103–105; February 3, 1938.

[8] F. C. Williams, "The properties of a resonant circuit loaded by a complex diode rectifier," *Wireless Eng.*, vol. 15, pp. 600–611; November, 1938.

[9] W. N. Weeden, "New detector circuit," *Wireless World*, vol. 40, pp. 6–8; January 1, 1937.

[10] C. P. Healy and H. A. Ross, "The linear reflex detector," *A.W.A. Tech. Rev.*, vol. 3, pp. 1–6; July, 1937.

[11] M. Chauvierre, "Distortion in diode detection," *L'Onde Electrique*, vol 17, p. 321; June, 1938.

be accentuated equally; in both the reflex and diode detectors the input electrode is biased back by the instantaneous total rectified output voltage; in neither case is the input electrode subject to simple modulation-frequency feedback voltages within its linear range of operation, as is usually the case in the application of negative feedback in amplifiers. On the other hand the output impedance, as measured by the application of a test voltage across the output terminals in the absence of a signal, is much higher than that of a cathode follower, because the mutual conductance of the valve is low at the working point.

(d) Negative Modulation-Frequency Feedback

The effective reduction in distortion achieved in amplifiers by the use of negative feedback inevitably suggests an analogous application for the reduction of detector distortion. Such experiments have been described by the Hazeltine Corporation in a licensee bulletin; it was concluded that detector distortion was not reduced by the application of negative feedback to the detector. I have myself confirmed this experimentally, and have indeed found an increase in distortion which is discussed in Section V.

It is known that negative current feedback in an amplifier valve may be utilized to reduce the input conductance if it differs from zero on account of a grid leak or other load[12] and the use of this device to reduce the load applied to the detector has been mentioned by van der Venn.[1] It has also been developed by Varrell[4] and used not only to reduce input conductance of the amplifier itself, but also to adjust the modulation-frequency conductance of the whole diode load, including the modulation-frequency conductance of an automatic-volume-control circuit, to equality with the direct-current conductance of the load. It will be shown in subsequent sections that this negative current feedback in the amplifier can be regarded as an incidental aspect; the essential feature common to these, and other circuits of which the incidental aspects may be either positive or negative voltage or current feedback in the amplifier, is the application of positive feedback to the detector load circuit.

This general conclusion is consistent with the experiments by the Hazeltine Corporation and myself, and is also consistent with a brief statement by van der Venn,[1] as follows: "Summarizing, it can be said that distortionless detection can be obtained with a diode for signals larger than 5 volts, if care is taken that the alternating-current and direct-current loads of the detector are equal when receiving signals of high modulation depth; this can often be realized by using the volume control as detector resistance, or by applying a small amount of positive feedback from the audio amplifier."

III. The Use of Positive Feedback

(a) General Considerations

The reduction of distortion in amplifiers by negative feedback inevitably suggests a similar application of feedback to reduce detector distortion. In an amplifier, the reduction in distortion results from appropriate combination or comparison of the input and feedback voltages; but in a signal detector, the signal input is a modulated wave of carrier frequency, while the output is the demodulated wave of modulation frequency, so that a corresponding simple combination or comparison of the input and output voltages is not feasible. There is, therefore, no relevant evidence to indicate that the application of negative modulation-frequency feedback to a detector should also lead to a reduction of distortion. It has been mentioned above that experimental work indicates that a reduction in distortion does not occur.

Distortion caused in the detector by "peak clipping" arises from a maladjustment of the modulation-frequency admittance of the detector load circuit. It is a well-known characteristic of feedback circuits that they permit the effective impedance of a circuit to be adjusted to any required value at any specified frequency by feeding back into that circuit a voltage of frequency and wave form identical to the test voltage. In principle, therefore, modulation-frequency energy fed back into a detector load circuit should permit its modulation-frequency admittance to be adjusted to equality with its direct-current conductance. It may be inferred, quite generally, that the feedback must be positive in the sense that it must be such as to reduce the modulation-frequency losses in the load circuit in the usual case in which these losses are excessive. It follows that any modulation-frequency feedback voltage applied to the detector must be approximately in the same phase as the detector output voltages existing at the point of application, and this corresponds to positive feedback in the sense in which the term is used in relation to feedback in amplifiers.

The effect of voltage feedback on the effective value of an impedance is readily expressed using the simple equivalent circuit of Fig. 2. An impedance Z is connected

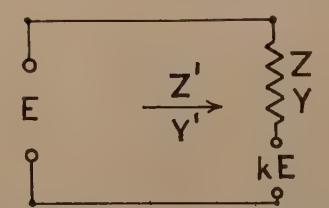

Fig. 2—An equivalent circuit for the effect of feedback on an impedance.

in series with a voltage kE and the effective impedance Z' of the series combination is measured by the application of a test voltage E. The effective impedance Z' may then be written

$$Z' = Z/(1 - k) \qquad (5a)$$

while the corresponding expression for the admittances is

$$Y' = Y(1 - k). \qquad (5b)$$

In general k, Z, Z', Y, and Y' may have any real or complex values and may also be nonlinear. It is clear that when k is real its value must be positive to effect an increase in the effective impedance or a decrease in the effective admittance; the feedback voltage is then in phase with the test voltage, and the term "positive

[12] H. Langford-Smith, "Radiotron Designer's Handbook," Third Edition, Wireless Press, Sydney, Australia, 1940. Complete reproduction, RCA Manufacturing Company, Harrison, N. J.

feedback" is properly applicable. It may also be noted that a complex admittance Y may be altered effectively to a pure conductance if an appropriate complex value is chosen for k.

Equation (5) may be used directly to obtain the usual expression for the effective output impedance of an amplifier with feedback, the test voltage being applied to the output terminals. It may also be used to calculate the input impedance of an amplifier with feedback; the test voltage is then applied to the input terminals and from this point of view the feedback must be positive if the input admittance is reduced, irrespective of whether the feedback produces an increase or decrease in gain, together with the associated characteristics of positive or negative feedback, respectively, in the amplifier.

(b) Equivalent Circuits

One method of applying modulation-frequency feedback to the detector is represented by the simple equivalent circuit of Fig. 3, in which the detector load circuit

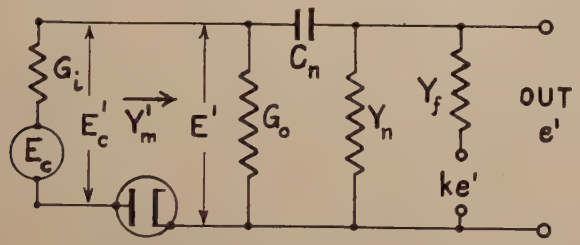

Fig. 3—An equivalent circuit of a diode detector with modulation-frequency feedback.

consists of a diode leak of uniform conductance G_0 in parallel with a modulation-frequency admittance Y_n which may be taken to include the admittance of any carrier-frequency filter and of any automatic-volume-control filter circuit. The total detector load voltage is denoted by E' while e' denotes the modulation-frequency output voltage. A feedback voltage ke', from a source of negligible impedance, is fed back to the load circuit through an admittance Y_f. The condition for the total load-circuit modulation-frequency admittance with feedback, to have the value G_0, uniform with its direct-current conductance, is

$$Y_n + Y_f(1 - k) = 0 \tag{6a}$$

which may be rewritten

$$Y_f = Y_n/(k - 1) \tag{6b}$$

so that, if k has a real value exceeding unity, the admittance Y_f will have a configuration similar to Y_n. Alternatively, if Y_f is fixed arbitrarily, k may be given an appropriate real or complex value. The application of feedback in accordance with (6) would obviously permit a high degree of freedom of choice of the detector load-circuit constants.

Fig. 4 depicts some other possible arrangements differing from that of Fig. 3 in that the feedback voltage is applied in series with one or more of the admittances already existing in the load circuit. In these circuits, Y_{n1} denotes the sum of the modulation-frequency admittances of any carrier-frequency or automatic-volume-control filter circuits, and Y_{n2} other modulation-frequency admittances such as the input admittance of the modulation-frequency signal amplifier fed from the detector. These circuits are, in the form shown, less flexible than that of Fig. 3, in that all parameters other than k are fixed by the design of the detector and associated circuits; but it is clear that the load-circuit admittances may be readily modified to permit equalization

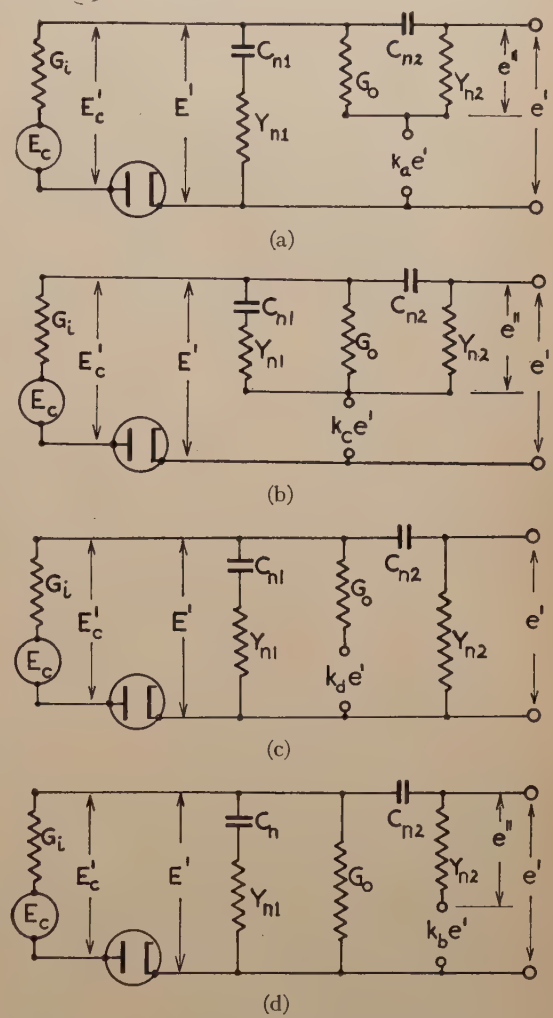

Fig. 4—Alternative arrangements for the application of modulation-frequency feedback to diode detectors.

of the load circuit for real values of k. The relations to be satisfied between the parameters are indicated by the following equations in which the subscripts a, b, c, and d refer respectively to the corresponding configurations in Fig. 4, and $Y_n = Y_{n1} + Y_{n2}$.

Fig. 4(a)

$$Y_{n1} + (G_0 + Y_{n2})(1 - k_a) = G_0$$

whence

$$k_a = (Y_{n2} + Y_{n1})/(Y_{n2} + G_0) \tag{7a}$$

and k_a must be complex unless $Y_{n1} = G_0$ or unless Y_{n1} and Y_{n2} are both pure conductances.

Fig. 4(b)

$$Y_{n1} + Y_{n2}(1 - k_b) = 0$$

whence

$$k_b = 1 + Y_{n1}/Y_{n2} \tag{7b}$$

and k_b can be real only if the configurations of Y_{n1} and Y_{n2} are made similar.

Fig. 4(c)

$$(Y_{n1} + Y_{n2} + G_0)(1 - k_c) = G_0$$

whence

$$k_c = Y_n/(G_0 + Y_n) \tag{7c}$$

and k_c can be real only if Y_n is a pure conductance.

Fig. 4(d)

$$Y_{n1} + Y_{n2} + G_0(1 - k_d) = G_0$$

whence

$$k_d = Y_n/G_0 \tag{7d}$$

and k_d can be real only if Y_n is a pure conductance.

In each of the cases shown in Figs. 3 and 4, the modulation-frequency output voltage e' from the detector, when (6) and (7) are satisfied, is the value given by (4) for a total load of uniform conductance G_0.

A modulation-frequency output voltage e'' may also be taken across the terminals of the modulation-frequency admittance Y_{n2} in Figs. 4(a), 4(b), and 4(d). The output voltage e'' is related to the voltage e' by

$$e'' = e'(1 - k) \tag{8}$$

where k has the values k_a, k_b, k_d. If the feedback voltage is derived from an amplifier fed with the output voltage e'', the feedback voltage may, for convenience, be written in the form

$$ke''/(1 - k). \tag{9}$$

The output voltage e'' is less than the total load voltage e' by the amount of the feedback voltage so that the over-all gain of detector and amplifier is correspondingly reduced.

(c) *Design Considerations*

The feedback voltage may be obtained from the modulation-frequency signal amplifier following the detector, or from an additional amplifier provided specifically for the purpose. In any case, the voltage fed back must be in amplitude and phase relation fixed with respect to the detector output voltage as defined by (6), (7), (8), and (9). Any manual or automatic volume or gain control must therefore be provided elsewhere in the complete arrangement except in special cases such as that described in Section IV(*d*) below. This imposes definite limitations on the general design and requires careful attention.

If the feedback voltage is obtained from a separate amplifier, the detector gain will be increased owing to the reduction in modulation-frequency losses in its load circuit; but the main modulation-frequency signal amplifier will not be affected by the feedback.

If the feedback voltage is obtained from the main modulation-frequency signal amplifier itself, it is necessary to consider carefully incidental feedback effects in this amplifier. The following cases may occur:

(1) The detector output voltage e' (at the output terminals shown in Figs. 3 and 4) is applied to the amplifier. The over-all gain is increased by the amount that can be ascribed to equalization of the detector load circuit, as determined from (3) and (4). Incidental effects of the feedback in the amplifier include an increase in distortion and noise and a modification of the amplifier output impedance corresponding to the over-all increase in gain.

(2) The detector output voltage e'' (referred to in (8) and (9)) is applied to the amplifier. The detector efficiency itself will be increased by the amount determined by (3) and (4), but only the fraction $(1-k)$ of the detector output voltage e' is fed to the amplifier, with a corresponding large loss of over-all gain (e.g., see Varrell's circuit in Section IV(*c*)). Incidental effects in the amplifier correspond to negative feedback.

In either case, the characteristics of the incidental feedback in the amplifier must depend on whether the voltage fed back to the detector is derived from a current or voltage in the amplifier circuits. The choice of the general arrangement (1) or (2) in combination with a selection of an amplifier current or voltage as a source of the detector feedback voltage permits the incidental effects in the amplifier to be so chosen as to be advantageous for any particular purpose, either in themselves, or in combination with additional feedback circuits in the amplifier.

The present investigation has been based on the assumption that the modulation-frequency voltages fed back to the detector are a close replica of the detector output voltages, and the design of the amplifier providing the feedback must conform to this condition. There is obviously scope for detailed investigation of the more general case in which this limitation is not imposed, and it is difficult to predict, without such detailed investigation, how much more widely useful this might be.

The detailed design of the detector and its associated amplifier and feedback circuits must depend largely on the frequencies of the carrier and modulation and on the relation between them. In many practical cases, at audible frequencies, the modulation-frequency admittances of the detector load circuit may be treated as pure conductances; but at higher modulation frequencies and with high ratios of modulation to carrier frequencies, the complex values of the admittances may with advantage be taken into account in the design, and the relevant equations given above have been put in the general form suitable for such applications.

IV. Some Typical Circuits

To illustrate the application of the foregoing principles, a few typical circuit arrangements will be described.

(a) *A Detector Circuit*

Fig. 5 shows a detector circuit which has advantages over both reflex and simple diode detectors. The arrangement is essentially that of Fig. 4(a), and equation (7a) is applicable.

A carrier-frequency circuit is connected to a diode rectifier valve V_1 through a capacitor C. The diode leak has a conductance G_0 and the modulation-frequency output e' is applied to a triode cathode follower through the coupling C_{n2}, G_{n2}. A filter G_{n1}, C_{n1} provides an automatic-volume-control voltage. The valve V_2 has a

cathode resistance R_4 tapped at a value of resistance R_3 measured from its low-potential end. The modulation-frequency voltage $k_a e'$ developed across R_3 is fed back to the rectifier load circuit in series with the parallel combination of G_0 and G_{n2}. The coupling circuits R_1C_1 and R_2C_2 permit the proper direct-current bias conditions for the two valves. The resistance R_4 may take the form of an output control potentiometer. It will be assumed, for simplicity in description, that R_1, R_2, and C have negligible admittance and C_{n1}, C_{n2}, C_1, and C_2 negligible impedance at modulation frequencies.

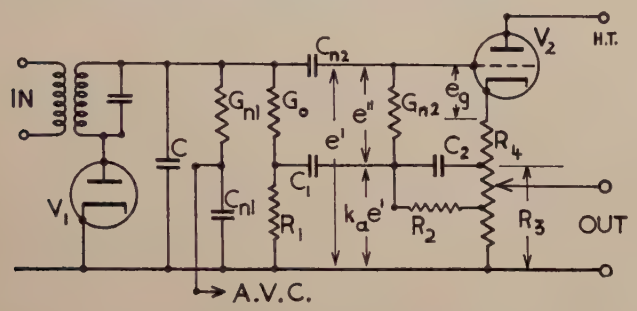

Fig. 5—A detector arrangement having a high input impedance and low output impedance.

The value of the factor k_a is determined from (7a) and is

$$k_a = (G_{n1} + G_{n2})/(G_0 + G_{n2}).$$

The value of the cathode resistance R_4 is determined primarily by the operating conditions of the triode V_2 and by the effective output impedance desired. A value of 10,000 ohms for R_4 and a mutual conductance g of 1.0 milliangstrom per volt for the valve V_2 will be arbitrarily assigned for illustration, and we will put

$$G_0 = 2.0 \text{ micromhos}$$

and

$$G_{n1} = G_{n2} = 1.0 \text{ micromhos}$$

so that

$$k_a = 2/3.$$

If we denote the modulation-frequency grid-cathode voltage of V_2 by e_g, we have

$$k_a e' = gR_3 \cdot e_g$$

and

$$e_g = e' - gR_4 \cdot e_g$$

whence

$$R_3 = (1/g + R_4) \cdot k_a$$

and, for the numerical values assigned,

$$R_3 = 7333 \text{ ohms} \qquad e_g = k_a e'/gR_3$$
$$R_4 = 10{,}000 \text{ ohms} \qquad = 0.136e'.$$

It is to be noted that the maximum modulation-frequency grid-cathode voltage e_g of the valve V_2 is a fraction k_a/gR_3 of the modulation-frequency detector output voltage so that appropriate choice of circuit constants

The maximum output voltage approximates closely to e'.

The advantages of this detector compared with the reflex are:

(1) The output impedance is much lower, partly because of the lower permissible value of the cathode resistor, and partly because valve V_2 operates at normal bias and mutual conductance.

(2) The detector provides automatic-volume-control voltages and compensates the load imposed thereby on the diode rectifier.

(3) The input to the detector may be permitted to rise to high levels by proper selection of the operating conditions of the triode cathode-follower.

Although the input admittance is not zero as in the reflex it may be made low enough for most purposes because choice of the leak conductance G_0 is relatively unrestricted and any modulation-frequency loading is compensated. The diode would be used in association with a reflex detector if automatic-volume-control were required, and in any case its provision in an existing valve envelope (other than that of V_2) is usually feasible.

The circuit may be varied in detail to allow compensation for modulation-frequency load-circuit admittances having complex values. The chief design limitation arises because the value of k_a may not exceed unity, owing to the cathode-follower operation of V_2, so that G_0 must be greater than G_{n1}.

(b) *An Alternative Detector Circuit*

For special purposes for which these limitations are a disadvantage, but for which the provision of a less economical circuit is justifiable, a more flexible general arrangement is shown in Fig. 6, corresponding to the equivalent circuit of Fig. 3. The arrangement may also be regarded and used as a detector-amplifier, the alternative output terminals then used being shown in the diagram.

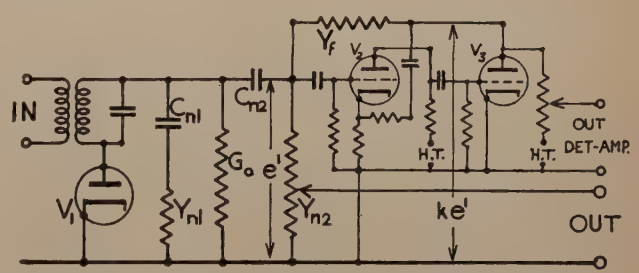

Fig. 6—A detector or detector-amplifier arrangement alternative to that of Fig. 5, and giving greater flexibility in design.

The rectifier output e' is applied to the input terminals of an amplifier of which the input admittance may be taken into account as part of the admittance Y_{n1} or may be reduced to a negligible effective value by feedback applied to the cathode circuit of the input valve V_2. A voltage output ke' from the amplifier output is applied to the rectifier load circuit in series with the modulation-frequency admittance Y_f, the relation between k and Y_f being determined by (6). The design of the amplifier itself will not be dealt with; negative feedback may be used to offset the incidental effects of the feedback to the detector, to reduce the output impedance and improve

the fidelity, or to decrease the input admittance; the gain must in any case be limited to prevent overloading; a double-triode valve may be used for economy.

As in the circuit of Fig. 5, a low output impedance can be achieved by negative feedback if the output is taken from the amplifier; but the chief advantage lies in the wide flexibility permissible in the values of k and Y_f.

(c) *Varrell's Circuit*

Varrell[4] has described the circuit arrangement shown in Fig. 7, in which the symbols used correspond to those in the foregoing discussion. The feedback voltage to the detector load is developed across the cathode resistance R_4 of the first modulation-frequency signal amplifier valve. The circuit constants may be determined from (7a) and the circuit is equivalent to that of Fig. (4a). The loss in over-all gain may be calculated using (8), the incidental effect in the amplifier being negative current feedback.

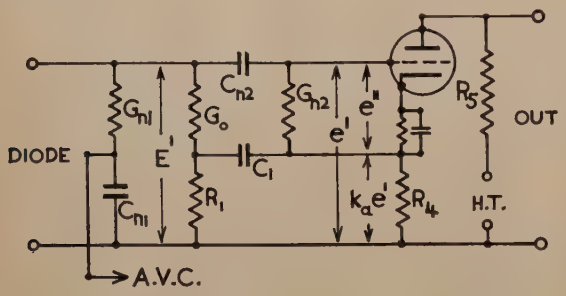

Fig. 7—A detector-amplifier arrangement described by Varrell.

Varrell has given a numerical example, using a valve of mutual conductance $g = 3$ milliamperes per volt and having an alternating-current anode resistance of 10,000 ohms

$G_0 = 5.0$ micromhos	$R_1 = 10{,}000$ ohms
$G_{n1} = 2.64$ micromhos	$R_4 = 5000$ ohms
$G_{n2} = 2.0$ micromhos	$R_5 = 30{,}000$ ohms

and states that the over-all reduction in gain was approximately 12 decibels. These figures, when the shunting of R_4 by R_1 is taken into account, agree closely with those obtained using (4a), the value of k_a being approximately 0.7.

Varrell has emphasized the aspect of reduction of the input admittance of the amplifier by the feedback, and from this point of view, the input circuit of the amplifier may be taken to include the whole of the detector load circuit. He also stresses the negative-feedback aspect of the arrangement.

A minor drawback of the arrangement is the loss in over-all gain, since this is due to negative current feedback in the first amplifier valve and is not offset by desirable feedback effects. If the anode load resistance R_5 of the amplifier is used as a gain control potentiometer, overloading of the amplifier may readily occur because the negative feedback is not sufficient from this point of view, while any increase results in further loss in gain. The use of a gain-control potentiometer between the detector and amplifier is not feasible.

(d) *A Detector-Amplifier with Volume Control*

It has been pointed out that the use of a volume-control potentiometer between the detector and amplifier is not generally permissible when the amplifier is used for feedback to the detector. Fig. 8 shows a special case in which the control can be used. The detector leak

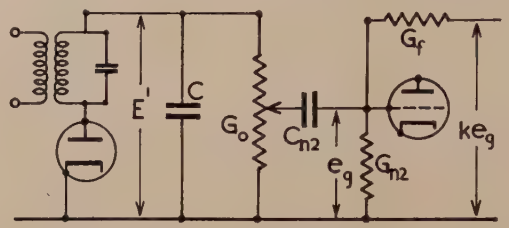

Fig. 8—A detector-amplifier arrangement with volume control.

resistance G_0 is in the form of a volume-control potentiometer and the input admittance G_{n2} of the amplifier is reduced to zero by means of positive feedback to the input grid in the form of a voltage ke_g applied in series with a conductance G_f, where

$$k - 1 = G_n/G_f.$$

The incidental effects in the amplifier itself correspond to positive voltage or current feedback, according to whether the feedback is derived from an amplified voltage or current respectively.

The adjustment of the feedback to reduce the input admittance of the amplifier to zero is obviously independent of the setting of the gain-control potentiometer. Similar arrangements applicable in this simple case include the use of feedback in the cathode circuit of the amplifier valve, with corresponding incidental negative-feedback effects in the amplifier itself. In any case, the arrangement does not permit the compensation of any additional modulation-frequency admittance, such as that of an automatic-volume-control filter, across the rectifier load circuit, except for one setting of the volume control; some compromise adjustment of the feedback might, on occasion, be useful in such cases, but is of limited general interest.

(e) *General*

These illustrations exemplify methods of applying positive modulation-frequency feedback to the detector and suggest some of the ways in which the general arrangement may be selected so that the incidental effects of the feedback may be made useful, or at least less undesirable.

V. The Effects of Negative Feedback

It is clear from the above discussion that negative modulation-frequency feedback to the detector (corresponding to negative values of k) must result in increased modulation-frequency losses and hence increased effective modulation-frequency admittances, leading to an increase in peak clipping. This was confirmed in my experiments mentioned in Section II(*d*). The matter is of more than passing interest, owing to the ease with which such feedback may occur incidentally, particularly when diode-triode or diode-pentode valves are used.

An example is shown in the simplified circuit of Fig. 9, in which a diode-triode valve V_1 is connected as a detector-amplifier. The detector has a leak of conductance G_0 and a volume-control potentiometer G_n is connected, in series with the blocking capacitor C_n, to earth. The output terminal of the potentiometer is connected to the

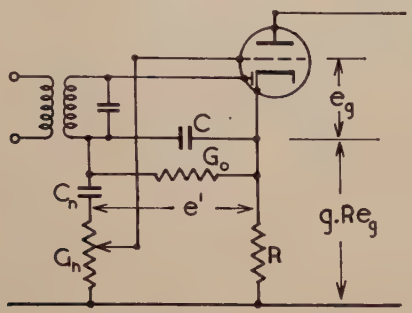

Fig. 9—Diode-triode detector-amplifier arrangement in which incidental negative modulation-frequency feedback to the detector may cause peak clipping.

amplifier grid which is biased by a cathode-bias resistor R. The resistor R is normally by-passed for modulation frequencies, but ineffective by-passing may permit modulation-frequency voltages to be developed across it. In other cases the by-pass is omitted and modulation-frequency voltages occur between cathode and earth for one or more of the following reasons: (1) The by-pass capacitor may be omitted owing to the practical difficulty of making it uniformly effective at all modulation frequencies, or to eliminate an undesirable component (e.g., an electrolytic capacitor). (2) Amplifier feedback voltages may be applied in series with the cathode, e.g., to provide negative voltage feedback from the amplifier output circuit. In any case, even if the grid is returned to cathode for modulation frequencies, any voltage between cathode and earth is effectively in series with the conductance G_n across the detector output circuit and must be considered as modulation-frequency feedback to the detector. It can readily be seen that, if this voltage is such as to cause a decrease in the over-all gain, it must represent negative modulation-frequency feedback to the detector.

Considering the case in which the control potentiometer is set at maximum, the grid-cathode modulation-frequency voltage is identical with the detector output voltage e'. Any reduction in over-all gain due to a modulation-frequency voltage between cathode and earth can therefore occur only as a result of a corresponding reduction in the effective modulation-frequency load impedance presented to the detector, and can be calculated by using (3) and (4). It is apparent that even small losses in over-all gain thus caused must correspond to drastic reduction of the effective modulation-frequency conductance of the detector load, resulting in increased peak-clipping effects. Similar effects will occur at lower settings of the control potentiometer but will in general be less marked for any particular circuit arrangement.

The use of a diode with a separate cathode, or associated with a valve not used at modulation frequencies, thus appears to be desirable to avoid incidental and undesired modulation-frequency feedback to the detector and to increase the flexibility of design of any modulation-frequency feedback circuit in the modulation-frequency amplifier itself.

VI. Conclusions

The following summarizes briefly the discussion in the previous sections, the relevant sections being indicated for ease of reference.

(a) The modulation-frequency losses in the load circuit of a detector may be reduced, so that its effective modulation-frequency conductance is equal to its direct-current conductance, by applying positive modulation-frequency feedback (III). Conversely, negative modulation-frequency feedback will increase the effective modulation-frequency admittance of the load (V).

(b) Incidental effects in the amplifier from which the positive feedback to the detector is taken may correspond to positive or negative, current or voltage, feedback depending on the circuits used (III(c), IV). If an additional amplifier is used to provide the feedback, no incidental feedback effects occur in the modulation-frequency signal amplifier fed from the detector (III(c), IV(b)).

(c) The emphasis on the negative-feedback aspect of the reflex detector tends to hide the essential similarity of the reflex and diode detectors and suggests negative-feedback characteristics that are not present in the usual sense (II(c)).

(d) A detector circuit is described which provides automatic volume control, has a low output impedance, and imposes a very light load on the carrier-frequency circuits. (IV(a)).

(e) The discussion is based on the assumption that the wave form of the energy fed back to the detector is a close replica of the detector output-voltage wave form. It may be worth investigating the more general case in which this condition is not satisfied (III(c)).

(f) Great care is required in the design of detector-amplifier circuits using multipurpose valves to ensure that negative modulation-frequency feedback to the detector is avoided (V).

(g) A circuit given by Varrell is consistent with the design procedure set out in Section III, although Varrell stresses aspects of the arrangement other than those stressed in this paper (IV(c)).

It is felt that the point of view adopted in the paper, which emphasizes the positive feedback to the detector as the common factor in various circuit arrangements, is desirable to avoid confusion.

The Ideal Low-Pass Filter in the form of a Dispersionless Lag Line*

MARCEL J. E. GOLAY†

Summary—Some theoretical and practical aspects of the design of the ideal low-pass filter in the form of a dispersionless lag line are considered. It is shown, in particular, that an artificial line made up of series inductances and shunt capacitances, with 18 per cent aiding mutual inductance between adjacent coils and 8 per cent shunt capacitance between alternate tie points, forms, for many purposes, a sufficiently good approximation of a dispersionless lag line. The mathematical study of the function $f(n)=\int_0^\pi (1-\cos\phi/\phi^2)\cos n\phi d\phi$, which is of pertinent interest in lag-line theory, is given in an appendix.

THE IDEAL low-pass filter, which is defined as a filter having linear phase characteristics and no attenuation up to the cutoff frequency, and infinite attenuation beyond, forms a useful mathematical concept in the theory of communication, as well as a challenge to the engineer to design as close an approximation to the ideal as possible.

Inasmuch as any delay networks with linear phase characteristics, and, in particular, the lag line, are, essentially, ideal low-pass filters, the theory presented herein will be concerned with the lag-line type of construction. This construction offers the advantage, over other types of delay networks, of having a multiplicity of tie points from which variously delayed but otherwise identical signals can be derived.

The original basic lag line was composed of equal series inductances and shunt capacitances. This arrangement offered good frequency cutoff, but poor phase characteristics. A notable improvement in the phase characteristics of lag lines was contributed by Pierce,[1] who discovered that a certain amount of negative (aiding) mutual inductance, between adjacent sections, unavoidable when the coils are coaxially mounted to yield a simple construction, actually is beneficial.[2] The consideration of mutual inductance between adjacent sections leads naturally to the consideration of mutual inductance between alternate and more distant sections, and an investigation of this possibility indicated that suitable design values for these various parameters yielded increasingly more linear phase characteristics. Unfortunately, the practical coaxial construction yields the wrong sign for the mutual inductance between alternate sections, when the connections are so made as to yield the correct value between adjacent sections. This situation could be circumvented by the device of providing special small additional coils designed to yield the mutual inductances of the correct sign and magnitude between alternate and more distant sections, but the resulting construction becomes unwieldy, besides introducing troublesomely large capacitances where they may not be wanted. This consideration led to the investigation of the effect of shunt capacitances across one or more coils, and the more general theory thus evolved yielded eventually such simple "recipes" for lag-line construction as the requirement of 18 per cent mutual inductance between coaxially mounted adjacent coils and of small capacitors between alternate tie points, the capacitance of these capacitors being 8 per cent of the capacitance of the line-to-ground capacitors.

For a simplified basic theory of the ideal lag line we need only consider a recurrent assembly of series inductances L with mutual inductance $\alpha_1 L$, $\alpha_2 L$, etc., between adjacent, alternate, and more distant sections, and capacitances C to ground (Fig. 1). The inductances and

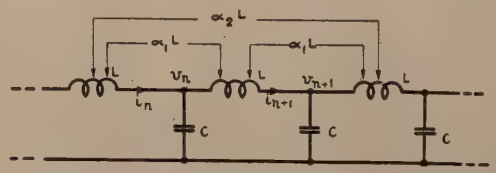

Fig. 1—Schematic diagram of lag line with mutual inductances.

capacitances are assumed to have infinite Q and zero power factor, respectively. Kirchhoff equations for the nth junction and the nth loop can be written

$$i_n - i_{n+1} = j\omega C v_n \tag{1}$$

$$v_n - v_{n+1} = j\omega L[i_{n+1} - \alpha_1(i_n + i_{n+2}) - \alpha_2(i_{n-1} + i_{n+3}) - \cdots]. \tag{2}$$

The recurrent character of the network permits us to write, generally

$$\frac{v_n}{v_{n+1}} = \frac{i_n}{i_{n+1}} = \frac{i_{n-1}}{i_n} = \frac{i_{n+1}}{i_{n+2}} = \cdots = e^{i\phi}. \tag{3}$$

Substitution in (1) and (2) of all i's and v's by their expressions in terms of i_n and v_n, multiplication of (1) and (2), member by member, and division by $i_n v_n$, yields

$$2(1-\cos\phi)=\omega^2 LC(1-2\alpha_1\cos\phi-2\alpha_2\cos 2\phi-\cdots). \tag{4}$$

The requirement of no attenuation below cutoff and of no phase distortion may be expressed by the condition that ϕ be real and proportional to ω

$$k\phi^2 = \omega^2 LC \tag{5}$$

* Decimal classification: R386. Original manuscript received by the Institute, March 15, 1945; revised manuscript received, September 5, 1945.

† Signal Corps Engineering Laboratories, Bradley Beach, N. J.

[1] G. W. Pierce, "Artificial electric lines," *Proc. Amer. Acad. Arts and Sci.*, vol. 57, pp. 195–212; 1921.

[2] The utilization of such a lag line in a special bridge network for the purpose of obtaining any desired impulse response, and, in particular, the impulse response of an ideal low-pass filter, has been described by M. Levy, in "The impulse response of electrical networks, with special reference to the use of artificial lines in network design," *Jour. I.E.E.* (London), Part III, pp. 153–164; December, 1943.

which, in combination with (4), yields the expression

$$\frac{2(1-\cos\phi)}{k\phi^2} = 1 - 2\alpha_1\cos\phi - 2\alpha_2\cos 2\phi - \cdots . \quad (6)$$

Equation (6) will be satisfied between the limits $\phi=0$ and $\phi=\pi$ if the second member is considered as the Fourier expansion of the first member between said limits. This leads to the following expressions for k and the α's:

$$k = \frac{2}{\pi}\int_0^\pi \frac{1-\cos\phi}{\phi^2}\,d\phi \quad (7)$$

$$\alpha_n = -\frac{2}{\pi k}\int_0^\pi \frac{1-\cos\phi}{\phi^2}\cos n\phi\, d\phi. \quad (8)$$

The mathematical treatment of this integral has been described in the Appendix, from which we borrow the values of k and of the first six α's, to five places.

$$\begin{aligned} k &= 0.77370 & \alpha_3 &= -0.01218 \\ \alpha_1 &= -0.16690 & \alpha_4 &= +0.00676 \\ \alpha_2 &= +0.02864 & \alpha_5 &= -0.00430 \\ & & \alpha_6 &= +0.00297 \end{aligned} \quad (9)$$

and, for higher values of n, the approximate formula

$$\alpha_n = (-1)^n\left(\frac{0.10615}{n^2} + \frac{0.030}{n^4}\right). \quad (10)$$

From (9) and (10) it appears that the successive odd-order mutual inductances of an ideal lag line should be aiding, while the even-order ones are opposing, and that their absolute value should vary roughly as the inverse square of their order. This is obviously not realized when the coils are axially mounted and regularly spaced, for if the connections are so made that the mutual inductance between adjacent coils is aiding, as it should be, all mutual inductances will be aiding, and their value will decrease roughly as the inverse cube of their order. As was mentioned earlier, auxiliary coils could serve to correct this situation, but such an arrangement would result in a rather inelegant construction, with a jumble of leads going to and fro, and stray capacitances between the various coils which would complicate matters at high frequencies.

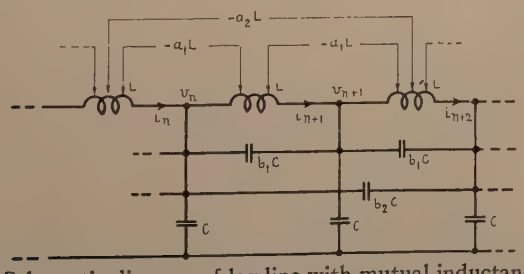

Fig. 2—Schematic diagram of lag line with mutual inductances, and capacitances between tie points.

Instead, let us determine how capacitances inserted between the various tie points affect the propagation characteristics of a lag line. In this calculation, the actual mutual inductances between adjacent, alternate, etc., coils will be designated by $-a_1L$, $-a_2L$, etc., where the a's will be all positive quantities when the mutual inductances are aiding (Fig. 2). Similarly, the capacitances between adjacent, alternate, etc., tie points will be designated by b_1C, b_2C, etc. The equations obtained from the application of Kirchhoff's law to this new arrangement become (formerly (1) and (2)).

$$i_n - i_{n+1} = j\omega C[v_n + b_1(2v_n - v_{n-1} - v_{n+1}) + b_2(2v_n - v_{n-2} - v_{n+2}) + \cdots] \quad (11)$$

$$v_n - v_{n+1} = j\omega L[i_{n+1} + a_1(i_n + i_{n+2}) + a_2(i_{n-1} + i_{n+3}) + \cdots]. \quad (12)$$

Former equation (3) is applicable, and substitution in (11) and (12) of all the i's and v's by their expression in terms of i_n and v_n, multiplication of (11) and (12) member by member, and division by i_nv_n, yields

$$2(1-\cos\phi) = \omega^2LC(1 + 2a_1\cos\phi + 2a_2\cos 2\phi + \cdots)\cdot[1 + 2b_1(1-\cos\phi) + 2b_2(1-\cos 2\phi) + \cdots]. \quad (13)$$

The requirement of no attenuation below cutoff and of no phase distortion can be written

$$k_1\phi^2 = \omega^2LC \quad (14)$$

which, in combination with (13), yields the expression

$$\begin{aligned} \frac{2(1-\cos\phi)}{k_1\phi^2} &= (1+2a_1\cos\phi+2a_2\cos 2\phi+\cdots)\cdot[1+2b_1(1-\cos\phi)+2b_2(1-\cos 2\phi)+\cdots] \\ &= [1+2(b_1+b_2+\cdots-a_1b_1-a_2b_2-\cdots)] \\ &\quad -2\cos\phi[-a_1(1+2b_1+2b_2+\cdots) \\ &\quad +b_1+a_1b_2+a_2b_1+a_2b_3+a_3b_2+\cdots] \\ &\quad -2\cos 2\phi[-a_2(1+2b_1+2b_2+\cdots) \\ &\quad +b_2+a_1b_1+a_1b_3+a_3b_1+a_2b_4+a_4b_2+\cdots] \\ &\quad -\cdots . \end{aligned} \quad (15)$$

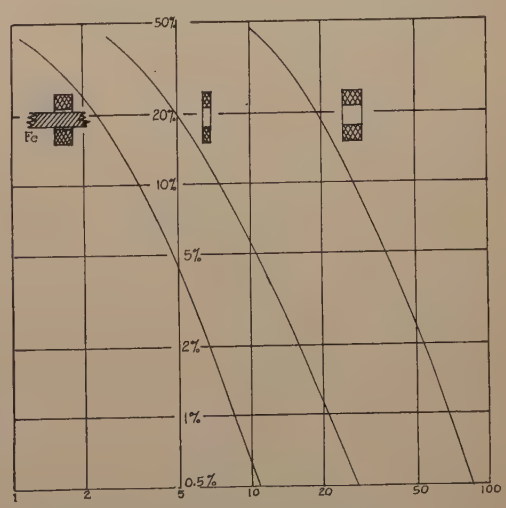

Fig. 3—Mutual inductance as a function of coil spacing.

Inasmuch as k_1 can have any fixed value, the comparison of (6) and (15) indicates that the necessary and sufficient condition for linear phase shift is that the successive brackets in the second member of (15) be proportional to 1, α_1, α_2, etc.

The b's can be chosen at will, but little choice is available for the a's when the practical coaxial construction is adopted, in which the mutual inductance between adjacent coils determines, substantially, all others. The three curves of Fig. 3 are plots, on doubly logarithmic paper, of the mutual inductance as a function of the distance, for the two different shapes of air-core coils illustrated, as well as for coils mounted on a common iron core of permeability 22. If the fuller air-core coils are used, and the spacing is adjusted for 18 per cent mutual inductance between adjacent sections, the mutual inductance between alternate, etc., sections can be verified to be 4.0 per cent, 1.4 per cent, 0.6 per cent, 0.3 per cent, etc., which gives the a's. If capacitance between alternate tie points only is used, so that $b_2 = 8$ per cent and all other b's vanish, it can be verified that the successive brackets of the last member of (15) are proportional to

$$1, \ -0.168, \ 0.029, \ -0.002, \ -0.003, \ -0.002, \text{ etc.},$$

and can be compared with the required values for the α's

$$1, \ -0.167, \ 0.029, \ -0.012, \ 0.007, \ -0.004.$$

If flatter coils are used, the slightly higher mutual inductances between far sections would yield more negative values for the 4th and 5th brackets, thereby improving the agreement of the 4th bracket with the theoretical value. The agreement of the 5th bracket would be slightly worsened, but this could be corrected with a little capacitance between every tie point and the 4th next, so as to yield a value for b_4 which will permit agreement of the 5th bracket with the required value. Thus if the coils are spaced for 18.2 per cent mutual inductance between adjacent sections, the other mutual inductance derived from the center curve of Fig. 3 will be: 5.2 per cent, 2.1 per cent, 1.05 per cent, 0.6 per cent, 0.4 per cent, etc. Assuming now for b_2 and b_4 the values of 9.6 per cent and 1.6 per cent respectively, the successive brackets of (15) will be proportional to

$$1, \ -0.167, \ 0.028, \ -0.004, \ 0.007, \ -0.002, \text{ etc.},$$

thereby yielding an appreciably better agreement with the theoretical values than the figures based on the curve for compact coils. Such an arrangement would appear to be of especial value in radio-frequency lag lines of many sections, for at such frequencies flat coils yield as good a Q as the more compactly shaped ones.

The curve of Fig. 3 representing the mutual inductance versus spacing of compact coils having a common iron core has approximately the same slope as the curve obtained for the same coils without the iron core, and offers, therefore, no possibility of a better agreement of the 4th bracket with the required value.

Preliminary measurements have indicated that if the coils are flanked with discs of magnetic material, in addition to the central magnetic core, the successive mutuals will decrease even less rapidly than in the case of flat air-core coils, thereby offering the possibility of even better phase characteristics. However, this case cannot be represented rigorously by a single curve, because a variation of the spacing between coils causes a change in their magnetic circuit.

It might be thought that placing the coils in closer proximity than is needed for approximately 18 per cent mutual inductance between adjacent coils, so as to increase the mutual inductance between every coil and the 3rd next, would yield a better agreement for the 4th bracket, but, as it turns out, the large capacitances needed across the coils and between alternate tie points yield values for the cross terms $a_1 b_2$, and $a_2 b_1$ which offset the increase obtained for a_3.

Reflecting Termination

Reflections with approximately the same small distortions that occur along a line of the design described above, can be obtained by a proper adjustment of the circuit constants at the end of the line. These adjustments are derived from the consideration of a virtual image of the line beyond its terminated end, in which positive or negative image pulses are propagated.

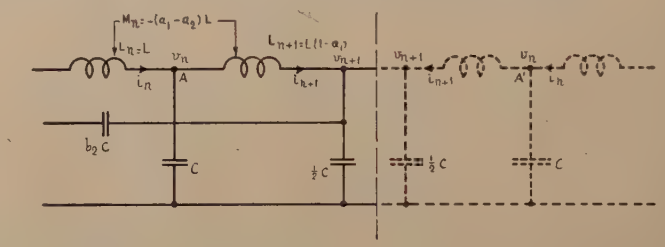

Fig. 4—Schematic diagram of lag line and its electrical image about the last tie point.

Fig. 4 illustrates the end of a lag line and its mirror image about its last tie point. The pulses in the image line are assumed to be the positive image of the pulses in the real line, and will become, therefore, the reflection without change of phase of the pulses in the real line if certain conditions are met. These conditions are that the voltages induced in the coils of the real line owing to their mutual inductance with the coils of the image line be actually induced as the result of a modification of the real line, and that the currents delivered by the various tie points of the image line to the various tie points of the real line be actually generated within the real line. If the line in question is assumed to have -18 per cent and -4 per cent mutual inductance between adjacent and alternate coils, respectively, and 8 per cent shunt capacitance between alternate tie points, it will be readily seen that the absence of a shunt capacitance between points A and A' will call for no modification of the real line, inasmuch as A and A' are always at the same potential by virtue of the assumption made. Conversely, the absence of a mutual inductance between the last coil of the real line and its image will require that a voltage having the value $-0.18\ j\omega L i_{n+1}$ be otherwise generated within the last coil of the real line, and this is accomplished by reducing the value of the inductance of this last coil to $0.82L$. Likewise, the absence of mutual inductance between the last coil of the real line and the second coil of the image

line will require that a voltage having the value $-0.04\,j\omega Li_n$ be otherwise induced in the last coil of the real line, and this is accomplished by changing the value of the mutual inductance between the last two coils of the real line from $-0.18L$ to $-0.14L$.

Another possible termination yielding reflections without change of phase can be obtained in a similar manner by the consideration of the end of a lag line and its mirror image about the center of the next coil. Thus, two "recipes" can be devised for in-phase reflections, and in the assumed case of -18 per cent and -4 per cent mutual inductance between adjacent and alternate coils, respectively, and 8 per cent shunt inductance between alternate tie points, they are as follows:

(a) The inductance of the last coil is $0.82L$, and its mutual inductance to the penult coil is $-0.14L$. It is terminated by a capacitance $\frac{1}{2}C$ to ground.

(b) The last coil is shunted by a capacitance $0.08C$ and its inductance is $0.96L$. It is terminated by a capacitance C to ground.

Similar considerations can be applied in the search for lag-line terminations yielding 180-degree out-of-phase reflections. The calculations are basically simple and lead to the following conclusions:

If the lag line is imaged about its last tie point, physically realizable conditions are obtained when the values of the alternate shunt capacitances form two descending series. Thus, in the case considered above, the following "recipe" is derived:

The end of the last coil is grounded, and its inductance and mutual inductance to the penult coil are, respectively, $1.18L$ and $-0.22L$. The capacitance from the last tie point to ground is $1.16C$, and the $0.08C$ normally connected between the end of the last coil and the penult tie point may be lumped with the capacitance from that point to ground.

Conversely, if the lag line is imaged about the center of its last coil, physically realizable conditions are obtained only when the values of all successive shunt impedances form a descending series. In all other cases, and in particular in the case considered above (18 per cent mutual inductance between adjacent coils and 8 per cent capacitance between alternate tie points) one is led to the requirement that negative capacitances be utilized in the circuit.

Constant-Voltage Lines

Inasmuch as some attenuation takes place as signals are propagated along a line, owing mostly to the effective resistance of the coils, only one of the variables, voltage or current, may be propagated without attenuation, at the expense of the other. If it is desired to have a line in which the signal voltage is not attenuated, the impedance of the line will be increased gradually in the direction of propagation, while maintaining the resistance-capacitance product constant. This impedance increase would be exponential if the Q's of all coils were the same, but need not be as rapid, as the Q of the successive coils increases with their size. In practice it is often sufficient to increase linearly the number of turns of each successive coil by a predetermined amount.

Time Delay and Impedance Computation

The time delay per section of a group of waves of average frequency ω is given by the well-known expression

$$t(\omega) = \frac{d\phi}{d\omega}. \tag{16}$$

When a lag line has been designed to have a nearly linear phase change with frequency, the value of $t(0)$ is fairly representative of the over-all delay per section. From (13) and (14) we deduce

$$t(0) = \frac{d\phi}{d\omega_{\omega=0}} = \frac{\phi}{\omega_{\omega=0}}$$
$$= \sqrt{LC}\sqrt{1 + 2a_1 + 2a_2 + \cdots} = \sqrt{k_1 LC}. \tag{17}$$

The characteristic impedance is not clearly definable, owing to the cross connections of the capacitances. If, however, we arbitrarily split one of the capacitances to ground in two equal components, connect all capacitances b_1C, b_2C, etc., to the nearer capacitance $\frac{1}{2}C$ and define the impedance as the ratio of the voltage at this point to the current flowing from the first half to the second half of the capacitance, we obtain

$$Z = \frac{v_n}{\frac{1}{2}j\omega C v_n + i_{n+1} + j\omega C[b_1(v_n - v_{n+1}) + b_2(v_n - v_{n+2}) + \cdots]}. \tag{18}$$

Substituting for i_{n+1}, v_{n+1}, v_{n+2}, etc., their values derived from (3) and (8), and for ω its value derived from (17), expanding in powers of ϕ and neglecting all terms in ϕ^2 and higher powers, we obtain

$$Z = \sqrt{\frac{L}{C}}\sqrt{1 + 2a_1 + 2a_2 + \cdots} = \sqrt{k_1 \frac{L}{C}}. \tag{19}$$

It has been found experimentally that lag lines terminated by a capacitance $\frac{1}{2}C$ shunted by a resistance of value Z exhibit negligible reflection. Conversely, it has also been found that a lag line beginning with a capacitance of value $\frac{1}{2}C$ connected to ground through a resistance of value Z exhibits, for many practical purposes, a substantially uniform resistive impedance at all frequencies.

Conclusions

Lag lines designed according to the theory described above have yielded phase-versus-frequency curves which, within the errors of bridge and frequency measurements, agreed with the formula

$$\omega = \frac{1}{\sqrt{LC}}\sqrt{\frac{2(1-\cos\phi)}{(1+2a_1\cos\phi+\cdots)[1+2b_1(1-\cos\phi)+\cdots]}}. \tag{20}$$

In designing lag lines for high frequencies and low impedances, it was found necessary to take into account the shunted capacitance of the coils, which contributes to the factor b_1, and which was compensated by making a_1 and consequently b_2 correspondingly larger. The limit to the application of the lag-line theory is met when the combination of high cutoff frequency, high impedance, and high coil capacitance yield values for b_1 which can just be compensated by placing the coils at an optimum proximity, beyond which the increased capacitance between the coils causes an effective increase in b_1 which is no more compensated by the increase in a_1.

Appendix

Power-Series Development of the Function

$$f(n) = \int_0^\pi \frac{1-\cos\phi}{\phi^2}\cos n\phi d\phi$$

From

$$f(n) = \int_0^\pi \frac{1-\cos\phi}{\phi^2}\cos n\phi d\phi \tag{21}$$

we derive, after two differentiations under the integral sign

$$f''(n) = -\int_0^\pi (1-\cos\phi)\cos n\phi d\phi = \frac{1}{2}\frac{\sin(n-1)\pi}{n-1} + \frac{1}{2}\frac{\sin(n+1)\pi}{n+1} - \frac{\sin n\pi}{n}. \tag{22}$$

If we define $F(n)$ as the second integral of $(\sin n\pi)/n$, $f(n)$ may be written

$$f(n) = \tfrac{1}{2}F(n-1) + \tfrac{1}{2}F(n+1) - F(n). \tag{23}$$

The circumstance that the second member of (23) is a second difference justifies the indetermination of the lower integral limits of $F(n)$. The Taylor expansion of $F(n-1)$ and $F(n+1)$ yields for $f(n)$

$$f(n) = \frac{1}{2!}F''(n) + \frac{1}{4!}F^{IV}(n) + \cdots = \frac{1}{2!}\frac{\sin n\pi}{n} + \frac{1}{4!}\left(\frac{\sin n\pi}{n}\right)'' + \cdots. \tag{24}$$

If its expansion in series is substituted for $\sin n\pi$ in the series above, the $(2l-2)$nd derivative of the $(l+m)$th expanded term of the lth term in (24) will be the term explicitly written out in the new summation obtained for $f(n)$ in (25)

$$(n) = \sum_{m=0}^{\infty}\frac{n^{2m}}{(2m)!} \cdot \sum_{l=1}^{\infty}(-1)^{l+m+1}\frac{(2l+2m-2)!}{(2l)!(2l+2m-1)!}\pi^{2l+2m-1}. \tag{25}$$

The absolute value of every term of the double series above is smaller than the corresponding term in the double series

$$\pi\sum_{m=0}^{\infty}\frac{|n|^{2m}}{(2m)!}\sum_{l=1}^{\infty}\frac{\pi^{2l+2m-2}}{(2l-2)!} = \pi\cosh\pi\cosh|n|\pi \tag{26}$$

therefore the expansion of $f(n)$ given in (25) is absolutely convergent for all values of n.

The value of $f(0)$, which will be designated by K_0 is equal to the partial sum corresponding to $m=0$ in (25)

$$f(0) = K_0 = \frac{\pi}{2!} - \frac{\pi^3}{3.4!} + \frac{\pi^5}{5.6!} - \cdots. \tag{27}$$

This series is not reducible to a simpler form, whereas all other partial series, corresponding to higher values of m, are.

For their reduction, use will be made of the identical relation

$$\frac{(2l+2m-2)!}{(2l)!} = \sum_{p=1}^{2m-1}(-1)^{p+1}\frac{(2m-2)!(2l+2m-1)!}{(2m-p-1)!(2l+p)!} \tag{28}$$

which can be verified by observing that both sides are polynomials in $2l$ of order $2m-2$ having the same coefficient for the highest power of $2l$ and the same roots, all of which are single. The identity of the roots can be derived from the circumstance that the pth term of the summation is identifiable with the coefficient of x^{2m-p-1} in the expression

$$(2m-2)!(1-x)^{2l+2m-1}$$

which vanishes for $x=1$ when $2l$ is an integer greater than $1-2m$, and all terms of which are included in the summation when $2l$ is a negative integer, for these conditions define also the values of $2l$ for which the polynomial in the first member of (28) vanishes.

The substitution of the second member of (28) for its equivalent expression in (25) yields for $f(n)$

$$f(n) = K_0 + \sum_{m=1}^{\infty}(-1)^m\frac{\pi^{2m-1}n^{2m}}{(2m-1)2m}\left[\sum_{p=1}^{2m-1}\frac{(-\pi)^{-p}}{(2m-p-1)!}\sum_{l=1-m}^{\infty}\frac{(-1)^l\pi^{2l+p}}{(2l+p)!} + \frac{1}{(2m-1)!}\right] \tag{29}$$

in which the summations have been extended to all integral values of l for which $2l$ is a root of the polynomial of (28), which adds only vanishing terms to the summations, as well as to the value $l=0$, the term thus added to the summations being subsequently subtracted within the brackets.

The partial summations with respect to l can be identified with $\sin(p-1)\pi/2$ and vanish for odd values of p. Equation (29) therefore can be rewritten, setting $p=2q$

$$f(n) = f(0) + \sum_{m=1}^{\infty}\frac{(-1)^m\pi^{2m-1}n^{2m}}{(2m-1)2m}\left[\sum_{q=1}^{m-1}\frac{(-1)^{q+1}}{\pi^{2q}(2m-2q-1)!} + \frac{1}{(2m-1)!}\right] = K_0 + \sum Q_m n^{2m} \tag{30}$$

where

$$Q_1 = -\frac{\pi}{2}$$

$$Q_2 = \frac{\pi}{3.4} + \frac{\pi^3}{3.4.3!}$$

$$Q_3 = \frac{\pi}{5.6} - \frac{\pi^3}{5.6.3!} - \frac{\pi^5}{5.6.5!} \tag{31}$$

$$Q_4 = \frac{\pi}{7.8} - \frac{\pi^3}{7.8.3!} + \frac{\pi^5}{7.8.5!} + \frac{\pi^7}{7.8.7!}.$$

The series defined by (30) is absolutely convergent for all values of n, as it was formed by reshuffling the terms of the absolutely convergent series of (25).

The application of the (symbolic) binomial theorem to the successive derivatives of (24) yields

$$f(n) = A \sin n\pi + B \cos n\pi. \tag{32}$$

The explicit expression of the contribution to A of the term containing the $(2l-2)$nd derivative of sin $n\pi$ in the $(m+l-1)$st term of (24) yields for A the sum

$$A = \sum_{m=1}^{\infty}\sum_{l=1}^{\infty} \frac{(-1)^{l+1}\pi^{2l-2}(2m+2l-4)!}{(2m+2l-2)!(2l-2)!n^{2m-1}}. \tag{33}$$

When

$$|n| \geqq 1 \tag{34}$$

the absolute value of the individual terms of this sum is equal to or smaller than the corresponding term in the sum

$$\sum_{m=1}^{\infty}\sum_{l=1}^{\infty} \frac{\pi^{2l-2}}{(2m-1)2m(2l-2)!} = \log_e 2 \cosh \pi \tag{35}$$

and the series defined by (33) is therefore absolutely convergent in the region defined by (34).

The partial summations of (33) for any one value of l over all values of m have a logarithmic character. For instance, the partial sum corresponding to $l=1$ is equal to

$$\frac{1}{1.2}\frac{1}{n} + \frac{1}{3.4}\frac{1}{n^3} + \cdots = \frac{1}{2}\log_e\left(1+\frac{1}{n}\right)^{n+1}\left(1-\frac{1}{n}\right)^{n-1}. \tag{36}$$

The divergent character of the sum above for all absolute values of n below unity indicates that the double series defining A is not absolutely convergent outside the region defined by (34).

The partial summations of (33) for any one value of m over all values of l have a circular character and yield more convenient expressions for $f(n)$.

To effect this summation, use is made of the identical relation

$$\frac{(2l+2m-4)!}{(2l-2)!} = \sum_{p=1}^{2m-1}(-1)^{p+1}p\frac{(2m-2)!(2m+2l-2)!}{(2m-p-1)!(2l+p-1)!} \tag{37}$$

which can be verified by observing that both sides are polynomials in $2l$ of order $2m-2$ having the same coefficient for the term $2l^{2m-2}$ and the same roots, all of which are single. The equality of the roots can be derived from the circumstance that the pth term of the second member is identifiable with the coefficient of x^{2m-p-1} in the expression

$$(2m-2)!(1-x)^{2m+2l-3}[2m-1+(2l-1)x]$$

which vanishes for $x=1$ when $2l$ is greater than $3-2m$, and all terms of which are included in the second member of (17) when $2l-2$ is a negative integer, these conditions for $2l$ being also the conditions under which the first member of (37) vanishes.

Substituting the second member of (37) for the ratio $(2m+2l-4)!/(2l-2)!$ in (33) yields

$$A = \sum_{m=1}^{\infty}\frac{(2m-2)!}{n^{2m-1}}\sum_{p=1}^{2m-1}\frac{(-1)^p p}{\pi^{p+1}(2m-p-1)!} \cdot \sum_{l=2-m}^{\infty}\frac{(-1)^l\pi^{2l+p-1}}{(2l+p-1)!} \tag{38}$$

in which the summation has been extended to all values of $2l$ which are even roots of the polynomial $(2m+2l-4)!/(2l-2)!$, as identically vanishing quantities only are added to the summation by this extension. Any one of the partial summations with respect to l can be identified with $-\sin p\pi/2$, except when $p=2m-1$, in which case the first term of the expansion of $\sin(m-1/2)\pi=(-1)^m\cos\pi$ is missing and must be subtracted separately. Setting $p=2q-1$, the expression finally obtained for A is

$$A = \sum_{m=1}^{\infty}\frac{(2m-2)!}{n^{2m-1}}\left[\sum_{q=1}^{m}(-1)^{q+1}\frac{2q-1}{\pi^{2q}(2m-2q)!} + (-1)^{m+1}\frac{2m-1}{\pi^{2m}}\right] = \sum_{m=1}^{\infty}\frac{R_m}{n^{2m-1}} \tag{39}$$

where

$$R_1 = \frac{2}{\pi^2}$$

$$R_2 = \frac{1}{\pi^2} - \frac{12}{\pi^4}$$

$$R_3 = \frac{1}{\pi^2} - \frac{36}{\pi^4} + \frac{240}{\pi^6} \tag{40}$$

$$R_4 = \frac{1}{\pi^2} - \frac{90}{\pi^4} + \frac{1800}{\pi^6} - \frac{10{,}080}{\pi^8}.$$

etc.

An entirely similar procedure would yield, for B, the double infinite series, absolutely convergent when $|n| \geqq 1$

$$B=\sum_{m=1}^{\infty}\sum_{l=1}^{\infty}\frac{(-1)^l\pi^{2l-1}(2m+2l-2)!}{n^{2m}(2m+2l)!(2l-1)!}$$

$$=\sum_{m=1}^{\infty}\frac{(2m-1)!}{n^{2m}}\sum_{p=1}^{2m}\frac{(-1)^{p+1}p}{(2m-p)!\pi^{p+1}}\sum_{l=1-m}^{\infty}\frac{(-1)^l\pi^{2l+p}}{(2l+p)!}$$

$$=\sum_{m=1}^{\infty}\frac{(2m-1)!}{n^{2m}}\left[\sum_{q=1}^{m}\frac{(-1)^q 2q}{(2m-2q)!}\frac{1}{\pi^{2q+1}}+\frac{(-1)^m 2m}{\pi^{2m+1}}\right]$$

$$=\sum_{m=1}^{\infty}\frac{S_m}{n^{2m}} \tag{41}$$

where

$$S_1=-\frac{4}{\pi^3}$$

$$S_2=-\frac{6}{\pi^3}+\frac{48}{\pi^5}$$

$$S_3=-\frac{10}{\pi^3}+\frac{240}{\pi^5}-\frac{1440}{\pi^7} \tag{42}$$

$$S_4=-\frac{14}{\pi^3}+\frac{840}{\pi^5}-\frac{15120}{\pi^7}+\frac{80640}{\pi^9}$$

etc.

$$S_m=(2m-1)!\sum_{q=1}^{m}\frac{(-1)^q 2q}{(2m-2q)\,\pi^{2q+1}}+(-1)^m\frac{(2m)!}{\pi^{2m+1}}.$$

The first six values of S_m are, to eight places

$$S_1=0.12900614 \qquad S_4=0.00752223$$
$$S_2=0.03665655 \qquad S_5=0.00427285$$
$$S_3=0.01502696 \qquad S_6=0.00265136.$$

Another general relation is of use in computing the value of $f(n)$ when n assumes integral values. The application of Fourier's expansion theorem to (1) yields

$$\pi\frac{1-\cos\phi}{\phi^2}=f(0)+2f(1)\cos\phi+2f(2)\cos 2\phi+\cdots$$
$$-\pi\leqq\phi\leqq\pi. \tag{43}$$

If, for instance, the values 0, $\pi/3$, $2\pi/3$, and π are substituted in (43), and the four relations thus obtained are given the weights 1, 2, 2 and 1 and added, we obtain

$$\pi\left(\frac{1}{2}+\frac{71}{\pi^2}\right)=6f(0)+12f(6)+12f(12)+\cdots$$
$$=6f(0)+12\left[\frac{s_1}{36}\left(1+\frac{1}{4}+\frac{1}{9}+\cdots\right)\right.$$
$$\left.+\frac{s^2}{1296}\left(1+\frac{1}{16}+\frac{1}{81}+\cdots\right)+\cdots\right]$$
$$=6f(0)+12\left(\frac{s_1}{36}\frac{\pi^2}{6}+\frac{s_2}{1296}\frac{\pi^4}{90}+\cdots\right) \tag{44}$$

wherefrom $f(0)$ can be calculated with convenience.

Its value to seven places is

$$f(0)=K_0=1.2153173. \tag{45}$$

Other convenient relations may be similarly derived for the first few integral values of n. The formula

$$f(n)=(-1)^n\sum_{m=1}^{\infty}\frac{s_m}{n^{2m}} \tag{46}$$

permits the ready calculation of $f(n)$ for higher integral values of n.

In certain problems of dispersionless energy propagation through recurrent electrical or mechanical networks the quantities

$$k=\frac{2}{\pi}K_0=0.77370 \tag{47}$$

and

$$\alpha_n=-\frac{f(n)}{K_0} \tag{48}$$

where n represents a natural number, are of practical interest. The first six values of α_n are, to five places,

$$\alpha_1=-0.16690 \qquad \alpha_4=+0.00676$$
$$\alpha_2=+0.02864 \qquad \alpha_5=-0.00430 \tag{49}$$
$$\alpha_3=-0.01218 \qquad \alpha_6=+0.00297.$$

For higher values of n we derive from (45), (46), and (48), the very approximate expression

$$\alpha_n=(-1)^n\left(\frac{0.10615}{n^2}+\frac{0.030}{n^4}\right). \tag{50}$$

It must be noted that for real values of n, $f(n)$ can be expressed by the formula

$$f(n)=-\frac{2}{\pi}\cos n\pi-n\mathrm{Si}(n\pi)$$
$$+\tfrac{1}{2}(n+1)\mathrm{Si}(n+1)\pi$$
$$+\tfrac{1}{2}(n-1)\mathrm{Si}(n-1)\pi \tag{51}$$

which was pointed out to the writer by Dr. A. N. Lowan. $f(n)$ could therefore be calculated in terms of known (that is, extensively tabulated) functions. It is thought that the developments presented above have some mathematical interest because $f(n)$ can be expressed by convergent series in the inverse powers of n, whereas, to the writer's knowledge, divergent series only are available for the development of the primary function $\mathrm{Si}(n)$ in inverse powers of n. The same remarks apply to the similar function defined by the integral

$$\int_0^{\pi}\frac{\sin\phi}{\phi}\cos n\phi d\phi.$$

Applications of Matrix Algebra to Filter Theory*

PAUL I. RICHARDS†, ASSOCIATE, I.R.E.

Summary—**After a brief introduction to matrix notation, methods are presented for the derivation of design equations for filter sections with special attention to symmetrical types. Finally, insertion and mismatch loss formulas, obtainable directly from the matrices, are given.**

I. Introduction

MATRICES are useful in circuit theory because circuit equations (even in transient analysis) are always *linear*. The matrix method was developed as a means of handling linear equations and almost all of its use occurs in this connection. One advantage of using matrices lies in the fact that there is a definite "turn-the-crank" procedure for most problems. Thus, no time is lost searching out blind alleys and trick methods, as is so often tempting if not necessary in the usual simultaneous-equations method. In addition, matrix notation is brief; it requires a minimum amount of lead pencil to express a given set of relations. This last fact becomes of greater and greater importance as the circuits become more complicated.

II. Elementary Definitions

We must first draw the distinction between a matrix and a determinant. The two look very much alike on paper. A determinant, however, is a single number; the various elements displayed in the expression for the determinant are always to be combined in a certain fashion, and, when this process is carried out, the single number found is then the value of the determinant. A matrix is *not* a single number; it has no "value." On the contrary, it is a *list* of numbers—no more, no less. The individual elements are no more to be combined to a single value than are the names in a telephone book. It is customary to respresent matrices symbolically in the following form:

$$\overline{A} = \begin{Vmatrix} a_{11} & a_{12} \cdots a_{1m} \\ a_{21} & a_{22} \cdots a_{2m} \\ \cdot & \cdot \quad\quad \cdot \\ \cdot & \cdot \quad\quad \cdot \\ a_{n1} & a_{n2} \cdots a_{nm} \end{Vmatrix} \quad \text{or} \quad \|a_{ij}\| \tag{1}$$

where the first subscript indicates the row and the second, the column. If $m=n$, the matrix is called a square matrix. All of the following theory remains valid if a nonsquare matrix is thought of as being a square matrix with zeros in the missing rows or columns. It is wise, however, to become accustomed to handling nonsquare matrices since they are much briefer than the corresponding square forms.

We next define operations on matrices. The first six operations defined are very simple; the operation in question is merely applied to each term of the matrix (or to corresponding terms if there is more than one matrix involved). They are

$$\begin{aligned}
&\overline{C} = K\overline{A} \ (K = \text{an ordinary number}) && \text{if } c_{ij} = Ka_{ij} \\
&\overline{C} = \overline{A}^* \ (\text{conjugate}) && \text{if } c_{ij} = a_{ij}^* \\
&\overline{C} = \overline{A} \pm \overline{B} && \text{if } c_{ij} = a_{ij} \pm b_{ij} \\
&\overline{C} = \frac{d}{dx}\overline{A} && \text{if } c_{ij} = \frac{da_{ij}}{dx} \\
&\overline{C} = \int \overline{A}dx && \text{if } c_{ij} = \int a_{ij}dx.
\end{aligned} \tag{2}$$

Matrix multiplication is more complicated. At this stage, one can see no reason for defining it in the strange fashion to follow. The reason is the same as that for many other complicated definitions (e.g., curl of a vector; dot product of vectors, which is a special case of matrix products); namely, the concept later turns out to be extremely useful. Matrix multiplication is defined as follows:

$$\overline{C} = \overline{A}\,\overline{B} \quad \text{if} \quad c_{ij} = \sum_{(k)} a_{ik}b_{kj}. \tag{3}$$

Note that $\overline{A}$ must have as many columns as $\overline{B}$ has rows; otherwise, the expression is meaningless. Second, in general:

$$\overline{A}\,\overline{B} \neq \overline{B}\,\overline{A}. \tag{4}$$

Equation (4) is the only point at which matrix algebra differs from ordinary algebra; it is, therefore, the point where caution must be observed in handling matrix expressions. The content of definition (3) is best remembered by the following diagram:

$$\overrightarrow{\quad\quad} \qquad \downarrow$$
$$\begin{Vmatrix} a_{11} & a_{12} \cdots a_{1m} \\ \cdot & \quad\quad \cdot \\ \cdot & \quad\quad \cdot \\ a_{1n} & \cdots\cdots a_{nm} \end{Vmatrix} \times \begin{Vmatrix} b_{11} & \cdots & b_{1k} \\ \cdot & & \cdot \\ \cdot & & \cdot \\ b_{m1} & \cdots & b_{mk} \end{Vmatrix}.$$

The arrows indicate that we take a row in $\overline{A}$, multiply each term by the corresponding term in a column of $\overline{B}$, and add the results. This number is then placed in the position in $\overline{C}$ where the particular row of $\overline{A}$ and column of $\overline{B}$ would intersect if $\overline{A}$ and $\overline{B}$ were laid on top of each other. Anticipating later notation, we have as examples (capital letters indicate ordinary numbers)

$$\left.\begin{aligned}
&\begin{Vmatrix} A & \cdot & B \\ \cdot & \cdot & \cdot \\ C & \cdot & D \end{Vmatrix} \times \begin{Vmatrix} A' & \cdot & B' \\ \cdot & \cdot & \cdot \\ C' & \cdot & D' \end{Vmatrix} \\
&\qquad = \begin{Vmatrix} AA'+BC' & \cdot & AB'+BD' \\ \cdot & \cdot & \cdot \\ A'C+C'D & \cdot & DD'+B'C \end{Vmatrix}; \\
&\begin{Vmatrix} A & \cdot & B \\ \cdot & \cdot & \cdot \\ C & \cdot & D \end{Vmatrix} \times \begin{Vmatrix} E \\ \cdot \\ I \end{Vmatrix} = \begin{Vmatrix} AE+BI \\ \cdot \\ CE+DI \end{Vmatrix}.
\end{aligned}\right\} \tag{5}$$

* Decimal classification: R143. Original manuscript received by the Institute, August 13, 1945; revised manuscript received, November 9, 1945.

† 49 Washington Avenue, Cambridge 40, Mass.

The operation represented in (5) is the one which requires the most practice in learning to use the matrix methods. Once this is mastered, the rest of the concepts are relatively simple.

There is a matrix, usually denoted by $\overline{I}$, which behaves like the number 1 in ordinary algebra; it is

$$\overline{I}=\begin{Vmatrix} 1 & 0 & 0 & \cdots & 0 \\ 0 & 1 & 0 & \cdots & 0 \\ 0 & 0 & 1 & \cdots & 0 \\ \cdot & & & & \cdot \\ \cdot & & & & \cdot \\ \cdot & & & & 0 \\ 0 & 0 & \cdot & \cdots & 1 \end{Vmatrix} = \|\delta_{ij}\| \text{ where } \delta_{ij}=\begin{cases} 1 \text{ if } i=j \\ 0 \text{ if } i\neq j. \end{cases} \quad (6)$$

This matrix has the property that for all $\overline{A}$

$$\overline{I}\overline{A}=\overline{A}\overline{I}=\overline{A}. \quad (7)$$

In view of this property, if there is a matrix $\overline{A}^{-1}$ such that

$$\overline{A}\overline{A}^{-1}=\overline{I}(=\overline{A}^{-1}\overline{A})$$

then $\overline{A}^{-1}$ is called the inverse of $\overline{A}$. Only those matrices whose determinants are not zero have inverses. When inverses exist, they are unique. *For a two-by-two matrix* (only), the inverse is obtained simply by (a) interchanging the diagonal terms ($i=j$); (b) changing the sign of the off-diagonal terms ($i\neq j$); (c) dividing each element by the determinant of the original matrix.

Thus

$$\begin{Vmatrix} A & B \\ C & D \end{Vmatrix}^{-1}=\frac{1}{AD-BC}\begin{Vmatrix} D & -B \\ -C & A \end{Vmatrix} \quad (AD-BC\neq 0). \quad (8)$$

Inverses are extremely useful in manipulating matrix expressions. As a simple example, if we represent (with obvious definitions) equations (9) and (10) by $\overline{T}_1=\overline{G}\overline{T}_2$ then, if $\overline{G}$ has an inverse, premultiplication by $\overline{G}^{-1}$ gives $\overline{G}^{-1}\overline{T}_1=\overline{G}^{-1}\overline{G}\overline{T}_2=\overline{I}\overline{T}_2=\overline{T}_2$, or

$$\begin{Vmatrix} E_2 \\ I_2 \end{Vmatrix}=\begin{Vmatrix} A & B \\ C & D \end{Vmatrix}^{-1}\times\begin{Vmatrix} E_1 \\ I_1 \end{Vmatrix}. \quad (8a)$$

III. Use of Matrices in Circuit Theory

A number of the problems of circuit theory are very easily handled by matrix methods. Some of these are (a) finding networks equivalent to a given network; (b) analyzing transient behavior of complicated networks; (c) analyzing alternating-current machinery, especially in unstable conditions ("hunting"); (d) elimination of various dependent currents and voltages; and (e) finding driving-point impedances of complicated (e.g., nonplanar) networks. These problems are treated by Pipes,[1,2] Guillemin,[3] and Kron.[4] We shall consider only the applications of the matrix method to filter design; i.e., to four-terminal networks.

IV. Four-Terminal Networks

In any linear four-terminal network, there is, by definition, a linear relation between the input current and voltage and output current and voltage (Fig. 1).

$$\begin{aligned} E_1 &= AE_2+BI_2 \\ I_1 &= CE_2+DI_2. \end{aligned} \quad (9)$$

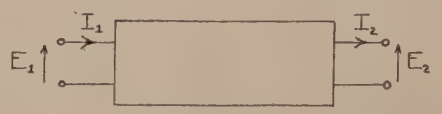

Fig. 1—Conventions employed in this paper.

This may be placed in matrix form as follows:

$$\begin{Vmatrix} E_1 \\ I_1 \end{Vmatrix}=\begin{Vmatrix} A & B \\ C & D \end{Vmatrix}\times\begin{Vmatrix} E_2 \\ I_2 \end{Vmatrix}. \quad (10)$$

The reader should check, by multiplying out the matrices, that (10) is really equivalent to (9). Notice that the essential properties of the equations are determined by the coefficients A, B, C, D; matrix algebra achieves its brevity by dealing only with these coefficients. It is thus unnecessary to write out repeatedly either the "+" and "=" signs of (9) or the variables E_1, I_1, E_2, I_2. The values of A, B, C, D, for several simple circuits are given in Table I. The reader should check a few of these so that he will understand the connection between this method of notation and the usual circuit equations.

Thus far, we have merely translated language of the type (9) into that of the type (10), and it might seem that we have gained little. The advantages appear, however, when we begin to interconnect various networks. The only connection which we shall employ in this paper is that of cascade. A large collection of formulas for this[2] and other types of connection[5] has already been given.

In the case of *cascade of several networks*, the rule is that *the over-all matrix of the new network is merely the matrix product of the matrices for the individual networks taken in the order of connection*. This rule is easily proved by setting up the relations (10) for each network and performing appropriate substitutions according to the

---

[1] L. A. Pipes, "Matrices in engineering," *Elec. Eng*, vol. 56, pp. 1177–1190; September, 1937. This paper gives basic matrix theory in very brief, easily understandable form. In addition, several applications are discussed.

[2] L. A. Pipes, "Matrix theory of four-terminal networks," *Phil. Mag.*, vol. 30, pp. 370–395; November, 1940. A large number of useful formulas are summarized and a full discussion of input impedances and iterative-termination parameters is included.

[3] E. A. Guillemin, "Communication Networks," vol. II, John Wiley and Sons, New York, N. Y., 1935, p. 140. A basic discussion of four-terminal networks is given with proofs of the propagation function and characteristic impedance formulas for both image and iterative termination. Also, a section on finding equivalent circuits is included.

[4] Gabriel Kron, "Tensor Analysis," "Tensor Analysis of Networks," and "Application of Tensors to Rotating Electrical Machinery." These works are written from a geometric point of view to a great extent, and contain techniques of a much more general character than any of the others listed here.

[5] In footnote reference 4 there appears to be an error in the formula for C in the case of parallel connection. The numerator should read $AD^1+A^1D+BC^1+B^1C-2$.

physical connection. As a simple example, we consider (Fig. 2)

Fig. 2—Low-pass filter.

$$\begin{array}{c|c}A & B\\ \hline C & D\end{array} = \begin{array}{c|c}1 & jL\omega\\ \hline 0 & 1\end{array} \quad \begin{array}{c|c}1 & 0\\ \hline jC\omega & 1\end{array} \quad \begin{array}{c|c}1 & jL\omega\\ \hline 0 & 1\end{array}$$

$$= \begin{array}{c|c}1 & jL\omega\\ \hline 0 & 1\end{array} \quad \begin{array}{c|c}1 & jL\omega\\ \hline jC\omega & 1-LC\omega^2\end{array}.$$

$$\begin{array}{c|c}A & B\\ \hline C & D\end{array} = \begin{array}{c|c}1-LC\omega^2 & 2jL\omega - jL^2C\omega^3\\ \hline jC\omega & 1-LC\omega^2\end{array}. \qquad (11)$$

TABLE I

Matrices for Simple Four-Terminal Networks

Network	*Matrix*
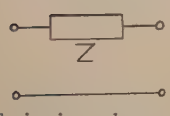 Series impedance	$\begin{array}{c\|c}1 & Z\\ \hline 0 & 1\end{array}$
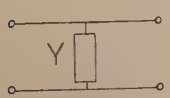 Shunt admittance	$\begin{array}{c\|c}1 & 0\\ \hline Y & 1\end{array}$
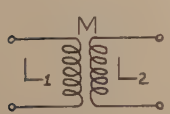 Coupled circuits	$\begin{array}{c\|c}L_1/M & j\omega\dfrac{(L_1L_2-M^2)}{M}\\ \hline \dfrac{-j}{M\omega} & L_2/M\end{array}$
Characteristic impedance $=Z_0$ Propagation constant $=\Gamma$ (complex) Transmission line	$\begin{array}{c\|c}\cosh\Gamma & Z_0\sinh\Gamma\\ \hline \dfrac{\sinh\Gamma}{Z_0} & \cosh\Gamma\end{array}$ If $\Gamma = j\theta = j\dfrac{\omega l}{c} = j\dfrac{2\pi l}{\lambda}$, then: $\begin{array}{c\|c}\cos\theta & jZ_0\sin\theta\\ \hline j\dfrac{\sin\theta}{Z_0} & \cos\theta\end{array}$
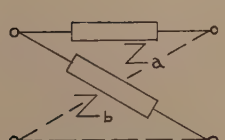 Symmetric lattice	$\begin{array}{c\|c}\dfrac{Z_a+Z_b}{Z_b-Z_a} & \dfrac{2Z_aZ_b}{Z_b-Z_a}\\ \hline \dfrac{2}{Z_b-Z_a} & \dfrac{Z_a+Z_b}{Z_b-Z_a}\end{array}$

Anticipating later results, we may then say that for this filter

$$\cosh\Gamma = 1 - LC\omega^2$$

$$K_0 = \sqrt{2\frac{L}{C} - L^2\omega^2}. \qquad (12)$$

By usual filter theory[6] the cutoff frequencies are given by $\cosh\Gamma = \pm 1$, or $\omega = 0$ and $\omega_C = \sqrt{2/LC}$, while K_0 at $\omega = 0$ is given by $\sqrt{2L/C}$. The usual design equations are then obtained by solving inversely for L and C.

In the case of lumped-constant, reactive T, π, and lattice sections, methods have been worked out which enable rapid determination of filter characteristics. In filters involving transmission lines or configurations not of the T, π, or lattice type, however, no such methods are available and the difficulties encountered in ordinary simultaneous-equations methods will soon convince the reader of the advantages of the present attack.

V. Some General Relations

Before considering the interpretation of the final matrix, we turn to some general relations which form useful checks in manipulations of the type considered above. *The following relations are valid in any four-terminal network in which the reciprocity theorem holds.* This includes in particular any passive lumped-constant network, and by the Rayleigh-Carson reciprocation theorem (see Additional Reference (1)), any "black box" not including nonlinear elements such as iron or vacuum tubes. Thus, the following relations hold for any system involving the conventional lumped constants, transmission lines, wave guides, antennas, etc.

The first relation is a direct consequence of the reciprocation theorem. When the latter is applied to (10), we obtain

$$AD - BC = 1. \qquad (13)$$

We now show that, *for lossless networks*,

$$\begin{aligned} &A, D \text{ are real}\\ &B, C \text{ are pure imaginary.}\end{aligned} \qquad (14)$$

In any lossless configuration (even transmission-line, wave-guide circuits, etc.), the input and output short- and open-circuit impedances must be reactive. Otherwise, the circuit could absorb power by itself contrary to definition. Hence,

$$A/C,\ B/D,\ D/C,\ B/A \text{ are pure imaginary.} \qquad (14a)$$

Dividing the first expression by the second, we see that AD/BC is pure real. From (13), this means that $1+1/BC$ and $(1-1/AD)^{-1}$ are real or that BC and AD are real. Multiplying and dividing these last and various terms in (14a), we easily find

$$A^2,\ B^2,\ C^2,\ D^2 \text{ are pure real.} \qquad (14b)$$

Thus, A, B, C, and D are all either pure real or pure imaginary. Equation (14a) then shows either (A, D) are pure imaginary with (B, C) pure real, or else (14) holds. Let the circuit be deformed gradually into, say, the first circuit of Table I. Considerations of continuity then show that (14) must hold in general.

[6] Leigh Page and N. I. Adams, "Principles of Electricity," D. Van Nostrand Company, New York, N. Y., 1931, p. 534.

The inverse of the matrix in (10) is given by (8). If we consider that, when the network is turned end for end, E_1, I_1, E_2, I_2 become $E_2, -I_2, E_1, -I_1$ respectively, we see from (8), (8a), and (13) that *the matrix for the network connected inversely is*

$$\begin{vmatrix} D & B \\ C & A \end{vmatrix}. \tag{15}$$

Thus, in particular, *if the network is symmetrical,*

$$A = D. \tag{16}$$

This follows from (15) and the fact that, if a symmetrical network is connected "backwards," there can be no change in its behavior.

Relations (14) and (16) are useful as checks on the matrix multiplication and, if watched carefully, will point out many errors. Relation (13) is an equally valid check, but is in general difficult to apply in complicated networks.

VI. Filter Parameters from Final Matrix

We consider only image-termination parameters. Iterative parameters have been fully discussed.[2,3] The parameters we use are

$$\begin{aligned} \Gamma &= \alpha + j\beta = \text{propagation function} \\ \phi &= \text{transformation ratio} \\ K_m &= \text{geometric mean image impedance.} \end{aligned} \tag{17}$$

The input and output image impedances are then

$$\begin{aligned} K_{I1} &= \phi K_m \\ K_{I2} &= \frac{1}{\phi} K_m. \end{aligned} \tag{18}$$

These parameters are obtained from the final matrix by the formulas

$$\begin{aligned} \cosh^2 \Gamma &= AD \\ \sinh^2 \Gamma &= BC \\ \tanh^2 \Gamma &= \frac{BC}{AD} = \frac{Z_{sc}}{Z_{oc}} \\ \phi^2 &= A/D \\ K_m^2 &= B/C. \end{aligned} \tag{19}$$

These relations have been proved by conventional methods.[3] For purposes of this paper, we may take them as *definitions* and justify their physical interpretation by (29) of Section VIII.

The edges of the pass bands of reactive networks are given by $\cosh^2 \Gamma = 1$ or 0. Note that this, in view of (13), means that *the edges of the pass bands are given by*

$$AD = 0 \quad \text{or} \quad BC = 0. \tag{20}$$

In the case of symmetrical filters, using (16) in (19), we obtain

$$\begin{aligned} \cosh \Gamma &= A \\ K_0 &= \sqrt{B/C} = K_{I1} = K_{I2}. \end{aligned} \tag{21}$$

Sometimes (20), and sometimes $\cosh \Gamma = \pm 1$ (or 0 also, for unsymmetrical networks) is easier to use. This depends on the particular problem. Equation (20) shows that the characteristic impedances are always zero or infinite at the edges of a pass band, and further, use of (13) shows that they are real in pass bands and reactive in stop bands.

Conclusion

To analyze a given filter:

(a) Break the structure up into a cascade of simple four-terminal networks, whose matrices are already known. (Table I and footnote reference 2.)

(b) Multiply the matrices in the order of connection.

(c) Obtain the filter parameters by (19), (20), or (21).

(d) Find the pass bands and stop bands and characteristic impedances at appropriate points in the pass bands. (See Section VIII.)

(e) Solve inversely to obtain design equations giving filter elements in terms of desired characteristics.

Remarks

Once the matrix product is set up, the *grouping* in which the matrices are multiplied is immaterial. On consideration of the definition (3), we have $\overline{A}(\overline{BC}) = (\overline{A}\,\overline{B})\overline{C}$. In general, it is best to leave factors which have 0's or 1's as elements until last, since these are easiest to multiply into more complicated expressions. It must be emphasized again that *the order of the matrices must not be changed*, since this would, in general, give incorrect results. (Compare (4).)

VII. Special Methods for Symmetrical Sections

It is evident that if we know all the characteristics of a half section of a symmetrical network, we must be

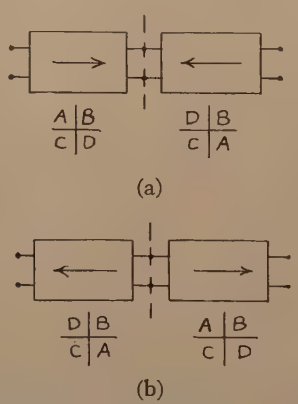

Fig. 3—Symmetrical network split into inversely connected half sections.

able to obtain from this information the characteristics of the whole section. This is indeed true. Let us assume that we have worked out the matrix for the first half section of the network and its expression is Fig. 3 (a).

The matrix for the second half section is then given by (15). Carrying out the multiplication, we find that for the whole section

$$\cosh \Gamma = AD + BC$$

$$K_0 = \sqrt{\frac{AB}{CD}}. \tag{22}$$

(Note that cosh Γ is simply cosh $2\Gamma_1$ where Γ_1 is the propagation constant of the half section.)

Now using (13), we see that *the edges of the pass band are given by*

$$AD = 0$$

or

$$BC = 0. \tag{23}$$

Thus we need only find where each of the elements of the matrix of the *half section* vanishes, and if the diagonally opposite one is not infinite, we have the edge of the pass band. Moreover, it is easily shown from (22) that for cosh $\Gamma = 0$

$$\pm K_0 = \frac{Z_{s\frac{1}{2}}}{j} = -\frac{Z_{0\frac{1}{2}}}{j} \tag{24}$$

where $Z_{s1/2}$ and $Z_{01/2}$ are the short- and open-circuited input impedances of the first half section.

Equation (24) is seldom simpler than (22) for finding the position of cosh $\Gamma = 0$, but (24) is invariably a very rapid way of obtaining K_0 for this condition.

Hence, in analyzing symmetrical-section filters, the amount of matrix multiplication may be cut almost in half since (22), (23), and (24) can be used to obtain the characteristics of the entire section from the matrix of the first half section. Moreover, the characteristics of the circuit of Fig. 3 (b) can be obtained easily merely by setting

$$K_0 = \sqrt{\frac{DB}{AC}}. \tag{22b}$$

Thus, "T" and "π" sections can be analyzed simultaneously by dealing with only one half section.

VIII. Insertion and Mismatch Losses

The foregoing discussion has treated the conventional filter-design methods which ignore the slight effects of mismatch in the pass band, etc. For more accurate determination, we need the actual insertion and mismatch losses.

Insertion loss is defined as the decibel loss in power (a) delivered to the load with the network inserted between the generator and load as compared with (b) that when the generator and load are connected directly. The formula is

$$L = 10 \log \left| \frac{AZ_l + DZ_g + B + CZ_gZ_l}{Z_g + Z_l} \right|^2 \tag{25}$$

where Z_g and Z_l are the generator and load impedances. This formula and (27) are derived by evaluating the voltage across the load under the two conditions involved and taking

$$10 \log \left| \frac{E_{21}}{E_{22}} \right|^2.$$

If $Z_g = Z_l = R$ (real), and the network is symmetrical and reactive

$$L = 10 \log \left(1 + \frac{1}{4}\left(\frac{B}{jR} - \frac{C}{j}R\right)^2\right). \tag{25a}$$

These formulas can be rewritten in numerous ways in special cases and give many second-order results not predicted by simpler theory. For example, if $Z_g = Z_l = R$ (real) and the network is a symmetrical, n-section reactive filter working the pass band, then (see (31), (32), and (33)).

$$L = 10 \log \left(1 + \frac{\sin^2 n\beta}{4}\left(\frac{K_0}{R} - \frac{R}{K_0}\right)^2\right). \tag{26}$$

Thus, if $n = 1$ and $K_0 = R$ at $\beta = \pi/2$ (i.e., cosh $\Gamma = 0$), we see that L will remain small as in Fig. 4 (a). If, however, n is large, we will obtain responses of the type shown in Fig. 4 (b).

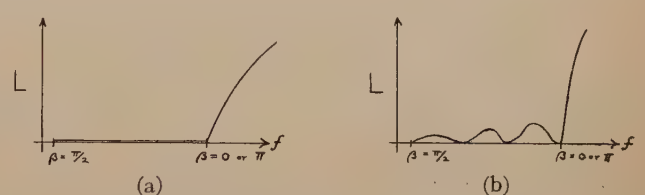

(a) (b)

Fig. 4—Effect on insertion loss due to addition of similar sections.

Mismatch loss is defined as the decibel loss in power (a) delivered to the load with the network inserted between generator and load as compared with (b) the power delivered to the load when a perfect *matching* network is inserted.

The general formula is

$$M = 10 \log \frac{|AZ_l + DZ_g + B + CZ_gZ_l|^2}{4R_gR_l}. \tag{27}$$

If $Z_g = Z_l^*$ (so that generator and load are already matched) then $M = L$. The mismatch loss is the quantity which best expresses the performance of an unsymmetrical filter. In such a filter, we are interested in matching generator to load over as wide a range of the pass band as possible. Again if $Z_g = R_g$, $Z_l = R_l$ and the network is lossless

$$M = 10 \log \left\{ 1 + \frac{\left(\sqrt{\left|\frac{X_1}{X_2}\right|\frac{R_l}{R_g}} - \sqrt{\left|\frac{X_2}{X_1}\right|\frac{R_g}{R_l}}\right)^2 + \left(\sqrt{\frac{|X_{1S}X_{2S}|}{R_lR_g}} - \sqrt{\frac{R_lR_g}{|X_{10}X_{20}|}}\right)^2}{4\left|1 - \frac{X_S}{X_0}\right|} \right\} \tag{28}$$

where subscripts 1 and 2 refer to input and output; S and 0 to short-circuit and open-circuit conditions; also

$$\frac{X_1}{X_2}=\frac{X_{1S}}{X_{2S}}=\frac{X_{10}}{X_{20}} \quad \text{and} \quad \frac{X_S}{X_0}=\frac{X_{1S}}{X_{10}}=\frac{X_{2S}}{X_{20}}.$$

This formula shows that, whenever $X_{iS}=X_{i0}(i=1 \text{ or } 2)$ and $|X_1|\neq R_g$, $|X_2|\neq R_l$, we have $M=\infty$ or *infinite insertion loss despite the behavior of* α. In particular, this frequently occurs if a shunt element becomes resonant or a series element antiresonant. These considerations are of importance in the choice of various filter types. As an example, the filter section shown in Fig. 5 (a) has[7] an "attenuation" (α) curve as in Fig. 5 (b) whereas the foregoing considerations show that the actual insertion loss of a number of such sections terminated in resistive loads would be of the general form of the dotted curve.

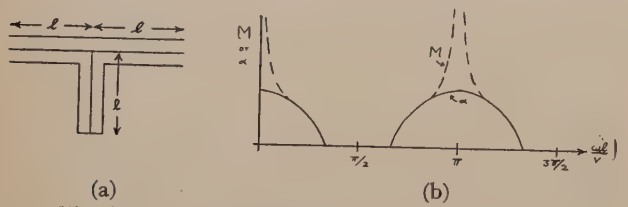

(a) (b)

Fig. 5—Difference of behavior of insertion loss and attenuation functions.

From (27) it is easily shown that if A and D have only small imaginary parts and B and C small real parts, then the change in M will be small. (Use the fact that, for any complex numbers, $|a+b|\leqq|a|+|b|$). *Thus small losses cause only slight differences in filter behavior.*

Finally, if $X_g=0$, $X_l=0$, and the network is reactive, M can be written

$$M=10\log\left\{\left(|\phi|\sqrt{\frac{R_l}{R_g}}-\frac{1}{|\phi|}\sqrt{\frac{R_g}{R_l}}\right)^2\frac{|\cosh^2\Gamma|}{4}+\left(\frac{|K_m|}{\sqrt{R_gR_l}}-\frac{\sqrt{R_gR_l}}{|K_m|}\right)^2\frac{|\sinh^2\Gamma|}{4}+\tfrac{1}{2}(1+|\cosh^2\Gamma|+|\sinh^2\Gamma|)\right\}. \tag{29}$$

This involved formula is interesting in that each of its terms gives us information on filter design. The last term, it will be seen, is equal to 1 throughout the passband and $\cosh^2\alpha$ in the stopband. Thus, if the other terms were not present, M would be zero throughout the passband and approximately 20 log $(e^\alpha/\sqrt{2})$ in the stopband. This explains why conventional "first-order" theory works so well.

Secondly, we shall see that in filter design we should make

$$K_m=\sqrt{R_gR_l} \text{ when or near } AD=0$$
$$\phi=\sqrt{\frac{R_g}{R_l}} \text{ when or near } BC=0. \tag{30}$$

This is contrary to usual practice which makes

$$K_{I1}=\phi K_m=R_g$$
$$K_{I2}=\frac{1}{\phi}K_m=R_l$$

somewhere in the middle of the passband. This latter requirement means that both parts of (30) are satisfied at one point and consequently that neither is satisfied at any other point. We have seen, however, that ideal filter behavior depends on keeping the first two terms small. Thus we want the coefficient of $\sin^2\beta$ to be zero when (or near) $\sin^2\beta=1$, and similarly the coefficient of $\cos^2\beta$ small when $\cos^2\beta=1$. These conditions give precisely (30). The behavior of the coefficients when $\sin\beta$ or $\cos\beta=0$ is immaterial.

In order to show that the parameters Γ, ϕ, K_m as *defined* by (19) for a single section, are immediately extensible to a cascade of any number of sections, we note that if (19) is solved inversely for A, B, C, D, and the sign properly chosen in extracting the square roots, then the matrix may be written

$$\begin{array}{c|c}\phi\cosh\Gamma & K_m\sinh\Gamma\\ \hline \dfrac{\sinh\Gamma}{K_m} & \dfrac{1}{\phi}\cosh\Gamma\end{array}. \tag{31}$$

(Note that the ambiguity of sign in extracting the square roots makes no difference in (29).)

If an odd number n of such sections is connected in cascade in the manner for image termination, then multiplying the matrices gives

$$\begin{array}{c|c}\phi\cosh n\Gamma & K_m\sinh n\Gamma\\ \hline \dfrac{\sinh n\Gamma}{K_m} & \dfrac{1}{\phi}\cosh n\Gamma\end{array}. \tag{32}$$

If an even number $2n$ is so connected, the structure, of course, becomes symmetrical with characteristic impedance $K_{I1}=\phi K_m$ and indeed matrix multiplication gives

$$\begin{array}{c|c}\cosh 2n\Gamma & \phi K_m\sinh 2n\Gamma\\ \hline \dfrac{\sinh 2n\Gamma}{\phi K_m} & \cosh 2n\Gamma\end{array}. \tag{33}$$

[7] W. P. Mason and R. A. Sykes, "The use of coaxial and balanced transmission lines in filters and wide-band transformers for high radio frequencies," *Bell Sys. Tech. Jour.*, vol. 16, pp. 275–302; 1937.

Additional References

(1) J. R. Carson, "A generalization of the reciprocation theorem," *Bell Sys. Tech. Jour.*, vol. 3, pp. 393–399; July, 1924. This paper contains a proof of the Rayleigh-Carson reciprocation theorem.

(2) R. S. Burrington and C. C. Torrence, "Higher Mathematics," Matrix Algebra, chap. 6, Part A, Electric Circuits: pp. 403–416.

"Electron Transit Time in Time-Varying Fields"*

ARTHUR B. BRONWELL

L. A. Ware[1] and H. B. Phillips:[1] In his paper, Bronwell gives an interesting result for the transit angle in klystron grids under the following conditions:

$d = 0.002$ meter
$V_1 = 300$ volts
$V_0 = 1.33\times10^7$ meters per second ($\sim$500 volts)
$\omega = 18\times10^9$

The result given for the entrance angle ϕ, equal to 180 degrees is 175 degrees or $T = 1.69\ 10^{-10}$ second.

It is of interest to check this result by a graphical method of calculation first presented by Kompfner.[2] In this paper, an equation is presented as follows: (equation (5a))

$$\frac{2z\theta^2}{d}=\frac{Q}{2}(y-x)^2+\left(\frac{2\theta}{\sqrt{M}}+\cos x\right)(y-x)-(\sin y-\sin x)$$

where $\theta=\omega d/v_0$, and $z=d=$grid spacing
$v_0=$electron velocity produced by maximum potential between grids
$M=$depth of modulation
$x=\omega t$, representing instant of passing first grid
$y=\omega t_1$, representing instant of passing second grid

Q is the ratio of the direct voltage across the grids to the maximum alternating potential across the grids. In this case $Q=0$ so the equation reduces to

$$2\theta^2=\left(\frac{2\theta}{\sqrt{M}}+\cos x\right)(y-x)-(\sin y-\sin x). \qquad (1)$$

Following Kompfner's method, this equation is solved by the following construction. (See Fig. 1.)

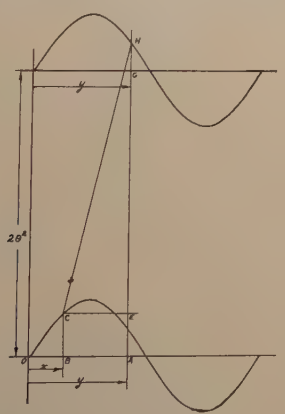

Fig. 1—Graphical construction for solving equation (1).

Two sine waves of unit amplitude are drawn with axes separated by the distance $2\theta^2$. A value of x is selected and the line BC is drawn. The line CH is then drawn by making tan $HCE=(2\theta/\sqrt{M}+\cos x)$. This determines the point H from which a perpendicular is dropped to the base line at A. Then $OA=y$. The difference $y-x$ is then the required transit angle to be determined. The proof of this construction is simple.

$$AE=\sin x \qquad GH=\sin y$$
$$EH=(2\theta/\sqrt{M}+\cos x)(y-x).$$

Then $AG=AE+EH-HG=(2\theta/\sqrt{M}+\cos x)(y-x)-\sin y+\sin x=2\theta^2$ by construction. Thus (1) is obtained.

The parameters necessary for the construction in this particular case are determined as follows:

The velocity v_0 is the velocity which would be produced by the maximum voltage existing continuously across the grids. This voltage is 300. M is 0.6. By the usual equation for electron velocities,

$$v_0 = 1.03\times10^7 \text{ meters per second.}$$

Then $$\theta=\omega d/v_0=\frac{18\times10^9\times0.002}{1.03\times10^7}=3.495 \text{ units}$$

and $2\theta^2=24.35$ units. Also $2\theta/\sqrt{M}=9.01$ units. Thus the distance between the sine curves is 24.35 and the tangent of the angle HCE varies from 8.01 to 10.01. Upon making the graphical calculations it is found that the transit-angle curve of Fig. 2 is obtained where it is

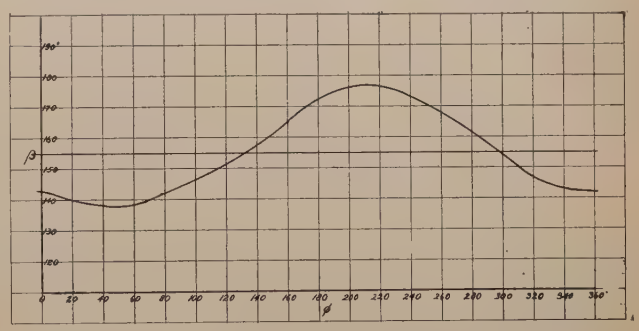

Fig. 2—Transit-time curve for conditions as given in Bronwell's paper.

seen that at $x=180$ degrees, the transit angle β is 173 degrees. The calculated values for this curve are shown in Table I.

TABLE I

ϕ degrees	β degrees	ϕ degrees	β degrees
0	142.6	180	173
20	140	200	175.6
40	138.5	220	176.3
60	138	240	173
80	142.5	260	167.5
100	146.6	280	162
120	151	300	154.5
140	157.5	320	146.8
160	165	340	143

The axis of the transit angle curve is indicated at the value corresponding to the transit angle due to the entrance velocity alone. It lies at $\beta=155$ degrees. It is interesting to note that the maximum transit angle occurs for electrons leaving the first grid after the alternating voltage already has become appreciably negative; i.e., at about 220 degrees.

Arthur B. Bronwell:[3] I believe that there is no need for my adding anything to this discussion since these results agree substantially with those in my published paper.

* PROC. I.R.E., vol. 33, pp. 712–716; October, 1945.
[1] State University of Iowa, Iowa City, Iowa.
[2] R. Kompfner, "Transit time phenomena in electron tubes," *Wireless Eng.*, p. 2, January, 1942.
[3] Northwestern University, Evanston, Illinois.

Contributors to Proceedings of the I.R.E. Section

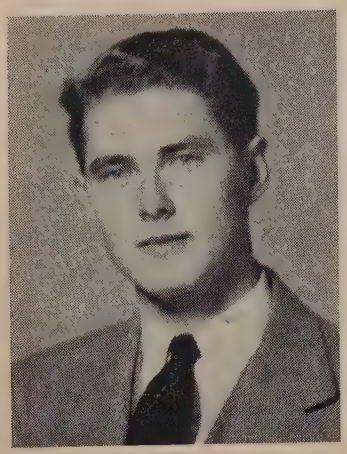

WALTER J. FRANTZ

Walter J. Frantz (S'42–A'45) was born on April 23, 1921, at Swayzee, Indiana. In 1942 he received the B.S. degree in electrical engineering from Purdue University. After graduation Mr. Frantz was employed by the test and measuring equipment section of the RCA Victor Division at Camden, New Jersey. During 1945 he transferred to the RCA Laboratories at Princeton, New Jersey, to continue work on radio circuits and systems. Mr. Frantz is a member of Eta Kappa Nu and Tau Beta Pi.

❖

Edward Leonard Ginzton (S'39–A'40) was born on December 27, 1915, in Russia. He received the B.S. degree in 1936 and the M.S. degree in 1937 from the University of California; the E.E. degree in 1938 and the Ph.D. degree in 1940 from Stanford University. From 1937 to 1939 Dr. Ginzton was an assistant in teaching and research at Stanford University and during 1939 and 1940 a research assistant in physics there. In 1940 he joined the Sperry Gyroscope Company, Inc., and is now a research engineer in charge of tube and microwave research and development. He is a member of Sigma Xi.

❖

Marcel J. E. Golay was born on May 3, 1902, in Switzerland. He received the

❖

EDWARD LEONARD GINZTON

❖

Baccalaureat Scientifique from the Gymnase de Neuchatel in 1920, the licenciate in electrical engineering from the Federal Institute of Technology at Zurich in 1924, and the Ph.D. in physics from the University of Chicago in 1930.

From 1924 to 1928 Dr. Golay was associated with the Bell Telephone Laboratories engaged in work on telephone cables. In 1930 and 1931 he worked on automatic telephone systems for the Automatic Electric Company, and since 1931 he has been connected with the Signal Corps Laboratories, Bradley Beach, New Jersey, working on subaqueous acoustics, terrestrial sound ranging, heat detection, radio relays, and electronic controls.

❖

Arthur E. Harrison (A'41–SM'45) was born on January 20, 1908, at San Luis Obispo, California. He received the B.S. degree in electrical engineering from the University of California in 1936. From 1936 to 1939 he was a teaching Fellow at the California Institute of Technology, and received the M.S. degree in 1937 and the Ph.D. degree in 1940. He did research work for the department of mechanical engineering at the University of California in 1940. Mr. Harrison joined the klystron laboratory of the

❖

MARCEL J. E. GOLAY

❖

Sperry Gyroscope Company at San Carlos, California, in May, 1940, and is now located at the Sperry Research Laboratories in Garden City, Long Island, New York. He is a member of Sigma Xi, Tau Beta Pi, and Eta Kappa Nu.

❖

A. E. Hastings (A'42) received the B.S. degree in electrical engineering in 1934 and the Ph.D. degree in physics in 1938 from Brown University. Since 1938 he has been associated with the Naval Research Laboratory in the development of radar and closely allied devices.

❖

Paul I. Richards (A'45) was born at Orono, Maine, on February 8, 1923. He studied physics and electronics at Harvard University from 1940 to 1943. In 1943, he left became a research associate at the radio research laboratory, Harvard University. His work was concerned primarily with the theory and design of distributed-constant filter circuits. Mr. Richards is now studying for his Ph.D. degree in physics at Harvard University. He is a member of Phi Beta Kappa.

❖

For a biographical sketch of Geoffrey Builder, see Contributors to Waves and Electrons Section, page 147 W, this issue.

❖

A. E. HASTINGS

PAUL I. RICHARDS

ARTHUR E. HARRISON

PROCEEDINGS OF THE I.R.E. AND WAVES AND ELECTRONS

Published Monthly
by
The Institute of Radio Engineers, Inc.

March, 1946

SECTION II—WAVES AND ELECTRONS SECTION

George R. Town—Chairman, Rochester Section ..... 108 W
When Radio Engineer is "Big Boss" ..... Orestes H. Caldwell 109 W
Induction Heating in Radio Electron-Tube Manufacture ..... Edwin E. Spitzer 110 W
Fine Wires in the Electron-Tube Industry ..... George A. Espersen 116 W
A Three-Beam Oscillograph for Recording at Frequencies up to 10,000 Megacycles ..... Gordon M. Lee 121 W
Synchronizing Generators for Electronic Television ..... A. Rufus Applegarth 128 W
The Effect of Negative Voltage Feedback on Power-Supply Hum in Audio-Frequency Amplifiers ..... Geoffrey Builder 140 W
High-Voltage Rectified Power Supply Using Fractional-Mu Radio-Frequency Oscillator ..... Robert L. Freeman and R. C. Hergenrother 145 W
Contributors to WAVES AND ELECTRONS SECTION ..... 147 W

Institute News and Radio Notes

Outstanding Events of 1946 Winter Technical Meeting ..... 149 W
Board of Directors ..... 154 W
Executive Committee ..... 155 W
I.R.E. People ..... 155 W
Sections ..... 159 W

Books

"Pulsed Linear Networks," by Ernest Frank ..... Reviewed by Albert Preisman 159 W
"Table of Arc Sin X," Prepared by The Mathematical Tables Project, Arnold N. Lowan, Project Director, and a Technical Staff of Six Persons ..... Reviewed by John R. Whinnery 160 W
Section Meetings ..... 36 A
Membership ..... 40 A
Positions Open ..... 54 A
Positions Wanted ..... 56 A
Advertising Index ..... 86 A

SECTION I—PROCEEDINGS OF THE I.R.E. SECTION CONTENTS ON PAGE 95 P

EDITORIAL DEPARTMENT

Alfred N. Goldsmith
Editor

Helen M. Stote
Publications Manager

Ray D. Rettenmeyer
Technical Editor

Winifred Carrière
Assistant Editor

William C. Copp
Advertising Manager

Lillian Petranek
Assistant Advertising Manager

Responsibility for the contents of papers published in the PROCEEDINGS OF THE I.R.E. and WAVES AND ELECTRONS rests upon the authors.
Statements made in papers are not binding on the Institute or its members.

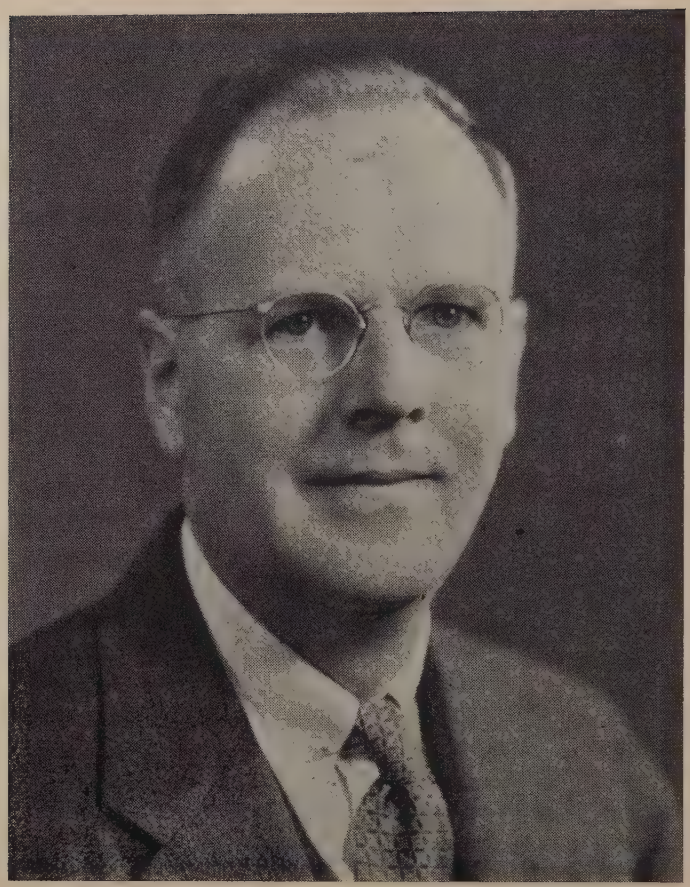

George R. Town

Chairman—Rochester Section

George R. Town was born on May 26, 1905, in Poultney, Vermont. He received the degree of E.E. from Rensselaer Polytechnic Institute in 1926, and the degree of D.Eng. from the same institution in 1929.

From 1929 until 1933 he was an engineer in the research laboratory at Leeds and Northrup Company. For seven months in 1933 he was a development engineer for Arma Engineering Company. From 1933 to 1936 he was an instructor at Rensselaer Polytechnic Institute serving one year as instructor in mathematics, and two years as instructor in electrical engineering.

In 1936 Dr. Town joined the engineering division of Stromberg-Carlson Company. He has worked successively as an engineer in the research department, as engineer-in-charge of the television laboratory, as assistant director of research, and in his present position as manager of engineering and research. In April, 1945, he was elected assistant secretary of the Company. He has served on various panels and committees of the Nationa Television System Committee and of the Radio Technical Planning Board, being chairman of one of the Television Standards Committees of the latter organization. He is, at present, chairman of the Frequency-Modulation Systems Committee of the Radio Manufacturers Association, and secretary of the RMA Television Systems Committee.

He was secretary of the Rochester Section from 1942 to 1944, and has served as chairman for the Rochester Section since 1944. He is chairman of the I.R.E. Committee on Organizational Research, and is a member of the I.R.E. Committee on Education. He is vice-chairman of the Rochester Section of the American Institute of Electrical Engineers.

Dr. Town joined the Institute of Radio Engineers as an Associate in 1937 and transferred to Senior Member grade in 1944.

Contributing substantially to the advancement of the radio-and-electronic field are the various periodicals which present the methods and advances in that field. Their Editors are a group of leaders of thought in the field. Guest editorials from the pens of these Editors have been requested, and it is accordingly possible to present below an analytical and stimulating discussion from the Editor of *Electronic Industries*, who is himself a Fellow of The Institute of Radio Engineers and a former Federal Radio Commissioner.

The Editor

When Radio Engineer is "Big Boss"

Orestes H. Caldwell

Radio engineers can be proud of the industrial wealth they have created and continue to create.

Last year, for example, some four-billion-dollars' worth of radio equipment and service—four-thousand-million dollars—was produced based on the technical discoveries and designs created by the members of The Institute of Radio Engineers and their fellow engineers. For each of the voting members of the I.R.E., this was nearly one and one-half million dollars per man. And all of this billions of dollars of actual wealth per year was created literally "out of thin air" by radio engineers and radio inventors.

Radio engineers have now had a taste of big-scale industrial production. Radio engineers have seen themselves playing a part in big-business operations. They have observed that their knowledge and their efforts are at the center of businesses which collect hard round dollars in the millions.

But from now on, we should insist, radio engineers must not be satisfied to be merely employees and staff aides in the huge industries they have created.

Radio engineers should themselves take business and industrial leadership. It is time for the radio engineer to be the "big boss" of his own concern and shape its general policies. Instead of avoiding and evading business responsibility in order to keep close to the design room and slide-rule, radio engineers should prepare to reach out themselves for the top management positions, for independent proprietorships, for public service in fitting radio into broader usefulness to humanity.

All too often, some skillful lawyer, clever salesman, or quick-minded accountant is chosen to fill the top place in a radio organization, a post which would have been far better served by a trained radio-minded man having the broad grasp necessary to relate our radio art to general business problems.

Radio engineers are perfectionists. And so they like to keep close to their technical work, improving detail parts into the highest possible efficiency.

But even from this aspect of perfectionism alone, radio men will admit that fullest perfection in radio cannot come unless the radio engineer has the greatest freedom in which to work. And this means that there must be radio engineers at the top who can give sympathetic encouragement to radio engineers throughout the organization.

Radio engineers have created a whole galaxy of great industries—industries tremendous in public service, industries imagination-defying in technical achievement, and industries now astronomic in dollar volume!

Let us look forward to the day when radio-electronic industries are officered by radio men, from top executive posts on down to the design rooms and production departments. This is absolutely necessary, for the good of the radio industries and the public they serve. Let radio men accept and even seek out these responsibilities of management and direction. And let us see that the radio man collects in full, for himself and his family, his share of the wealth he is producing.

Induction Heating in Radio Electron-Tube Manufacture*

EDWIN E. SPITZER†, SENIOR MEMBER, I.R.E.

Summary—**The radio electron-tube industry was one of the first to use induction heating extensively. The metal parts of electron tubes must be heated to 500 to 1500 degrees centigrade during evacuation in order to liberate gases occluded in the parts. Since the parts are in a vacuum and are usually surrounded by a glass bulb, induction heating is the ideal method. The heating coils are usually made to fit the bulbs and may be used either on stationary evacuation systems or on rotary systems. Other similar applications are "getter"-flashing and vacuum-firing systems. Still other applications are in sealing metal to glass, in brazing tube parts together, and in welding. In all of these applications the chief advantages are accurate control and speed of heating. The radio-frequency generators are usually of the vacuum-tube type operating at about 200 to 500 kilocycles. Units of about 2 to 15 kilowatts are used. The theory of heating is developed from simple air-cored transformer considerations and an example is given.**

Introduction

INDUCTION heating is very widely used in the radio electron-tube industry. This has been true starting from the early 1920's. The main use has been in degassing the electrodes of radio tubes during evacuation of the tubes. In evacuating, or exhausting, any type of electron tube it is necessary not only to remove the air from the tube envelope, but also to remove, to a great extent, gases and vapors occluded in the internal tube parts so that they will not be liberated later during use of the tube. The higher the temperature to which these parts can be brought during the exhaust process, the more rapidly the undesired gases can be pumped out. The temperature is limited by such considerations as evaporation of the electrode materials, melting of parts, or melting of the glass envelope. The temperature range is roughly 500 to 1500 degrees centigrade, although higher temperatures may be used in the case of high-power tubes.

In the earliest days of the radio electron-tube industry, heating of tube electrodes was accomplished by lighting the filament so that it would emit electrons, and then applying voltage to the other electrodes so that they would be bombarded by electrons. Under these conditions, the heat dissipated in an electrode is simply the product of the applied voltage and the current to the electrode. This method is still used in many cases, but it has been largely supplanted by induction heating. The reason for this change is that it is inadvisable to require modern filaments and cathodes to emit heavy electron current while the vacuum in the tube is poor. Modern cathodes are usually of the barium-strontium, oxide-coated filament type or of the thoriated-tungsten type. Both of these types of cathodes are very efficient sources of electron emission, but they are also sensitive to gas bombardment or oxidation by oxidizing gases. It is, therefore, very desirable not to heat the cathodes to operating temperature during poor vacuum conditions such as would be present while electrodes are giving off gas and vapor. Induction heating is, consequently, an ideal method of heating the electrodes of tubes, because the cathode may remain unenergized while the electrodes are being degassed. In addition, induction heating may be controlled very easily. It is small wonder, therefore, that this type of heating is so widely used in the tube industry.

Applications

A number of typical induction-heating applications will be described. Application to tube exhausting has already been mentioned. There are two main types of such applications, the first to stationary exhausting positions and the second to automatic rotary machines. Fig. 1 shows a stationary application. Here a 500-watt

Fig. 1—Induction heating applied to radio tubes.

tube is being exhausted. The tube has been sealed to a glass exhaust manifold which leads to a vapor-diffusion pump. The anode of the tube, which is 2 inches (51 millimeters) in diameter and 3 inches (76 millimeters) long,

* Decimal classification: R590×R331. Original manuscript received by the Institute, June 25, 1945; revised manuscript received, August 22, 1945. Reprinted by permission from the *Transactions of the Electrochemical Society*, vol. 86, 1944.

† RCA Victor Division, Radio Corporation of America, Lancaster, Pennsylvania.

and made of tantalum sheet, is being heated to about 1300 degrees centigrade by the multiple-turn heating coil or inductor. The inductor is made of standard 0.25-inch (2.5-millimeter) copper tubing and carries a cur-

Fig. 2—Automatic rotary exhausting machine.

rent of about 150 amperes at about 300 kilocycles. This current is generated by an 8-kilowatt radio-frequency generator, which will be described later. The radio-frequency current is controlled by changing of voltage taps

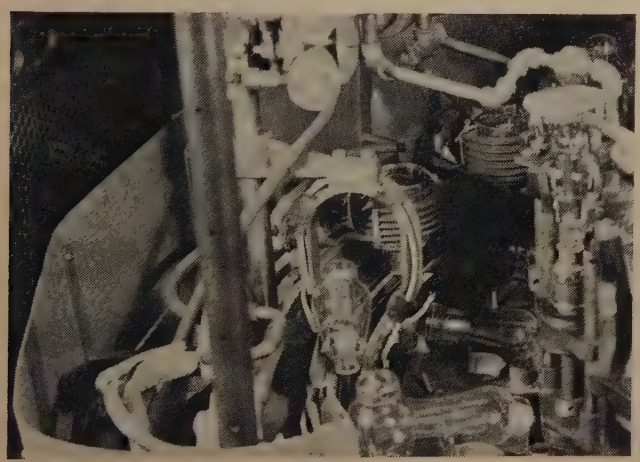

Fig. 3—Induction-heating position on rotary exhausting machine.

on the high-voltage-supply transformer and by variation of the filament voltage of the oscillator tubes in the generator.

Fig. 2 shows an automatic rotary exhausting machine. The exhaust tubing of the tubes is inserted into a rubber exhaust opening and connected by means of manifolds and a rotary valve to diffusion and mechanical pumps. The rotary table carrying the tubes turns at intervals which may be 0.1 to 3 minutes long. To the rear of the machine, the carbon anodes of the tubes may be seen heated to incandescence by high-frequency inductors. Just before the rotary table indexes, the inductors are raised up high enough to clear the tubes. Due to this arrangement, it is not necessary to have the inductors rotate. The radio-frequency generator may be seen in the left background; the heavily insulated leads carrying the current to the machine are in clear view. Several inductors are usually connected in series in order to utilize fully the capabilities of the generator.

Fig. 3 shows a closer view of the machine in Fig. 2. Fig. 4 shows a typical inductor held over a tube. The inductors shown in these two figures are made of flattened 0.5-inch (51-millimeter) diameter copper tubing through which cooling water is circulated. Inductor

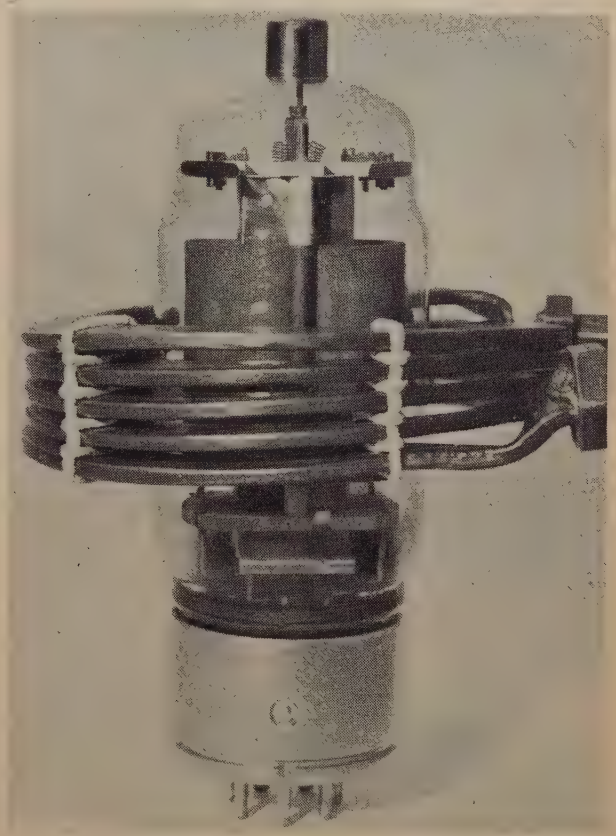

Fig. 4—Typical inductor and radio tube.

currents of 50 to 150 amperes are used; temperatures of 700 to 1200 degrees centigrade are commonly produced in the electrodes of the tubes being exhausted. The inductors are designed to be readily interchangeable by the use of standard pipe couplings. In this way, inductors of varying diameter and construction to suit the job at hand may be installed.

Fig. 5 shows an application of induction heating to vacuum firing. It is often desirable to heat tube parts to high temperature in good vacuum prior to assembly of the tubes. Occluded gases can be removed in this manner and it is also possible to remove vaporizable contaminating materials. In the particular case shown in Fig. 5, small tube parts are being vacuum-fired. Since these parts have very poor coupling to the inductor, they are placed in a box made of tantalum sheet. The induction currents heat the box which in turn heats the parts by

radiation and conduction. The box is supported within the long, 5-inch (127-millimeter) diameter glass bell jar, which rests on a rubber gasket lubricated with castor

Fig. 5—Induction-heated vacuum firing station.

oil. The vacuum pumps are mounted below the table. The inductor can be seen surrounding the bell jar. A multiple-turn inductor of 0.25-inch (6 millimeters) copper tubing is used; its power supply is a 16-kilowatt radio frequency generator.

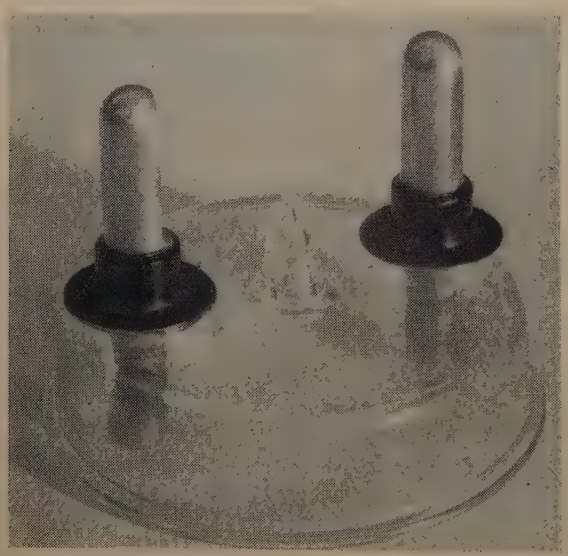

Fig. 6—Metal-to-glass seals made with induction heat.

Sealing Metal to Corning Glass

A considerably different application is sealing metal to glass. Fig. 6 shows a completed assembly consisting of a molded glass "dish" and two terminals of Kovar which have been sealed to the "dish." Kovar, an iron-nickel-cobalt alloy, has an expansion curve which closely matches that of Corning No. 705FN glass. As a result, butt glass-to-metal seals of the type shown are readily possible. To make a seal of this type the Kovar and glass can be heated by gas-oxygen flames, but much more uniform results are obtained by heating the Kovar by induction. Fig. 7 shows the setup used for making the

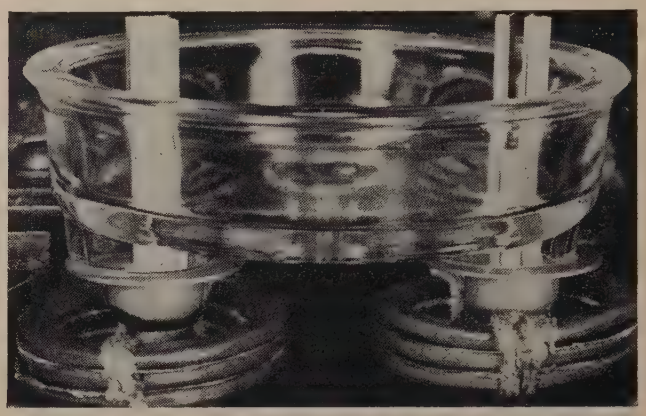

Fig. 7—Metal-to-glass sealing setup

seal just described. The glass dish and two terminals are held in position by suitable means. The two Kovar cups are heated by the small inductors. The glass dish

Fig. 8—Typical silver-soldered assembly.

may be moved up and down. The Kovar cups are heated until they oxidize slightly and then the glass dish is pressed down so that the two flat-ground openings in the dish contact the cups. Moderate pressure is applied while the cup heating is continued. In a short time the glass softens and flows. In this state it dissolves the surface oxide on the cups, and an intimate bond results. Heating is then stopped and the assembly is placed in a continuous annealing oven so as to remove any strains introduced in the glass. The entire sealing operation requires only about one minute. An 8-kilowatt vacuum-tube radio-frequency generator is used. This method, which has been in use about 5 years with women

operators, has been singularly free of difficulties although the operation itself was once regarded as a job requiring many years of training.

Brazing

Still another application of induction heating is in brazing. Fig. 8 shows a typical case. The large flange is made of Kovar and four Kovar glass assemblies are brazed to the flange using Handy and Harman "BT" silver solder. The joint must be vacuum-tight. The flange is mounted, as shown in Fig. 9, over a 5-turn

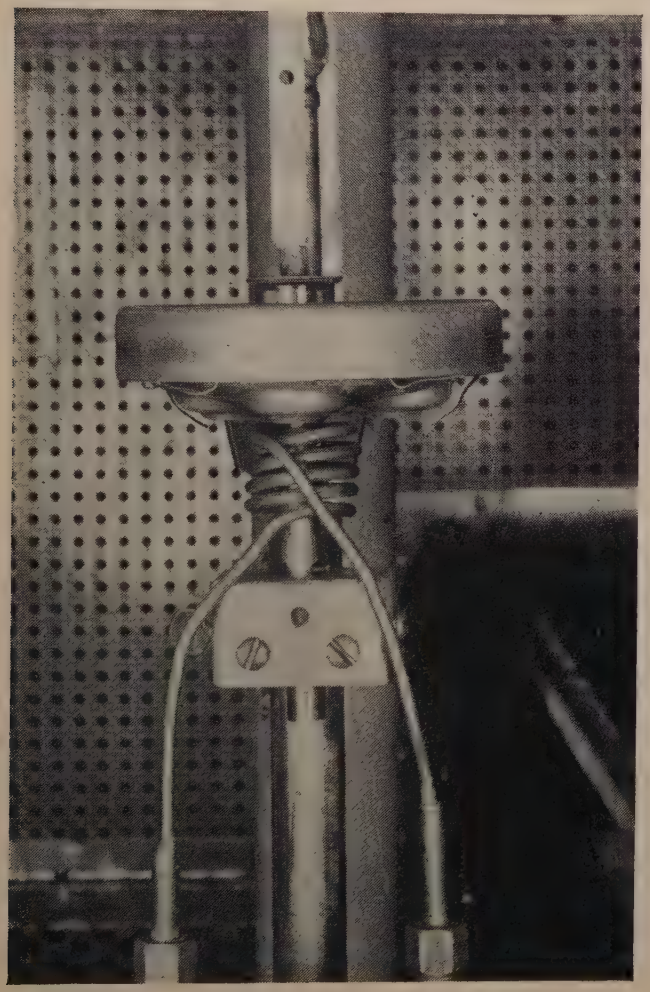

Fig. 9—Silver-soldering setup.

inductor. A single turn of wire solder is placed around the joint to be brazed. A bell jar fed with hydrogen from the top is placed over the work. The radio-frequency generator is then turned on until the silver flows as observed through a window. Since the heating is done in a reducing atmosphere, all metal parts stay bright. An 8-kilowatt furnace is used, although a smaller one would be satisfactory. Experience has shown that soldering of Kovar is much more satisfactory when done this way. Furnace soldering, where the parts are held above the soldering temperature for several minutes, and then cooled slowly, often gives difficulty because the solder can enter grain boundaries in the Kovar and split it open. For certain sizes and shapes, induction soldering may be effected with sufficient speed and the heat so localized that splitting does not occur.

Radio-Frequency Generators

Fig. 10 shows a typical 8-kilowatt radio-frequency generator as used in manufacturing operations. These generators use two Type 892 water-cooled triodes. These

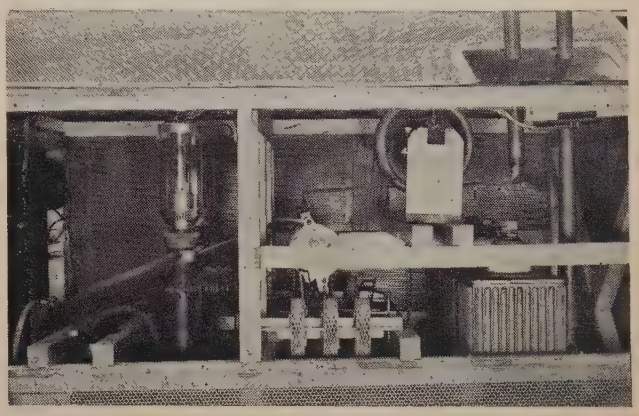

Fig. 10—Eight-kilowatt radio-frequency generator.

tubes have tungsten filaments and are rated for operation as oscillators with a direct-current power input of 30 kilowatts at 15 kilovolts and 2 amperes. The anodes are rated to dissipate up to 10 kilowatts.

Fig. 11 is a simplified circuit diagram of the above generator. In this generator the tubes are operated with 60-cycle alternating-current plate voltage in order to simplify the design of the generator. (When it is desired to utilize the full capability of the oscillator tubes, they are operated with direct-current rather than with alternating-current plate voltage.) Since the oscillator tubes

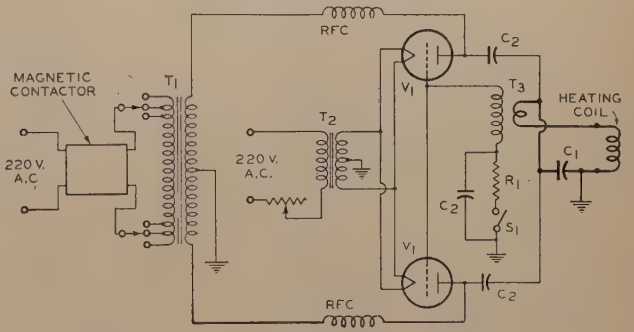

Fig. 11—Eight-kilowatt radio-frequency generator circuit.
Range = 250 to 400 kilocycles.
V_1 = RCA-892 water-cooled power tube
T_1 = 12.5-kilovolt power transformer. Total secondary voltage 7 to 18 kilovolts
T_2 = filament transformer
T_3 = feedback transformer
RFC = radio-frequency choke coil
C_1 = mica capacitor, 0.014 to 0.021 microfarad, 140 to 210 amperes
C_2 = mica capacitor, 0.004 microfarad
R_1 = grid-bias resistor, 1000 to 6000 ohms
S_1 = output control switch

themselves act as rectifiers of the 60-cycle power, it is necessary to use two tubes, operating on opposite secondary-winding terminals of a 60-cycle transformer with the center tap of the secondary grounded. Thus,

one oscillator tube operates on one-half cycle and the other on the other one-half cycle. The rectified currents supplied by the tubes buck each other and there is, therefore, no direct-current flux produced in the transformer.

The Type 892 tubes are effectively connected in parallel for radio-frequency currents by means of mica capacitors. The radio-frequency circuit consists partly of a bank of mica capacitors of 0.014- to 0.021-microfarad capacitance and rated to carry 140 amperes to 210 amperes at 300 kilocycles, and partly of a parallel inductance composed of the external inductors and leads, and an internal coil which couples to a second coil for feedback of excitation voltage to the grids of the Type 892 tubes.

Control of output current is obtained by means of taps on the primary of the plate-supply transformer and by means of a filament voltage control. The latter gives fine control by varying the electron emission of the Type 892 filaments. The generator is equipped with a filament voltmeter, plate-current meter, and a radio-frequency output-current meter.

Since the Type 892 tubes are water-cooled, a water-flow meter and interlock are provided so that the generator is shut off automatically if the water flow drops below a safe value. A plate-current overload relay is also provided.

The generator is turned on and off when in service by opening the grid-leak resistor. This method very effectively cuts off the generator and, since the current in the grid resistor is only a few hundred milliamperes, no unusual relay is needed. Generators of this type have proved very reliable and flexible.

Theory of Induction Heating

Many cases of induction heating in the radio industry concern thin-walled cylinders. In other cases, the depth of penetration of the current is so small that the load can be considered a thin-walled cylinder, with the wall thickness equal to the depth of penetration. The inductor and the load can thus be considered as an air-cored transformer. The mathematical solution of this heating problem is very simple.[1,2,3] The expression for the efficiency of heating is

$$n = \frac{1}{1 + \frac{1}{K^2}\left(\frac{1 + Q_2^2}{Q_2 Q_1}\right)} \qquad (1)$$

where K = coefficient of coupling between inductor and the load
$Q_1 = Q$ of the inductor
$Q_2 = Q$ of the load.

[1] W. Esmarch, "Zur Theorie der kernlosen Induktionsöfen," *Wiss. Veröffent. Siemens-Konzern*, vol. 10, pp. 172–196; 1931.
[2] H. B. Dwight and M. M. Bagai, "Calculations for coreless induction furnaces," *Elec. Eng.*, vol. 54, pp. 312–315; March, 1935.
[3] G. H. Brown, "Efficiency of induction heating coils," *Electronics*, vol. 17, pp. 124–129, 382–385; August, 1944.

Q is defined as the ratio of reactance of a circuit element to the series resistance of the element.

In the case of an inductance L having a resistance R at a frequency of f,

$$Q = \frac{2\pi fL}{R} = \frac{\omega L}{R}.$$

A study of (1) shows that efficiency increases with Q_2 and is essentially at its maximum value when $Q_2 = 3$.

Further, the current required in the inductor to produce W watts in the load is

$$I = \frac{\sqrt{W}}{K\sqrt{\omega L_1}}\sqrt{\frac{1 + Q_2^2}{Q_2}} \qquad (2)$$

where L_1 = unloaded inductance of the inductor.

The voltage across the inductor is

$$E \cong I\omega L_1\left(1 - K_2\frac{Q_2^2}{1 + Q_2^2}\right). \qquad (3)$$

In the application of the above equations, practical units are to be inserted; i.e., henries, ohms, watts, root-mean-square volts and amperes, and cycles per second.

The question now arises, how are these quantities to be determined? If both the inductor and load are coaxial cylinders, the inductance of each and also their mutual inductance may be calculated.[4] The coupling coefficient is then the mutual inductance divided by the square root of the product of the two individual inductances. The reactance of the load can be calculated at the operating frequency. The resistance around the periphery of the load can also be easily calculated. If the thickness of the wall of the load is greater than the depth of penetration of the current, the thickness should be taken as equal to the depth of penetration. The Q of the load and the reactance ωL_1 of the inductor are next calculated. Thus, all constants for (2) and (3) are known, and with further insertion of the watts desired in the load, both inductor current and voltage may be obtained. Since it may not be practical to calculate the Q of the inductor very reliably, measurement may be necessary if determination of efficiency is desired.

If neither the inductor nor the load possesses geometrical shapes for which there are formulas for inductance and mutual inductance, measurement can be made. A Boonton Model 160-A Q meter is very convenient for this purpose. First, a model of the inductor is made of the same length and cross section and wound with enough turns of wire to bring the inductance up to 600 to 1000 microhenries so as to permit obtaining resonance with the variable Q meter capacitance of 450 micromicrofarads. The Q meter is resonated at the desired frequency and a reading of Q and the required resonant capacitance are noted. This permits calculation

[4] Bureau of Standards Circular No. 74, Radio Instruments and Measurements, 1938.

of L_M, ωL_M, and R_M, where the subscript M refers to the model. The load is then inserted. (If the load is magnetic at room temperature, but not at the desired temperature, an identical load of nonmagnetic metal should be used.) The Q meter is reresonated and the new values of Q and capacitance are noted. Again L_M', $\omega L_M'$, and R_M' are calculated. The original values are subtracted giving $\Delta\omega L_M$ and ΔR_M. The theory shows that

$$\frac{\Delta\omega L_M}{\omega L_M} = K^2 \frac{Q_M^2}{1 + Q_M^2} \tag{4}$$

and that

$$Q_M = \frac{\Delta\omega L_M}{\Delta R_M}. \tag{5}$$

Equation (5) gives Q_M which is inserted in (4). Equation (4) can be solved for the coupling coefficient K. Knowing the resistivity of the actual load at the desired temperature and the resistivity of the load used during the test above, we find that the true Q of the load is

$$Q_2 = Q_M \sqrt{\frac{\rho_M}{\rho_2}} \tag{6}$$

where ρ_M is the model load resistivity and ρ_2 the actual load resistivity. Equation (6) assumes that the depth of penetration is less than about one fifth of the radius of the load. Finally, the measured ωL_M must be reduced by the ratio of the square of the inductor turns to the square of the model turns, so as to get the true inductor reactance ωL_1. All values are then known for (2) and (3).

Both of the above methods have been used with good results. One example will be given. The load and inductor were those shown in Fig. 4. A model of the inductor was made by winding 91 turns on a coil form. The model had the same length as the inductor, but the diameter was 3.75 inches (95 millimeters) instead of 3.5 inches (89 millimeters). This requires a later correction in K. The model connected to a Boonton Q meter, gave at 300 kilocycles a Q of 180 and a resonant capacitance of 272 micromicrofarads. By a second measurement at 600 kilocycles, it was found that the model had 7 micromicrofarads stray capacitance. Therefore the corrected capacitance was 279 micromicrofarads. From the usual formula connecting L, C, and f, the inductance of the model was 1010 microhenries and its reactance was 1905 ohms at 300 kilocycles. Thus the model had a resistance of $1905/180 = 10.6$ ohms.

Next, the anode of Type 813 tube was inserted in the model and it was found that at 300 kilocycles the Q was 29 and the resonant capacitance was 286 micromicrofarads. Repeating the calculations above the new model reactance was 1810 ohms and the new resistance was $1810/29 = 62.4$ ohms. The change in reactance was, thus, $1905 - 1810 = 95$ ohms, and the change in resistance was $62.4 - 10.6 = 51.8$ ohms. Applying (5) we find that

$$Q_M = \frac{95}{51.8} = 1.83.$$

In this case, since an actual anode and not a model was used, $Q_M = Q_2$. However, the anode was not at operating temperature, so the correction of (6) is still necessary. The ratio of hot-to-cold resistance in this case was 0.85. Therefore the hot

$$Q_2 = 1.83 \sqrt{\frac{1}{0.85}} = 1.99.$$

Applying (4), we obtain

$$\frac{95}{1905} = K^2 \cdot \frac{\overline{1.83^2}}{1 + \overline{1.83^2}}.$$

From this equation

$$K = 0.25.$$

This value needs revision, due to the fact that the inductor model had too large a diameter. As an approximation, K is inversely proportional to diameter. Thus the corrected K became

$$0.25 \times \frac{3.75}{3.5} = 0.268.$$

The reactance of the model inductor was then reduced by the square of the number of turns in order to get the reactance ωL_1 of the actual inductor, which had 4.5 turns. We obtain

$$\omega L_1 = 1905 \times \left(\frac{4.5}{91}\right)^2 = 4.63 \text{ ohms.}$$

The power required in the anode was calculated by assuming that the temperature was 1100 degrees centigrade and the radiation coefficient was 0.8, and by allowing 5 per cent for end effects. This gave 1200 watts.

Now applying (2) and (3), we obtain

$$I = \frac{1}{0.268} \sqrt{\frac{1200(1 + \overline{1.99^2})}{4.63 \times 1.99}} = 95 \text{ amperes}$$

and

$$E = 95 \times 4.63 \left(1 - \overline{0.268^2} \frac{\overline{1.99^2}}{1 + \overline{1.99^2}}\right) = 415 \text{ volts.}$$

Actual measurements on an exhausting machine gave $I = 87$ amperes, $E = 365$ volts at a frequency of 308 kilocycles and with an anode temperature of 1100 degrees centigrade. This comparison shows that satisfactory results can be obtained by this method.

Additional References

(1) T. P. Kinn, "R-F generator characteristics for induction heating," *Radio-Elec. Eng.*, vol. 4, pp. 20–22, 28–30; January, 1945.
(2) R. M. Baker and C. J. Madsen, "High-frequency induction heating of conductors and nonconductors," *Elec. Eng.*, vol. 64, p. 64; February, 1945.
(3) F. W. Curtis, "High-Frequency Induction Heating," McGraw-Hill Book Company, New York, N. Y., 1944.

Fine Wires in the Electron-Tube Industry*

GEORGE A. ESPERSEN†, ASSOCIATE, I.R.E.

Summary—This article discusses primarily the application of fine wires in the electron-tube industry. Some fundamental basic properties which confront the wire manufacturer are briefly discussed. Design formulas, including a nomograph, are given for electron-tube filaments. The use of platings of gold, platinum, and zirconium on metals of the refractory group have assisted in the reduction of grid emission. A unique method of utilizing zirconium, both to accelerate the vacuum exhaust process and to serve as a continuous "getter," is described. A novel method of securing a uniform rate of evaporation of thin films of metals is discussed.

Methods of Specifying Characteristics

FINE WIRES such as nickel, nickel alloys, tungsten, thoriated tungsten, molybdenum, and tantalum have been used by the electron-tube industry from the date of its inception. The practices set up for manufacturing incandescent-lamp filaments were readily applied to filaments, heaters, and grids for electron tubes. Through a period of years, various standards for wire quality and characteristics have been established independently by individual electron-tube manufacturing companies. These standards in most cases are practically identical, with minor deviations occurring where certain other fabricating processes are to be considered.

The basic properties which have been considered are: (1) finish; (2) weight; (3) diameter; (4) elongation; (5) tensile strength; (6) straightness; (7) electrical resistance; (8) chemical composition; (9) brittleness.

The finish of a wire may vary from a clean, shiny surface to a dark matt surface. Manufacturing specifications may also include such statements as freedom from kinks, waves, cracks, slivers, seams, burrs, roughness, soap drawing compounds, oil, foreign matter, and oxides.

The weight of the fine wires is usually expressed in milligrams per 200 millimeters. Tolerances on weight usually vary from plus or minus 2 per cent for filaments to plus or minus 4 per cent for grid wires, these values depending upon the degree of control required to maintain the specified characteristic tolerances.

The diameter of the wire is usually specified as a nominal value for fine wires, and it can readily be computed by using either of the following formulas:

$$D = K_1\sqrt{W} \qquad (1)$$

$$W = K_2D^2 \qquad (2)$$

where D = the mean diameter of the wire in mils
W = the weight of the wire in milligrams per 200 millimeters of length
K_1 and K_2 = constants depending upon the densities of the wire.

Table I indicates values for K_1 and K_2 for the materials named.

TABLE I

Material	K_1	K_2
Molybdenum	0.989	1.022
Tungsten	0.717	1.950
Tantalum	0.771	1.682
Thoriated Tungsten	0.725	1.903
Nickel	1.055	0.898
Magno Nickel	1.064	0.883

The diameter of a wire is usually checked by the wire manufacturer for any out-of-round tendencies, which usually indicate excessive die wear and serve as a warning to change defective dies. Lack of uniform diameter may cause localized bright spots, if the wire is used as a filament, which would tend to shorten its useful life; if utilized as a grid, no detrimental effects should be observed providing the specified weight tolerance is maintained.

Out-of-roundness is usually expressed as a percentage equal to

$$\frac{A - B}{A} \times 100$$

where A = the maximum diameter of the cross section in inches, and
B = the minimum diameter of the cross section in inches.

The elongation of fine wires is usually specified if this material is to be used for grid material, in particular for grids requiring stretching of the laterals to maintain a specified shape. Typical values of elongation range from 17 to 22 per cent.

The straightness is usually specified for grid lateral material and tungsten heaters of the spiral type. This quality indicates the relative freedom from strain resulting from proper annealing of the wire. No standard method of testing this characteristic has been established in the electron-tube industry.[1] The usual crude test is to suspend a three-foot length at the ends in a horizontal plane approximately twenty inches apart and observe that the sample assumes the shape of a catenary free from bulges or irregular rises or twists.

Brittleness tests are specified for tungsten wire, which is used either as direct or indirect heaters. Stringent

* Decimal classification: R331×R282.1. Original manuscript received by the Institute, June 22, 1945; revised manuscript received, October 10, 1945.

† North American Philips Company, Inc., Dobbs Ferry, N. Y.

[1] See "American Society for Testing Materials Standards Handbook," 1944, p. 1794.

vibration testing of tubes has made such tests imperative. Manufacturers of electron tubes differ only in detail as to how this quality is measured. The usual procedure consists of supporting one end horizontally by clamping and bending the wire downward to a specified angle at which value the specimen shall not break or show a tendency towards splitting.

Electrical-resistance and chemical-composition tests are usually established only as additional tests. These properties have usually been well adhered to by most wire manufacturers, since it is very difficult to have any undue quantities of volatile impurities at the temperatures at which wires of the refractory group are sintered. Manufacturers who make alloys consisting of two or more metals of the refractory group conduct thorough tests on electrical conductivity as well as the chemical composition. In cases where the heaters or filaments are formed in the shape of coils, either inductive, noninductive, flat pancake, or spiral, nonsag material is usually specified.

It is clear that if the tube engineer puts such rigid quality requirements on his wires, the wire manufacturers can supply a satisfactory product only if they are equipped with up-to-date wire-drawing and wire-plating machinery.

In addition, a scientific control system, using the latest apparatus handled by a skilled staff to check the finished product is necessary. These features can be provided only by wire manufacturers in intimate contact with the electron-tube manufacturers.

Fine wires employed as a base metal for emitters usually consist of pure nickel, aluminum nickel, cobalt nickel, silicon nickel, tungsten, thoriated tungsten, and nickel-plated tungsten. Wires containing nickel are base metals for oxide-coated filaments of the alkaline earth group, usually barium, strontium, and calcium. Tungsten wires have been utilized either as a base metal for indirectly heated cathode-type tubes or as a direct emitter for high-power water-cooled copper-anode tubes. Thoriated-tungsten wire has been successfully employed as a direct emitter for power-transmitter tubes where the maximum plate dissipation does not exceed 1000 watts or the maximum plate voltage does not exceed 4000 volts. Nickel-plated tungsten wires having

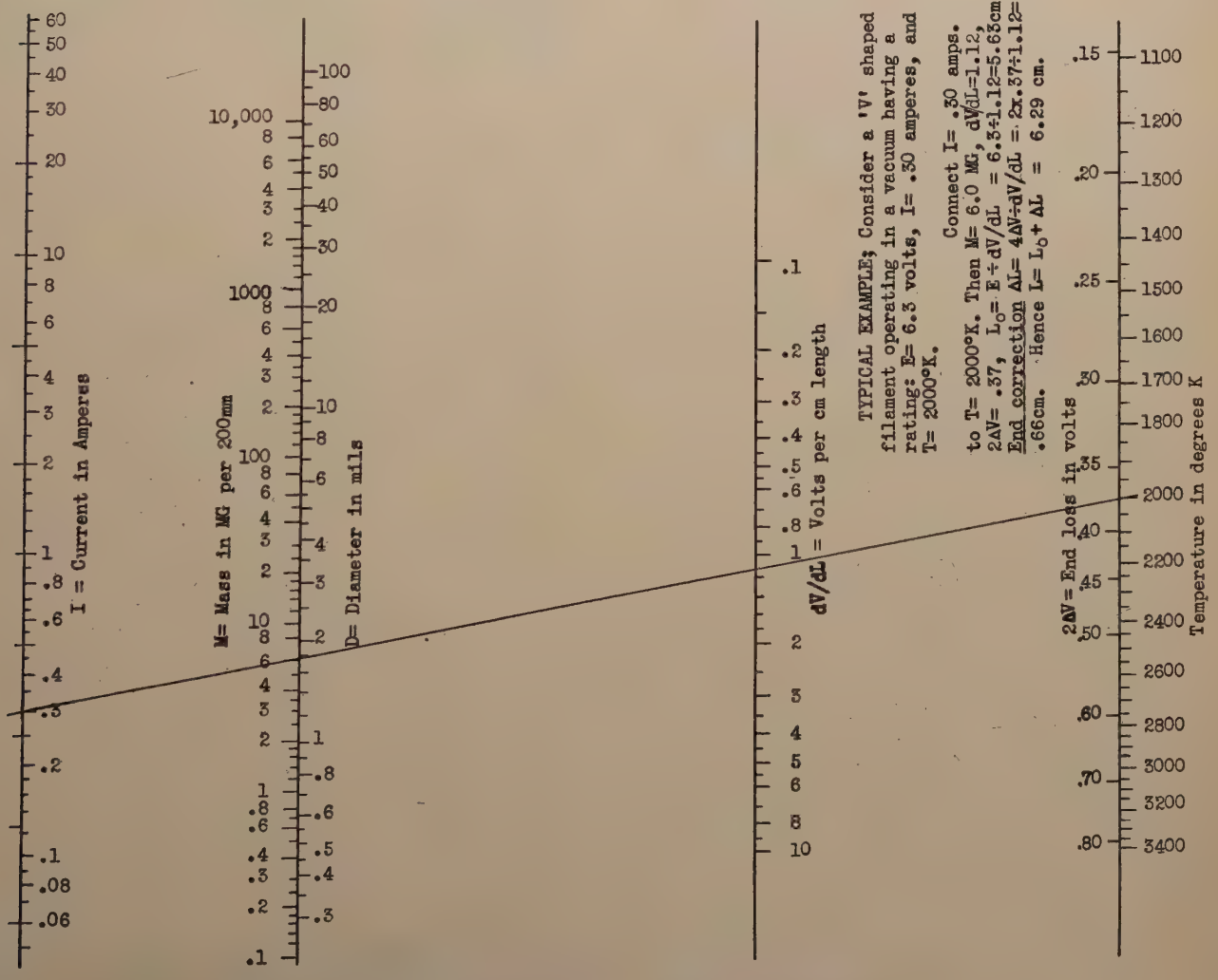
I = Current in Amperes
M= Mass in MG per 200mm
D= Diameter in mils
dV/dL = Volts per cm length
2ΔV = End loss in volts
Temperature in degrees K
TYPICAL EXAMPLE; Consider a 'V' shaped filament operating in a vacuum having a rating: E= 6.3 volts, I= .30 amperes, and T= 2000°K.
Connect I= .30 amps.
to T= 2000°K. Then M= 6.0 MG, dV/dL=1.12,
2ΔV= .37, L0= E÷dV/dL = 6.3÷1.12=5.63cm.
End correction ΔL= 4ΔV÷dV/dL = 2x.37÷1.12=
.66cm. Hence L= L0+ ΔL = 6.29 cm.

Fig. 1—Nomograph for design of tungsten filaments. (See footnote reference 2.)

diameters of less than 0.001 inch are suitable as a base metal for oxide-coated filaments of the alkaline earth group on minature and hearing-aid-type tubes.

Design Fundamentals

The following formula is generally employed by electron-tube engineers in the design of filaments. (End losses are not considered.)

$$R_h = \frac{2\rho L_h d}{W_h}$$

where R_h = heater resistance at operating temperature expressed in ohms
ρ = specific resistance in ohms at the operating diameter
d = density of the heater material in milligrams per cubic centimeter
W_h = heater-wire weight in milligrams per 200 millimeters of length
L_h = heater-wire length in millimeters.

Fig. 1 takes into consideration the correction factor for end losses due to conduction to the leads to which the filament is welded and the contact with the filament tension hook.[2]

Grid Emission

Grids on most receiving tubes and a number of transmitting types use lateral wires having diameters of less than 0.010 inch. The most common materials being used are manganese-nickel, nickel-chromium-iron alloys, tantalum, molybdenum, molybdenum-iron alloys, zirconium-clad molybdenum, platinum-clad molybdenum, and gold-plated molybdenum.

To reduce grid emission, manganese-nickel material has been utilized on most receiving-type tubes while zirconium-clad molybdenum, platinum-clad molybdenum, and gold-plated molybdenum have been used on most transmitter-type tubes.

To date, a controversy still exists as to whether platinum-clad molybdenum is superior to gold-plated molybdenum for the prevention of grid emission. Both materials are being used successfully, and data should be available in the near future as to which displays superior qualities. However, the use of platinum is recommended when either the degassing or operating temperature during processing is above or dangerously close to the melting point of gold. The gold-plating of molybdenum wire in a continuous process to provide a well-adherent nonporous coating offers certain fabricating difficulties which have now been overcome.

To date, it has been virtually impossible for the wire manufacturer to obtain the same results with plating of platinum as with gold, hence we must resort to a mechanical cladding process to produce platinum-clad molybdenum. From the stand of the wire manufacturer, plating is a simpler process than applying a platinum tube to a molybdenum core prior to the drawing operation.

The application of grid-emission inhibiting wires has found usage in grids (Fig. 2) of close-spaced triodes, pentodes, and velocity-modulated tubes where spacings from the cathode to the grid may range from 0.004 inch to 0.015 inch. The relative merits of zirconium-clad molybdenum for the prevention of grid emission has been explored on a number of medium-power high-frequency pentodes.

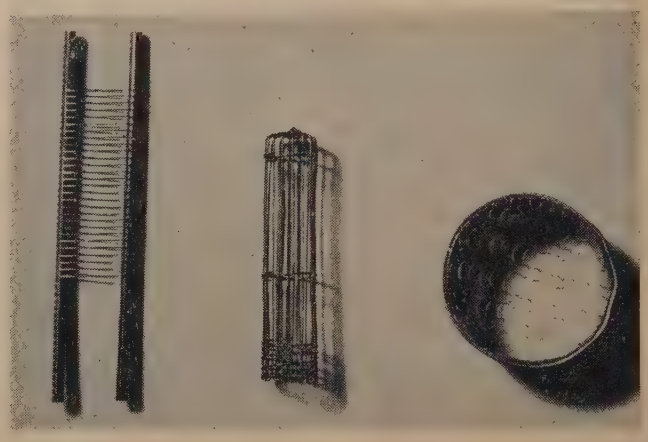

Fig. 2—Grid assemblies of various designs.

Electron-tube manufacturers who specialize in miniature or acorn-type tubes have usually had difficulties with molybdenum wire on grids due to heavy oxidation resulting from the heat generated during the sealing operations. Where possible, inert gases have been introduced into the envelope to reduce the degree of oxidation, but this method has not been entirely satisfactory. Molybdenum oxide on the grid laterals has a tendency to poison the emitting cathode, particularly if it consists of the alkaline earth type. Gold and silver plating of the molybdenum wire, prior to grid making, has offered considerable relief in reducing the degree of oxidation. Platinum and zirconium cladding have also been highly successful in this respect.

Getter Wires of Zirconium

The use of fine zirconium wire as a getter material has had numerous applications in X-ray tubes where the barium getter has proven to be unsatisfactory due to its higher vapor pressure at the operating temperature of the tube. Zirconium has the peculiar property of absorption of hydrogen at temperatures ranging from 300 to 400 degrees centigrade, and absorption of all other gases (excepting rare gases) at temperatures ranging from 1000 to 1600 degrees centigrade.

Zirconium wire which is unsupported is not sufficiently strong to maintain its preformed shape at a

[2] W. E. Forsythe and A. G. Worthing, "The properties of tungsten and the characteristics of tungsten lamps," *Astrophys. Jour.*, vol. 61, pp. 146–185; 1925.

temperature of 1600 degrees centigrade.[3] It has been found desirable to support it by winding zirconium wire (0.005 inch in diameter) alongside a tungsten wire (0.007 inch in diameter) on a tungsten or molybdenum core that is 0.008 inch in diameter. Zirconium wire exposed to the atmosphere has a tendency to oxidize slightly on the surface. This oxidation does not seriously impair the gettering qualities since it can be removed by glowing at 1600 degrees centigrade in a vacuum of approximately 1×10^{-6} millimeter of mercury. The combination zirconium-tungsten assembly wound on a molybdenum core has the advantage of serving as a support

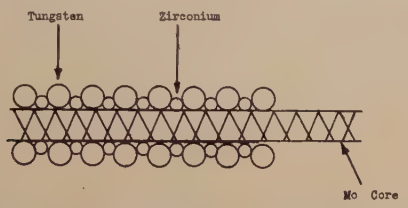

Fig. 3—Sketch showing cross section of a zirconium getter assembly.

for the rather weak zirconium and also makes possible glowing of the assembly at a temperature slightly higher than the melting point of zirconium, so a zirconium mirror can be formed on the glass retainer envelope.

Fig. 4—View of helical coil sealed in glass envelope.

This assembly has the advantage that it prevents the liquid zirconium from forming globules about the core wire, since it is retained between two tungsten wires which serve as a trough preventing the zirconium from flowing along the length of the wire.

[3] See United States Patent No. 2,336,138. A. J. van Hoorn and G. Thurmer, "Vaporization of metals," December 7, 1943.

Fig. 3 shows a cross section of a zirconium getter assembly. To obtain continuous gettering action in a tube, it is suggested that the getter assembly be assembled either in series or parallel with the tube filaments.

Test runs using assemblies as indicated in Fig. 4 were employed to accelerate the vacuum exhausting process. This assembly is inserted between the diffusion pump and the tube to be exhausted. Prior to exhausting a given tube, the getter coil is glowed at 1650 to 1700 degrees centigrade for approximately one minute. The

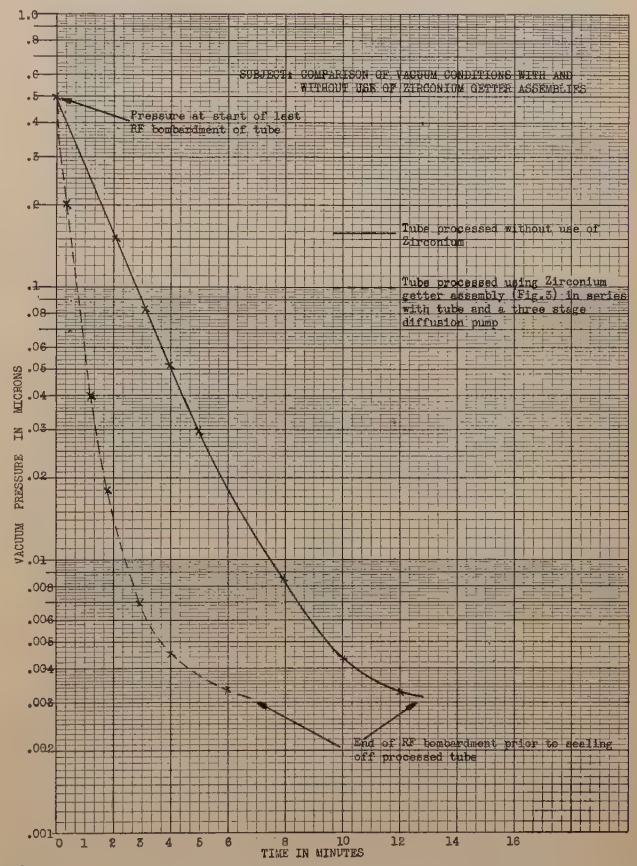
SUBJECT: COMPARISON OF VACUUM CONDITIONS WITH AND WITHOUT USE OF ZIRCONIUM GETTER ASSEMBLIES
Pressure at start of test RF bombardment of tube
Tube processed without use of Zirconium
Tube processed using Zirconium getter assembly (Fig.3) in series with tube and a three stage diffusion pump
End of RF bombardment prior to sealing off processed tube
VACUUM PRESSURE IN MICRONS
TIME IN MINUTES

Fig. 5—Curves showing comparison of vacuum conditions with and without the use of zirconium getter assemblies.

tube is exhausted in a normal manner, out-gassing the metal parts at a high frequency and internally bombarding the elements as required. When the vacuum approaches 1.0×10^{-3} millimeter of mercury, the getter coils are heated slowly to a temperature of 1650 degrees centigrade and maintained at this temperature for approximately five minutes. At the end of this period the vacuum pressure ranged from 1.0×10^{-5} to 1.0×10^{-6} millimeter of mercury. The time of pumping schedule of electron tubes exhausted with the use of zirconium getter coils was reduced approximately 25 per cent depending upon the type of tube (Fig. 5).

The zirconium getter coil can be used repeatedly for gettering until the coil fails mechanically. The author has utilized a single coil as many as fifty times without noticing any impairment of the gettering qualities.

Wires for Evaporating Metals in Vacuums

The evaporation of metals has been successfully effected through a design of coil similar to the one shown in Fig. 6. Evaporation of thin films of silver, copper, gold, aluminum, etc., on glass, quartz, mica, etc. has

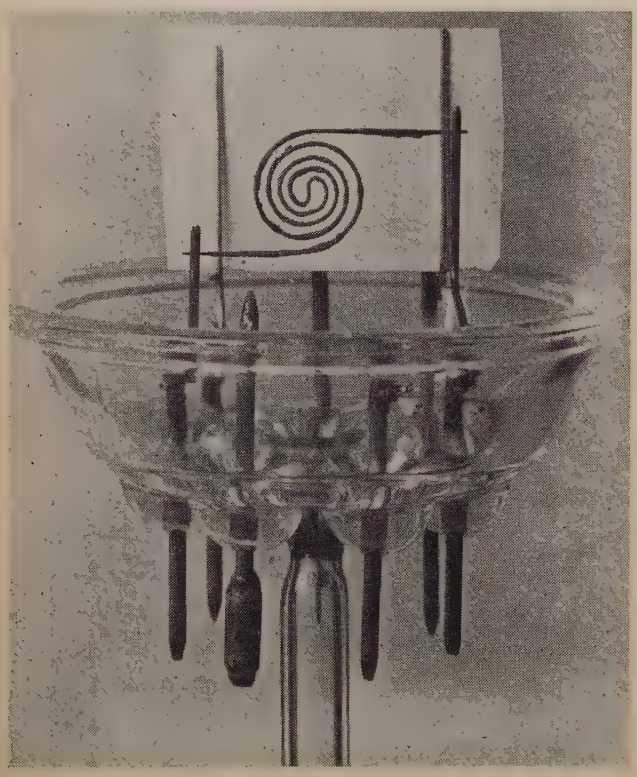

Fig. 6—View of evaporating coil.

been accomplished by replacing the zirconium (Fig. 3) with the metal to be evaporated. This type of assembly insures a uniform rate of evaporation and reduces the tendency of the evaporating metal towards forming globules, which result in an uneven diameter causing localized spheres of evaporation. Evaporation of silver, aluminum, copper, gold, etc., with the pancake-type coil (Fig. 6) which had a center-core rod of molybdenum was carried out at a pressure of 10^{-3} millimeter of mercury.

The intimate contact of the plating wire in the coiled coil assembly made possible uniformity of control of evaporation. All assemblies using the same type of plating wire evaporated at approximately the same glow current would plate at the same rate. Measurements on a number of mica plates indicated that the weight of the evaporated material did not deviate by more than five per cent on approximately 100 specimens. Using fine wires rather than heavy wires in the order of 0.025 inch in diameter insured a minimum heating of the specimen to be plated, thus preventing a chemical breakdown of the sample as well as insuring a cool surface for the sample, which also resulted in a plating free from oxides, bubbles, and peeling. It was observed that the more rapid the plating process the better was the quality of the plating.

Bibliography

(1) "Thorium," Bureau of Mines Information Circular No. 6321.
(2) Fansteel Pamphlets on Tantalum and Columbium, 1935, 1937, 1939, 1942.
(3) "Bibliography of Tungsten," United States Geological Survey, Bulletin No. 666, 1919.
(4) Molybdenum, United States Geological Survey, Bulletin No. 846C, 1933.
(5) Colin J Smithelles, "Tungsten—A Treatise on Its Metallurgical Properties and Application," D Van Nostrand Co., Inc., New York, N. Y., 1926
(6) K. C. Li and Chung Yu Wang, "Tungsten," Reinhold Publishing Co., New York, N. Y., 1943
(7) J. D. Fast, "Zirconium as a getter," *Foote Prints*, vol. 13, pp. 22–30; June, 1940.
(8) S. Hukagawa and J. Nambo, "Absorption properties of metallic zirconium for gases and its application to electronic tubes," *Elec. Tech. Jour.* (Japan), pp. 27–30; February, 1941.
(9) J. Strong, "Procedures in Experimental Physics," Prentice Hall, Inc., New York, N. Y., 1944
(10) H. P. Edinga, "Some problems influencing the drawing of fine wires," *Wire and Wire Prod.*, pp. 650–653; October, 1944.
(11) "Tungsten Molybdenum and Wire Products," North American Philips Co., Dobbs Ferry, N. Y.
(12) "Resistance Hand Book," Wilbur B. Driver Co., Newark, New Jersey, 1938.
(13) "Data Book—Electrical Alloys," Driver Harris Co., Newark, New Jersey, 1939.
(14) M. Benjamin, "Influence of metallic impurities in the core of oxide cathodes," *Phil. Mag.*, vol. 20, pp. 1–24; July, 1935.
(15) A. L. Reiman, "Thermionic Emission," John Wiley and Sons, Inc., New York, N. Y., 1934.
(16) W. Espe and M. Knoll, "Werkstoffkunde der Hockvakuumtechnik," Julius Springer, Berlin, Germany, 1936.
(17) U. S. Patent No. 2,050,820, K. M. van Gessel and W. D. van Wijk, "Method of making metal bodies consisting of a core and a shell," August 11, 1936.
(18) E. M. Wise, "Nickel in the radio industry," Proc. I.R.E., vol. 25, pp. 714–753; June, 1937.

A Three-Beam Oscillograph for Recording at Frequencies up to 10,000 Megacycles*

GORDON M. LEE,† ASSOCIATE, I.R.E.

Summary—A fundamental limiting factor in the application of high-speed cathode-ray oscillographs to the recording of high-frequency voltages or fast transients has been the error introduced by the finite time required for an electron to traverse the deflecting fields. A description is given of a three-beam high-speed micro-oscillograph which extends the range of application of single-sweep oscillographic recording by a factor of approximately 10 in frequency over previous limits imposed by transit-time distortion. The reduction in deflection sensitivity attributable to transit-time effect is calculated to be 4 per cent at 3000 megacycles and 40 per cent at 10,000 megacycles. Single-sweep oscillograms of 3000 and 10,000-megacycle oscillations and breakdown transients with fronts on the order of 10^{-9} second duration are shown.

Introduction

Nature and Importance of Transit-Time Distortion

UNTIL recently limitations in the application of oscillographic techniques imposed by transit-time distortion have caused but little concern because there was seldom occasion to use or study frequencies so high or transients so fast that the effect was of great consequence. However, the rapid growth of the microwave art and its very important applications made the development of an oscillograph for single-trace recording in the microwave region a matter of considerable importance. It was also realized that such an instrument would be exceedingly useful for fundamental studies on dielectric breakdown.

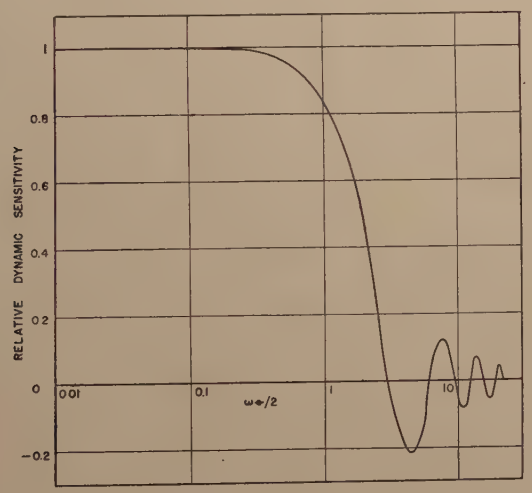

Fig. 1—Effect of electron transit time on sensitivity.

Considering an oscillograph with parallel electrostatic deflecting plates, it is well known that the decrease in sensitivity at high frequencies due to transit-time effect is given by

$$\text{relative dynamic sensitivity} = \frac{\sin \omega\theta/2}{\omega\theta/2} \qquad (1)$$

where ω is the angular frequency of the deflecting voltage and θ is the time taken for the electron to pass between the plates.[1] This formula neglects the action of the stray field at the ends of the deflecting plates, but it is sufficiently accurate for most purposes, particularly if a somewhat longer effective plate length is used in calculating θ. The variation in sensitivity with increasing values of $\omega\theta/2$ is shown in Fig. 1.

If a pure sine wave, the period of which is comparable in magnitude to the transit time, is impressed upon the deflecting plates, a reduction in sensitivity is the only undesirable result. As long as sufficient sensitivity remains for a particular application, this gives little cause for concern. However, if a complex voltage containing components of sufficiently high frequency is to be studied, distortion will occur since the sensitivity will vary with each harmonic, and for harmonics in certain regions a relative phase shift of 180 degrees will appear.

In applying an oscillograph to transient problems, the distortion to be expected in reproducing an exponential voltage front of the form

$$E(t) = E(1 - \epsilon^{-t/\tau}) \qquad (2)$$

is frequently a good criterion of the instrument's usability.[2] The nature of this distortion is best shown graphically as in Fig. 2. It will be seen that the ratio of the voltage time constant τ to electron transit time θ should have a minimum value of about 5 for accurate reproduction.

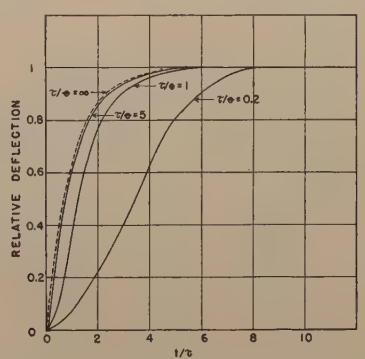

Fig. 2—Transit-time distortion in the recording of exponential fronts.

* Decimal classification: R388. Original manuscript received by the Institute, October 10, 1945. Presented, 1946 Winter Technical Meeting, New York, N. Y., January 25, 1946.

† Formerly, Laboratory for Insulation Research, Massachusetts Institute of Technology, Cambridge, Massachusetts; now, Central Research Laboratories, Inc., Red Wing, Minnesota.

[1] H. E. Hollman, "Die Braunsche Rohre bei sehr hohen Frequenzen," *Hochfrequenz. und Elektroakustik*, vol. 40, pp. 97–103; September, 1932.

[2] Hans Klemperer and Otto Wollf, "Die Verzerrungen im Kathodenoszillographen bei hohen Messgeschwindigkeiten," *Arch. für Elektrotech.*, vol. 26, pp. 495–502; July, 1932.

Typical values of effective deflecting-plate length and accelerating voltage for a conventional high-speed oscillograph are 5 centimeters and 50 kilovolts respectively. For these constants the reduction in deflection sensitivity is 5 per cent at 500 megacycles, and in recording an exponential voltage, τ may have a minimum value of about 2×10^{-9}.

Where writing speed did not impose a lower limit, these values remained as approximate limits to the application of all high-speed oscillographs described in the literature up until 1939. The reason for this is that the upper frequency and lower time limits are, respectively, inversely and directly proportional to the transit time. The transit time in turn varies directly with the effective plate length and inversely with the square root of the electron-beam accelerating voltage. To decrease the effective plate length very much below 5 centimeters is not feasible in the conventional high-speed oscillograph for a number of reasons. One of these is that an already low voltage sensitivity would be decreased. Another is that the diameter of the electron beam demands a certain plate separation; hence, as the plate length is decreased, the stray field at the edge of the plates becomes more important, and little is gained. Increasing the accelerating voltage is a relatively fruitless proposition since the transit time varies inversely only as the square root of the voltage, which is already high, and furthermore, above 50 kilovolts the relativity correction for the electron velocity starts to become important so that even less is gained.

Principles and History of the Microoscillograph

In 1939, von Ardenne[3] presented an original idea on oscillograph design which seemed to offer good possibilities for developing an instrument which would extend considerably the range of oscillographic recording. His instrument, which he designates as a microoscillograph, is designed according to electron microoptical principles which he developed in his work on the electron-scan microscope. In the microoscillograph the writing spot is made very fine, on the order of 10^{-2} to 10^{-3} millimeter in diameter, and the entire oscillogram is reduced in size by a factor of 100 compared to normal-size records. To preserve detail, the record is of necessity made directly on the photographic emulsion, which must be inserted into the vacuum chamber. The record is examined through a low-power microscope, or a photographic enlargement of it may be made. The fine writing spot is obtained by imaging the effective electron source with a short-focal-length magnetic or electrostatic lens. As a result of reducing the scale of the beam and oscillogram, all the deflecting-plate dimensions may be decreased by a factor of 10 or more, which means a corresponding reduction in transit time of 10 or more.

Von Ardenne's oscillograph was not designed for the purpose of resolving ultra-high-frequency phenomena, however, so the reduction in transit time was only of incidental interest. Another result of the reduced scale employed in the microoscillograph is that the actual velocity of travel of the trace over the recording plane is small enough so that mechanical sweep methods, such as a rotating film drum, may be used to obtain reasonably small minimum resolving times. Von Ardenne was chiefly interested in this feature which enabled him to obtain oscillograms with a total duration of 0.4 second and a minimum resolvable time of 5×10^{-7} second. A 10-centimeter-diameter drum rotating at a little under 10,000 revolutions per minute was used to provide the linear sweep for this application.

The only worker who seems to have made any use of the low transit time afforded by the microoscillographic technique to permit oscillography in the microwave region is Hollmann.[4] His instrument, however, was designed for the analysis of steady-state high-frequency voltages by means of Lissajou figures, and with his design, in which a sealed-off tube and fluorescent screen is used, it is very doubtful whether either the writing speed or optical resolving power of the screen would be adequate to permit the photographing of single-trace oscillograms of very short duration.

In addition to the reduction in transit-time distortion, the microoscillograph possesses a number of other advantages over the conventional high-speed instrument. One of these is that the reduction in deflecting-plate size causes a corresponding reduction in capacitance and particularly distributed capacitance and stray capacitance to ground. This is clearly of considerable importance at ultra-high frequencies. Owing to the small dimensions and fine beam used in the microoscillograph, it is also considerably easier to design and construct a multiple-beam microoscillograph than a multiple-beam instrument of the conventional type. The advantages of a multiple-beam instrument are quite obvious. In transient research, the recording of simultaneous current, voltage, and timing waves is a common requirement. In von Ardenne's original instrument, two beams were obtained from a single electron source by a relatively simple twin aperture and magnetic focusing system. A later design using electrostatic focusing provided for recording six traces simultaneously on a rotating drum.[5] Another advantage of the microtechnique is that a large amount of information in the form of an oscillogram can be contained in a very small area. A complete oscillogram of usual proportions need occupy an area of but a few square millimeters. This means that a large number of records can be made on a small photographic plate. This last advantage is somewhat offset, of course, by the necessity for examining the records with a microscope, microprojector, or making photographic enlargements.

[3] M. von Ardenne, "Der Elektronen-Mikrooscillograph," *Hochfrequenz. und Elektroakustik*, vol. 54, pp. 181–188; December, 1939.

[4] H. E. Hollmann, "Ultra-high-frequency oscillography," Proc. I.R.E., vol. 28, pp. 213–220; May, 1940.

[5] M. von Ardenne, "A six-trace cathode-ray micro-oscillograph," (abstract) *Wireless Eng.*, vol. 19, p. 231; May, 1942.

With these facts in mind, a three-beam microoscillograph for recording single-trace oscillograms of low transit-time distortion at ultra-high frequencies was developed.

Construction Details

An assembly drawing of the completed mechanical design of the oscillograph proper is shown in Fig. 3. The entire assembly is designed to be easily demountable for adjustment and experimentation. Vacuum-tight connections between the various sections are made by tongue-and-groove flange joints using $\frac{1}{16}$-inch-thick neoprene as a gasket material. Where allowance for slight variations in alignment must be made, such as in

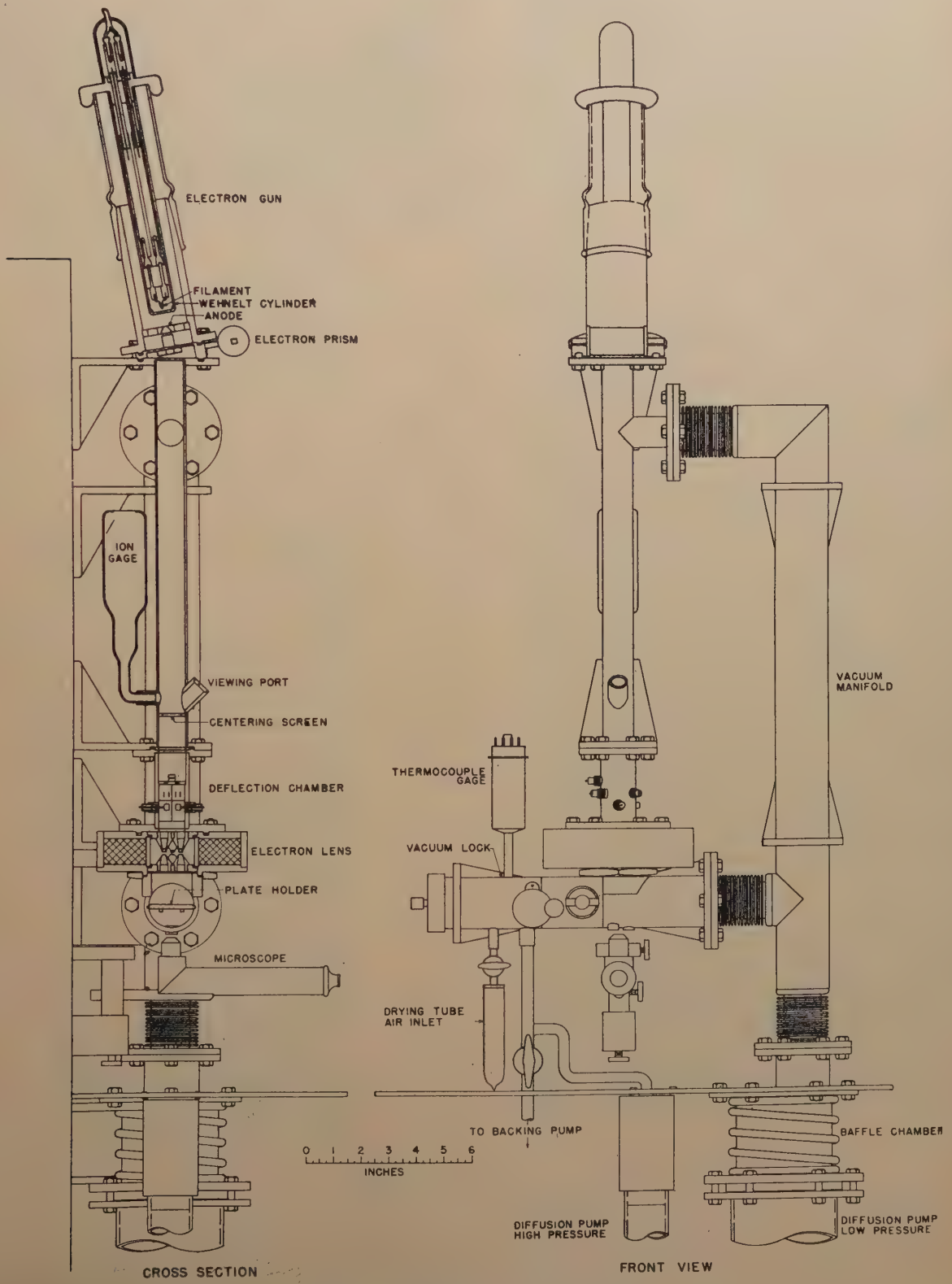

Fig. 3—Oscillograph assembly drawing.

the connections to the vacuum manifold, hydron bellows are used. The chief construction material is brass, and both hard and soft solders were used in making permanent joints. A vacuum as low as 5×10^{-6} millimeter of mercury may be maintained by the pumping system which consists of a glass-metal oil diffusion pump, using Octoil as the pumping fluid, backed by a two-stage mechanical pump. An ionization gage is used to measure the pressure during operation, and a thermocouple gage is used to determine when the diffusion pump may be turned on and to measure the pressure in the vacuum lock when photographic plates are exchanged.

To prevent undesired deflection of the beam by the earth's magnetic field, a cylindrical liner of 30-gage annealed high-permeability alloy extends from the electron gun to the deflecting-plate system.

A view of the complete oscillograph mounted on the chassis containing power supplies and vacuum-gage circuits is shown in Fig. 4. In the following paragraphs, various of the more important components will be described individually.

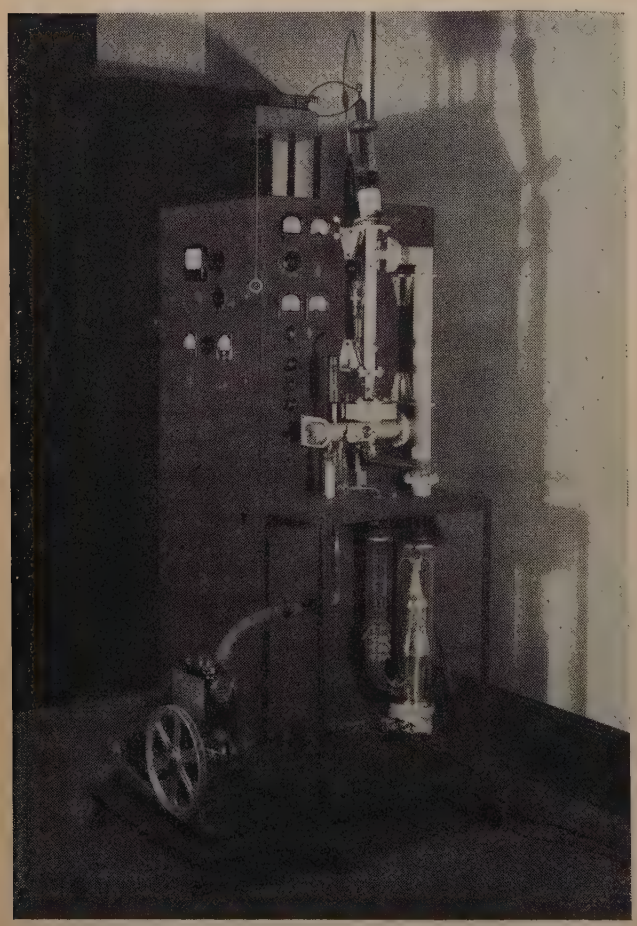

Fig. 4—Three-beam high-speed microoscillograph.

The electron gun, shown in Fig. 5, is of the hot-cathode type using a hairpin filament of 0.005-inch-diameter tungsten as the cathode. The filament is held in place by a simple set-screw arrangement to permit easy replacement and adjustment. A pyrex standard-taper ground joint insulates the corona shield, filament assembly, and Wehnelt cylinder from the anode tube. Apiezon "W" wax is used to make the vacuum-tight seals between the metal and glass portions of the assembly, except for the ground joint which is a grease seal. To prevent fogging of the photographic plate by

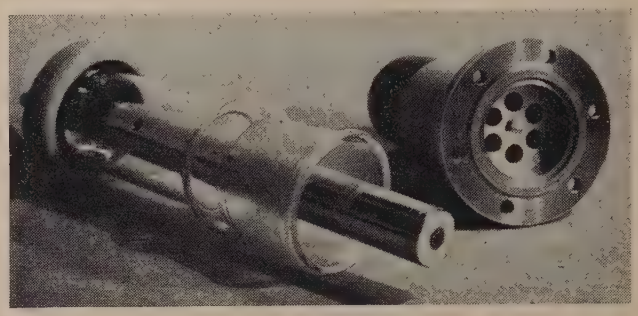

Fig. 5—Electron gun, partially disassembled.

direct light from the filament, the electron gun is tilted at an angle of 10 degrees with the main oscillograph body, and the electron beam is deflected through the angle by the magnetic field of an electromagnetic electron prism.

Incorporated in the main body of the oscillograph are a viewing port and annular fluorescent screen to aid in centering the electron beam. To prevent undesirable X-radiation of the operator while adjustments are being made, the viewing-port window is made of suitable lead glass.

Mechanical considerations and the desire to keep sensitivity and writing speed as high as possible dictated placing the deflection chamber on the electron-source side of the main lens. Included in the deflection chamber are a shielded pickup probe (used for triggering the sweep and phenomenon-initiating circuits as will be explained later), a three-aperture beam diaphragm,

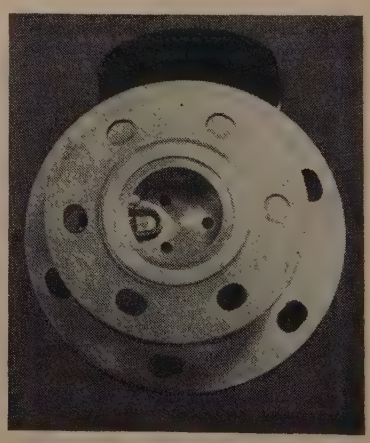

Fig. 6—Deflection chamber, top view showing shielded pickup probe and three-aperture beam diaphragm.

and the six pairs of deflecting plates. The deflecting plates are 0.2 inch long, 0.16 inch wide, with a separation of 0.14 inch. In each pair one plate is grounded and the other is waxed into a low-loss fused-quartz bushing.

The leads are designed to accommodate Sperry-type coaxial microwave fittings. An individual shielded compartment isolates each deflecting-plate pair from every other pair. A top view of the deflection chamber showing the shielded probe and three-aperture beam diaphragm is shown in Fig. 6. Fig. 7 is an external view showing the coaxial leads to the deflecting plates and probe. Fig. 8 is a bottom view showing the three pairs of plates normally used for time deflection and the lower three divisions in the shielding arrangement.

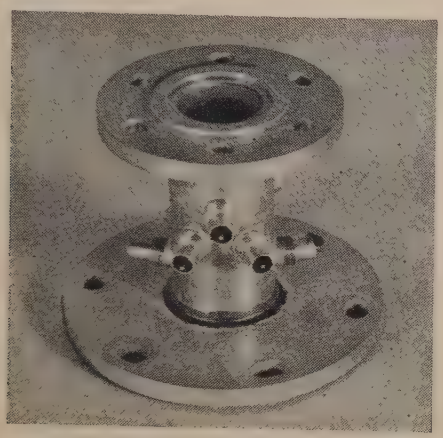

Fig. 7—Deflection chamber, external view.

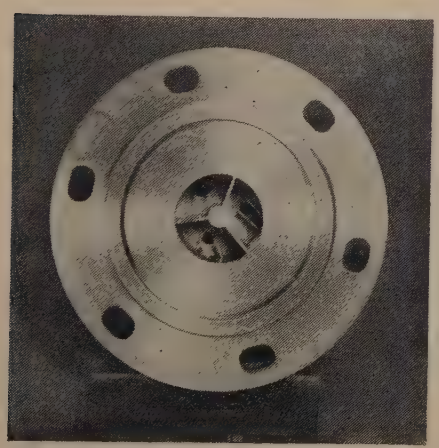

Fig. 8—Deflection chamber, bottom view showing the three lower plate pairs and shielding compartments.

The construction of the electron lens is shown by Fig. 9 in which the top pole-shoe carrier has been removed to reveal the interior. A single winding provides the magnetomotive force for the three parallel lens elements. To permit regulation of the coil current by a single receiving-type vacuum tube, a high-resistance, low-current winding of 20,000 turns is provided.

A close-up view of the vacuum lock and recording chamber together with the focusing microscope is shown in Fig. 10. The vacuum lock permits insertion and removal of photographic plates without breaking the vacuum on the main portion of the instrument. Removing one plate, inserting another, and establishing operating vacuum requires about 10 minutes. The plate holder is translated from the vacuum lock into recording position by a rack and pinion drive which enters the vacuum through a neoprene diaphragm known as a "Wilson seal."[6] The internal position of the plate holder is shown by an external indicator which is geared directly to the pinion drive shaft.

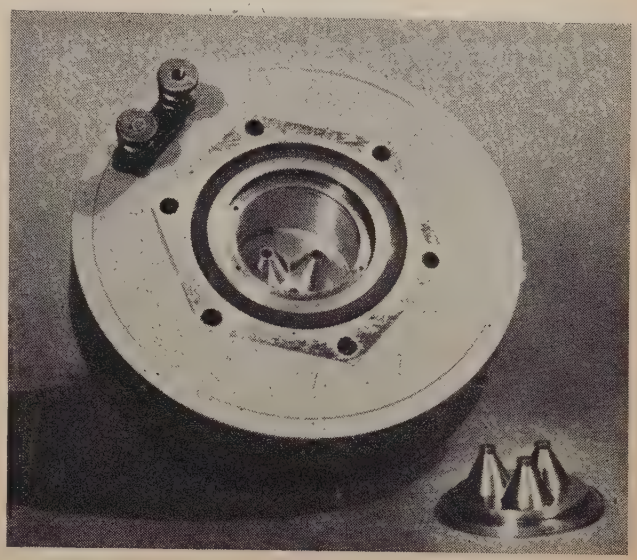

Fig. 9—Electron lens with top pole-shoe carrier removed.

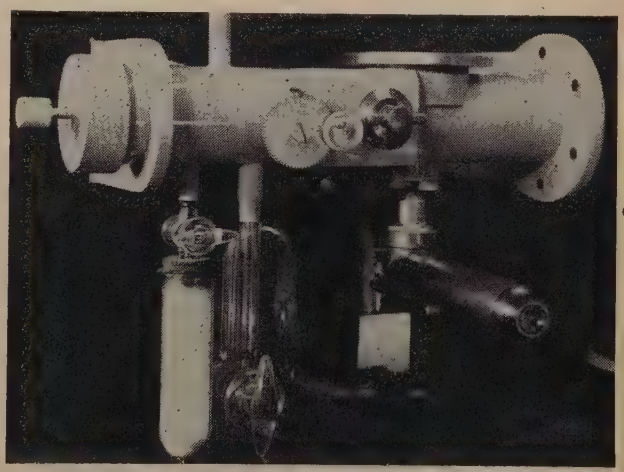

Fig. 10—Vacuum lock and recording chamber.

Fig. 11 shows the photographic-plate holder and light cover designed to take $1\frac{1}{4}$-by $1\frac{5}{8}$-inch plates. On a single plate, 8 complete sets or 24 oscillograms in all may be recorded. For focusing, a fine-grained translucent luminescent screen is attached to one end of the plate holder. The screen is viewed with the 42-power prism microscope through viewing ports on the under side of the recording chamber.

A block diagram of the circuits housed in the oscillograph chassis is given in Fig. 12. A voltage stabilizer of the saturable-core type is used to reduce line-voltage fluctuations to less than 1 per cent and thus reduce the range over which the electronic stabilizers must operate.

[6] R. R. Wilson, "A vacuum-tight sliding seal," *Rev. Sci. Instr.*, vol. 12, pp. 91–93; February, 1941.

The main high-voltage source is a conventional rectifier-doubler circuit, with a maximum output of 50,000 volts.

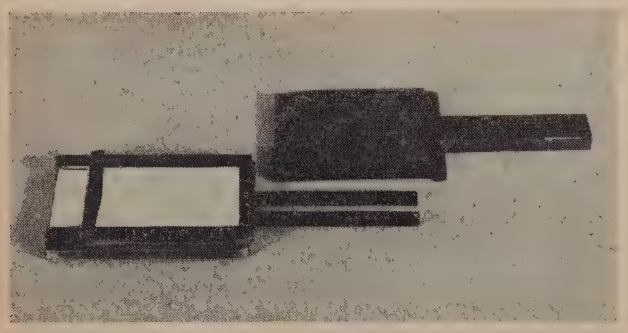

Fig. 11—Photographic plate holder and light cover.

A 5-megohm resistor is included in the high-voltage lead as a safety precaution, and during the short time of actual operation, it is short-circuited out by a manually-operated short-circuiting switch. The high voltage is stabilized to better than 0.05 per cent by a two-stage voltage-feedback circuit.

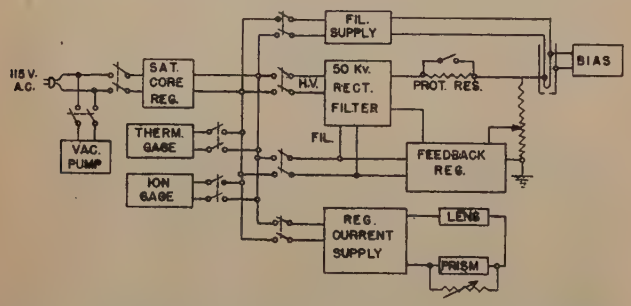

Fig. 12—Block diagram of circuits housed in oscillograph chassis.

The electron lens and prism current supply is taken from a design by Vance.[7] It more than adequately meets the oscillograph stability requirement of 0.05 per cent. Since the circuit regulates for both input-voltage variations and changes in output-circuit resistance, it is possible to operate the lens and prism winding in series by incorporating a variable shunt resistor across the prism winding to provide the necessary degree of independence in adjustment.

Bias supply for the electron-gun Wehnelt cyclinder is obtained from miniature dry-cell batteries. During standby the electron gun is biased beyond cutoff so that the photographic plate will not be fogged by scattered and secondary electrons. A tripping switch modeled after the principle of a double-action camera shutter is used to reduce the bias to the operating value for about 0.001 second. The switch is actuated by pulling on an insulating glass-fiber cord, the switch and bias batteries being mounted on an insulated platform as shown in Fig. 4.

Operation and Performance

Synchronization of the time sweep and phenomenon with the initiation of the electron beam is accomplished in the following manner. When the electron-gun bias is switched from cutoff to operating value, the full electron beam passes down the oscillograph and approximately 2 per cent of it strikes the pickup probe in the deflection chamber. Thus the probe acts as a constant-current source during this interval and may be used to actuate an electronic relay circuit, which in turn may initiate the sweep, the phenomenon, or both. For recording in the microwave region an accelerating voltage of 50,000 volts and a total beam current on the order of 5 milliamperes is used.

The deflection sensitivity of the instrument is 0.001 millimeter per volt on the recording plane. Since the trace diameter is 0.01 millimeter, the records may be enlarged 100 diameters to give an oscillogram of normal trace width. Thus the useful deflection sensitivity, referred to a trace width of 1 millimeter, is 0.1 millimeter per volt; or in other terms, the deflection factor is 10 volts per trace width.

To calculate the reduction in sensitivity owing to electron transit time through the deflecting fields, an effective plate length 40 per cent greater than the physical plate length of 0.2 inch was assumed to allow for fringing of the electric field at the ends of the deflecting plates. For 50,000 volts accelerating potential then, formula (1) gives a reduction in deflection sensitivity of 4 per cent at 3000 megacycles and 40 per cent at 10,000 megacycles.

For the generation of very fast single-sweep time bases, resistance-capacitance spark-gap circuits, and vacuum-tube circuits have been used. The spark-gap circuit has the advantage of simplicity, while a vacuum-tube circuit is much more reliable in synchronization characteristics.

Performance of the instrument is shown by the typical enlarged oscillograms shown in Figs. 13 through 16. Fig. 13 shows an oscillogram of a 3000-megacycle voltage obtained with a spark-gap sweep circuit. A vacuum-tube sweep circuit was used to record the 10,000-megacycle voltage shown in Fig. 14. The utility of the instrument in recording simultaneous phenomena is demonstrated by Figs. 15 and 16 in which current and voltage transients occurring in a particular circuit upon the breakdown of a spark gap are shown. The time scale was taken from a timing wave simultaneously recorded by the third beam.

In conclusion it may be said that a three-beam high-speed microoscillograph has been developed which extends the range of application of single-sweep oscillographic recording by a factor of approximately 10 in frequency over previous limits imposed by conventional high-speed oscillographs. The instrument in its present state of development opens up entirely new fields of research for the application of oscillographic techniques. Some of these are microwave transients, reflection and traveling-wave phenomena on small systems, and research on the fundamental electric-breakdown characteristics of dielectrics using very steep impulse voltages.

[7] A. W. Vance, "Stable power supplies for electron microscopes," *RCA Rev.*, vol. 5, pp. 293–300; January, 1941.

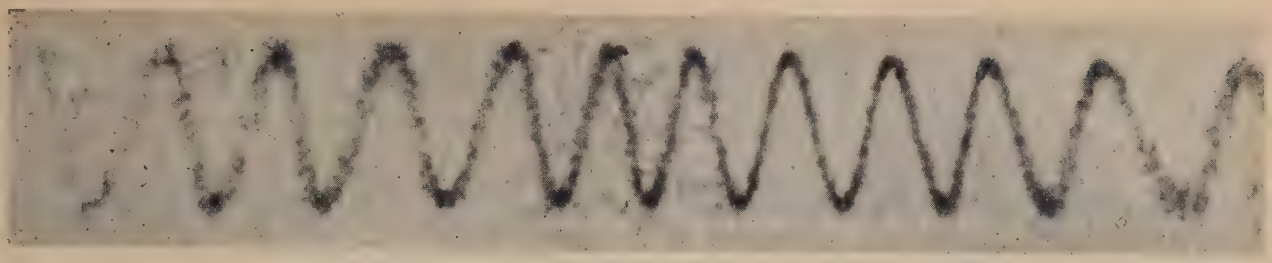

Fig. 13—Single-sweep oscillogram of 3000-megacycle voltage. Enlargement, 100 diameters.

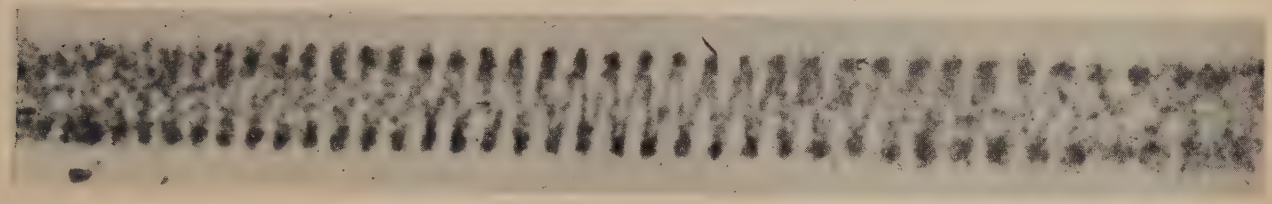

Fig. 14—Single-sweep oscillogram of 10,000-megacycle voltage. Enlargement, 100 diameters.

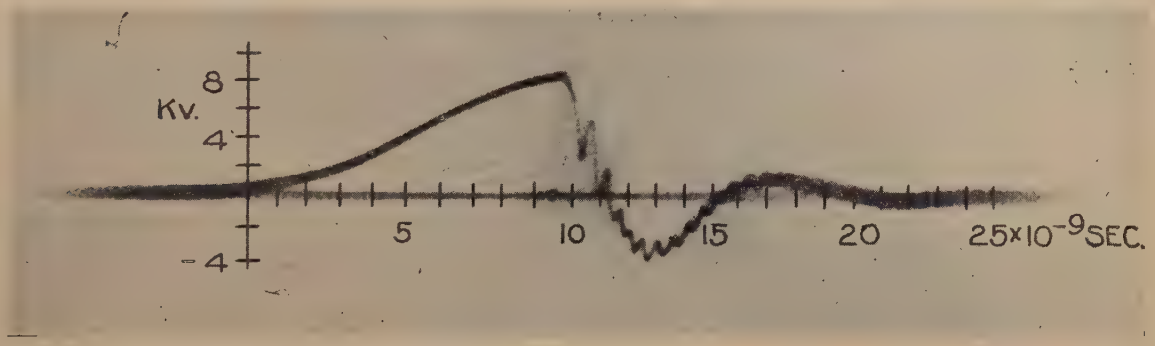

Fig. 15—Voltage transient in spark-gap circuit. Enlargement, 50 diameters.

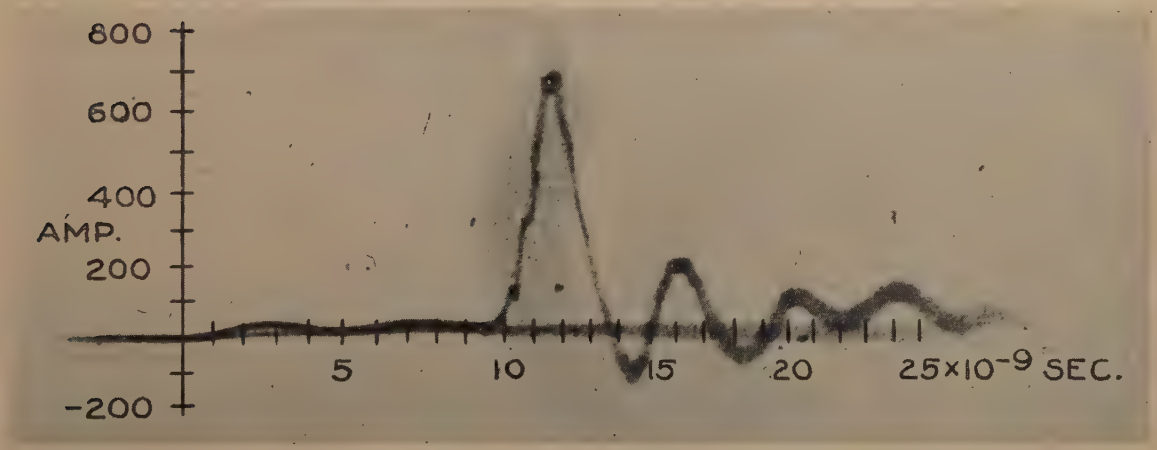

Fig. 16—Current transient in spark-gap circuit recorded simultaneously with voltage transient in Fig. 15. Enlargement, 50 diameters.

Acknowledgment

This development was made as part of the program of the Laboratory for Insulation Research, Department of Electrical Engineering, Massachusetts Institute of Technology, in partial fulfillment of the requirements for the Doctor of Science degree in electrical engineering, and was financed in part by a grant from the General Radio Company, of Cambridge, Massachusetts. The writer also wishes to acknowledge the constant encouragement and helpful counsel of Professor Arthur R. von Hippel, Director of the Laboratory for Insulation Research; the co-operation of Mr. George Gale, who performed the major part of the machine shop work; and the welcome suggestions and assistance of Dr. Demetrius Jelatis, Mr. Merlin Haugen, and Mr. Robert Fletcher in setting up microwave equipment used in part of the research.

Synchronizing Generators for Electronic Television*

A. RUFUS APPLEGARTH†, ASSOCIATE, I.R.E.

Summary—**The system of electronic circuits employed to generate the complex wave forms required as a base for television picture transmission is described. It comprises four principal sections which are: (1) source of accurately timed pulses; (2) frequency-divider chain; (3) components-generating circuits; and (4) signal-synthesis circuits. The various means for accomplishing these functions is briefly discussed, and illustrated by circuits which have been used successfully for such purposes in practical applications.**

I. Introduction

MUCH has been written about the general subject of television. There are available several good texts which discuss the general requirements of television systems, but which do not delve into the problems involved in generating the modern electronic-television synchronizing signal. The subject matter of this paper includes a discussion of the problems concerning the design of synchronizing generators and also some detailed circuits to illustrate the discussion.

The synchronizing generator is the heart of any electronic-television system. It provides the many component synchronizing and pedestal signals to which the picture signal, having been generated and amplified elsewhere, is added to form the complete composite video signal. This video signal is then modulated upon a suitable carrier for radio-television transmission. The basic components of a television synchronizing generator are illustrated in Fig. 1. It is necessarily a complex assembly of electronic devices, interlocked in such a way as to produce a stable composite signal which must conform to the standards set by the Federal Communications Commission (see Fig. 2).

The Federal Communications Commission standards specify an interlaced scan. The timing of the vertical scan must be precisely related to that of the horizontal scan, if accurate interlacing is to be obtained. Not only must the horizontal and vertical scanning frequencies be harmonically related, but precisely controlled in relative phase position as well. For example, a shift in the timing of the vertical scan by an interval equal to one half of a horizontal line will completely destroy the interlace. Furthermore, the maintenance of a satisfactory interlace (defined as one in which the unbalance between adjacent line spacing is no greater than 40 to 60 per cent) requires that timing precision be held to 0.1 line, or to one part in 5250 in a 525-line system. Such narrow tolerance restrictions in the timing between horizontal and vertical scanning frequencies preclude most of the simple harmonic-generating systems used successfully for other purposes.

* Decimal classification: R583. Original manuscript received by the Institute, July 2, 1945.

† 5722 Greene Street, Philadelphia 44, Pa.

The design of electronic synchronizing generators generally includes a high-frequency master oscillator from which the various signal components are derived by frequency-divider systems and wave-shaping circuits. It is desirable to have the 60-cycle vertical-scanning frequency synchronous with the 60-cycle power system of the local utility, to eliminate the slow vertical drift imparted to any hum pattern which might originate anywhere in the over-all television system.

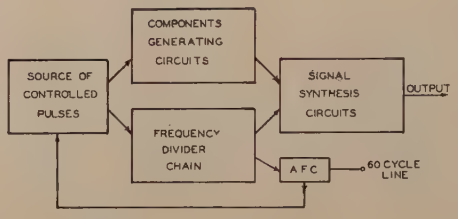

Fig. 1—Block diagram of synchronizing generator showing principal components.

Television standards for some years have included a line structure specifically chosen to facilitate frequency-divider design. The frequency-division ratio to relate the vertical scan to the second harmonic of the horizontal scan is equal to the number of lines. Thus, for easy frequency-divider design, the number of lines must be a number capable of being broken into several small prime factors. For example, 343 could be factored into $7\times7\times7$. Likewise, 441 can be factored into $3\times3\times7\times7$, and 525 into $3\times5\times5\times7$. Future standards undoubtedly will be chosen to factor similarly. The illustrative circuits described herein are designed for the 525-line standard, but, by suitable modification, could be made to function on any standard likely to be adopted for some time to come.

II. The Frequency-Divider Chain

As pointed out above, the system of circuits called the frequency-divider chain which links the vertical-scanning frequency to the second harmonic of the horizontal-scanning frequency forms a vital part of the synchronizing generator. Various circuits can be used for the several links of the chain, including multivibrators, blocking-tube oscillators, and counters.

The multivibrator comprises two resistance-coupled amplifier stages in cascade, with the output of the second stage fed directly back to the input of the first stage, to form an oscillator (see Fig. 3a). The frequency of oscillation is determined primarily by the time

constants of the coupling networks, but depends also on the tube characteristics, power-supply voltages, and the amplitude of the driving signal. The multivibrator offers a versatile means for generating oscillations of

The resonant stabilizer is shock excited by the pulse of grid current that flows through it during the positive-grid portion of each cycle. The voltage that appears across the stabilizer is a damped transient oscillation

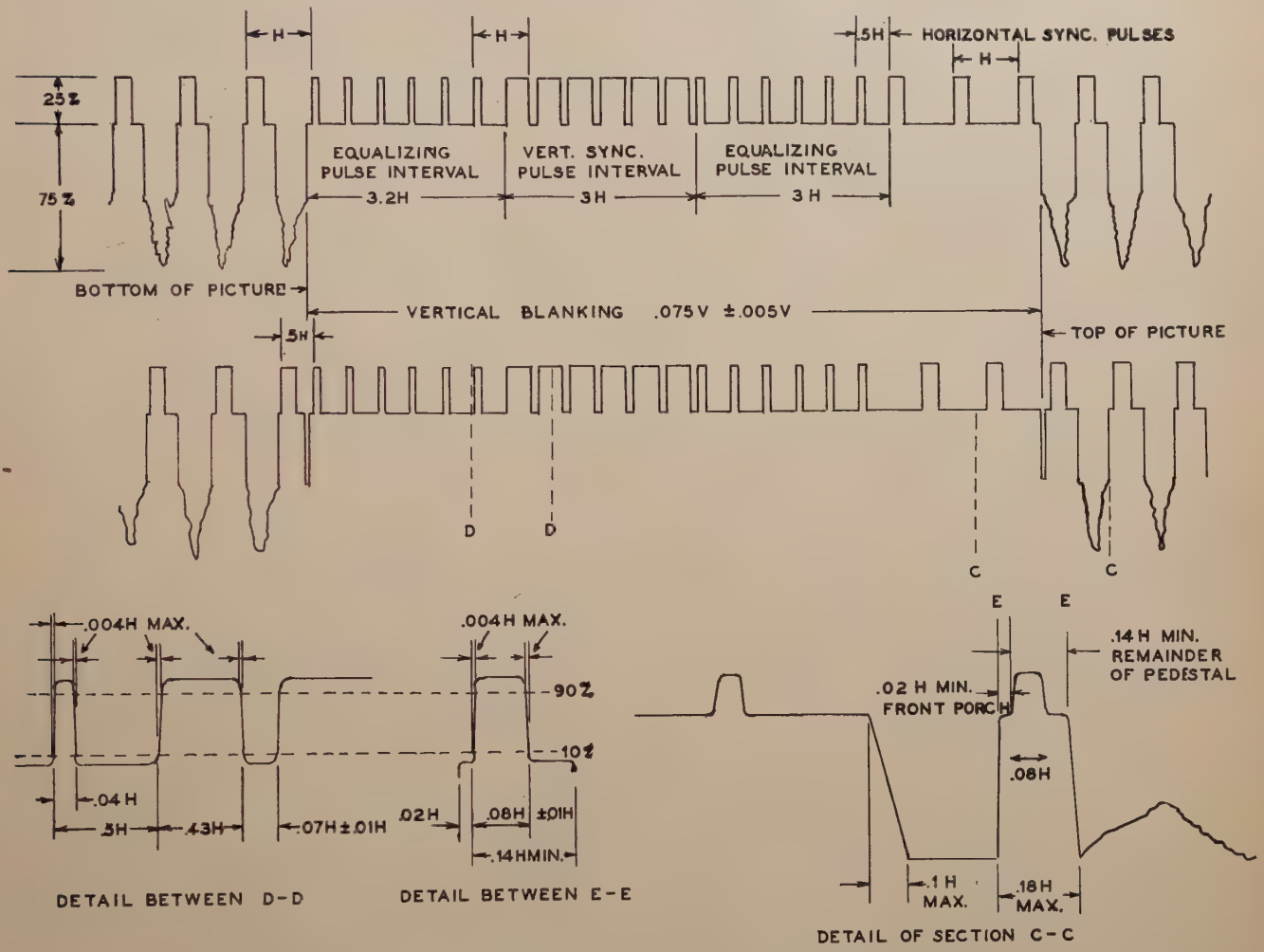

Fig. 2—Federal Communications Commission's standard television signal.

rectangular wave form, but its stability is inadequate for its use as a frequency divider for factors greater than about 3:1.

The blocking-tube oscillator represents a distinct improvement in stability over the multivibrator (see Fig. 3b). This improvement comes primarily from the substitution of a transformer of inherently stable characteristics for one of the tubes of the multivibrator. This type of oscillator, although more stable, is also subject to frequency dependence upon tube characteristics, power-supply voltage variations, and the amplitude of the driving signal used to synchronize it.

A resonant stabilizer comprising a parallel-connected tuned circuit can be inserted in series with the oscillator grid circuit to increase greatly its frequency stability. This will cause it to divide by a factor primarily determined by the tuning of the resonant circuit, and to a far lesser degree by unwanted variables (see Fig. 4).

whose period is determined by the tuning of the resonant stabilizer. This transient voltage, which is repeated each time a pulse of oscillator-grid current flows, is added to the exponential capacitor-discharge voltage, and to the train of driving pulses to form the composite oscillator-grid signal. Thus, by tuning the stabilizer to the proper frequency (about one and one-half times the desired oscillator frequency) the transient oscillation will elevate the desired driving pulse substantially above its neighbors, and thereby insure synchronization of the blocking-tube oscillator on the desired driving pulse, despite the usual variations in tube characteristics, power-supply voltages, and the amplitude of the driving pulses.

The stabilizing effect increases as the amplitude of the damped transient signal is increased, up to the point where this transient signal becomes strong enough to fire the blocking-tube oscillator without the aid of the

desired driving pulse, which defeats the purpose of the stabilizer. The amplitude of the stabilizing signal is determined by the magnitude and wave form of the pulse of grid current exciting it, and by the Q and resistance-capacitance ratio of the resonant stabilizer. The Q should be made as high as conveniently practicable, and the final amplitude of the stabilizing signal set by adjusting the resistance-capacitance ratio.

Pulse-counting circuits similar to the one shown in Fig. 3c are frequently used as frequency dividers. They usually comprise blocking oscillators in which the grid-leak resistors are replaced by a pair of diodes. The driving signal is applied to the oscillator grid capacitor through a diode to cause the voltage to be built up in a series of steps. The circuits are adjusted so that the desired firing pulse causes the blocking-tube oscillator

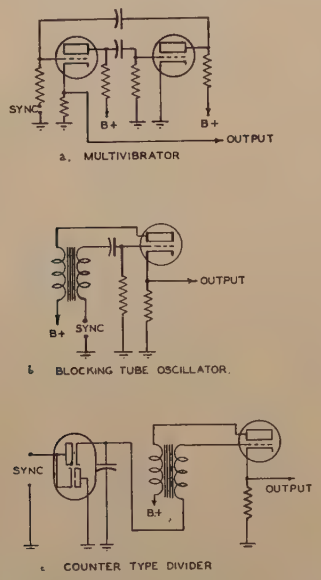

Fig. 3—Frequency-divider circuits.

to fire on the top step, thus discharging the grid capacitor to complete the cycle.

The frequency divider shown in Fig. 5 comprises four stages, dividing in the ratios $3\times5\times5\times7$ to reduce 31,500 cycles per second to 60 cycles per second, for use in a 525-line television system.

III. The Master Oscillator and Automatic-Frequency-Control System

The master oscillator should be a fairly stable sine-wave oscillator whose frequency can be readily controlled by a reactance tube. The drift stability is not of great importance, since the frequency average is maintained through automatic frequency control, but a high degree of cycle-to-cycle regularity, difficult to obtain in relaxation-type oscillators, is necessary to produce a television picture with straight vertical edges.

The transitron oscillator is well suited to this purpose. It is a very simple circuit of inherently high stability requiring simple components. The frequency of the master oscillator should be set to the second harmonic of the horizontal-scanning frequency, which is the fundamental of the frequency used for the equalizing pulses and the serrated vertical-synchronizing blocks. For a 525-line picture (30 frames per second) this would be 31,500 cycles per second, as determined by multiplying

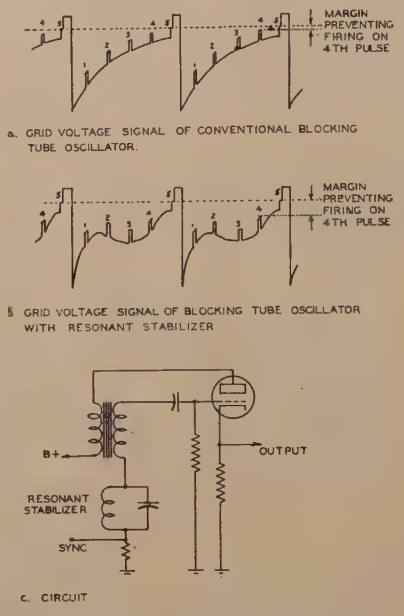
MARGIN PREVENTING FIRING ON 4TH PULSE
a. GRID VOLTAGE SIGNAL OF CONVENTIONAL BLOCKING TUBE OSCILLATOR.
MARGIN PREVENTING FIRING ON 4TH PULSE
b GRID VOLTAGE SIGNAL OF BLOCKING TUBE OSCILLATOR WITH RESONANT STABILIZER
B+
OUTPUT
RESONANT STABILIZER
SYNC
c. CIRCUIT

Fig. 4—Stabilized frequency divider.

the number of lines by the number of frames per second and by the interlace ratio ($525\times30\times2=31{,}500$).

The reactance tube in the circuit illustrated in Fig. 6 is of conventional design, employing a resistance-capacitance network bridged between grid and plate to provide a grid excitation shifted approximately 90 degrees in phase from the plate voltage. The reactance-control circuit should have sufficient frequency-control range to

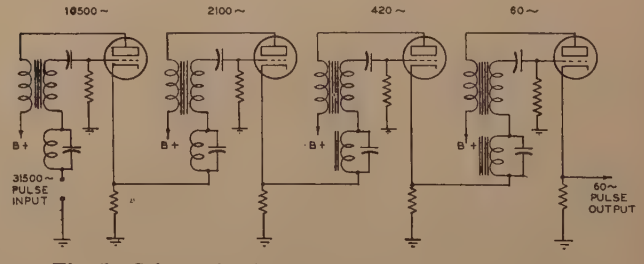

Fig. 5—Schematic diagram of frequency-divider chain.

correct for any drift of the master oscillator, but should not be locked so tightly to the oscillator as to cause reasonable line-voltage fluctuations (particularly momentary phase disturbances) to introduce frequency variations in the master oscillator of sufficient magnitude to show as irregularities in the vertical edges of the picture.

The direct-current frequency-control signal is derived from a phase discriminator sensitive to phase-angle variations between the 60-cycle output from the

frequency-divider chain and the 60-cycle signal taken from the power line. The time constant of the control circuit must be made high enough to prevent sudden power-line irregularities of momentary duration from affecting the master oscillator. A circuit suited to this purpose is shown in Fig. 6. The signal from the 60-cycle vertical-blanking (pedestal) multivibrator is used as a driving source because it is the widest 60-cycle pulse used as a component part of the composite synchronizing and pedestal signal. This wide pulse is amplified, and partially shaped into a sine wave by the tuned secondary of the audio transformer. The Q of the resonant-transformer secondary is so low that the wave form across it more nearly resembles a saw tooth, but it is usable as such. The circuit of the discriminator, as shown, is similar to the one commonly used as a detector for frequency-modulation, but the tuning of the transformer plays no active part in the functioning of the device other than wave shaping. The discriminator develops a direct-current output dependent upon the relative phase of the two input signals.

made up of precisely timed "edge" signals connected by constant voltage-time intervals represented by the straight horizontal portions of the wave forms. The multivibrator is ideally suited to generating such signal components, because they can be precisely synchronized and the pulse width can be controlled easily. The stability of such circuits is adequate, if they are not expected to subdivide frequencies by large factors.

Some component wave forms may also be derived by a wave-shaping process not requiring synchronized oscillators. This method of generating prescribed wave forms is to be preferred where the circuits involved are simple, and do not require critical tube characteristics or operating voltages. It is also the best means for generating component wave forms which do not require such close pulse-width control, such as the set of serrated vertical-synchronizing blocks.

The keying signals, particularly the one for inserting the group of six vertical synchronizing blocks, must be timed with high precision. This accuracy in timing is necessary to insure eventual synthesis of signal groups

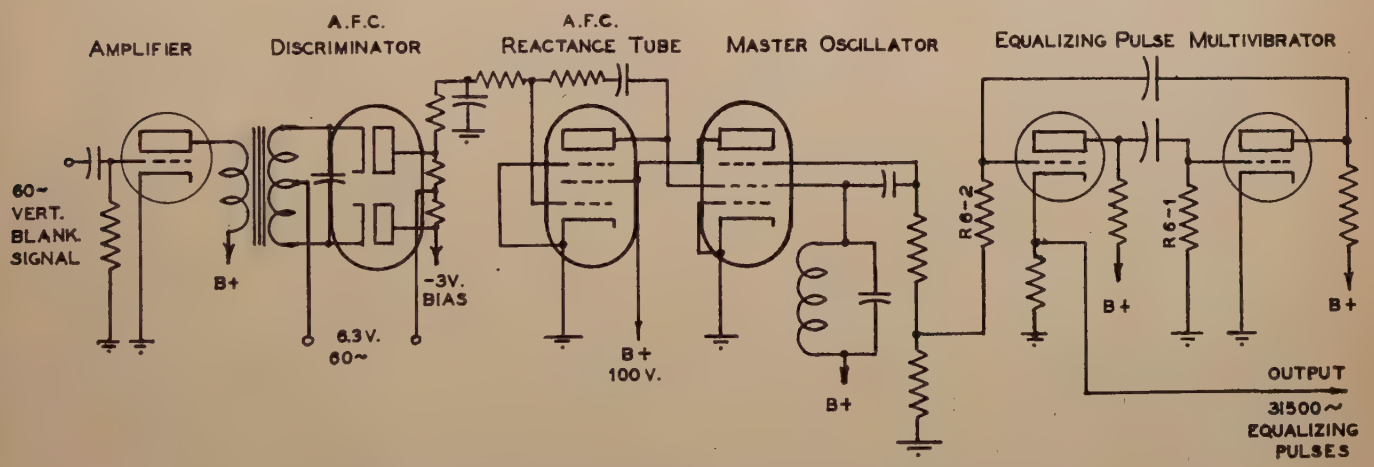

Fig. 6—Master oscillator and automatic-frequency-control system.

IV. The Components-Generating Circuits

The next logical step in the design of a television-synchronizing generator is to produce the various component wave forms that comprise the complete signal. An analysis of the Federal Communications Commission standard television signal (see Fig. 2) discloses that it is made up of five different periodic wave forms, plus the picture signal, lasting for time intervals from a few closely spaced pulses to an appreciable fraction of the 60-cycle period. These various component signals are most easily generated as continuous trains of pulses, or blocks, for later modulation into groups suitable for composite-signal synthesis.

The derivation of certain desired wave forms from related source signals is a fascinating branch of the electronic art. The television synchronizing and pedestal signals comprise essentially rectangular wave forms, containing the correct number of pulses or blocks, with smooth and correctly timed change-overs.

A. The Equalizing-Pulse Signal

Two groups, each containing six narrow pulses that are half as wide as normal horizontal-synchronizing pulses but spaced at half-line time intervals, form a part of the composite synchronizing signal. One such group is transmitted immediately prior to the vertical synchronizing signal, and the other immediately following it. Their purpose is to equalize the two sets of alternate fields which comprise a frame, but which are staggered one-half line apart in order to produce the interlace, so that they are made identical for a short interval before and after the vertical-synchronizing signal. Thus, simple signal-integrating circuits can be used in television receiving apparatus to separate the vertical-synchronizing

signal from the remainder of the composite signal.

A continuous train of equalizing pulses would have a frequency of 31,500 cycles per second. This has been previously chosen as the master-oscillator frequency, and so a multivibrator, or other means for generating the signal, can be driven by the master oscillator as shown in Fig. 6. The pulse width of this multivibrator can be adjusted to standard by *R6-1*, after which *R6-2* can be reset for tightest synchronization to the master oscillator. Both resistances can be replaced by fixed units of suitable value, since the exact pulse width is not critical, and the synchronization at fundamental frequency is very tight.

The output of this multivibrator can be used for many purposes including driving the frequency-divider chain, driving the horizontal-pedestal and synchronizing-pulse oscillators (dividing 2:1 in frequency), generating the vertical-synchronizing block signal, and providing a reference leading edge for all of the synchronizing-signal components, in addition to the direct generation of the equalizing-pulse signal.

B. The Horizontal-Pedestal Signal

The horizontal-pedestal signal, or blanking signal as it is sometimes called, forms the base on which the picture signal is later built. It also serves to black out the television-receiver screen during the flyback of the horizontal scan. The frequency of this signal must be equal to the horizontal scanning rate, which is 15,750 cycles per second for a 525-line, 30-frame-per-second, 2:1-interlaced picture.

In order to facilitate the separation of the synchronizing signals from the picture and pedestal signals in the television receiver, particularly under conditions of adverse radio transmission, the edges of the horizontal pedestals terminating each line are made to precede the leading edge of the horizontal synchronizing pulses by a small but definite time interval sometimes referred to as the "front porch" (see Fig. 7d). Since the horizontal-pedestal signal is derived from the equalizing pulses by synchronization, and since time cannot be anticipated, the firing of the horizontal-pedestal oscillator relative to the leading edges of the equalizing pulses driving it is delayed by a time interval of slightly less than one half line (the interval between equalizing pulses).

A means for accomplishing this time delay is shown in Fig. 7. It consists of forming a saw-tooth signal by integration of the equalizing pulses and using a portion of this signal to fire the horizontal-pedestal multivibrator. The range of adjustment should be limited to a few per cent of the horizontal-scan period, or the control may be replaced by suitable fixed resistances since the exact length of the "front porch" is not critical provided that timing of the horizontal-synchronizing pulses does not depend on it, as is incorporated in this design.

A multivibrator is suggested as the pedestal oscillator as shown in Fig. 7. The pulse width is determined by resistance *R7-2*, and the "front-porch" interval set by the adjustment of voltage divider *R7-1*.

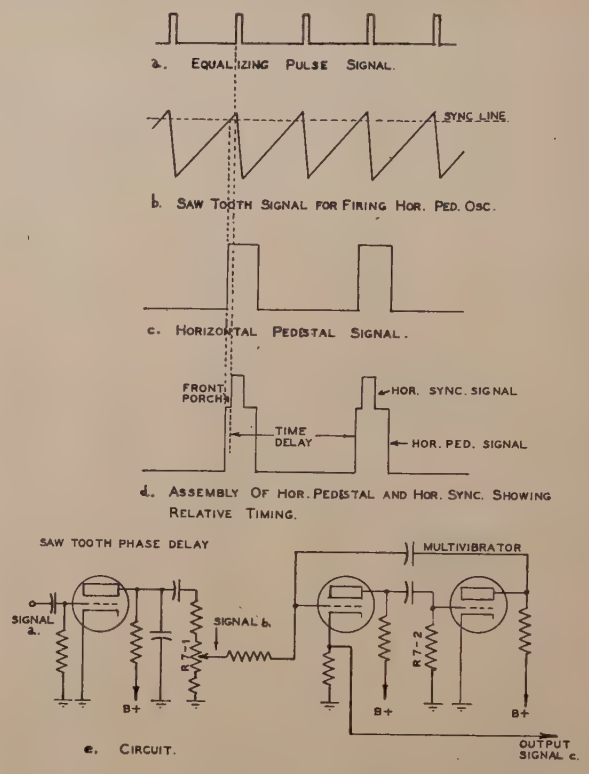

Fig. 7—Horizontal-pedestal multivibrator system.

C. The Horizontal-Synchronizing Pulse

Synchronization of the horizontal-scanning system of the television receiver depends directly upon the transmission of accurately formed and timed horizontal-synchronizing pulses, except for short time intervals during the transmission of the equalizing pulses and the vertical-synchronizing blocks.

The horizontal-synchronizing pulses must be timed to coincide approximately with the wider horizontal-pedestal pulses. Thus, if they are to be synchronized separately by the source of equalizing pulses which occur at twice the horizontal-repetition rate, means must be provided to guard against the possibility of the two horizontal-signal components synchronizing on alternate equalizing pulses.

It is entirely possible to use the horizontal-pedestal pulses to fire the horizontal-synchronizing-pulse oscillator through a time-delay network similar to the one used to delay the firing of the horizontal-pedestal oscillator. However, by so doing, the timing of the leading edges of the horizontal-synchronizing pulses relative to the leading edges of the equalizing pulses and vertical-synchronizing blocks will become dependent upon the sum of the two time-delay adjustments, creating an undesirable situation. The use of an alternate equalizing-pulse selector, or modulator, whereby the proper set of alternate equalizing pulses for the synchronization of the horizontal-synchronizing-pulse oscillator is selected by the horizontal-pedestal signal is to be preferred (see

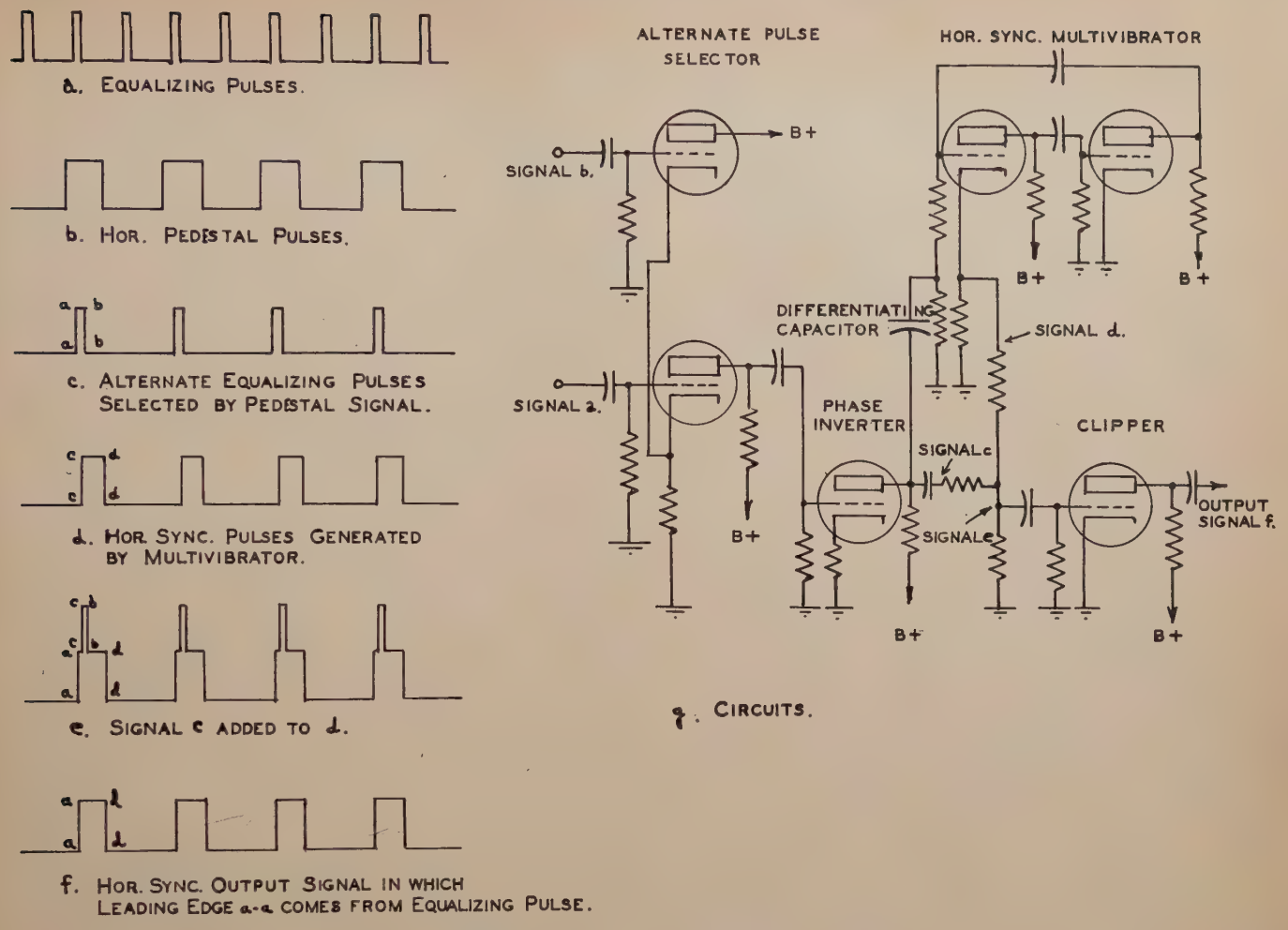

Fig. 8—Horizontal-synchronizing-pulse generating system.

Fig. 8). Thus, the adjustment of the "front-porch" time delay over a reasonable range cannot affect the timing of the horizontal-synchronizing pulses.

The horizontal-synchronizing-pulse oscillator may well be another multivibrator, as shown in Fig. 8. Resistance *R8-1* controls the pulse width. The problem of mixing the selected equalizing-pulse signal with the generated horizontal-synchronizing-pulse signal will be discussed in the section devoted to signal-synthesis circuits.

D. The Vertical-Synchronizing Blocks

The synchronization of the vertical-scanning system of the television receiver is accomplished by integrating a series of six wide pulses, or blocks, which are transmitted as a component of the composite synchronizing signal. These groups of blocks must be identical for each of the interlaced fields comprising a frame if a satisfactory interlace is to be obtained in the receiver. As explained previously, the equalizing pulses which precede and follow this group of vertical-synchronizing blocks help further to unify the composite synchronizing signal to facilitate the interlace. The vertical-synchronizing signal is serrated, or split, into blocks, so as not to interrupt the regularly timed firing of the horizontal-scanning system during the transmission of the vertical-synchronizing signal.

An oscillator could be used to generate these blocks, or inverted pulses, if properly synchronized by the equalizing pulses, but for this application wave-shaping circuits can be used to reshape the equalizing pulses into suitable blocks. The advantage resulting from this practice is the substitution of a highly stable system for a relatively unstable synchronized oscillator where it is not necessary to have the high degree of pulse-width flexibility obtainable from the multivibrator. Fig. 9 shows such a system of circuits. The equalizing pulse is formed into a saw tooth and thence clipped in two successive stages to produce the desired wave form.

E. The 60-Cycle Keying Signals

Two 60-cycle keying signals are required for the eventual synthesis of the composite signal. One such keying signal is used to interrupt the otherwise continuous transmission of the horizontal-synchronizing pulses for a time interval corresponding to nine such pulses, and to insert in their stead a group of eighteen equalizing pulses. The other 60-cycle keying signal is used to add the group of six vertical-synchronizing blocks to the center six equalizing pulses of the above selected group. This one is referred to as the 60-cycle, 3-line keying signal.

The final 60-cycle, blocking-tube oscillator of the frequency-divider chain can be used as the 60-cycle 9-line keying signal, if it is designed to produce a pulse of the proper width.

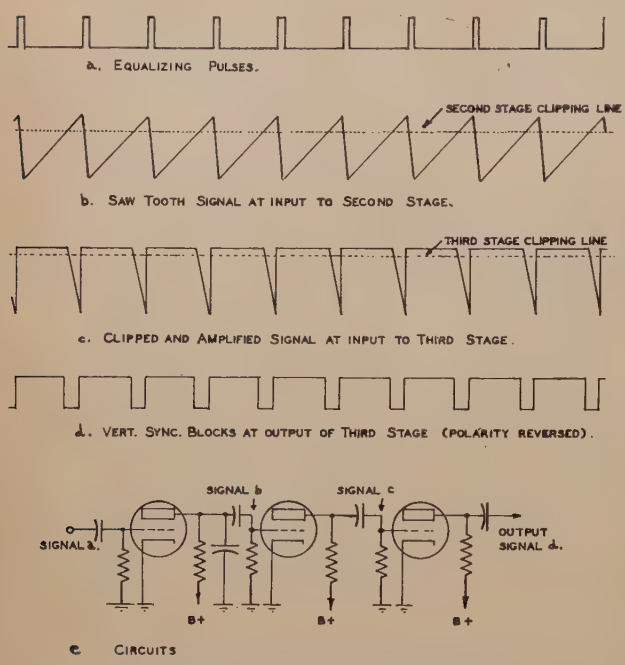

Fig. 9—Shaping circuits for generating the vertical-synchronizing blocks.

The 60-cycle 3-line keying signal must be more precisely controlled. It can be either a properly designed multivibrator or a simple blocking-tube oscillator, or can be derived from the 60-cycle 9-line keying signal by suitable wave-shaping circuits. Experience has shown that the blocking-tube oscillator provides a satisfactory solution to the problem.

The timing of the leading edge of the 60-cycle 3-line keying signal is very critical and must be held within the time interval represented by the width of an equalizing pulse. The most certain means for accomplishing this degree of precision is to fire the oscillator generating the 60-cycle 3-line signal from the leading edge of a particular equalizing pulse. Synchronization on the leading edge can be obtained readily by electrical differentiation of the equalizing pulse prior to its use for the synchronization of the 60-cycle 3-line oscillator. The more difficult problem is to insure synchronization on the particularly chosen equalizing pulse out of the 525 which are generated during each 60-cycle period.

A means for obtaining the required timing precision with proven stability is shown in Fig. 10. The 60-cycle 9-line keying signal, which is used to time the keying

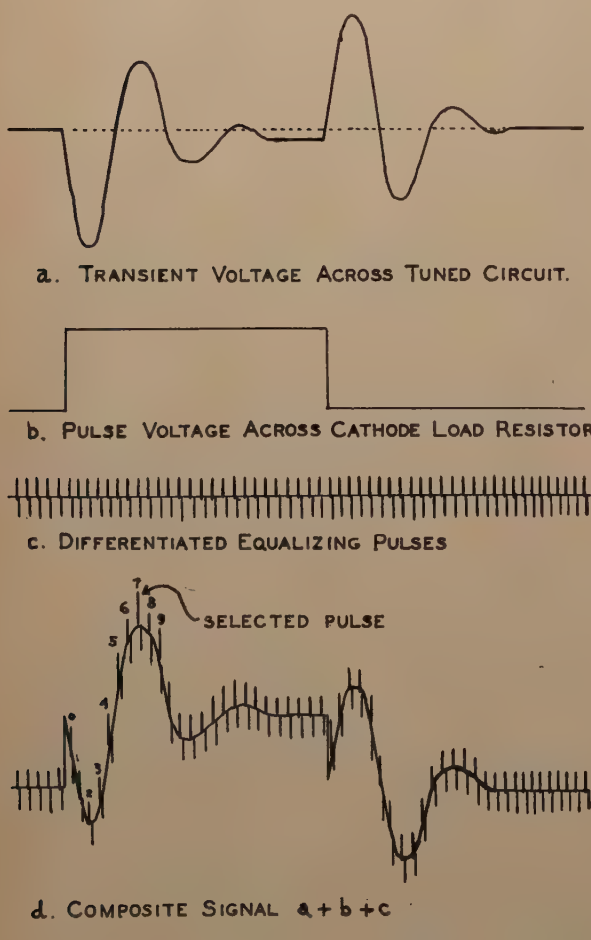
a. TRANSIENT VOLTAGE ACROSS TUNED CIRCUIT.
b. PULSE VOLTAGE ACROSS CATHODE LOAD RESISTOR
c. DIFFERENTIATED EQUALIZING PULSES
SELECTED PULSE
d. COMPOSITE SIGNAL a+b+c
1 2 3 4 5 6
1. CORRECT TUNING OF RESONANT CIRCUIT. 6 EQUALIZING PULSES.
1 2 3 4 5
2. INCORRECT TUNING. ONLY 5 EQUALIZING PULSES.
1 2 3 4 5 6 7
3. INCORRECT TUNING. 7 EQUALIZING PULSES.
e. EFFECT OF RESONANT CIRCUIT TUNING ON COMPLETED COMPOSITE SYNCHRONIZING SIGNAL.
EQUALIZING PULSE
DIFFERENTIATING CAPACITOR
SIGNAL c.
OUTPUT SIGNAL d.
SIGNAL a.
60 CYCLE 9 LINE KEYING SIGNAL
B+
SIGNAL b.
f. CIRCUIT.

Fig. 10—Details of precision time-delay system.

of the equalizing-pulse group, is also used to drive a pulse of current through a resonant circuit, causing it to develop two trains of damped sinusoidal oscillations, one following each pulse edge. The resonant circuit is tuned so that the second half cycle of the damped oscillations following the excitation produced by the leading edge of the 60-cycle, 9-line signal can serve as a pedestal to elevate the seventh equalizing pulse following the leading edge of the 60-cycle 9-line signal. The use of the second half cycle for pulse selection results in a gain in pulse selectivity of about three times, as compared to the use of the first half cycle. This improvement results from the obvious fact that the frequency to which the resonant circuit must be tuned is three times as great when the desired time interval is three quarters of a cycle as compared to one-quarter cycle (peak of the transient).

The second half cycle of a highly damped transient oscillation is considerably reduced in amplitude as compared to the first half cycle. Thus, if the polarity of the transient signal is chosen to cause the second half cycle of the initial damped oscillation excited by the leading edge of 60-cycle, 9-line pulse to reinforce the desired equalizing pulse, the first half cycle of the second train of damped oscillations excited by the trailing edge of the 60-cycle, 9-line pulse will be greater in amplitude than the desired reinforcement signal, and will probably cause erroneous synchronization. The resistance component of the inductor forming part of the tuned circuit adds a voltage component of the same wave form as the 60-cycle 9-line pulse, which further accentuates the undesired reinforcement. Both of these factors can be overcome by mixing with the transient oscillations and differentiated equalizing pulses a third component comprising a 60-cycle, 9-line pulse of proper polarity to elevate the initial transient relative to the second one (see Fig. 10). The result of adding the three components is to produce a very precise synchronizing signal for the 60-cycle 3-line oscillator, accurate to about one part in 25,000, without requiring any critical circuits. The tuning of the resonant circuit is the only adjustment, and its tolerance is about ± 10 per cent in resonant frequency.

F. The Vertical Blanking Signal

The vertical-blanking signal corresponds in the vertical-scanning system to the horizontal pedestal. It is sometimes called the vertical-pedestal signal, and it serves to black out the television-receiver screen during the vertical flyback, but does not serve as a base upon which to build the picture signal, as does the horizontal pedestal.

The timing of this signal is not of great importance so long as it comes within a line or two of its specified phase relative to the vertical-synchronizing signal. It is a wide pulse, and therefore a multivibrator is suggested. The frequency should be 60 cycles per second, and simple synchronization from the leading edge of the 60-cycle, 9-line keying signal will suffice. The output signal from this oscillator is also used to drive the discriminator for the automatic frequency control of the master oscillator (see Fig. 6).

G. Conclusions

It seems advisable at this point to tabulate the various signals (Table I) that have been generated, before proceeding with the synthesis of these signal components into the composite television signal.

TABLE I

Signal	Frequency	Wave form	Timing Source
Master oscillator	31,500	sine wave	power line through automatic-frequency-control system
Equalizing pulse	31,500	narrow pulse	master oscillator
Horizontal-synchronizing pulse	15,750	medium pulse	equalizing pulses selected by horizontal-pedestal modulator
Vertical synchronizing blocks	31,500	wide block	equalizing pulses
Horizontal pedestal	15,750	wide pulse	equalizing pulses (delayed)
Vertical blanking	60	wide pulse	60-cycle, 9-line keying
60-cycle, 9-line keying	60	medium pulse	frequency-divider chain
60-cycle, 3-line keying	60	narrow pulse	60-cycle, 9-line keying (delayed)

V. Signal-Synthesis Circuits

The synthesis of the composite television signal from the various components generated (Section IV) is done in several successive stages.

In a television synchronizing generator, uniform and precisely regular timing of the leading edges of the three components used to synchronize the horizontal-scanning system at successive time intervals is essential to the reproduction of a picture with straight vertical edges and tight horizontal synchronization. For example, if the leading edges of the equalizing pulses or the vertical-synchronizing blocks are delayed by but a microsecond relative to the uniform regularity of the horizontal-synchronizing pulses, a "tear" or horizontal displacement of several of the lines at the top of the picture may appear due to the transient disturbance set up in the receiver horizontal-scanning system. Thus, unusual precautions must be taken to insure leading-edge regularity between the various horizontal-synchronizing components.

It is, of course, possible to use adjustable delay circuits between the master timing signal and each of the three horizontal-synchronizing components, which can be individually adjusted to provide uniform timing. Such an arrangement would be subject to the variations in timing that might arise from nonuniform drifting of the time-delay circuits and to the component-generating circuits derived therefrom.

A more stable system not requiring any such critical adjustments for obtaining the exact timing of the leading edges of these various components has been successfully used. In this system, the leading edges of one reference timing signal are used directly for all components, and the various trailing edges corresponding to

the desired pulse widths are introduced by the signal-synthesis circuits. This may sound difficult, but it can be done fairly easily, as will be described in the following subsections.

The circuits required for synthesis are mostly modulators, mixers, and clippers. Various systems of modulation can be used, but the one found easiest to apply for these purposes is a type of grid modulation in which one signal is impressed on the grid of the modulator, and the other on its cathode. In some cases such modulation is accomplished by exciting the grids of two tubes with the signals to be intermodulated, and operating them with a common cathode load resistor. Mixing can be accomplished by simple addition, by paralleled-plate connections of two tubes with a common load resistor, or by paralleled-cathode connections. The method to be used in a particular case will depend on the polarity and wave form of the signals, and on any clipping that may be done simultaneously.

A. Assembly of the Horizontal-Synchronizing Signal

The leading edge of the equalizing-pulse signal has been selected as the time reference to be used as a part of all three horizontal-synchronizing components because it is the narrowest pulse and because it can be timed directly from the sine-wave master oscillator.

The circuits for assembling a horizontal-synchronizing signal from the leading edge of the equalizing-pulse signal and the trailing edge of the horizontal-synchronizing pulse signal as generated (Section IV *C*) are shown in Fig. 8. The synthesis of the composite pulse comprises adding the selected alternate equalizing pulses to the horizontal-synchronizing pulses as generated and thence clipping off the overlap.

B. Insertion of the Equalizing Pulses into the Horizontal-Synchronizing Signal

The newly assembled precision horizontal-synchronizing-pulse signal (from Section V *A*) is fed into a modulator. Here a gap of nine pulses is removed by the 60-cycle, 9-line keying signal, as shown in Fig. 11. The equalizing pulses are also fed into another modulator in which a group of eighteen pulses is selected by the 60-cycle, 9-line keying signal. The outputs of the

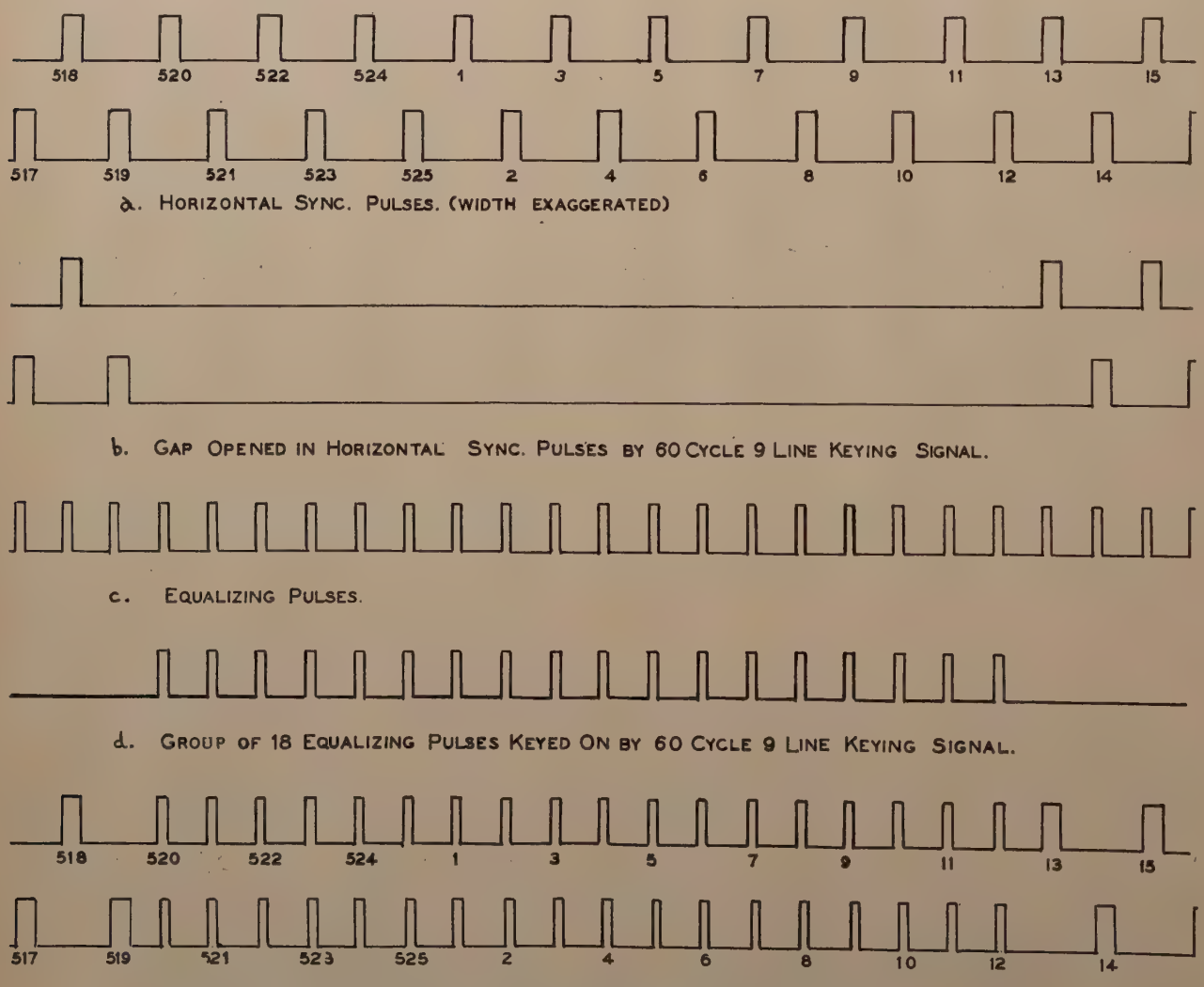
518 520 522 524 1 3 5 7 9 11 13 15
517 519 521 523 525 2 4 6 8 10 12 14
a. Horizontal Sync. Pulses. (width exaggerated)
b. Gap Opened in Horizontal Sync. Pulses by 60 Cycle 9 Line Keying Signal.
c. Equalizing Pulses.
d. Group of 18 Equalizing Pulses Keyed On by 60 Cycle 9 Line Keying Signal.
518 520 522 524 1 3 5 7 9 11 13 15
517 519 521 523 525 2 4 6 8 10 12 14
Properly Inserted Equalizing Pulses. Signal b added to signal d.

Fig. 11—Insertion of equalizing pulses into horizontal-synchronizing signal.

two modulators are mixed together, and clipped, to form a composite horizontal-synchronizing signal in which the normal train of horizontal-synchronizing pulses is interrupted at 60-cycle intervals by a group of eighteen equalizing pulses. The circuits are shown in Fig. 12.

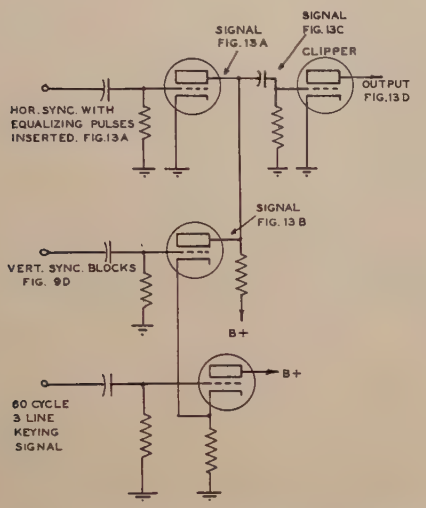

Fig. 12—Circuit of modulator for inserting equalizing pulses.

C. Insertion of the Vertical-Synchronizing Blocks

This same process of modulation is used in the next stage of the signal synthesis. Here, for exactly the center six equalizing pulses, the vertical-synchronizing blocks are added as shown in Figs. 13 and 14. The modulating

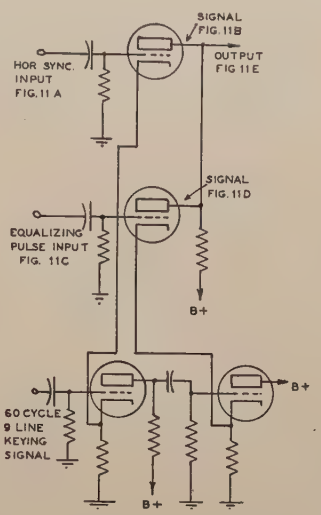

Fig. 14—Circuit of modulator for inserting the vertical-synchronizing blocks.

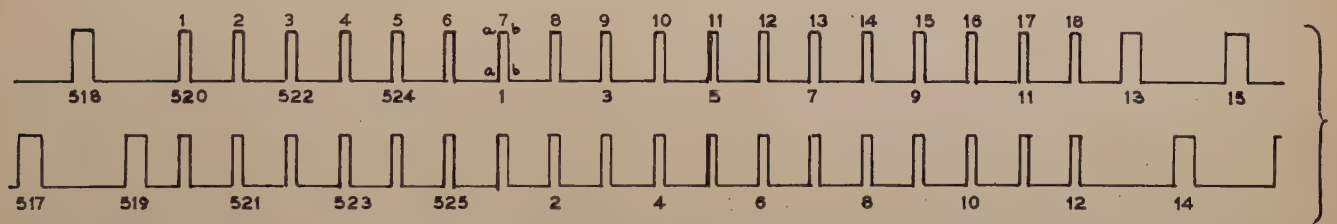

a. HOR. SYNC. SIGNAL WITH EQUALIZING PULSES INSERTED. (FROM FIG. 11E)

b. GROUP OF 6 VERT. SYNC. BLOCKS KEYED ON BY 60 CYCLE 3 LINE KEYING SIGNAL.

c. RESULT OF ADDING a TO b. NOTE LEADING EDGE a-a OF VERT. SYNC. NOW COMES FROM EQUALIZING PULSE.

d. OVERLAP IS CLIPPED OFF TO COMPLETE SYNTHESIS OF COMPOSITE SYNC. SIGNAL.

Fig. 13—Insertion of the vertical-synchronizing blocks into the composite synchronizing signal.

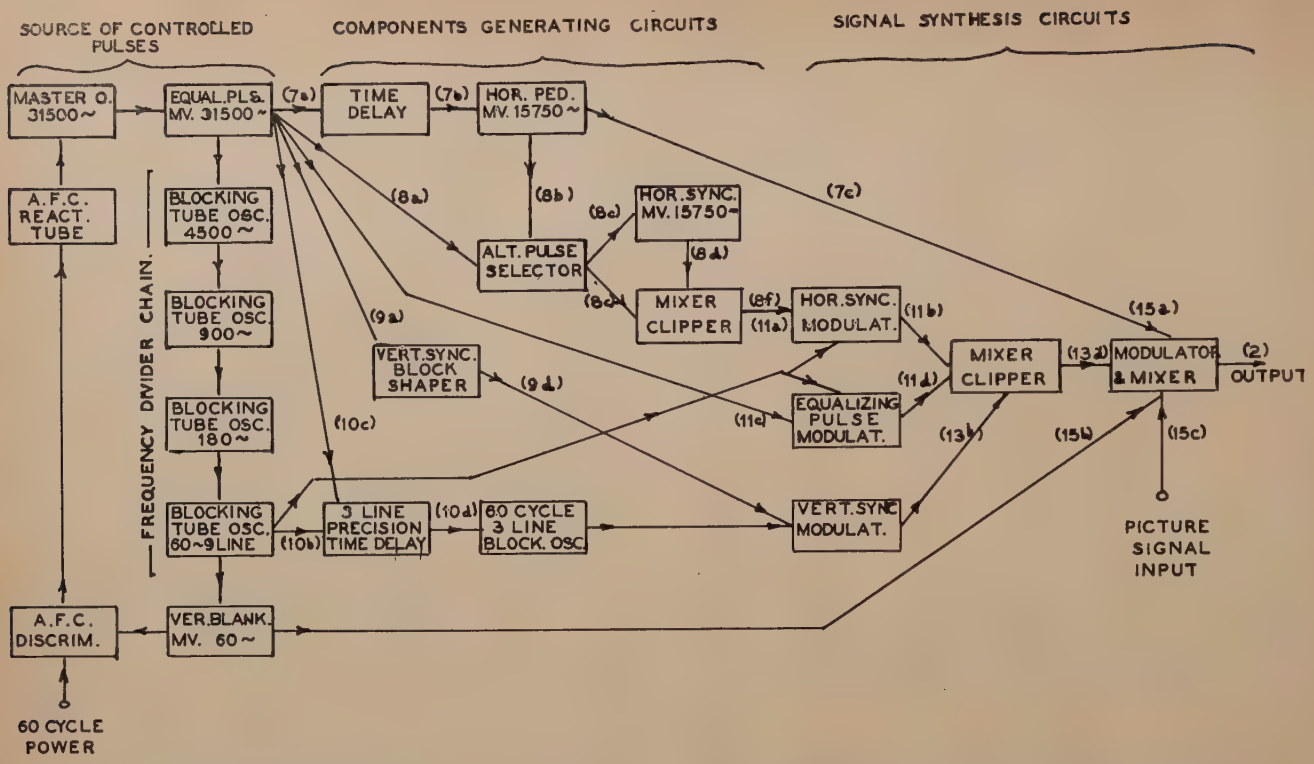

Fig. 16—Detailed block diagram of synchronizing generator. References in parentheses are to wave-form figures.

signal is the 60-cycle, 3-line keying signal, and the modulation process does not include interruption of the eighteen equalizing pulses, but merely the addition of the vertical-synchronizing blocks to the center six equalizing pulses. The resulting composite synchronizing signal is then clipped to remove the overlap existing between the center six equalizing pulses and the vertical-synchronizing blocks. By this process, once more, the leading edges of the equalizing pulses have been made to form the final leading edges of the vertical-synchronizing blocks, to complete the assembly of all three of the horizontal-synchronizing components from the same train of leading-edge signals.

D. Mixing the Picture and Pedestal Signals

The horizontal-pedestal signal is modulated by the vertical-blanking signal so as to blank it off during the vertical-retrace interval. The picture signal is then added to the horizontal-pedestal signal. The modulation and mixing circuits should be arranged to cut off the picture modulator during the horizontal- and vertical-blanking periods, so as to prevent spurious components

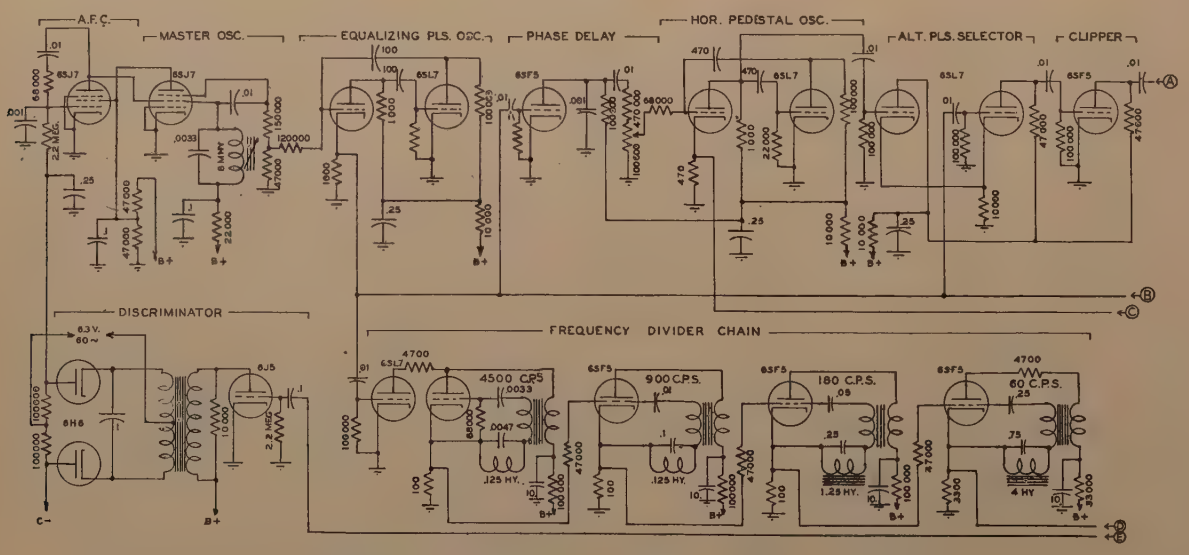

Fig. 17—Detailed schematic diagram of a television synchronizing generator.

of the picture signal occurring during these intervals from interfering with the synchronizing signals (see Fig. 15).

E. Final Stage: Adding the Composite Picture and Blanking Signal to the Composite Synchronizing Signal

These two composite signals can be mixed or simply added together to form the complete video signal suitable for radio transmission via ultra-high-frequency carrier. Television receivers used with such a signal should be properly designed to utilize the Federal Communications Commission standard television signal.

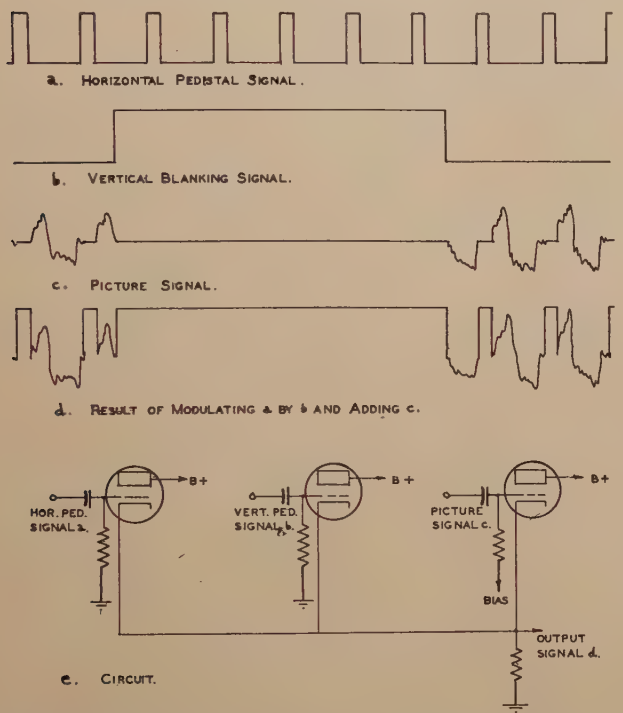

Fig. 15—Modulation of the horizontal pedestal by the vertical blanking signal and mixing with the picture signal.

VI. The Complete Synchronizing Generator

A block diagram and also a complete circuit schematic for a television synchronizing generator are shown in Figs. 16 and 17, respectively. Because it will seldom be possible for the experimenter to duplicate exactly all the conditions of an original working model, some variations in the values of the various electrical parameters can be expected.

A photograph of a television synchronizing generator made along the described lines is shown in Fig. 18. This particular unit was designed for the 441-line standard as formerly existed, and was used for some time as a part of a portable television demonstration unit. No controls, screwdriver operated or otherwise, were provided for the maintenance of the unit in proper adjustment, except for a vernier tuning capacitor in the master-oscillator tank circuit.

Fig. 18—Synchronizing generator for 441-line television.

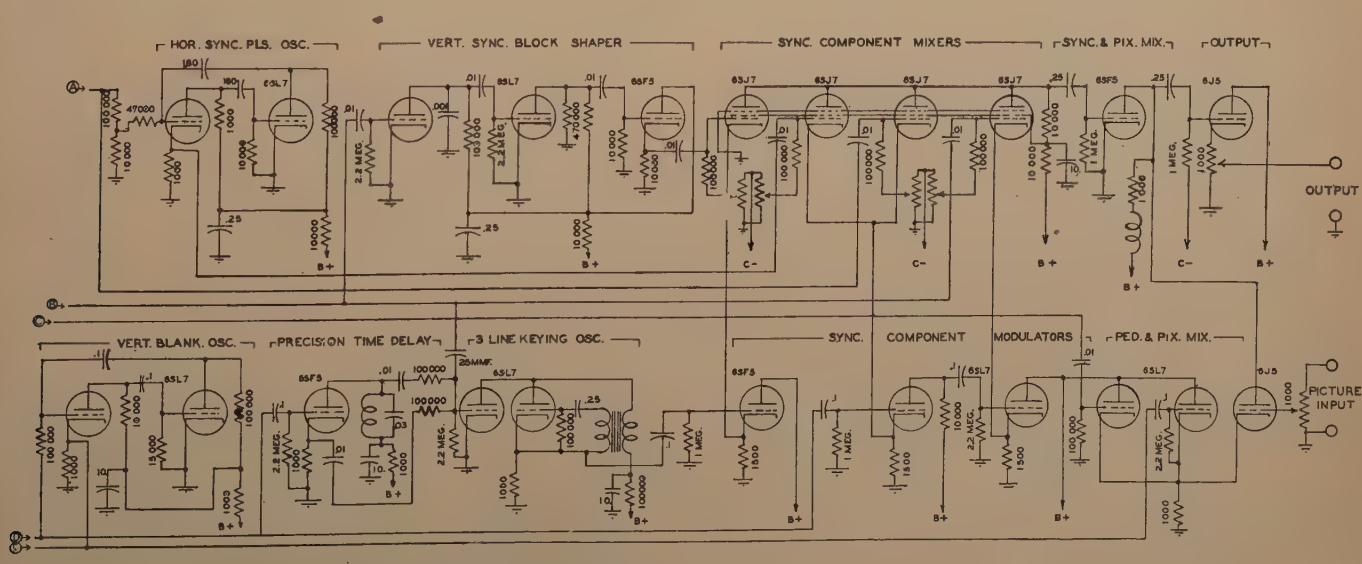

Fig. 17, continued. (A, B, C, D, and E indicate continuous lines.)

The Effect of Negative Voltage Feedback on Power-Supply Hum in Audio-Frequency Amplifiers*

GEOFFREY BUILDER†, FELLOW, I.R.E.

Summary—Some confusion exists regarding the effect of negative voltage feedback on the signal-to-hum ratio in the output of an audio-frequency amplifier. This appears to be due to lack of care in interpretation of the negative-feedback equations and to the application of these equations to circuit arrangements which do not conform to the conditions implied in their formulation. Various cases are discussed to illustrate the proper interpretation and application of the equations. The conclusions to be derived from these discussions may be summarized briefly as follows:

(1) Where the negative voltage feedback circuits satisfy the relevant conditions implied in the formulation of equations for simple negative feedback, the signal-to-hum ratio, for constant signal output, is improved by the gain-reduction factor $(1-\beta M)$.

(2) This improvement must be interpreted in relation to the complex value of the factor $(1-\beta M)$ and its variation with frequency, in relation to the frequencies of the signal and hum voltages.

(3) Failure to achieve the improvement in signal-to-hum ratio thus predicted may be due to the feedback voltage including voltage other than the fraction β of the output voltage required for simple negative feedback. A further specific analysis is then necessary to determine the effect of the feedback on the signal-to-hum ratio.

(4) In general, hum balancing within the amplifier is independent of the feedback only when the conditions for simple negative feedback are satisfied.

(5) Although, without feedback, it is legitimate to calculate the hum output voltage due to the high-tension hum voltage e by considering simple potential division of this voltage between the load impedance and the valve anode resistance R_a, this procedure is not generally valid when applied to an amplifier with feedback if the effective value of the anode impedance Z_a' of the valve is taken to be $R_a/(1-\mu\beta)$. This arises because Z_a' is the effective value of the valve impedance as viewed from the amplifier output terminals and is not necessarily significant when potential division of the voltage e is considered. It has, however, been shown in Section III(c) that, when the feedback voltage is proportional to $(e+e_0)$, the effect of the feedback on the hum output due to e is identical with that obtained on the basis of simple potential division, using the effective value Z_a'.

I. Introduction

NEGATIVE voltage feedback is commonly applied to audio-frequency amplifiers in radio receivers and similar equipment for reduction of nonlinear distortion and frequency discrimination in the amplifier itself or in its load circuit. The theory of negative feedback suggests that hum and other noise voltages introduced by the amplifier and its associated circuits should also be reduced. There is, however, some confusion as to what improvement in signal-to-hum ratio may, in fact, be expected from the application of negative feedback. This appears to arise from two main causes; lack of care in interpretation of the significance of the negative-feedback equations, and application of these equations to circuit arrangements which do not conform to the conditions implied.

* Decimal classification: R363.2×R263. Original manuscript received by the Institute, June 18, 1945.

† Merino House, 57 York Street, Sydney, Australia.

It is the object of the following discussion to clarify these points. The second of them arises from the fact that there is in common use[1–5] a number of negative-feedback circuits that do not conform to the conditions implied in the negative-feedback equations formulated by Black.[6] The term "simple negative feedback" will be used to distinguish circuit arrangements conforming to Black's implied condition that the feedback voltage should be a definite fraction of the output voltage and should not include any other voltages. For simplicity, attention is restricted to the use of negative voltage feedback, and the discussion is illustrated by circuit arrangements typical of its application; but it is obvious that similar considerations might arise in the application of other types of feedback.

The symbols and abbreviations used in the text are summarized below for convenient reference:

M = voltage gain of an amplifier or valve (vacuum tube), measured between the input and output terminals.

M_s = voltage gain from the screen grid to anode of a pentode valve.

μ = amplification factor of the amplifier or valve between input and output terminals.

μ_s = amplification factor of a pentode valve, from screen grid to anode.

β = that fraction of the output voltage fed back to the input circuit of the amplifier.

R_a = alternating-current anode resistance of the output valve of an amplifier.

Z_a = output impedance of the amplifier.

Z = load impedance into which the amplifier works.

e = hum voltage across the output of the high-tension rectifier filter supplying the amplifier.

e_i = an equivalent hum voltage referred to the input terminals of the amplifier and arising from sources within the amplifier *from which the hum is independent of the signal level.*

e_0 = output hum voltage developed across the amplifier output circuit.

e_0' = corresponding output hum voltage when simple

[1] Laboratory staff of Amalgamated Wireless Valve Company, "Negative feedback in R-C amplifiers," *Wirless World*, vol. 43, pp. 437–438; November 17, 1938.

[2] Amalgamated Wireless Valve Company, "Inverse feedback," *Radio Rev. Australia*, vol. 5, p. 64; March, 1937.

[3] G. Robert Mezger, "Feedback amplifier for C.R. oscilloscopes," *Electronics*, vol. 17, pp. 126–131, 254; April, 1944.

[4] F. Langford-Smith, "Radiotron Designer's Handbook," Wireless Press, Sydney, Australia, 1940, pp. 40–45. Complete reproduction, RCA Manufacturing Company, Harrison, N. J.

[5] F. Langford-Smith, "The relationship between the power output stage and the loudspeaker," *Proc. World Radio Convention*, Sydney, Australia, 1938.

[6] H. S. Black, "Stabilized feedback amplifiers," *Bell. Sys. Tech. Jour.*, vol. 13, pp. 1–19; January, 1934.

negative voltage feedback is applied to the amplifier.

e_0'' = corresponding output hum voltage when feedback, other than simple negative feedback, is applied to the amplifier.

In each case, the suffixes t and p are used for amplifiers having the output valve connected as a triode or pentode, respectively.

The amplification factor μ is defined by

$$(de_a/de_g) \text{ for } i_a \text{ constant}$$

where e_a is the anode voltage of the output valve, e_g the potential of the input control grid, and i_a the anode current of the output valve. For a single valve μ is real and negative, in agreement with the actual physical value of the amplification factor. In any case, the sign of μ is consistent with that of M, and in the case of a single valve, corresponds to the change of phase of 180 degrees (for resistive load) between input and output voltages.

II. Simple Negative Voltage Feedback

The general theory and equations of simple negative voltage feedback are well known; but, for clarity, those equations relevant to the discussion will be set out briefly in convenient form. In deriving these equations it is implied that the feedback voltage is derived from, and is directly proportional to, the voltage developed across the amplifier output terminals.

If the voltage gain of an amplifier without feedback is M, and if a *fraction β of the voltage across the output circuit* is fed back to the amplifier input in series with the signal voltage, the gain becomes

$$M' = M/(1 - \beta M) \tag{1}$$

and the quantity $(1-\beta M)$ is conveniently referred to as the gain-reduction factor. The gain M is related to the amplification factor μ of the amplifier, the load Z, and the anode resistance R_a of the output valve, by

$$M = \mu \cdot Z/(Z + R_a). \tag{2}$$

The effect of the feedback on the output impedance of the amplifier is to reduce it, from the anode resistance R_a of the output valve, to a value Z_a' (which will in general have a complex value) given by

$$Z_a' = R_a/(1 - \beta\mu). \tag{3}$$

It is to be noted that μ is always greater than M, and may be much greater when a pentode valve is used, so that the output impedance is reduced by a factor correspondingly greater than the gain-reduction factor.

It can be shown readily that distortion, hum, and noise voltages generated in the amplifier and its associated circuits and *developed across the output circuit* are also reduced by the gain-reduction factor $(1-\beta M)$. When, as is usually the case, the signal input voltage is increased by the factor $(1-\beta M)$ to maintain the signal output at the same level as without feedback, one might expect an improvement in the signal-to-hum and signal-to-distortion ratios across the output circuit by the factor $(1-\beta M)$, insofar as the hum or distortion originates within the amplifier.

These equations are valid for all real and complex values of the parameters μ, M, β, and Z, and the value of the gain reduction factor $(1-\beta M)$ is generally complex and dependent on frequency even for a single-valve amplifier; some of the advantages of negative feedback are in fact due to this.

It is obvious that great care is required to ascertain the exact significance of "an improvement in signal-to-hum ratio by the gain-reduction factor $(1-\beta M)$." An analysis can readily be made for any specific case, and it is clear that the reduction of signal-to-hum ratio must depend on the relative frequencies of the signal and hum voltages; only when the frequencies are identical will the gain-reduction factor be the same for both. It is not unusual to refer to an amplifier having negative feedback giving a gain reduction stated in decibels; the reference is usually to the numerical value of the gain-reduction factor at the center of the transmitted band and the gain-reduction factor at the hum frequency may be very much less, and may even in some cases be less than unity.

Proper application of the theory thus permits a correct assessment of the improvement to be expected in signal-to-hum ratio from the use of negative voltage feedback. Failure to achieve this in practice may be due to the use of feedback circuits that fail to satisfy the conditions implied. One departure from these conditions occurs when the voltage fed back includes voltages other than the fraction β of the amplifier output voltage. In practice, this probably occurs most often if the output valve of the amplifier is transformer-coupled to the load and is series fed, and if the feedback voltage is taken from between anode and cathode of the output valve; the voltage fed back then includes some fraction of any hum voltage in the high-tension supply to the output valve.[1–5]

III. Amplifier with Transformer Coupling to the Load

Transformer coupling is sometimes used for voltage amplification but is chiefly of interest in radio-receiver design for coupling the amplifier power output to a load. For illustration, an amplifier using a series-fed output valve transformer-coupled to the load, and operated under class A conditions, will be considered.

Such an amplifier may use either a pentode or triode output valve. For immediate comparison of the two types it is convenient to consider the same pentode (or beam-power) amplifier valve connected as a triode or pentode. Denoting its anode resistance as a pentode by R_{ap} and as a triode by R_{at}, we have the approximate relation

$$R_{ap} = \mu_s \cdot R_{at} \tag{4}$$

where μ_s is the amplification factor from screen grid to anode. Typical series-fed power-amplifier circuits are shown in Fig. 1. In Fig. 1(a) the output valve is triode-connected and works into a load Z_t presented to it by the output transformer, while in Fig. 1(b), the output valve is pentode-connected and works into a load Z_p. In each case, the anode is fed from a high-tension source with output filter L, C; the impedance of C to hum and signal voltages will be neglected in comparison with the load impedance. Bias arrangements are not shown but are also assumed to have negligible impedance at signal and hum frequencies. Although a single-valve amplifier is depicted in Fig. 1 for purposes of illustration, the ensuing discussion must be taken to be equally applicable to a multistage amplifier.

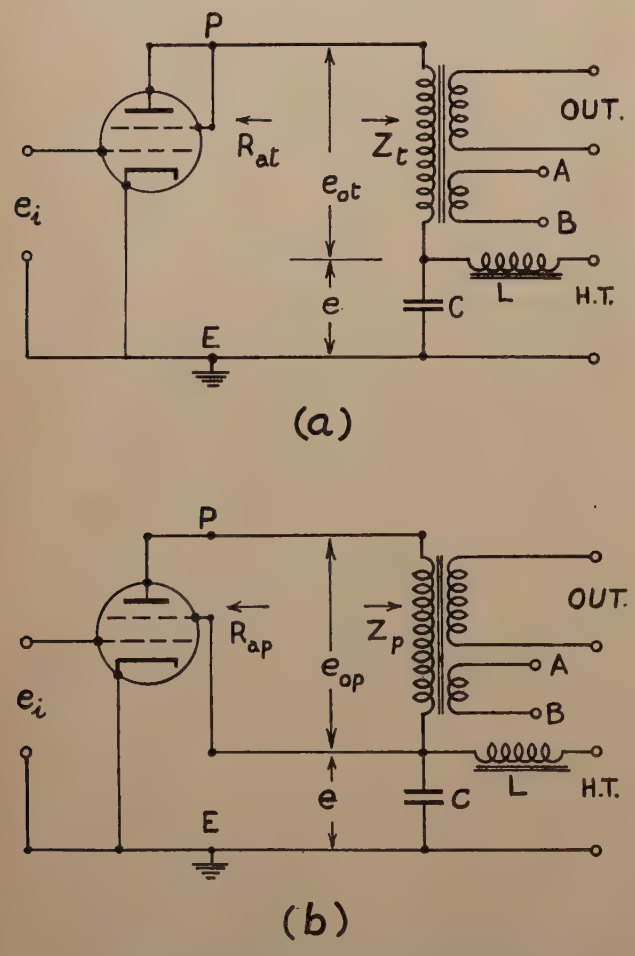

Fig. 1—Series-fed transformer-coupled amplifier (a) triode connection (b) pentode connection.

The hum voltage across the filter capacitor C is denoted by e. Hum arising from other sources within the amplifier is represented by an equivalent hum voltage e_i applied to the input terminals in series with the signal input voltage, and it is assumed that e_i is independent of the signal voltage. It is clear that, should the signal voltage itself include hum voltages, the signal-to-hum ratio in the amplifier output, insofar as it is due to hum from the signal source, will not be affected by the application of negative feedback to the amplifier except insofar as the gain-reduction factor is frequency-dependent and the signal and hum frequencies are different; that is to say, insofar as the frequency-response characteristic of the amplifier is affected by the feedback.

(a) Hum Output Without Feedback

The hum voltage developed across the output circuit is readily calculated. For the triode we have

$$e_{0t} = -Z_t \cdot e/(Z_t + R_{at}) + M_t \cdot e_i \qquad (5)$$

where M_t is the voltage gain from grid to anode, and is given by

$$M_t = Z_t \cdot \mu_t/(Z_t + R_{at}).$$

The first term of (5) corresponds to simple potential division of the hum voltage e between the load and anode impedances, while the second represents the amplification of the equivalent hum voltage e_i referred to the amplifier input circuit.

For the pentode, account must also be taken of the hum voltage e applied to the screen grid, and the output ripple voltage is given by

$$e_{0p} = -Z_p \cdot e/(Z_p + R_{ap}) + M_s \cdot e + M_p \cdot e_i \qquad (6)$$

where M_p is the voltage gain from grid to anode and M_s that from screen grid to anode, and

$$M_p = Z_p \cdot \mu_p/(Z_p + R_{ap}) \qquad M_s = Z_p \cdot \mu_s/(Z_p + R_{ap}).$$

Comparison of (5) and (6), taking into account (4), indicates that the hum output voltage for a pentode, arising from the hum voltage e applied to its anode and screen circuits, will usually exceed the corresponding output hum voltage for the triode owing to the magnitude of the term $M_s e$. For example, the beam-power valve type 6V6G has the typical operating conditions.

$R_{at} = 2500$ ohms	$R_{ap} = 50{,}000$ ohms
$Z_t = 4000$ ohms	$Z_p = 5000$ ohms
$\mu_s = -20$	$M_s = -1.8$

and (5) and (6) give the respective hum output voltages

$$e_{0t} = -0.6e \qquad e_{0p} = -1.7e.$$

Such a comparison will, of course, apply only when series feed is used and the screen supply includes the hum voltage e. If the screen supply is further filtered to such an extent that the hum voltage applied to the screen is negligible, the output hum voltage due to e is determined by the first term of (6) and will be considerably less than in the case of the triode, owing to the large value of the anode resistance R_{ap} in comparison with the load impedance.

(b) The Effect of Simple Negative Feedback on the Hum Output Voltage

The application of simple negative voltage feedback to the amplifier, as defined in Section II, requires that the voltage fed back be a fraction of the voltage developed across the output load circuit; i.e., across Z_t or Z_p. This condition is most readily satisfied by taking the feedback voltage across an appropriate winding AB on the output transformer as indicated in

Fig. 1. When this is done, the hum output voltage is reduced by the factor $(1-\beta M)$. We then have, for the triode and pentode connections, respectively,

$$e_{0t}' = e_{0t}/(1 - \beta M_t) \quad (7)$$

$$e_{0p}' = e_{0p}/(1 - \beta M_p). \quad (8)$$

These expressions cannot be formulated in terms of the reduction in effective output impedance Z_a' of the amplifier because the voltage e is not included in the feedback and the effective output impedance Z_a' is not applicable to such a calculation; i.e., it is not the effective impedance as viewed from the terminals of the voltage e.

It is obvious that, in this case, the reduction in the hum output voltages occurs equally for hum from the various sources and any hum balancing within the amplifier will not be affected by the feedback. However, if the output transformer feeds a moving-coil loudspeaker of which the field coil is used for smoothing the rectified high-tension supply to the amplifier, the speaker may have a hum-balancing coil wound over the field coil and connected in series with the voice coil. In general, a hum voltage will then be produced across the transformer secondary and reduction of this voltage by the feedback may require compensation by adjustment of the hum-balancing coil.

(c) The Effect of Other Feedback Circuits on the Hum Output Voltage

It is a common, and undoubtedly convenient, practice to utilize a feedback voltage other than that required for simple negative feedback as specified in Section II above. Among the most common of such modified circuits is that in which the feedback voltage is obtained by potential division from the anode-cathode voltage of the output amplifier; i.e., the voltage between points P and E in Figs. 1(a) and 1(b). This arrangement departs from the simple feedback circuit in that the feedback voltage is a fraction, not of the output load voltage, but of the output voltage plus the hum voltage e across the capacitor C. It is not, therefore, to be expected that the modification of the hum output voltage indicated by the theory of simple feedback will occur.

If the output valve is triode-connected, the effect of this feedback circuit will be to change the output hum voltage from its value e_{0t} without feedback (equation (5)), to a value e_{0t}'' given by

$$e_{0t}'' = -Z_t \cdot e/(Z_t + Z_{at}') + M_t' \cdot e_i \quad (9)$$

where

$$Z_{at}' = R_{at}/(1 - \beta\mu_t).$$

$$M_t' = M_t/(1 - \beta M_t)$$

and for large amounts of feedback this approximates to

$$e_{0t}'' = -e + M_t' \cdot e_i \quad (10)$$

indicating that, owing to the reduction in the effective output impedance of the amplifier by the feedback, practically the whole of the hum voltage e is developed across the load; but that hum voltages represented by e_i are reduced by the gain-reduction factor. It happens in this case, because the feedback voltage is proportional to $(e+e_0)$, that the effect of the feedback on the hum due to e can be expressed in terms of the change in effective output impedance of the amplifier.

If the output valve is pentode connected, the effect of this feedback arrangement will be to change the hum voltage output from its value e_{0p} without feedback, as given in (6), to a value e_{0p}'' given by

$$e_{0p}'' = -Z_p \cdot e/(Z_p + Z_{ap}') + M_s' \cdot e + M_p' \cdot e_i \quad (11)$$

where

$$Z_{ap}' = R_{ap}/(1 - \beta\mu_p)$$

$$M_s' = M_s/(1 - \beta M_p)$$

$$M_p' = M_p/(1 - \beta M_p).$$

Without feedback, the first term of (11) is small but increases to the limiting value $-e$ for large values of feedback, as in the case of the triode. The hum arising in the screen and input circuits is decreased by the gain-reduction factor.

(d) Hum Balancing

For either connection of the output valve, the net result of the feedback on the total output hum depends on the relative phases and amplitudes of the various hum voltages. Equations (5), (6), (9), and (11) state the conditions necessary for reduction of the output hum voltage to zero by any process of hum-balancing within the amplifier such as those described[7,8] in the literature. It is to be noted that any such balance generally depends on the degree and nature of the feedback, but that *when the conditions for simple negative feedback are satisfied, the balance is independent of the feedback*, as indicated by the form of (7) and (8).

IV. Other Amplifiers

In amplifiers having an output circuit other than the series-fed transformer arrangement discussed in relation to Fig. 1, the output voltage is usually identical with the anode-to-cathode voltage of the output valve, and the relevant conditions for simple negative feedback are satisfied by almost any convenient circuit arrangement. This applies, for example, to a parallel-fed transformer-coupled output circuit, or to a resistance- or choke-coupled voltage amplifier. Simplified circuits corresponding to these cases are shown in Figs. 2(a) and 2(b) and can be used to represent a wide range of practical cases.

In Fig. 2 the high-tension supply is fed to the amplifier anode through an impedance Z_1 which may be a

[7] Wen-Yuan Pan, "Circuit for neutralizing low-frequency regeneration and power-supply hum," Proc. I.R.E., vol. 30, pp. 411–412; September, 1942.

[8] K. B. Gonser, "A method of neutralizing hum and feedback caused by variations in the plate supply," Proc. I.R.E., vol. 26, pp. 442–449; April, 1938.

resistance (e.g., resistance-capacitance-coupled voltage amplifier) or a choke (e.g., parallel-fed transformer-coupled amplifier). The anode of the valve is coupled through a blocking capacitor to a load Z_2 which may be the grid leak of a succeeding stage, or may be presented

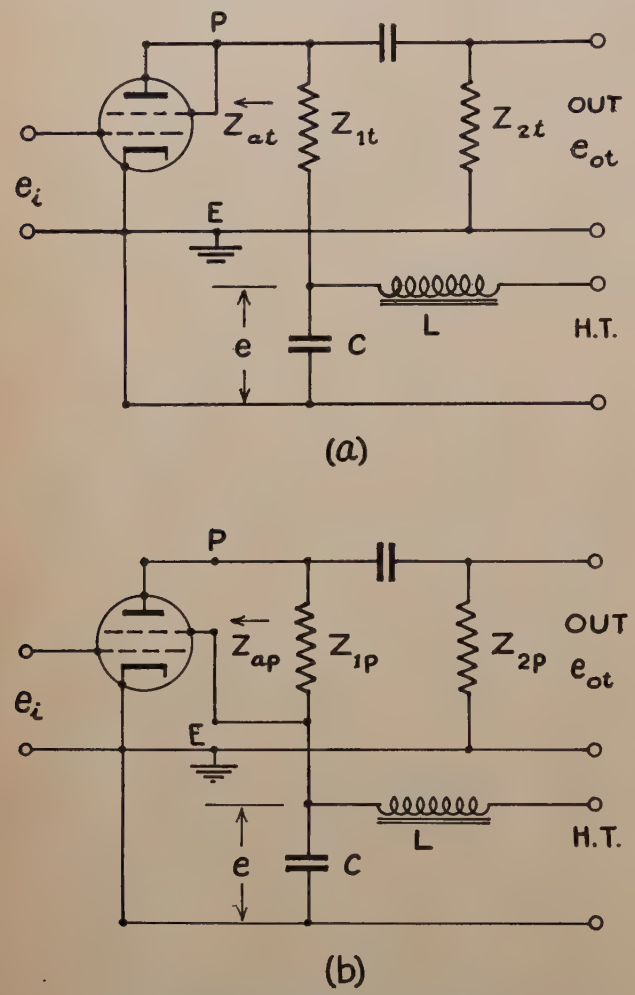

Fig. 2—Parallel-fed amplifier (a) triode connection (b) pentode connection.

by the primary of an output transformer. In Fig. 2(a) the output valve is triode-connected, and in Fig. 2(b), pentode-connected. In each case the hum and signal voltages applied are the same as in the foregoing discussion.

Without feedback, the hum output voltage may readily be shown to be, for the triode and pentode connections respectively,

$$e_{0t}=\frac{-R_{at}\cdot Z_{2t}}{R_{at}\cdot Z_{2t}+R_{at}Z_{1t}+Z_{1t}\cdot Z_{2t}}\cdot e+M_t\cdot e_i \qquad (12a)$$

$$e_{0p}=\frac{-R_{ap}\cdot Z_{2p}}{R_{ap}\cdot Z_{2p}+R_{ap}\cdot Z_{1p}+Z_{1p}\cdot Z_{2p}}\cdot e+M_s\cdot e+M_p\cdot e_i \qquad (12b)$$

where

$$Z = Z_1\cdot Z_2/(Z_1+Z_2)$$
$$M = Z\cdot\mu/(Z+R_a)$$
$$M_s = Z\cdot\mu_s/(Z+R_a)$$

and the subscripts t and p refer to the triode and pentode connection respectively. Z, M, and M_s have the same significance as in the cases discussed previously. In (12a) and (12b) the first term represents simple potential division of the hum voltage e between the feed impedance Z_1 and the load Z_2 in parallel with the anode resistance R_a of the valve. It is clear that the hum output voltage will, in general, in the case of parallel feed be less for a triode, but greater for a pentode, than in the case of series feed.

Negative voltage feedback may be provided by simple potential division of the anode-cathode voltage of the valve or from a winding on an output transformer. In any straightforward method, the feedback voltage will be proportional to the amplifier output voltage, because this is identical with the anode-cathode voltage and the conditions for *simple negative feedback* are satisfied. The effect of the negative voltage feedback is, therefore, to reduce the hum output voltage from all sources by the gain-reduction factor. As in the case discussed in Section III(b) above, the effect of the feedback on the hum output voltage due to e, as given by the first term of (12), cannot be formulated in terms of the change in effective output impedance Z_a' of the amplifier with feedback, because the impedance Z_a' is the effective output impedance viewed from the output terminals and is not significant for the purpose of considering potential division of the hum voltage e.

Because the feedback satisfies our definition of *simple negative feedback*, hum-balancing arrangements within the amplifier are unaffected by the feedback. Hum across the load due to a loudspeaker hum-balancing coil can be treated as part of the hum output voltage Me_i and is reduced by the gain-reduction factor; some readjustment of the hum-balancing arrangement in the loudspeaker will be necessary.

V. Acknowledgment

I am deeply indebted to Mr. F. Langford-Smith for his interest and assistance in the preparation of this paper.

High-Voltage Rectified Power Supply Using Fractional-Mu Radio-Frequency Oscillator*

ROBERT L. FREEMAN†, SENIOR MEMBER, I.R.E., AND R. C. HERGENROTHER‡, ASSOCIATE, I.R.E.

Summary—**An oscillator circuit designed to operate with a vacuum tube having a small fractional mu has been used to develop across its grid-leak resistor a bias voltage whose value is over ten times as great as the anode-supply voltage. The principle can be demonstrated by connecting a triode so that its grid and anode are interchanged. However, special tubes of unconventional design were constructed for generating several thousand volts. The rectified voltage is negative in polarity relative to cathode, and thus is adapted for oscilloscopes. A slight modification permits a positive-polarity voltage to be obtained for use with television-picture tubes.**

THE PURPOSE of this paper is to describe a novel electronic system of producing direct-current voltages of the order of a few thousand volts from a lower direct-current voltage by means of a single vacuum tube. The system has application as a voltage source for high-impedance devices, such as cathode-ray tubes. The system, like that described by Schade (see bibliography), utilizes radio frequencies and thus has the advantage that low-capacitance filter capacitors may be employed with consequent reduction of shock hazards.

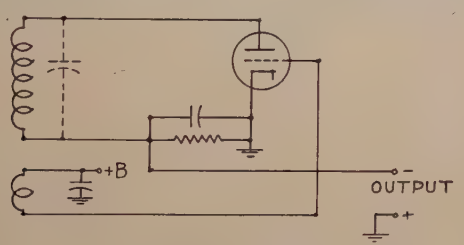

Fig. 1—Fractional-mu oscillator using conventional triode.

The circuit, in general, is that of a vacuum-tube oscillator with self-biased grid. During operation a negative potential is built up across the grid capacitor by electrons which the grid collects during the positive excursions of the grid-voltage swing. If the tube has certain characteristics, it is possible to build up a grid bias voltage which is many times greater than the direct-current voltage applied to the anode of the tube. This grid bias voltage constitutes the high-voltage direct-current output.

Consideration of the characteristics which an oscillator tube and associated circuit must have in order to build up a high bias voltage indicate that the oscillator circuit should have a large voltage step-up ratio from anode to grid, and the amplification factor or mu of the tube should be fractional; that is, less than unity. In order for oscillations to build up, the transconductance of the tube at small grid voltages should exceed the total circuit conductance.

* Decimal classification: R356.1×R388. Original manuscript received by the Institute, June 19, 1945. Presented, 1945 Winter Technical Meeting, New York, N. Y., January 26, 1945.

† Lewyt Corporation, Brooklyn, N. Y.; formerly, Hazeltine Corporation, Little Neck, Long Island, N. Y.

‡ Raytheon Manufacturing Company, Waltham, Mass., formerly, Hazeltine Corporation, Little Neck, Long Island, N. Y.

In Fig. 1 is shown a fractional-mu oscillator circuit using a conventional triode. The grid of the tube is here connected to a direct-current source and acts as the oscillator anode, whereas the plate of the tube is connected to a high-impedance tank circuit and acts as the grid or control element of the oscillator. The control-electrode bias voltage which is built up across the parallel control-electrode resistor and capacitor constitutes the stepped-up direct-current output voltage. Tests on the circuit proved that a direct-current output voltage greater than the direct-current input could be obtained. However, it was found that a conventional tube was not practicable for high-voltage output, since the direct-current input voltage had to be kept quite low to avoid overheating of the grid structure in the tube.

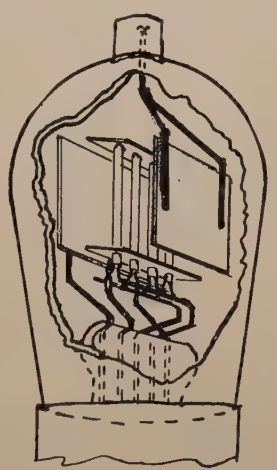

Fig. 2—Sketch of fractional-mu tubes A and B.

The next step was to design a fractional-mu tube which could stand direct-current input voltages of the order of 300 volts without overheating the anode. One such design is shown in Fig. 2. On both sides of an array of cylindrical cathodes are placed flat plates, one of which serves as the anode and the other as the control electrode.

The cross section and control-electrode-voltage-versus-anode-current characteristics of this tube are shown in Fig. 3. These curves show that this tube has a very remote cutoff characteristic which caused the tube to operate poorly as an oscillator. The prolonged tail on the curve is produced by uncontrolled emission from that part of the cathode surface facing the anode. The electric field produced at the cathode by the control electrode is greatest at that portion of the cathode facing the control electrode and is quite weak at the portion of the cathode facing the anode. Conversely, the electric field produced at the cathode by the anode is strongest

at that portion of the cathode facing the anode and is weak on the opposite side of the cathode. These two effects combined give the poor cutoff characteristic in Fig. 3.

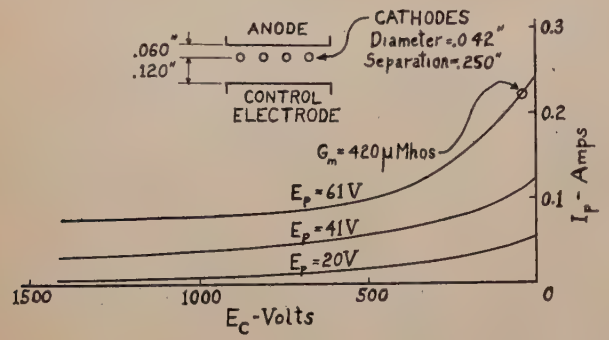

Fig. 3—Dimensions and characteristics of fractional-mu tube A. Cathodes are completely coated with oxide emitter. At $E_p=60$ volts and $I_p=0.10$ ampere, $\mu=0.046$. At $E_p=60$ volts and $I_p=0.15$ ampere, $\mu=0.060$.

In order to improve the cutoff, a similar tube was constructed in which the cathode coating extended only halfway around each cathode cylinder and faced the control electrode. The cross section and characteristics of this tube are shown in Fig. 4, wherein a substantial

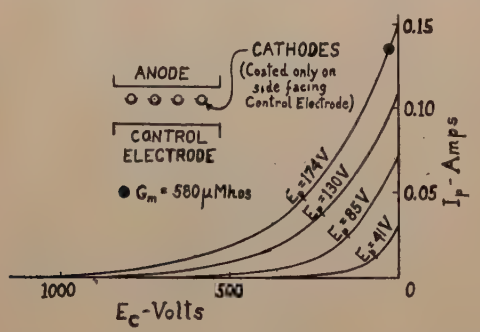

Fig. 4—Dimensions and characteristics of fractional-mu tube B. Cathodes are coated only on side facing control electrode. Dimensions are the same as tube A. At $E_p=107$ volts and $I_p=0.05$ ampere, $\mu=0.39$. At $E_p=152$ volts and $I_p=0.10$ ampere, $\mu=0.56$.

improvement in cutoff is indicated. The transconductance shows improvement, although the active cathode area has been decreased to one half. The mu of the tube was increased about fourfold by this change.

The performance of this tube as a fractional-mu oscillator was measured using the circuit shown in the Fig. 5, which oscillates at 190 kilocycles.

The details of the radio-frequency coil are shown in Fig. 6. This shows a cross-sectional view of the transformer, the axis of the coil being vertical. The secondary-to-primary turns ratio is 13. The coupling coefficient and Q are made fairly large by using an iron-dust core and Litz wire for the windings.

The performance data obtained with this tube and circuit are shown in Table I. The direct voltage developed across a 23-megohm resistor was from 14 to 17 times as great as the direct voltage applied to the anode of the oscillator tube. If the efficiency of the circuit is defined as the ratio of the power absorbed in the output resistor to the power input to the anode, the values shown in the extreme right-hand column are representative.

The fractional-mu oscillator tube with partly coated cathodes as in Fig. 4 made rather inefficient use of cathode heating power, since only one half of the cathode sleeve is coated with emitter and the remaining half

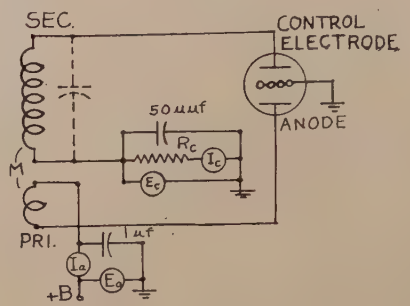

Fig. 5—Oscillator circuit for tube B.

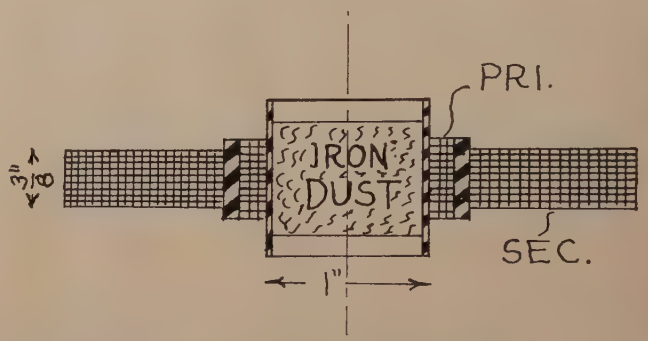

Fig. 6—Details of coil used in circuit of Fig. 5. Primary, next to core, is universal wound with 60 turns of 7/41 Litz wire; inductance=220 microhenries. Secondary, insulated by $\frac{1}{8}$-inch-thick layer of varnished cambric, is universal wound with 780 turns of 7/41 Litz wire; inductance=36 millihenries. The Q of the secondary measures 75 at 125 kilocycles. The coefficient of coupling =0.5.

absorbs just as much cathode power but produces no emission. An improved design of fractional-mu oscillator tube which makes use of the entire cathode area is shown in Fig. 7. The control-electrode-voltage versus anode-

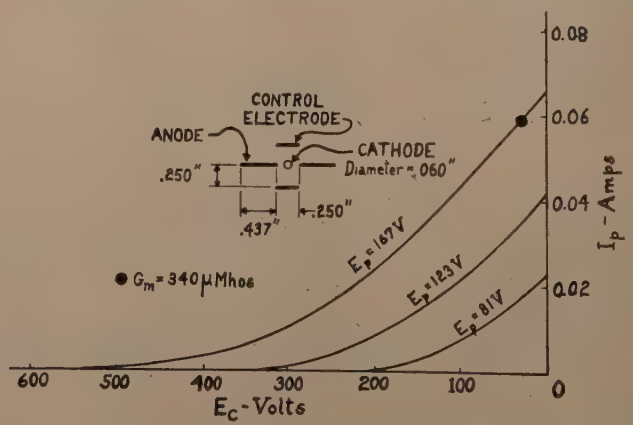

Fig. 7—Dimensions and characteristics of fractional-mu tube of improved design which uses a completely coated cathode.

current characteristic of this tube, shown in Fig. 7, is comparable with that of the preceding tube, and shows further improvement in cutoff. This tube was tested in

TABLE I
PERFORMANCE AF TUBE B IN CIRCUIT OF FIG. 5.

E_a Volts	E_c Volts	I_a Milli-amperes	I_c Milli-amperes	R_c Megohms	E_c/E_a	E_cI_c/E_aI_a
220	3160	14.7	0.134	23.6	14.4	0.13
312	4900	21.5	0.208	23.6	15.7	0.152
362	5900	25.5	0.250	23.6	16.3	0.16
490	8400	35.2	0.355	23.6	17.2	0.171
300	4540	25.0	0.360	12.6	12.0	0.217
485	7750	43.0	0.617	12.6	12.6	0.228

the circuit of Fig. 4 and gave substantially the same performance as the previous tube.

The output voltage developed across the control-electrode resistor and capacitor has considerable sawtooth component. Increasing the time constant will reduce this component to some extent, but a time constant will ultimately be reached where the oscillator will intermittently block. Thus, an additional resistance-capacitance filter is used preferably between the control-electrode resistor and the utilization device.

The potential derived is negative with respect to chassis and is thus of correct polarity for cathode-ray tubes used as oscilloscopes. In such applications the second anode and deflector plates are usually at chasis potential and the cathode at a large negative potential.

In television receivers it is most convenient to apply a large positive potential to the second anode while maintaining the cathode and grid near chasis potential. This permits simplified coupling between the last video stage and the cathode-ray-tube grid. It is possible, however, to connect the picture tube so that its cathode and grid are highly negative. However, a high-voltage capacitor and a direct-current reinsertion diode are necessary to couple the last video stage to the cathode-ray-tube grid.

If the cathode-ray tube is to be operated with its grid and cathode near chassis potential, the fractional-mu oscillator can be operated with the chassis connection at the negative-potential end of the grid resistor instead of at the cathode end. A separate low-wattage power supply operating above chassis potential can be used to supply the anode voltage and heater voltage for the fractional-mu tube. This supply will fluctuate in potential above chassis by an amount equal to the ripple present across the grid resistor, and thus the auxiliary power supply preferably should be shielded.

ACKNOWLEDGMENT

It is to be acknowledged that an associate of the authors, A. H. Reesor Smith, made the proposal of using a fractional-mu oscillator to generate high voltages.

Bibliography

(1) F. E. Terman, "The inverted vacuum tube, a voltage-reducing power amplifier," PROC. I.R.E., vol. 16, pp. 447–461; April, 1928.
(2) O. H. Schade, "Radio-frequency-operated high-voltage supplies for cathode-ray tubes," PROC. I.R.E., vol. 31, pp. 158–163; April, 1943. (Also U. S. Patent No. 2,374,781, May 1, 1945).
(3) U. S. Patent No. 2,300,451, A. H. R. Smith, November 3, 1942, "High-voltage power-supply system."
(4) U. S. Patent No. 2,324,776, R. C. Hergenrother, July 20, 1943, "Vacuum tube."

Contributors to Waves and Electrons Section

A. Rufus Applegarth, Jr., (A'36) was born at Patchogue, New York, on February 1, 1913. He received the S.B. and S.M. degrees from the Massachusetts Institute of Technology in 1936, after which he became associated with the Philco Radio and Television Corporation as a television development engineer. He joined the RCA Manufacturing Company in 1939 to engage in the design of aviation-radio receivers and airborne radar equipment. Shortly after the outbreak of the war with Japan, he was called to active duty with the Signal Corps, and sent to the aircraft radio laboratory, Wright Field, Dayton, Ohio, where he was assigned to the radar division. He is now vice-president of the Aeronautical Corporation, Camden, New Jersey.

A. RUFUS APPLEGARTH, JR.

❖

Geoffrey Builder (A'32–F'41) was born at Cue, Western Australia, on June 21, 1906. He received the B.Sc. degree from the University of Western Australia in 1928, and the Ph.D. degree from London University in 1933. From 1928 to 1930 he was an observer at the Walheroo, Western Australia, Magnetic Observatory of the Carnegie Institution of Washington. During 1931 and 1932 he was engaged in research work in radio physics at the University of London, and during 1933 and 1934 was a research physicist of the Australian Radio Research Board. From 1934 to 1941 he was in charge of the research and development laboratories

GEOFFREY BUILDER

EDWIN E. SPITZER

❖

of Amalgamated Wireless (Australasia), Ltd. Since 1941 he has been a consulting engineer.

Dr. Builder is a Fellow of the Institute of Physics, London, a Fellow of the Institution of Radio Engineers (Australia), and an Associate member of the Institution of Engineers (Australia).

❖

George A. Espersen (A'34) was born at Jersey City, New Jersey, on May 17, 1906. He received the B.S. degree in physics in 1931 from New York University. From 1932 to 1939 Mr. Espersen was employed by Hygrade Sylvania Corporation as a development engineer engaged in the development and production of receiving type tubes. He was tube-development engineer for National Union Radio Corporation in 1939 and 1940.

From 1940 to 1942 Mr. Espersen was engaged in research and development of ultra-high-frequency tubes in the research laboratories of the Sperry Gyroscope Company. Since 1942 he has been a development engineer with the North American Philips Company at Dobbs Ferry, New York.

Mr. Espersen is a member of the American Physical Society.

❖

Edwin E. Spitzer (A'28–M'38–SM'43) was born at Fitchburg, Massachusetts, on February 22, 1905. He received the B.S. and M.S. degrees in electrical engineering from the Massachusetts Institute of Technology in 1927. Mr. Spitzer was associated with the research laboratory and the vacuum-tube engineering department of the General Electric Company from 1927 to 1933. From 1933 to date he has been head of the power-tube division of the engineering department, RCA-Victor Division of the Radio Corporation of America, Harrison, New Jersey, and since 1943 located at Lancaster, Pennsylvania.

❖

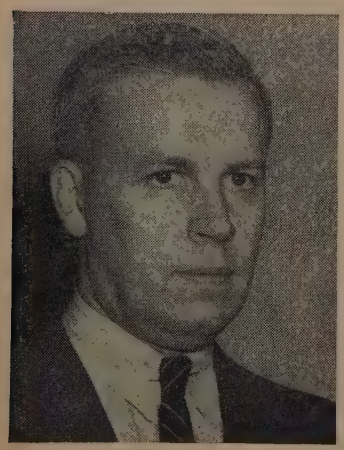

GEORGE A. ESPERSEN

❖

Gordon M. Lee (A'45) was born on January 3, 1917, at Minneapolis, Minnesota. He received the B.E.E. degree from the University of Minnesota in 1938. For the following year he was employed as a research and teaching assistant in electrical engineering at the University of Missouri and received the M.S. degree in electrical engineering from that school in 1939. From 1939 to 1945 he was associated with the Laboratory for Insulation Research at the Massachusetts Institute of Technology, receiving the D.Sc. degree in electrical engineering from M.I.T. in 1944.

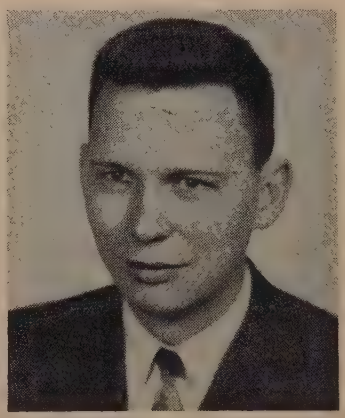

GORDON M. LEE

In 1945 he became one of the technical directors of the newly organized Central Research Laboratories, Inc., of Red Wing, Minnesota, an organization devoted to consultation, research, development, and limited production in the fields of chemistry, physics, and electrical engineering.

Dr. Lee is a member of the American Institute of Electrical Engineers, the American Physical Society, Sigma Xi, Tau Beta Pi, and Eta Kappa Nu.

❖

Robert L. Freeman (S'32–A'33–SM'45) was born on February 1, 1909, at Cleveland, Ohio. He received the A.B. degree in 1931, the E.E. degree in 1933, and the Ph.D. degree in electrical engineering in 1934 from Stanford University. He was engaged in receiver development with the Crosley Radio Corporation from 1934 until 1937. During 1937 he was transmitter engineer for Farnsworth Television, Inc. From September, 1937, to August, 1945, he was employed by Hazeltine Corporation as senior engineer and as consulting engineer. In August, 1945, he was employed by Lewyt Corporation as chief engineer.

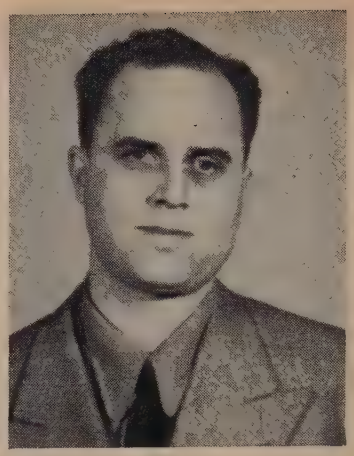

ROBERT L. FREEMAN

Dr. Freeman is a member of Sigma Xi and a Fellow of the Radio Club of America.

❖

R. C. Hergenrother (A'37) was born on September 5, 1903, in Chemnitz, Germany. He received the A.B. degree from Cornell University in 1925. During 1925 and 1926 he was employed in vacuum-tube development work at Westinghouse Lamp Company in Bloomfield, New Jersey. He went to the Pennsylvania State College in 1927 as an instructor in physics and there received the M.S. degree in 1928. He received the Ph.D. degree from California Institute of Technology in 1931.

Dr. Hergenrother held a Rockefeller Foundation Research Fellowship in physics at Washington University, St. Louis, Missouri, from 1932 to 1934. From 1934 to 1935 he was employed by the Farnsworth Television Laboratories of Philadelphia, Pennsylvania, on research and development work on television tubes. From 1935 until recently he worked for the Hazeltine Corporation on electron-tube research and development. He has now joined the communications division of the Raytheon Manufacturing Company in Waltham, Massachusetts.

He is a member of the American Physical Society, Sigma Xi, and Sigma Pi Sigma.

R. C. HERGENROTHER

Institute News and Radio Notes

Outstanding Events of 1946 Winter Technical Meeting

Keynoted by the remarkable public response to the first announcement of radar contact with the moon, the theme of the largest and most successful Winter Technical Meeting in the history of The Institute of Radio Engineers might be characterized, in the words of Dr. Frederick B. Llewellyn, president of the Institute, as one of "intense enthusiasm and a sense of the importance of this field of electronics in the daily lives of men now and in the future."

The four-day meeting from January 23–26, 1946, at the Hotel Astor drew a record registered attendance of 7020 radio-and-electronic engineers and scientists, over 2500 more than had been anticipated. Last year, an estimated 3000 members of the professions attended.

Opening the four-day gathering on Wednesday evening, January 23, was a joint meeting between the Institute of Radio Engineers and the American Institute of Electrical Engineers at the Engineering Societies Auditorium, 33 West 39th Street, New York City, at which Major General Leslie R. Groves, director of the Manhattan District, code name for the atomic-bomb project, was the principal speaker before an overflow crowd. Commenting on many of the background aspects of the gigantic atomic-bomb project, General Groves noted "The United States Army and Navy would have fought the Spanish-American War with radar in all its present uses, if radar progress had advanced as speedily from its beginnings as the atomic-bomb project." The

Some of the Sections' Representatives Who Attended the 1946 Winter Technical Meeting

First Row (left to right): C. A. Norris, Chairman, Meetings and Papers Committee, Toronto; Alexander Bow, Secretary-Treasurer, Toronto; H. E. Kranz, Chairman, Detroit; W. O. Swinyard, Board of Directors, I.R.E.; W. L. Everitt, Retiring President, I.R.E.; Samuel Gubin, Vice-Chairman, Philadelphia; R. A. Heising, Chairman, Sections Committee; and M. C. Jensen, Representative, Twin Cities.
Second Row (left to right): E. B. Swan, Vice-Chairman, Canadian I.R.E. Council, Toronto; G. T. Royden, Sections Committee; F. A. Polkinghorn, Sections Committee; Richard White, Chairman, Kansas City; R. S. Ould, Representative, Washington; C. W. Tirrell, Secretary, San Diego; R. F. Field, Executive Committee, Boston; G. H. Browning, Vice-Chairman, Boston; A. E. Newlon, Secretary, Rochester; and E. M. Dupree, Representing Houston.
Third Row (left to right): N. L. Kiser, Chairman, Emporium; H. E. Smithgall, Chairman, Williamsport; L. A. W. East, Chairman, Montreal; R. R. Desaulniers, Secretary, Montreal; B. E. Shackelford, Sections Committee, New York; E. S. Skelsey, Vice-Chairman, Montreal; R. R. Batcher, Representative, New York; Roy M. Flynn, Chairman, Dallas-Fort Worth; Durward J. Tucker, Representative, Dallas-Fort Worth; W. H. Crew, Assistant Secretary, I.R.E., and H. E. Hartig, Chairman, Twin Cities.
Fourth Row (left to right): F. L. Burroughs, Secretary, Williamsport; F. H. R. Pounsett, Chairman, Toronto; Burwell Graham, Chairman, London; G. B. Hoadley, Chairman, New York; N. J. Zehr, Secretary, St. Louis; R. B. Jacques, Technical Secretary, I.R.E.; B. B. Miller, Chairman, St. Louis; S. L. Bailey, Sections Committee; R. A. Holbrook, Chairman, Atlanta; and J. E. Breeze, Representative, Ottawa.
Fifth Row (left to right): Alois W. Graf, Vice-Chairman, Chicago; R. H. Herrick, Executive Committee, Chicago; F. S. Howes, Chairman, Canadian I.R.E. Council, Montreal; H. D. Reid, Chairman, Cincinnati; W. L. Webb, Board of Directors, I.R.E.; T. A. Hunter, Chairman, Cedar Rapids; R. S. Conrad, Secretary, Cedar Rapids; R. N. Harmon, Chairman, Baltimore; V. A. Bernier, Secretary, Indianapolis; and F. W. Albertson, Chairman, Washington.

1946 WI
TECHNICA

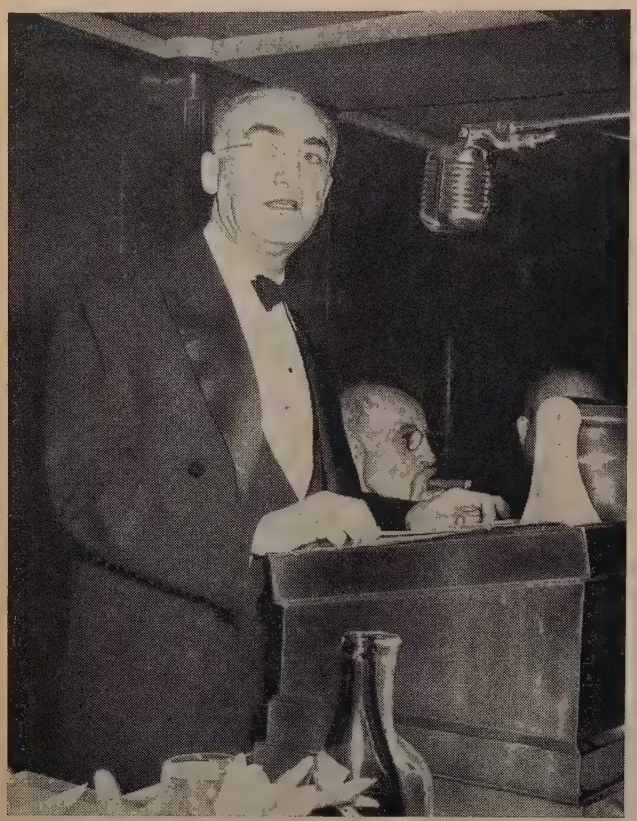

MR. EDGAR KOBAK, President of the Mutual Broadcasting System, acts as Toastmaster at Banquet. Dr. Jewett in background.

DR. LLEWELLYN presents Morris Liebmann Memorial Prize for 1945 to Dr. Peter C. Goldmark.

DR. RALPH VINTON HARTLEY receives Medal of Honor for 1946 from Dr. Frederick B. Llewellyn.

MR. RAYMOND A. HEISING Presides over Annual Meeting of Sections' Representatives.

TER I.R.E. MEETING

DR. LLEWELLYN presents Certificate of Fellowship to Dr. Julius A. Stratton who made Speech of Acceptance for all recipients of Fellow Award.

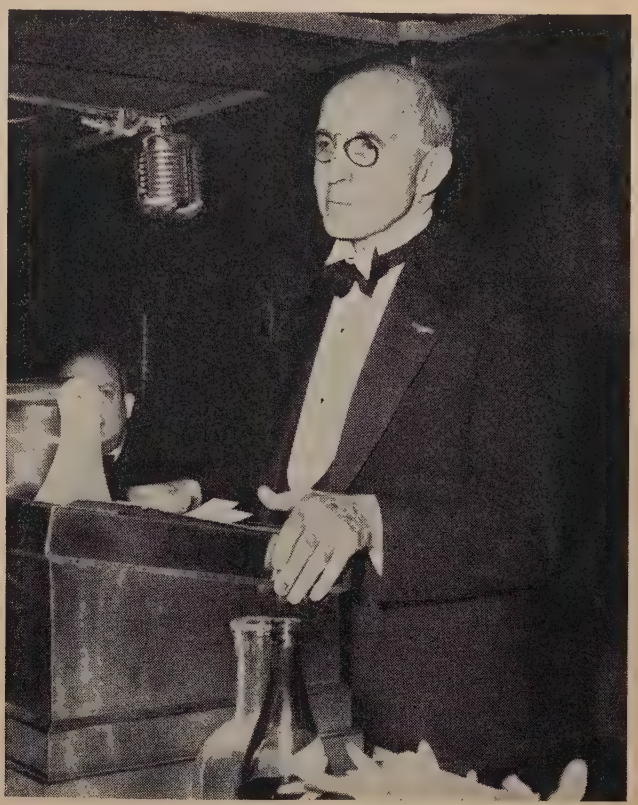

DR. FRANK B. JEWETT, President of the National Academy of Sciences, is Guest Speaker at Banquet.

MR. LEWIS M. CLEMENT, Vice-President in Charge of Research and Engineering, The Crosley Corporation, is Master of Ceremonies at President's Luncheon. Dr. Everitt in background.

DR. WILLIAM L. EVERITT, Retiring President of the I.R.E., Presents Gavel to Dr. Frederick B. Llewellyn, President for 1946, at Annual Meeting.

title of the General's talk was "Some Electrical, Engineering, and General Aspects of the Atomic-Bomb Project."

Presenting a panoramic view of the new world of electronics, a major assembly of radio engineering equipment was shown. One hundred and seventy exhibits of new devices by 135 companies included everything from latest developments in radio receivers to the latest frequency-modulation and television transmitters, from a preproduction model of a camera for the photographic recording of patterns which may appear on a cathode-ray-oscilloscope screen to "packaged antennas," easy to erect 30-foot antenna towers and 150-foot masts.

Radars and radar devices for peacetime use, amplitude- and frequency-modulation radio, television, sound recording, communications, photography, vacuum tubes, magnetic recording, remote-control devices, testing devices, time- and heat-control devices, rectifiers and converters, electronic navigation and direction-finding instruments, and X-ray equipment were a few of the many categories of electronic equipment featured in the exhibit.

Under *radar* were a number of superior designs of signal generators, wave guides, and other components of radars displayed for the first time together with examples of some of the newest radars for peacetime use.

In the *radio field*, one of the newer developments was a new supersensitive loop antenna for receivers. Occupying a section of an entire stage on the main exhibit floor was a radiotelegraph printer system in actual operation and a transmitting and receiving facsimile circuit at work. One feature of particular interest to broadcast engineers was a device shown in actual operation known as a "frequency watchman" which insured synchronized frequency control in frequency-modulation transmitters.

In *television*, a new television pickup and transmission system containing an extremely compact television camera weighing 40 pounds was included among the latest developments.

In *sound recording*, new phonograph pickups, recording turntables, transcription playback units for radio and other professional uses highlighted improved models of home and studio recording. Also on exhibit was a highly developed model of a new magnetic recorder.

In *communications*, mobile radiotelephone equipment of the type suggested for installation in vehicles operating within urban areas was among the new equipment shown.

One of the features in *vacuum tubes* was a 2,000,000-volt X-ray tube in an insulating column consisting of 180 metal-to-glass seals which has a precision control of the electron beam making possible a focal spot as small as one hundredth of an inch.

Other displays of unusual interest were a remote-control system which remotely tunes radio equipment in aircraft; extremely high vacuum pumps; pulse timers for automatic control equipment; a new type of voltage stabilizer for photographic purposes; dual remote-control automatic direction finders, and a new type current converter for automobile radios.

The third major feature of the Meeting was the Annual Banquet held Thursday evening, January 24, at which Dr. Frank B. Jewett, president of the National Academy of Sciences, was the principal speaker. Dr. Jewett declared on his talk before the 2000 members and their guests present, that our Nation's fundamental scientific resources were dangerously depleted. "We drew heavily on our scientific resources in this war," Dr. Jewett said, "and must get back again as soon as possible to serious researches in fundamental sciences. We must remember that our success in applied science adds very little to the source of all science which is fundamental research, and indeed the amazing success of such programs as the atomic-bomb project and the radar program draw heavily upon fundamental science and mobilize the brains and resources of our best men on a limited number of projects to the detriment of other equally vital fields."

At the Banquet also, two special awards and fifteen Fellowships were presented. The Institute Medal of Honor was awarded to Ralph Vinton Lyon Hartley, engineer of Bell Telephone Laboratories "for his early work on oscillating circuits employing triode tubes and likewise for his early recognition and clear exposition of the fundamental relationship between the total amount of information which may be transmitted over a transmission system of limited bandwidth and the time required." Dr. Peter C. Goldmark, engineer of the Columbia Broadcasting System, was the recipient of the Morris Liebmann Memorial Prize, "for his contributions to the development of television systems, particularly in the field of color." Fellowships were awarded to the following engineers: Gregory Breit, Henri G. Busignies, Howard A. Chinn, Thomas Lydwell Eckersley, Walter C. Evans, Clarence W. Hansell, Harold Lester Kirke, Elmer D. McArthur, Harold S. Osborne, Ronald J. Rockwell, Arthur L. Samuel, Joseph Slepian, Julius A. Stratton, William O. Swinyard, and Merle A. Tuve.

The fourth major feature of the Meeting was the President's Luncheon, honoring the incoming president, Dr. Frederick B. Llewellyn. The principal speaker was Paul Porter, then chairman of the Federal Communications Commission, who told 1000 luncheon guests that the radio industry has three main and immediate assignments: the construction of an entirely new system of aural broadcasting—frequency modulation—complete with thousands of transmitters, millions of receivers, and a nationwide network; the construction of a nationwide system of television, and the construction of scores of radio systems for a wide variety of uses to promote safety and efficiency.

Mr. Porter stressed the need for continued support

of the Federal Government in the realm of pure scientific research. "No one knows better than the radio engineer the frontiers that still remain to be conquered in the field of communications," he asserted. "These are tasks of such magnitude and of such general benefit to the entire field that no one company can or should be expected to undertake them. They are proper concerns of the Federal Government. It is plain that we shall have no alternative in this matter. Either research into pure science is to be aided by the Federal Government or much of it will simply be left undone."

At the cocktail party, which was held in the Grand Ballroom of the Hotel Astor on January 25, over 1700 members of the Institute and friends attended.

The women's activities were participated in by 171 guests who registered. On Thursday, January 24, 89 women were taken for a trip through the Cathedral of St. John the Divine; luncheon was served at Stoddard's Restaurant; and a tour of Riverside Church was provided. On Friday, January 25, 107 women were the guests of the I.R.E. and were conducted to the Museum of Costume Art, Sloane's House of Years, and the Public Library. Luncheon was served at the Town Hall Club where Mr. E. Stanley Turnbull had his pictures on display and painted a portrait of one of the women guests. Later in the afternoon, the group was taken to Radio City for a television tour.

Finally, the major features of every annual meeting—the reading of scientific papers and the sessions and symposia on the latest electronic developments—took on particular significance this year with a record number of 87 papers in 16 categories of subjects, many hitherto restricted by military security. The subjects of the sessions were: Military Applications of Electronics; Frequency Modulation and Standard Broadcasting; New Circuit Developments; Television; Radio Navigation Aids; Vacuum Tubes; Microwave Vacuum Tubes; Antennas; Radar; Microwave Techniques; Crystal Rectifiers; Industrial Electronics; Communications Systems and Relay Links; Radio Propagation; Broadcast Receivers; and Quartz Crystals.

One of the important papers of these sessions was recorded and played before a special meeting of the British Institution of Electrical Engineers in London, while its author, J. A. Pierce of the Radiation Laboratory of the Massachusetts Institute of Technology was delivering the paper in person at the meeting in New York. The subject was loran, a radar system that holds great promise for peacetime application and the title of the paper was "An Introduction to Hyperbolic Navigation." In his talk, Mr. Pierce outlined the possibilities of ships and planes automatically navigating straight to their destinations half a world away in any kind of weather; pilotless aircraft being controlled and guided from a great distance with unheard-of accuracy and large areas of the earth's surface being surveyed and charted in far less time than is required by conventional methods through development of loran.

Among other interesting facts which emerged from the many outstanding papers presented was the fact that more than 2,500,000 tons of Japanese shipping had been sunk during the war through the use of sonar, a supersonic device mounted on the hulls of submarines and surface vessels of many types. This information came from a paper entitled: "Navy Radio and Electronics in World War II," by Commodore J. B. Dow of the Navy's Bureau of Ships. Successful invasion of the ultra-high frequencies by high-power, high-definition, full-color television was described in a paper by Dr. Peter C. Goldmark of Columbia Broadcasting System, entitled "Television in the Ultra-High Frequencies." In a paper on "Metal-Lens Antennas", by W. E. Kock of the Bell Telephone Laboratories, new lens antennas made of thin metal strips which resemble venetian blinds were discussed and demonstrated and their use in the future in radio-relay links pointed out.

A Naval radar-directed bomb known under the code name of the "Bat" originated and sponsored by Captain Dundas P. Tucker of the Naval Bureau of Ordinance was described in a paper entitled "Radar Aspects of Naval Fire Control" before the session on Radar. The Bat was a flying bomb with a small fire-control type of fully automatic radar placed in its nose which guided the bomb to its assigned target. "Here," Captain Tucker pointed out, "was a robot 'suicide pilot' far better than his Japanese counterpart."

In a paper entitled "From Wiring to Plumbing" E. M. Purcell of the Radiation Laboratory of Massachusetts Institute of Technology told why engineers must be familiar with plumbers' techniques, in order to put together wave guides, which are metal pipes used for the transmission of ultra-high-frequency radio waves.

Proceedings of the I.R.E. and Waves and Electrons

From month to month, it is hoped more clearly to differentiate the nature of the contents of the Proceedings of the I.R.E. Section from those of Waves and Electrons Section, and to develop in the latter Section an increasingly distinctive character. In the meantime, the Board of Editors will be grateful for any comments, criticisms, or suggestions relative to Waves and Electrons Section. Only through the accumulation of viewpoints, and careful consideration of such proposals, can normal progress and improvement be anticipated.

Board of Directors

January 9 Meeting: At the final meeting of the 1945 Board of Directors, which was held on January 9, 1946, the following were present: F. B. Llewellyn, president-elect (guest); G. W. Bailey, executive secretary; S. L. Bailey, W. R. G. Baker, Alfred N. Goldsmith, editor; V. M. Graham, R. F. Guy, Keith Henney, B. E. Shackelford, D. B. Sinclair, and W. C. White.

Approval of Executive Committee Actions: The actions of the Executive Committee taken at its December 5, 1945, meeting were unanimously approved.

January 9 Meeting: At the annual meeting of the Board of Directors for 1946, the following were present: F. B. Llewellyn, president; G. W. Bailey, executive secretary; S. L. Bailey, W. R. G. Baker, Alfred N. Goldsmith, editor; V. M. Graham, R. F. Guy, Keith Henney, L. C. F. Horle, B. E. Shackelford, D. B. Sinclair, and W. C. White.

1946 Budget: After a careful consideration of the various items of the budget, the Board adopted the recommendation of the Executive Committee that the Budget, as presented, be approved.

Appointments and Committees: The following appointments were unanimously approved:

SECRETARY
Haraden Pratt

TREASURER
William C. White

EDITOR
Alfred N. Goldsmith

APPOINTED DIRECTORS—1946

R. A. Hackbusch	W. O. Swinyard
F. R. Lack	W. L. Webb
G. T. Royden	E. M. Webster

TECHNICAL SECRETARY
Robert Blair Jacques

GENERAL COUNSEL
Harold R. Zeamans

Committees

The following members were appointed.

AWARDS

E. W. Engstrom, *Chairman*

Ralph Bown	W. B. Lodge
D. E. Harnett	G. T. Royden
Keith Henney	W. C. White

CONSTITUTION AND LAWS

R. F. Guy, *Chairman*

G. W. Bailey	L. C. F. Horle
I. S. Coggeshall	B. E. Shackelford
R. A. Heising	F. E. Terman

H. R. Zeamans

EXECUTIVE

S. L. Bailey R. F. Guy
Keith Henney

NOMINATIONS

S. L. Bailey, *Chairman*

E. J. Content	D. D. Israel
Beverly Dudley	R. C. Poulter
W. L. Everitt	P. F. Siling

W. C. White

TELLERS

Trevor Clark, *Chairman*

H. A. Chinn	W. G. Moran
H. M. Lewis	J. E. Shepherd

WAR MEDALS

(Subcommittee of Awards Committee)

Ralph Bown, *Chairman*

F. S. Barton	G. F. Metcalf
J. B. Dow	J. A. Stratton
L. A. DuBridge	A. H. Taylor
Melville Eastham	F. E. Terman
E. W. Engstrom	M. A. Tuve
W. L. Everitt	A. F. Van Dyck
J. W. McRae	W. C. White

RTPB REPRESENTATIVE

D. B. Sinclair
Alfred N. Goldsmith (alternate)

Building-Fund: B. E. Shackelford, chairman of the I.R.E. Building-Fund Committee, reported that the amount subscribed to date is $625,545.77.

Code of Ethics: The recommendations that the functions of the Code of Ethics Committee be combined with the Committee on Professional Recognition and that the membership of the first-named committee be discharged with thanks and that the records of the first-named committee be forwarded to the chairman of the Committee on Professional Recognition was unanimously approved.

Office-Quarters: The Executive Secretary read a report of the Office-Quarters Committee, and a letter from General Counsel Zeamans, reporting the acquisition of the new I.R.E. Building at Fifth Avenue and 79th Street, New York, N. Y.

Constitution and Bylaws

Article II, Sec. 9: It was approved that the following wording be adopted for Article II, Sec. 9, and the amendment as modified be submitted to the membership:

"Sec. 9—Graduation from a radio or electrical course of a school of recognized standing shall be accepted as equivalent to two years experience in radio or allied fields. Full-time graduate work, or part-time graduate work with teaching in radio or allied courses in a school of recognized standing, shall be accepted as equivalent to professional experience, for a period not exceeding one year."

Article V: Unanimous approval was given to the proposed Constitutional Amendment to change the title of Article V from "Officers" to "Officers and Directors," to be submitted to the membership.

Article V, Sec. 5: It was unanimously approved that the following wording be adopted for Article V, Sec. 5, and the amendment as modified be submitted to the membership:

"Sec. 5—No Officer nor Director shall receive, directly or indirectly, any salary, traveling expense, compensation, or emolument from the Institute, unless authorized by the Board of Directors, or by the Bylaws."

Article VI. Sec. 7: The following wording was approved for adoption for Article VI, Sec. 7, and the amendment as modified submitted to the membership:

"Sec. 7—All committees shall be appointed by the Board of Directors or in such manner as the Board may designate."

Bylaw Section 22: The recommendation of the Constitution and Laws Committee that Bylaw Section 22 be eliminated was unanimously approved.

Bylaw Section 46: Unanimous approval was given to the following wording to be adopted for Bylaw Section 46:

"Sec. 46—The standing committees, each of which shall normally consist of five or more persons, shall include the following:

Admissions	Annual Review
Appointments	Antennas
Awards	Circuits
Board of Editors	Electroacoustics
Constitution and Laws	Electron Tubes
Education	Facsimile
Executive Committee of the Board of Directors	Frequency Modulation
	Handbook
	Industrial Electronics
Investments	Medical Electronics
Membership	Radio Receivers
Nominations	Radio Transmitters
Papers Procurement	Radio Wave Propagation and Utilization
Papers Review	
Public Relations	Railroad and Vehicular Communication
Sections	
Tellers	Research
	Standards
	Symbols
	Television

"On matters which are reasonably described by the committee names, these committees shall be advisory to the Board of Directors or the Executive Committee, whichever appoints them and directs their activities.

"The terms of appointments of the Admissions, Awards, Board of Editors, Constitution and Laws, Education, Investments, Membership, Nominations, Papers Procurement, Papers Review, Public Relations, Sections, and Tellers Committees shall start with the first day of the month following appointment and continue until the date the succeeding terms of appointments take effect. The Board may specifically advance or delay the terminating date of any committee and the starting date of a succeeding committee. Appointments shall be made to the following committees: Annual Review, Antennas, Circuits, Electroacoustics, Electron Tubes, Facsimile, Frequency Modulation, Handbook, Industrial Electronics, Medical Electronics, Radio Receivers, Radio Transmitters, Radio Wave Propagation and Utilization, Railroad and Vehicular Communication, Research, Standards, Symbols, and Television, each year between January first and May first and the terms of appointment shall be from May first of the year when the appointments are made until April thirtieth of the following year. Additional appointments may be made to fill vacancies or to care for special cases as the need arises, with the term of the appointment expiring April thirtieth."

Bylaw Section 49: Approval was given to the following wording to be adopted for Bylaw Section 49:

"Sec. 49—The Appointments Committee shall be appointed by the Board of Directors at its regular November meeting.

Its membership shall be chosen from the continuing and newly elected members of the Board of Directors. At least fourteen days before the next annual meeting of the Board of Directors, the Appointments Committee shall mail to the members of the new Board of Directors, a list of candidates for the Offices of Secretary, Treasurer, Editor, and Appointed Directors, and Chairmen and members of the Awards, Constitution and Laws, Executive, Investments, Nominations, and Tellers Committees."

Bylaw Section 53: It was unanimously approved that Bylaw Section 53 be changed to read as follows:

"Sec. 53—The President is authorized to appoint teachers of science or engineering who are Institute members as Institute Representatives. Each such Institute Representative is charged with promoting the welfare of the Institute at his school, particularly in matters relating to Student membership."

Bylaw Section 54—It was unanimously approved that the following wording be adopted for Bylaw Section 54:

"Sec. 54—The Board of Directors may appoint or direct the appointment of representatives of the Institute on joint committees, boards, and other local, national, and international bodies."

Awards: It was approved that all awards in the future shall be made by the Board, upon the recommendation of the Awards Committee, and the Board shall reserve the right to make such changes and additions as it deems desirable.

Morris Liebmann Memorial Fund: On recommendation of Mr. Heising, Treasurer, and the Board, Executive Secretary Bailey, wrote to Mr. Emil J. Simon, donor of the Morris Liebmann Memorial Fund, requesting his approval of a set of modified terms with reference to the Award as follows:

"First—That the award be made to that member of the Institute, who, in the opinion of the Board or its appointed committee, shall have made the most important contribution to the radio art during the preceding calendar year, but that the Board may deviate from these terms when, in its opinion, there are suitable and sufficient reasons, and when it believes the spirit of the award will still be properly satisfied.

"Second—That the fund may be invested in such securities as the Investments Committee of the Institute of Radio Engineers elects, including both stocks and bonds.

"Third—That the Committee on the award may be either a special Committee or the regular Committee of the Institute on other awards.

"Fourth—That the Board in its discretion may estimate the proper amount of an annual award giving effect to possible fluctuations in income so as to have the amount of the award substantially the same for each year in the future, and pay such sum annually, accumulation of any excess to be finally paid out by change in annual award.

"Fifth—The time of the award may be varied by the Board in charge provided it is once for each year."

Mr. Simon replied that he was agreeable to modifying the terms of the Award as outlined above.

Sections

Columbus: Approval was given to the recommendation of the Executive Committee that the petition of Columbus members for the formation of a Columbus Section be approved.

Executive Committee

January 9 Meeting: The Executive Committee Meeting, held on January 9, 1946, was attended by F. B. Llewellyn, president-elect (guest); G. W. Bailey, executive secretary; S. L. Bailey, W. L. Barrow, W. H. Crew, assistant secretary; Alfred N. Goldsmith, editor; and R. A. Heising, treasurer.

Membership: Approval was given to the 360 applications for membership in the Institute as listed on page 42A in the February, 1946, issue of the PROCEEDINGS OF THE I.R.E. and WAVES AND ELECTRONS. These applications are as follows:

For Transfer to Senior Member Grade	14
For Admission to Senior Member Grade	12
For Transfer to Member Grade	71
For Admission to Member Grade	81
For Admission to Associate Grade	131
For Admission to Student Grade	51
Total	360

Fifth Avenue at 79th Street: Mr. Heising, chairman of the Office-Quarters Committee, reported that the final purchase of the property at Fifth Avenue at 79th Street, New York, N. Y. had been consummated on December 28, 1945, that the architect is making up drawings, copies of which were not available as yet, and that the plans would have to be presented to the Department of Housing.

Office-Quarters Committee: The Office-Quarters Committee for the year 1946 will consist of R. A. Heising, chairman; F. B. Llewellyn, Haraden Pratt, Alfred N. Goldsmith, and George W. Bailey.

Papers Procurement Committee: The Editorial Department, on behalf of the Papers Procurement Committee, some time ago sent out a letter from Dorman D. Israel and E. T. Dickey to all Group and Subgroup Chairmen of the Papers Procurement Committee furnishing information which was secured from the postcard survey on promised papers. Thus, it was made possible for each Group chairman to secure papers systematically from the survey made on the postcards.

Appointments

The following appointments were unanimously approved:

Mr. R. F. Guy to serve as Mr. A in charge of technical committees.

Mr. S. L. Bailey to serve as Mr. B in charge of Sections' activities.

Mr. Keith Henney to serve as Mr. C in charge of certain standing committees such as Admissions, Membership, and Public Relations.

FACSIMILE COMMITTEE

Pierre Mertz

Technical Secretary: Executive Secretary Bailey announced that, in accordance with authorization by the Executive Committee and the Board of Directors, Robert Blair Jacques had been engaged as the new technical secretary to take office on February 1, 1946.

American Standards Association: The Executive Committee authorized the payment of $500 membership fees to the ASA Standards Council, subject to the approval of the 1946 Budget.

I.R.E. People

C. P. SWEENEY

C. P. Sweeney has returned to the National Broadcasting Company's engineering department as a member of the technical staff of the television transmitter in the Empire State Building in New York after service with the United States Navy as a Lieutenant Commander.

Mr. Sweeney joined NBC in 1939 as development laboratory engineer and was called to the Navy as a Lieutenant (s.g.) in 1941. He served as radio officer and radio materiel officer at Casablanca before returning to the United States to head the major shore section of the electronic field service group at the Naval Reserve Laboratory, Washington, D. C. In 1944, Mr. Sweeney was transferred to the Radio Engineering Planning Board of the Commander-in-Chief of the Pacific Fleet, serving as executive officer with the group which designed and supervised installation of Radio Guam. He completed his naval service in 1945 as an electronic ship superintendent at Mare Island, California.

J. B. SCHAEFER

J. B. Schaefer (A'37–SM'45) has been appointed plant manager of the New York Transformer Company. He will direct engineering and manufacturing activities at the Alpha, New Jersey, plant and have charge of reconversion.

Mr. Schaefer formerly was associated with the Sperry Gyroscope Company as engineering manager. He was responsible for several of Sperry's most important war projects and acted as transformer consultant for the company.

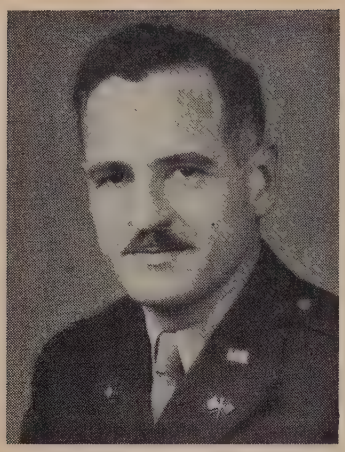

VERNON B. BAGNALL

VERNON B. BAGNALL

Vernon B. Bagnall (A'30–M'40–SM'43) has returned to the long-lines department of the American Telephone and Telegraph Company as division plant superintendent for the territories of Maryland, Virginia, West Virginia, and District of Columbia, after four years in the United States Signal Corps.

Colonel Bagnall received his B.S. degree in electrical engineering at the University of Wisconsin in 1927 and the M.S. from New York University in 1933. He joined the long-lines department in 1927 as technical employee in Chicago, Illinois, after which he was transferred to New York as radio engineer and circuit-layout engineer.

In 1942, he entered the Signal Corps as Captain and was assigned Officer in Charge, Radio Branch, Plant Division. In 1943, Colonel Bagnall was appointed Chief, Communications Engineering Branch, Army Communications Service, Office of the Chief Signal Officer, with responsibility for the over-all engineering of the world-wide radio and wire network established by ACS. He participated in making practicable the use of teletypewriters on radio circuits which formed the basis of the Army's telegraph communications system. He supervised the engineering of the communications arrangements for the Anglo-American and Big-Three conferences at Quebec, Cairo-Teheran, Malta-Yalta, and Potsdam, and also supervised the installation and operation of facilities at the Pottsdam and first Quebec conferences.

Colonel Bagnall made two other trips to the European theater, the first in connection with planning communications for the invasion of Europe, and the second in connection with rehabilitation and establishment of communications in France following the Allied Armies' push through that country. He also participated in an engineering survey of communications on the Air Transport Command's South Atlantic air-ferry route to establish radioteletype facilities which would expedite the movement of aircraft. Colonel Bagnall was awarded the Bronze Star and the Legion of Merit for his services.

❖

BEVERLY F. FREDENDALL

RAY H. DE PASQUALE

RAY H. DE PASQUALE

Ray H. de Pasquale (A'43) has been appointed vice-president and general manager of the recently organized Press Wireless Manufacturing Corporation of New York. Mr. Pasquale formerly was director of manufacturing for Press Wireless, Inc.

❖

BEVERLY F. FREDENDALL

Beverly F. Fredendall (A'29) is now associated with Frederick Hart and Company, Inc., specializing in the design and manufacture of recording equipment. Mr. Fredendall previously was with the National Broadcasting Company for sixteen years in operation and design of audio and video broadcast systems including the field of recording. Until recently, he was located at the NBC midwest headquarters in Chicago.

❖

WALTER S. LEMMON

Walter S. Lemmon (SM'45) has been named a vice-president of Globe Wireless, Ltd. Globe has acquired from International Business Machines Corporation its interest in the radio-type developments of Walter S. Lemmon and Associates.

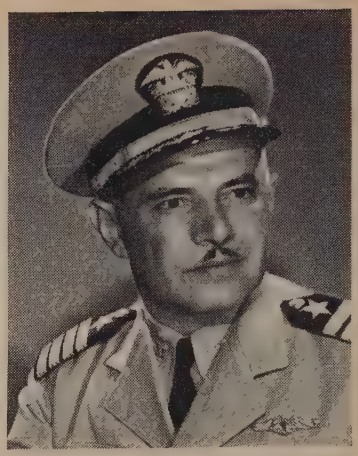

ADOLPH B. CHAMBERLAIN

ADOLPH B. CHAMBERLAIN

Adolph B. Chamberlain (A'27–M'30–F'42) was commissioned a Captain (SE3)T in the United States Naval Reserve in July, 1945. Captain Chamberlain has been active in radio work since 1920, and has served on general and technical committees of the I.R.E. He is a past chairman of the Rochester and Buffalo Sections. On December 24, 1945, he resumed his position as chief engineer of the Columbia Broadcasting System.

❖

HOWARD S. FRAZIER

Howard S. Frazier (A'27–M'43–SM'43) has announced the formation of a radio management consulting practice, with offices in Washington, D. C.

Mr. Frazier entered the amateur radio field in 1919, and in 1922, engaged in the manufacture and sale of radio parts and the custom building of broadcast receivers. From 1925 to 1932, he was located in Philadelphia, Pennsylvania, as control operator of WCAU, chief engineer of WABQ, partner and chief engineer of WPSW, and chief engineer of WPEN and WRAX. He was also chief engineer of WOAX, Trenton, New Jersey, and WOAB, New York City. In 1933, he became chief engineer of the General Broadcasting System and two years later was consulting

HOWARD S. FRAZIER

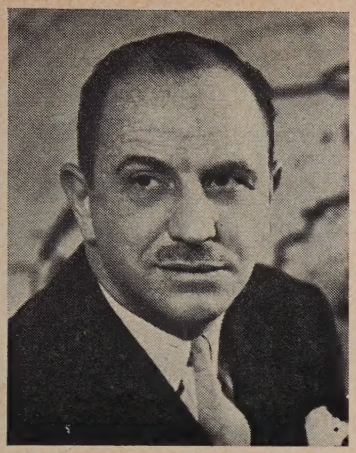

ROYAL V. HOWARD

❖

broadcast engineer practicing before the Federal Communications Commission. In 1937, Mr. Frazier became president and general manager of WSNJ, Bridgeton, New Jersey. As sales engineer for the Radio Corporation of America in 1942, he was in charge of United States Navy contracts, and later that year, he was named director of engineering of the National Association of Broadcasters.

Mr. Frazier is vice-chairman of the Radio Technical Planning Board and chairman of its Panel 4 on Standard Broadcasting. He is chairman of the Radio Manufacturers Association's Subcommittee on Satellite Amplitude-Modulated Broadcast Transmitters, acting director of engineering and secretary of the Executive Engineering Committee of NAB, alternate representative of RTPB on the Radio Propagation Executive Council, and a member of H. V. Kaltenborn's "Twenty-Year Club." He has recently been elected vice-president of Freeland and Olschner Products, Inc., of New Orleans, Louisiana, in charge of sales and finance. Mr. Frazier served as a member of the I.R.E. Winter Technical Meeting Committee and is a member of the I.R.E. Papers Committee.

❖

UNIVERSAL RESEARCH LABORATORIES

Royal V. Howard (M'41–SM'43) has been named director of the Universal Research Laboratories in San Francisco, California, established for the performance of radio engineering consultant work. His associates are F. Richard Brace (A'36–M'44), Allan A. Kees (M'44), Alfred E. Towne (A'30), and Melvin P. Klein (A'43).

Mr. Howard, one of the early workers in short-wave and aircraft communications, has been engaged in the radio field for the past twenty years. During the last twelve years of this period, he was director of engineering for KSFO, KWID, KWIX, and KPAS. He returned from Europe early in 1945 where he headed a special scientific staff and directed the Operational Analyst Staff at United States Army Headquarters for one year. Mr. Howard is vice-president of engineering of both the Associated Broadcasters, Inc., and the Universal Broadcasting Company, and is chairman of the San Francisco Section of the I.R.E. for 1946.

A graduate of the United States Naval Academy, Mr. Brace studied radio at the University of California and the Radio Institute of California. After a period of active duty with the Navy, he became chief of engineering plans of the Associated Broadcasters, Inc., and is in charge of directional-antenna design and engineering plans at the Laboratories.

Mr. Kees, engineering expert and studio construction specialist for the Laboratories, attended Shanghai American School and St. John's University, Shanghai, China. He served with the United States Navy for five years specializing in Naval radio and underwater sound. Mr. Kees performed radio research and was chief engineer of a prominent broadcast station for seven years before joining KSFO where he is chief of audio facilities.

Mr. Towne received the B.S. degreee in electrical engineering from the California Institute of Technology. Before becoming chief of transmitter facilities for KSFO, KWID, and KWIX in 1937, he served as test engineer for the Radio Corporation of

F. RICHARD BRACE

America and General Electric Company, and as radio test and design engineer in San Francisco. Besides design, Mr. Towne handles transmitter and antenna field engineering for the Laboratories.

Mr. Klein received his electrical engineering training at Denver University, University of Colorado, and the University of California. He was associated with the Aircraft Radio Laboratory in Denver, and was consulting engineer for the Air Transport Command in Alaska. In San Francisco, he was affiliated with the Office of War Information, after which he became engaged in broadcast consultant work in Washington, D. C. Mr. Klein served with the Office of Scientific Research and Development as scientific consultant in radar in the southwest Pacific area.

❖

CARMAN RANDOLPH RUNYAN, JR.

Carman Randolph Runyan, Jr., (A'18) was recently awarded the Armstrong Medal of The Radio Club of America for outstanding contributions to the radio art. The citation stresses his development of the multispark synchronous-gap transmitter, the crystal-controlled frequency-modulated telegraph system, the single-signal radiotelegraph receiver, and the 100-megacycle frequency-modulated broadcast transmitter.

❖

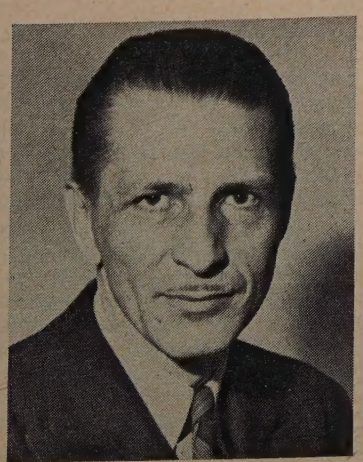

ALLAN A. KEES

MELVIN P. KLEIN

ALFRED E. TOWNE

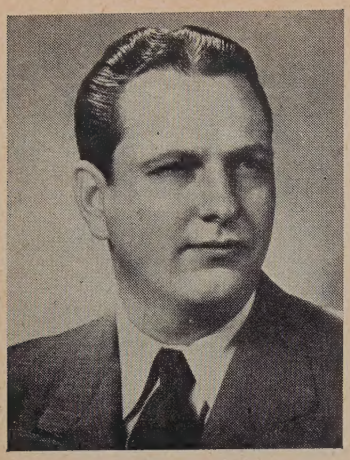

LEONARD F. CRAMER

LEONARD F. CRAMER

Allen B. DuMont (M 30–F'31), president of the Allen B. Du Mont Laboratories, Inc., Passaic, New Jersey, recently announced the appointment of Leonard F. Cramer (A'44) as director of the newly established television-broadcast division. Mr. Cramer has been the vice-president and a director of the Company since 1942.

❖

NORMAN S. KORNETZ

Norman S. Kornetz (A'39) has recently been appointed project engineer in charge of Westinghouse television-receiver development. He will have charge of all Westinghouse home television-receiver development, with emphasis on receiving units to be used in flight tests of stratovision.

Born in Boston, Massachusetts, Mr. Kornetz was graduated from Massachusetts Institute of Technology in 1935 with a B.S. degree in electrical engineering. He remained at M.I.T. during the next three years serving with the Division of Industrial Co-operation. In 1938, he joined the American Television Corporation of New York City. Later that year, Mr. Kornetz went to Buffalo to become a member of the staff of the Colonial Radio Corporation where he was located until he joined the U. S. Signal Corps in September, 1942. Mr. Kornetz has recently returned to this country from India where, as a captain with the 3105th Signal Service Battalion, he was in charge of all administrative radio communications in the Calcutta area.

❖

L. W. CHUBB AND EDWIN H. COLPITTS

L. W. Chubb (M'21–F'40) was elected vice-chairman of The Engineering Foundation, and Edwin H. Colpitts (A'14–F'26) was re-elected director at the annual meeting of that organization held on October 18, 1945. Dr. Chubb is director of the Westinghouse Electric Company's research laboratories, and Dr. Colpitts formerly held the position of director of the Bell Telephone Laboratories.

The Engineering Foundation was established in 1913 for "the furtherance of research in science and engineering and for the advancement in any other manner of the profession of engineering and the good of mankind."

❖

AUSTEN M. CURTIS

Austen M. Curtis (M'13–SM'43), member of the transmission research staff of Bell Telephone Laboratories, died in South Orange, New Jersey, on December 22, 1945, Mr. Curtis was born in Brooklyn, New York, in 1890.

Leaving Heffley Institute in 1907, he shipped as wireless operator for the United Wireless Company. Three years later, he became chief operator and installer for the radio systems of a Brazilian shipping company, and in 1912 had charge of radio operations on an exploring expedition for the Brazilian Department of Agriculture. Mr. Curtis joined the Western Electric engineering department in 1913 engaging in telephone instruments study and the radio research that took him to Paris for the transatlantic tests of 1915. It was he who listened at the Eiffel Tower radio receiver when spoken words were first transmitted across the Atlantic.

A member of the Army Signal Corps in World War I, he became a Captain in the Division of Research and Inspection in Paris. Returning to Western Electric's research department after the war, Mr. Curtis developed systems for telegraph communication over submarine cable, with particular emphasis on his work in recording oscillographs. He was responsible for the development of echo suppressors and volume limiters, and engaged in the study of contact phenomena which occupied his attention until his death. During World War II, Mr. Curtis made important contributions to secret scientific projects undertaken by Bell Telephone Laboratories for the United States Government.

AUSTEN M. CURTIS

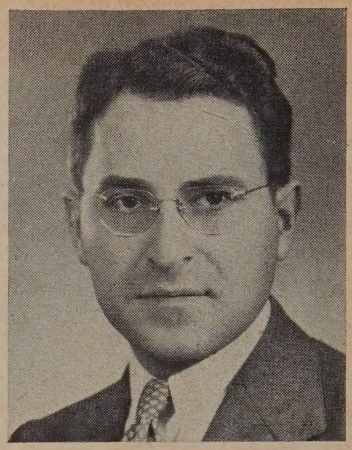

NORMAN S. KORNETZ

❖

G. ROBERT MEZGER

G. Robert Mezger (A'37) has rejoined the Allen B. DuMont Laboratories, Inc., Passaic, New Jersey, as manager of instrument sales after four and one-half years in the United States Navy.

Commander Mezger first joined the DuMont engineering department in 1936 following his graduation from Rensselaer Polytechnic Institute with a degree in electrical engineering. His first Naval assignment in 1941 was with the electronics section of the David Taylor Model Basin, Washington, D. C., where he was concerned with the development of electrical equipment for studies in stress, strain, and vibration problems on ships. In 1944, Commander Mezger attended the Navy's preradar and radar schools, after which he was appointed to the staff of the Electronics Maintenance School at Pearl Harbor.

❖

LEROY C. ANDERSON

Sergeant Leroy C. Anderson (A'39) lost his life when the ship on which he was being transported from the Philippine Islands was torpedoed and sunk on October 24, 1944. Sergeant Anderson was born April 2, 1918, and he was graduated from Burlington High School, Burlington, Wisconsin, in 1936, and later from a radio and television school in Chicago. At the time of his induction into the Armed Forces, Sergeant Anderson was employed at the Burlington Mills. In February, 1942, General Douglas MacArthur awarded Sergeant Anderson the Distinguished Service Cross for extraordinary heroism in action, he being the first selectee to be so honored.

SECTIONS

Chairman		Secretary
R. A. Holbrook 146 Lawrenceville Rd. Decatur, Ga.	ATLANTA March 15	I. M. Miles 554—14 St., N.W. Atlanta, Ga.
R. N. Harmon 1920 South Rd. Mt. Washington, Baltimore 9, Md.	BALTIMORE March 26	F. W. Fischer 714 S. Beechfield Ave. Baltimore, Md.
C. C. Harris Tropical Radio Telegraph Co Box 584, Hingham, Mass.	BOSTON March 22	A. G. Bousquet General Radio Co. 275 Massachusetts Ave. Cambridge 39, Mass.
A. DiMarco Carabobo 105 Buenos Aires, Argentina	BUENOS AIRES	H. Krahenbuhl Transradio Internacional San Martin 379 Buenos Aires, Argentina
J. M. Van Baalen 282 Orchard Dr. Buffalo 17, N. Y.	BUFFALO-NIAGARA March 20	H. W. Staderman 264 Loring Ave. Buffalo, N. Y.
T. A Hunter Collins Radio Co. 855—35 St., N.E. Cedar Rapids, Iowa	CEDAR RAPIDS March 20	R. S. Conrad Collins Radio Co. 855—35 St, N.E. Cedar Rapids, Iowa
Cullen Moore 327 Potomac Ave. Lombard, Ill.	CHICAGO March 15	D. G. Haines 4000 W. North Ave. Chicago 39, Ill.
J. D. Reid Box 67 Cincinnati 31, Ohio	CINCINNATI April 16	P. J. Konkle 5524 Hamilton Ave. Cincinnati 24, Ohio
R. A. Fox 2478 Queenston Rd. Cleveland Heights 18, Ohio	CLEVELAND March 28 Magnetic Recording, Physical Aspects and Recent Developments Otto Kernei	Walter Widlar 1299 Bonnieview Ave. Lakewood 7, Ohio
R. C. Higgy 2032 Indianola Ave. Columbus, Ohio	COLUMBUS April 12	Warren Bauer 376 Crestview Rd. Columbus 2, Ohio
H. W. Sundius Southern New England Telephone Co. New Haven, Conn.	CONNECTICUT VALLEY March 14 Bridgeport Offensive Aspects of Radar	L. A. Reilly 989 Roosevelt Ave. Springfield, Mass.
R. M. Flynn Station KRLD Dallas 1, Texas	DALLAS-FT. WORTH April 12	J. G. Rountree Box 5238 Dallas 2, Texas
L. B. Hallman 3 Crescent Blvd. Southern Hills Dayton, Ohio	DAYTON April 25 Dayton Engineers Club Presentation of Local Papers Annual Meeting Election of Officers	Joseph General 411 E. Bruce Ave. Dayton 5, Ohio
H. E. Kranz International Detrola Corp. 1501 Beard Ave. Detroit 9, Mich.	DETROIT March 15	A. Friedenthal WJR Fisher Building Detroit 2, Mich.
N. L. Kiser Sylvania Electric Products, Inc. Emporium, Pa.	EMPORIUM	D. J. Knowles Sylvania Electric Products, Inc. Emporium, Pa.
H. I. Metz Civil Aeronautics Authority Experimental Station Indianapolis, Ind.	INDIANAPOLIS	V. A. Bernier 5211 E. 10 Indianapolis, Ind.
E. M. Dupree Star Electric and Engineering Co. 613 Fannin St. Houston, Texas	HOUSTON	
R. N. White 4800 Jefferson St. Kansas City, Mo.	KANSAS CITY	Mrs. G. L. Curtis 6003 El Monte Mission, Kansas

Books

Pulsed Linear Networks, by Ernest Frank

Published (1945) by McGraw-Hill Book Co., Inc., 330 W. 42 St., New York 18, N. Y. 260 pages+7-page index+vii pages. 179 illustrations. $5\frac{1}{2}\times8\frac{1}{2}$ inches. Price, $3.00.

The scope of this book is the analysis by means of the classical method of the transient response of various forms of networks to a rectangular pulse. The networks are of the series resistance-capacitance, resistance-inductance, and resistance-inductance-capacitance type, as well as some special series-parallel combinations of the above parameters. The author very carefully emphasizes that other methods of solution, such as Laplacian transforms, will be necessary in more involved networks, but he intends using the classical method only, and to apply it to those circuits that are simple enough to be amenable to its application.

It might, therefore, be expected that the utility of this book (which is a first edition) will be limited accordingly, but actually quite a number of practical and useful circuits are treated, and the author covers the scope of his book quite thoroughly. Indeed, the first reaction is that he covers it too thoroughly, and that the first part of the book dealing with series networks, could be condensed into possibly three chapters instead of five.

However, the information contained in these five chapters is quite worthwhile for the busy design engineer who wants a summary of the results. The curves furnished serve this purpose, and since they are plotted in generalized co-ordinates involving the ratio of pulse width to time constant, they apply to all circuits of the type considered.

Thus, although the book is planned essentially for undergraduates in their junior or senior year, it will be found of value by the practicing engineer, particularly if he is a little rusty in his knowledge of elementary transient analysis. This is particularly true of the latter part of the book dealing with the series-parallel combinations of resistance, inductance, and capacitance.

It is here that some rather interesting equivalent series circuits are presented, and the method employed is that of transforming the differential equations for the various meshes into a single differential equation that suggests the equivalent series circuit. In some cases Thevenin's theorem is employed for the purpose, and thus more than one series equivalent can be found. This latter half is probably the more important part of the book, and makes the reader feel that if the first part had been condensed (since it is available in scores of other textbooks) more space would have been available for further examples of equivalent circuits and practical applications.

In line with this, the discussion of power and energy relations in the resistance-capacitance and resistance-inductance single-energy circuits seems to be somewhat unnecessary since no additional practical information is obtained that is not already contained in the current and voltage rela-

tions. The material appears more of academic interest, and could be summarized.

The book is very clearly written and is easy to follow. However, this is in considerable measure due to the simple networks studied and to the avoidance of some of the more complicated circuits actually in use. While many of the latter may be classified material, there are many circuits used in television, for example, that could be discussed profitably and the book would gain considerably in utility by the inclusion of such material. In short, while the author covers the scope of his book, it seems unfortunate that he did not expand its scope to include many useful and important circuits that are employed today. Incidentally, the classical method would appear particularly suited to the analysis of that type of nonlinear circuit involving switching actions, such as that of a unilateral circuit element. An example is given in Chapter IX in the form of a diode stage.

Nevertheless the book is quite worthwhile, and will be of value to many engineers engaged in pulse technique. The illustrations and diagrams are well done, and as stated previously, the style is clear and simple. In addition, a systematic mode of presentation is followed throughout.

ALBERT PREISMAN
Capitol Radio Engineering Institute
Washington, D. C.

Table of Arc Sin *X*

Prepared by the Mathematical Tables Project, Arnold N. Lowan, Project Director, and a Technical Staff of six persons, together with five Supervisory and Editing Assistants, and Conducted under the Sponsorship of the National Bureau of Standards, Lyman J. Briggs, Director, and Official Sponsor of the Project.

Published (1945) by Columbia University Press, 2960 Broadway, New York, N. Y. 124 pages+xix pages. $7\frac{1}{2}\times10\frac{3}{4}$ inches. Price, $3.50.

The tables of fundamental mathematical functions prepared by The Mathematical Tables Project under the direction of Dr. Lowan are well known to workers in applied mathematics; this latest volume will be found a welcome addition to the series. The main body of the tables in this volume gives values of arc sin X in radians to twelve decimal places, with intervals between successive arguments of 0.0001 from zero to 0.9890 and intervals of 0.00001 from 0.98900 to unity. In order to make the full accuracy of the table available when interpolation is necessary, special interpolation aids are included. Second central differences are listed in the main table for values of the argument from zero to 0.99900, second and fourth differences from 0.99900 to 0.99950, and a thirteen-place auxiliary table of a special function for greater accuracy in the range from 0.99950 to unity. Corresponding coefficients for the interpolation formulas are also tabulated in auxiliary tables, as are multiples of $\pi/2$, and conversion tables between radians, degrees, and decimal fractions, and degrees, minutes, and seconds.

JOHN R. WHINNERY
General Electric Co.
Schenectady, N. Y.

	Chairman	Secretary
LONDON, ONTARIO March 15	B. S. Graham Sparton of Canada, Ltd. London, Ont., Canada	C. H. Langford Langford Radio Co. 246 Dundas St. London, Ont., Canada
LOS ANGELES March 19	Frederick Ireland General Radio Co. 1000 N. Seward St. Hollywood, Calif.	Walter Kenworth 1427 Lafayette St. San Gabriel, Calif.
MILWAUKEE	P. B. Laeser 9410 Harding Rd. Milwaukee, Wis.	E. L. Cordes 3304 N. Oakland Ave. Milwaukee, Wis.
MONTREAL, QUEBEC March 21	L. A. W. East Canadian Pacific Railway 204 Hospital St. Montreal, Que., Canada	R. R. Desaulniers Canadian Marconi Co. Box 1690 (Place D'Armes) Montreal 1, Que., Canada
NEW YORK April 3	G. B. Hoadley 85 Livingston St. Brooklyn, N. Y.	J. T. Cimorelli RCA Victor Div. 415 S. Fifth St. Harrison, N. J.
OTTAWA, ONTARIO March 21	W. A. Steel 298 Sherwood Dr. Ottawa, Ont., Canada	L. F. Millett 33 Regent St. Ottawa, Ont., Canada
PHILADELPHIA April 4	D. B. Smith Philco Corporation Philadelphia 34, Pa.	P. M. Craig Philco Corporation Philadelphia 34, Pa.
PITTSBURGH April 8 "New Frequency-Modulation Transmitters" L. O. Krause General Electric Company Schenectady, N. Y.	J. A. Hutcheson 852 N. Meadowcroft Ave. Pittsburgh 16, Pa.	C. W. Gilbert 52 Hathaway Ct. Pittsburgh 21, Pa.
PORTLAND	C. W. Lund Rt. 4, Box 858 Portland, Ore.	L. C. White 3236 N.E. 63 Ave. Portland 13, Ore.
ROCHESTER April 18	G. R. Town Stromberg-Carlson Co. Rochester 3, N. Y.	A. E. Newlon Stromberg-Carlson Co. Rochester 3, N. Y.
ST. LOUIS March 28 March 20	B. B. Miller 2356A Lawrence St. St. Louis 10, Mo.	N. J. Zehr 1538 Bradford Ave. St. Louis 14, Mo.
SAN DIEGO April 2	David Kalbfell 941 Rosecrans San Diego, Calif.	Clyde Tirrell U. S. Navy Radio and Sound Laboratory San Diego 52, Calif.
SAN FRANCISCO	R. V. Howard Mark Hopkins Hotel San Francisco, Calif.	Lester Reukema 2319 Oregon St. Berkeley, Calif.
SEATTLE March 14	E. H. Smith 823 E. 78 St. Seattle 5, Wash.	W. R. Hill University of Washington Seattle 5, Wash.
TORONTO, ONTARIO	F. H. R. Pounsett Research Enterprises, Ltd. Leaside, Ont., Canada	Alexander Bow 137 Oxford St. Guelph, Ont., Canada
TWIN CITIES	H. E. Hartig University of Minnesota Minneapolis, Minn.	M. R. Ludwig 315 E. 24 St. Minneapolis, Minn.
WASHINGTON April 8	F. W. Albertson Room 1111, Munsey Bldg. Washington 4, D. C.	G. P. Adair Federal Communications Commission Washington 4, D. C.
WILLIAMSPORT March 6 April 3	Harry Smithgall Sylvania Electric Products, Inc. Plant No. 1 Williamsport, Pa.	F. L. Burroughs 2030 Reed St. Williamsport 39, Pa.

SUBSECTIONS

MONMOUTH (New York Subsection)	N. F. Schlaack Bell Telephone Laboratories 463 West St. New York 14, N. Y.	C. D. Samuelson 5 Russel Ave. Fort Monmouth, N. J.
PRINCETON (Philadelphia Subsection)	W. C. Johnson Princeton University Princeton, N. J.	J. G. Barry Princeton University Princeton, N. J.
SOUTH BEND (Chicago Subsection) March 21	H. E. Ellithorn 417 Parkovash Ave. South Bend 17, Ind.	J. E. Willson WHOT, St. Joseph and Monroe Sts. South Bend, Ind.